



# Influence des oxydes de manganèse et de la matière organique sur le cycle géochimique externe des terres rares

Olivier Pourret

## ► To cite this version:

Olivier Pourret. Influence des oxydes de manganèse et de la matière organique sur le cycle géochimique externe des terres rares. Géochimie. Université de Picardie Jules Verne, 2013. tel-02266954

HAL Id: tel-02266954

<https://hal.science/tel-02266954>

Submitted on 17 Aug 2019

**HAL** is a multi-disciplinary open access archive for the deposit and dissemination of scientific research documents, whether they are published or not. The documents may come from teaching and research institutions in France or abroad, or from public or private research centers.

L'archive ouverte pluridisciplinaire **HAL**, est destinée au dépôt et à la diffusion de documents scientifiques de niveau recherche, publiés ou non, émanant des établissements d'enseignement et de recherche français ou étrangers, des laboratoires publics ou privés.

***HABILITATION A DIRIGER DES RECHERCHES***

**Influence des oxydes de manganèse et de la matière organique sur le cycle géochimique externe des terres rares**

***PRESENTEE***

***PAR***

***OLIVIER POURRET***

***MEMOIRE PRESENTE LE 18 JUILLET 2013***

***DEVANT LE JURY DE***

***l'École Doctorale en Sciences, Technologies et Santé n°547***  
***du***

Pôle de Recherche et d'Enseignement Supérieur  
Université Fédérale Européenne Champagne Ardenne Picardie

Section CNU 36 Terre solide : géodynamique des enveloppes supérieure, paléobiosphère

**Composé de :**

**M. Dominique GUYONNET - Rapporteur**

**M. André MARIOTTI - Rapporteur**

**M. Jean-Luc SEIDEL - Rapporteur**

**M. Guillaume DECOCQ - Examinateur**

**M. Thierry AUSSENAC - Examinateur**

**M. Gérard GRUAU - Invité**



"These elements perplex us in our researches, baffle us in our speculations, and haunt us in our very dreams. They stretch like an unknown sea before us - mocking, mystifying and murmuring strange revelations and possibilities."

Williams Crookes (1887) talking about Rare Earths



## Table des matières

|  |            |
|--|------------|
| <b>Curriculum Vitae.....</b>   | <b>7</b>   |
| Curriculum Vitae .....   | 9          |
| Publications et communications.....  | 11         |
| Contrats publics et privés .....   | 19         |
| Collaborations.....  | 22         |
| Responsabilités collectives et administratives.....  | 23         |
| Appartenance à des sociétés savantes .....   | 23         |
| Expertises .....   | 24         |
| Activités et responsabilités d'enseignement.....   | 25         |
| Encadrement d'étudiants, doctorants et post-doctorants .....   | 30         |
| <b>Bilan de mes activités de recherche .....</b>   | <b>35</b>  |
| Avant-propos .....   | 37         |
| Introduction .....   | 40         |
| Partie I .....   | 45         |
| Impact des colloides sur le comportement des terres rares en solution .....  | 45         |
| I.1. Expériences d'adsorption/oxydation sur oxydes de manganèse .....  | 47         |
| I.3. Complexation des terres rares à la surface d'acides humiques .....  | 51         |
| I.4. Compétition acides humiques/carbonates .....  | 56         |
| I.5. Nouveau processus de formation d'anomalie de cérium .....   | 58         |
| Partie II .....  | 61         |
| Quantification des rôles respectifs de la matière organique et des oxydes de Fe et de Mn sur la spéciation des terres rares dans des eaux naturelles (eaux souterraines et de rivières)..... | 61         |
| II.1. Eaux souterraines de versant .....   | 63         |
| II.2. Eaux souterraines de zone humide .....   | 68         |
| II.3 Eaux de rivières .....  | 70         |
| Partie III.....  | 79         |
| Utilisation du fractionnement des terres rares dans la compréhension de minéralisations .....  | 79         |
| III.1. Altération et mise en solution.....   | 81         |
| III.2. Cycle externe des terres rares revisité .....   | 84         |
| III.3. Contrôle par matière organique .....  | 90         |
| III.4. Contrôle par oxydes de manganese et carbonates .....  | 94         |
| III.5. Contrôle par matière organique, oxydes de Fe/Mn et fluide .....   | 99         |
| Bilan.....   | 103        |
| <b>Projet de recherche .....</b>   | <b>105</b> |
| Fractionnement et spéciation des terres rares en solution .....  | 106        |
| Ecodynamisme des terres rares .....  | 107        |
| <b>Bibliographie.....</b>  | <b>109</b> |
| <b>Publications.....</b>   | <b>117</b> |



# **Curriculum Vitae**



# Curriculum Vitae

# Olivier POURRET

34 ans

## Enseignant-Chercheur

Institut Polytechnique LaSalle-Beauvais  
19 rue Pierre Waguet  
60026 Beauvais cedex

Géologue Géochimiste, Docteur en Sciences de la Terre

# Diplômes universitaires

**Thèse de doctorat** (Sciences de la Terre) de l'Université de Rennes 1 – soutenue le 06 octobre 2006 – mention très honorable, Géosciences Rennes, Université de Rennes 1.

## Impact de la matière organique sur le comportement des terres rares en solution : étude expérimentale et modélisation.

|                        |  |
|------------------------|--|
| Directeur de thèse     | Gérard Gruau                                 |
| Co-directrice de thèse | Mélanie Davranche                            |
| Rapporteurs            | Marc Benedetti<br>Bernard Dupré              |
| Examinateurs           | Françoise Elbaz-Poulichet<br>Michael Bau     |
| Invité                 | Aline Dia                                    |
| Financement            | Octobre 2003 - Septembre 2006 : Bourse MNERT |
| Partenaires financiers | Région Bretagne et Rennes Métropole          |

Ma thèse est consultable à cette adresse :

[http://www.caren.univ-rennes1.fr/doc/memoires/mem18/Olivier\\_Pourret\\_these.pdf](http://www.caren.univ-rennes1.fr/doc/memoires/mem18/Olivier_Pourret_these.pdf)

D.E.A., Géosciences, mention Bien (Université de Rennes 1)

2003

Impact de la complexation organique sur l'oxydation du Cerium (III) et sur l'adsorption des terres rares sur de la ferrihydrite : étude expérimentale, sous la direction de M. Davranche et de G. Gruau

**Maîtrise** Sciences de la Terre et de l'Univers (Université de Rennes 1) 2002

**Licence** Sciences de la Terre et de l'Univers (Université de Rennes 1) 2001

**DEUG** Sciences de la Matière (Université de Rennes 1) 2000

## Fonctions exercées

---

2003-2006 **Allocataire et Moniteur** de l'Enseignement Supérieur à l'Université de Rennes 1

2006-2007 **Attaché Temporaire d'Enseignement et de Recherche** à l'Université de Rennes 1

## Fonction actuelle

---

Depuis 2007 **Enseignant-Chercheur** en Géochimie à l'Institut Polytechnique LaSalle Beauvais. Unité de rattachement HydrISE.

## **Publications et communications**

### **Articles de rang A**

1. Davranche M., **Pourret O.**, Gruau G. et Dia A. (2004) Impact of humate complexation on the adsorption of REE onto Fe oxyhydroxide. *Journal of Colloid and Interface Science* **277**, 271-279.
2. Davranche M., **Pourret O.**, Gruau G., Dia A. et Le Coz-Bouhnik M. (2005) Adsorption of REE(III)-humate complexes onto MnO<sub>2</sub>: Experimental evidence for cerium anomaly and lanthanide tetrad effect suppression. *Geochimica et Cosmochimica Acta* **69**, 4825-4835.
3. **Pourret O.**, Davranche M., Gruau G. et Dia A. (2007) Competition between humic acid and carbonates for rare earth elements complexation. *Journal of Colloid and Interface Science* **305**, 25-31.
4. **Pourret O.**, Davranche M., Gruau G. et Dia A. (2007) Organic complexation of rare earth elements in natural waters: Evaluating model calculations from ultrafiltration data. *Geochimica et Cosmochimica Acta* **71**, 2718-2735.
5. **Pourret O.**, Dia A., Davranche M., Gruau G., Hénin O. et Angée M. (2007) Organo-colloidal control on major- and trace-element partitioning in shallow groundwaters: Confronting ultrafiltration and modelling. *Applied Geochemistry* **22**, 1568-1582.
6. **Pourret O.**, Davranche M., Gruau G. et Dia A. (2007) Rare earth elements complexation with humic acid. *Chemical Geology* **243**, 128-141.
7. Davranche M., **Pourret O.**, Gruau G., Dia A., Jin D. et Gaertner D. (2008) Competitive binding of REE to humic acid and manganese oxide: Impact of reaction kinetics on development of cerium anomaly and REE adsorption. *Chemical Geology* **247**, 154-170.
8. **Pourret O.**, Davranche M., Gruau G. et Dia A. (2008) New insights into cerium anomalies in organic-rich alkaline waters. *Chemical Geology* **251**, 120-127.
9. **Pourret O.** et Martinez R. E. (2009) Modeling lanthanide series binding sites on humic acid. *Journal of Colloid and Interface Science* **330**, 45-50.
10. **Pourret O.**, Gruau G., Dia A., Davranche M. et Molénat J. (2010) Colloidal control on the distribution of rare earth elements in shallow groundwater. *Aquatic Geochemistry* **16**, 31-59.
11. **Pourret O.**, Dia A., Gruau G., Davranche M. et Bouhnik Le-Coz M. (2012) Assessment on vanadium distribution in shallow groundwaters. *Chemical Geology* **294-295**, 89-102.
12. Voegelin A.R., Nägler T.F., Pettke T., Neubert N., Steinmann M., **Pourret O.** et Villa I.G. (2012) The impact of igneous bedrock weathering on the Mo isotopic composition of

- stream waters : Natural samples and laboratory experiments. *Geochimica and Cosmochimica Acta* **86**, 150-165.
13. Faucon M.P., Chipeng F., Verbruggen N., Mahy G., Colinet G., Shutcha M., **Pourret O.**, Meerts P. (2012) Copper tolerance and accumulation in two cuprophytes of South Central Africa: Crepidorhopalon perennis and C. tenuis (Linderniaceae). *Environmental and Experimental Botany* **84**, 11-16.
  14. Khalil A., Hanich L., Bannari A., Zouhri L., **Pourret O.**, et Hakkou R. (2013) Assessment of soil contamination around an abandoned mine in a semi-arid environment using geochemistry and geostatistics. *Journal of Geochemical Exploration* **125**, 117-129.
  15. **Pourret O.** et Davranche M. (2013) Rare earth element sorption onto hydrous manganese oxide: A modeling study. *Journal of Colloid and Interface Science* **395**, 18-23.
  16. Tuduri J., **Pourret O.**, Chauvet A., Barbanson L, Gaouzi A. et Ennaciri A. Supergene alteration of primary ore assemblage from the giant Imiter silver deposit (eastern Anti-Atlas, Morocco). *Economic Geology* **In review** (manuscrit SEG-D-10-00051R1).
  17. **Pourret O.**, Colinet G., Shutcha M., Mahy G., Meerts P., et Faucon M.P. Assessing the mobility of cobalt in soils from Katanga (Democratic Republic of Congo) by confronting speciation modeling and chemical extraction. *Geoderma* **In review** (manuscrit GEODER7497).
  18. Hoang L.V., Acha V., Bak A., Marion R., Coste C. et **Pourret O.**, Phenol oxidation in a semi industrial ozone pilot plant: the effect of some operating parameters. *Ozone: Science & Engineering* **In review** (manuscrit BOSE-2013-0008).
  19. Martinez R.E., **Pourret O.**, et Takahashi Y., Modeling of rare earth element sorption to the Gram positive Bacillus subtilis bacteria surface. *Journal of Colloid and Interface Science* **In review** (manuscrit JCIS-S-13-01151).
  20. **Pourret O.**, Steinmann M., Catrouillet C., et De Bardon De Segonzac C., Colloidal control on the distribution of major- and trace-elements and rare earth elements in stream water of the Malaval river (Massif Central, France). *Chemical Geology* **In Preparation**.
  21. Shutcha M., **Pourret O.**, Colinet G., Meerts P., Mahy G., et Faucon M.-P. (2012) Assessment on cobalt and copper speciation in metalliferous soils from Katanga (DR Congo): a tool to improve phytoremediation efficiency. *International Journal of Phytoremediation* **In Preparation**.
  22. Decrée S. et **Pourret O.**, Origin of heterogenite as illustrated by rare earth element fractionation. *Chemical Geology* **In Preparation**.
  23. Tuduri J., **Pourret O.**, Gouin J., Colin S., Gloaguen E., Potel S., Formation of gray monazite-(Eu) from paleozoic schists of the Armorican massif: Roles of host rock chemical composition and organic material. *Lithos* **In Preparation**.

24. Lange B., Faucon M.-P., Meerts P., Colinet G., Mahy G., et **Pourret O.** Prediction of edaphic factors influence upon the copper and cobalt accumulation in two metallophytes using copper and cobalt speciation in soils. *Plant and Soil In Preparation*.
25. **Pourret O.**, Lange B., Jitaru P., Meerts P., Mahy G., Faucon M.P., Transfer of rare earth elements from natural metalliferous (copper and cobalt rich) soils into plant shoot biomass of metallophytes from Katanga (Democratic Republic of Congo). *Plant and Soil In Preparation*.
26. **Pourret O.**, Tuduri J., Armand R., Bayon G., et Steinmann M., Rare earth elements as tracer of transfer – revisiting the biogeochemical continental cycle. *Journal of Geochemical Exploration In Preparation*.
27. **Pourret O.**, Steinmann M., Chaux L., Routier T., Bontemps S., Mobility of rare earth elements during igneous rocks weathering and associated stream water transport (Malaval catchment, Massif central, France). *Aquatic Geochemistry In Preparation*.
28. Armand R., Lange B., Faucon M.P, Colinet G., Shutcha M., Mahy G., **Pourret O.**, Assessment of soil metal distribution around Tenke-Fungurume mining (Democratic Republic of Congo) using geochemistry and geostatistics. *Journal of Geochemical Exploration In Preparation*.

## Autre article

1. **Pourret O.** (2009) Elements in the classroom. *Elements* 5, 195.

## Rapports

1. **Pourret O.** (2011) Optimisation des paramètres d'ozonation en phase liquide des polluants multiples de site pollué. Rapport d'avancement Phase 1, ADEME, 22p.
2. **Pourret O.**, Bak A., Hoang L.V., Acha V. (2011) Optimisation des paramètres d'ozonation en phase liquide des polluants multiples de site pollué. Rapport d'avancement Phase 2, ADEME, 61p.
3. **Pourret O.**, Trapy P.H., Hoang L.V., Acha V. (2012) Optimisation des paramètres d'ozonation en phase liquide des polluants multiples de site pollué. Rapport d'avancement Phase 3, ADEME, 64p.
4. **Pourret O.**, Hoang L.V., Trapy P.H., Duquennoy J., Acha V. (2013) Optimisation des paramètres d'ozonation en phase liquide des polluants multiples de site pollué. Rapport d'avancement Phase 4, ADEME, 32p.

## **Conférences internationales**

### **Communications invitées**

1. Faucon M.-P., Shutcha M., Colinet G., Meerts P., Mahy G., et **Pourret O.** (2012) Assessment on Cobalt and Copper speciation in metalliferous soils from Katanga (DR Congo): a tool to evaluate environmental risk and to improve phytoremediation efficiency. *Workshop Copper Flora*, 23 août 2012, ULB, Bruxelles.
2. Lange B., Faucon M.-P., Meerts P., Colinet G., Mahy G., et **Pourret O.** (2012) New insights into copper and cobalt concentrations among metallophyte from Katanga (DR Congo). *Workshop Copper Flora*, 23 août 2012, ULB, Bruxelles.
3. **Pourret O.**, Colinet G., Shutcha M., Meerts P., Mahy G., et Faucon M.-P. (2012) Cobalt and copper speciation in metalliferous soils from Katanga (DR Congo). *Workshop Copper Flora*, 23 août 2012, ULB, Bruxelles.

### **Communications orales**

1. Dia A., Morin E., **Pourret O.**, Gruau G., Davranche M., et Hénin O. (2005) Organo-colloidal control on trace element distribution in shallow groundwaters: fingerprinting by ultracentrifugal cells. *Goldschmidt Conference, Moscow, USA. Geochimica et Cosmochimica Acta* 69 (10): A185-A185.
2. Dia A., Pedrot M., Davranche M., **Pourret O.**, Petitjean P., Hénin O. et Le Coz-Bouhnik M. (2006) Unraveling the organo-colloidal control on trace element distribution in shallow groundwaters : an experimental contribution. *AGU Fall Meeting Conference, San Francisco, USA, Eos Trans. AGU, 87(52), Fall Meet. Suppl., Abstract B32B-08.*
3. Steinmann M., et **Pourret O.** (2009) The role of the colloidal pool for transport and fractionation of the rare earth elements in stream water. *7th Swiss Geoscience Meeting 20-21 November, Neufchâtel, Switzerland. p. 47.*
4. Voegelin A.R., Nägler T.F., Neubert N., Pettke T., Steinmann M., et **Pourret O.** (2011) Marine Mo isotope inventory: the role of igneous rock weathering. *Goldschmidt Conference 14-19 August 2011, Prague, Czech Republic. Mineralogical Magazine*, 75 (3), 2096.
5. Voegelin A. R., Nägler T. F., Neubert N., Heri A. R., Pettke T., Schlunegger F., Steinmann M., **Pourret O.** et Villa I.M. (2011) Molybdenum isotopes in river water: sources, fractionation processes and their importance for Mo cycling in the marine environment. *9th Swiss Geoscience Meeting 11-13 November, Zurich, Switzerland, p. 148.*
6. Acha V., Hoang L.V., Bak A., Marion R., et **Pourret O.** (2012) Phenol oxidation in a semi industrial ozone pilot plant: the effect of some operating parameters. *IOA-EA3G Conference & Exhibition, June 4-6, 2012, Toulouse, France, p. 271-278.*

## ***Communications par affichage***

1. Gruau G., Davranche M., **Pourret O.**, et Dia A. (2004) Impact of organic complexation on Ce(III) oxidation and REE adsorption onto Mn and Fe oxides. *Goldschmidt Conference*, Copenhagen, Denmark, Abstract 971. *Geochimica et Cosmochimica Acta* 68 (11): A375-A375.
2. **Pourret O.**, Gruau G., Davranche M., et Dia A. (2005) Organic speciation of rare earth elements in natural waters: comparing speciation models and ultrafiltration experiments. *Goldschmidt Conference, Moscow, USA, Geochimica et Cosmochimica Acta* 69 (10): A188-A188.
3. Davranche M., **Pourret O.**, Gruau G., et Dia A. (2006) Competition between organic matter and solid surface for cation sorption: Ce and rare earth element as Proxy. *AGU Fall Meeting Conference, San Francisco, USA, Eos Trans. AGU, 87(52), Fall Meet. Suppl., Abstract B33A-1148.*
4. **Pourret O.**, Davranche M., Gruau G., et Dia A. (2006) Modelling of rare earth elements complexation with humic acid. *AGU Fall Meeting Conference, San Francisco, USA, Eos Trans. AGU, 87(52), Fall Meet. Suppl., Abstract B33A-1150.*
5. Zouhri, L., **Pourret, O.**, Lutz, P., Groschaus, B., Laurent, E., Obry, F. et Ouattara, Y. (2009) Seasonal local recharge characterisation of the chalk aquifer, Beauvais experimental watershed (France). *Magmatism, Metamorphism and Associated Mineralization 3MA, Beni Mellal, Morocco.*
6. Bourges, M., Brès, M.-C., Carillo, M., Tuduri, J., **Pourret, O.** et Besnard, K. (2009) An example of hard rock aquifer concept for water prospection. *Magmatism, Metamorphism and Associated Mineralization 3MA, Beni Mellal, Morocco.*
7. Zouhri L., **Pourret O.**, Barrier P., Saj S., Deloges T. et Gielen A. (2009) The Beauvais experimental watershed (France): an outlook of the seasonal local recharge of the chalk aquifer. In Kovar P., Maca P., Redinova J. (eds.) 2009: *Water Policy 2009, Water as a Vulnerable and Exhaustible Resource. Proceedings of the Joint Conference of APLU and ICA, 23 – 26 June 2009, Prague, CULS Prague, Czech Republic.* p. 177.
8. **Pourret O.**, Marsac R., Davranche M. et Fauvain L. (2009) Rare earth elements fractionation modelling between manganese oxide and humic materials. *Goldschmidt Conference, Davos, Switzerland, Geochimica et Cosmochimica Acta* 73, A1048-A1048.
9. **Pourret O.** et Davranche M. (2010) Modeling rare earth elements adsorption onto manganese oxide using a surface complexation model. *IMA2010 - 20th General Meeting of the International Mineralogical Association 21-27 August, Budapest, Hungary. Mineralogica-Petrographica Absract Series, 6, 830.*

10. Acha V. et **Pourret O.** (2011) Development of biomimetic sensors for measuring trace-metal element concentrations. *43<sup>rd</sup> International Liege Colloquium on Ocean Dynamics 2-6 May, Liege, Belgium.*
11. Faucon M.P., Verbruggen N., Jitaru P., **Pourret O.**, Colinet G., Chipeng G., Shutcha M., Mahy G., et Meerts P. (2011) Cu and Co accumulation in metallophytes from Cu/Co soils in Katanga (D.R. Congo). *VII Serpentine Ecology Conference 12-16 June 2011, Coimbra, Portugal. p. 104.*
12. Bonhoure J. et **Pourret O.** (2011) Rare earth elements as proxies of unconformity uranium deposit mineralized fluids. *Goldschmidt Conference 14-19 August 2011, Prague, Czech Republic. Mineralogical Magazine, 75 (3), 550.*
13. Catrouillet C., De Bardon De Segonzac C., **Pourret O.** et Steinmann M. (2011) Colloidal control on the distribution of major and trace elements in a small mountain stream (Malaval catchment, Massif Central, France). *Goldschmidt Conference 14-19 August 2011, Prague, Czech Republic. Mineralogical Magazine, 75 (3), 633.*
14. Chaux L., Routier T., **Pourret O.**, Steinmann M., et Bontemps S. (2011) Mobility of rare earth elements during igneous rocks weathering and associated stream water transport (Malaval catchment, Massif central, France). *Goldschmidt Conference 14-19 August 2011, Prague, Czech Republic. Mineralogical Magazine, 75 (3), 647.*
15. Faucon M.P., Colinet G., Jitaru P., Verbruggen N., Shutcha M., Mahy G., Meerts P. et **Pourret O.** (2011) Relation between cobalt fractionation and its accumulation in metallophytes from South of Central Africa. *Goldschmidt Conference 14-19 August 2011, Prague, Czech Republic. Mineralogical Magazine, 75 (3), 832.*
16. Tuduri J., **Pourret O.**, Chauvet A., Barbanson L., Gaouzi A. et Ennaciri A. (2011) Rare earth elements as proxies of supergene alteration processes from the giant Imiter silver deposit (Morocco). In: Barra, F., Reich, M., Campos, E., and Tornos, F., eds., *Let's Talk ore deposits, Proceeding of the eleventh biennial SGA meeting, 2: Antofagasta, Ediciones Universidad Católica des Norte, Antofagasta, Chile, p. 826-828.*
17. Voegelin A.R., Nägler T.F., Pettke T., Neubert N., Steinmann M., **Pourret O.** et Villa I.G. (2011) The impact of igneous bedrock weathering on the Mo isotopic composition of stream waters : Natural samples and laboratory experiments. Abstract PP13C-1840 presented at 2011 Fall Meeting, AGU, San Francisco, Calif., 5-9 Dec.
18. **Pourret O.**, Tuduri J., Armand R., Bayon G., et Steinmann M. (2012) Reassessment of the rare earth elements external cycle in french watersheds - a high potential resource for the future. *Goldschmidt Conference 24-29 June 2012, Montréal, Canada.*
19. Shutcha M., **Pourret O.**, Colinet G., Meerts P., Mahy G., et Faucon M.-P. (2012) Assessment on Cobalt and Copper speciation in metalliferous soils from Katanga (DR Congo): a tool to improve phytoremediation efficiency. *9th IPS Conference on Phytotechnologies, September 11-14, Hasselt 2012, Belgium.*

20. Tuduri J., **Pourret O.** Boulvais P., Chauvet A., Barbanson L., Gaouzi A. (2012) A reassessment of fluid-mineral relations in the world-class Imiter silver deposit (Anti-Atlas, Morocco). *SEG Conference, 23-26 September 2012, Lima, Perou.*

## **Conférences nationales**

### **Communications orales**

1. **Pourret O.**, Davranche M., et Gruau G. (2004) Impact of organic complexation on cerium oxidation and REE adsorption onto Fe and Mn oxides: experimental evidence. *Réunion des Sciences de la Terre (RST Conference), Strasbourg, France, Abstract RSTGV-A-00028.*
2. Tuduri J., **Pourret O.**, Chauvet A., Barbanson L., Gaouzi A., et Ennaciri A. (2010) Supergene silver enrichment from the Imiter deposit (Easter Anti-Atlas, Morocco). *Réunion des Sciences de la Terre (RST Conference), Bordeaux, France. 25-29 Octobre. p. 285.*
3. Josso P., Dupouy M., Dutour E., du Peloux A., Combaud A., Laurent-Charvet S. et **Pourret O.** (2011) Impact des facteurs géologiques sur le développement du réseau hydrographique en Montagne Noire. *SIG2011, conférence francophone ESRI, 5-6 Octobre 2011, Versailles, France.*
4. Poujol M., Ballouard C., Bonhoure J., Boulvais P., Cathelineau M., Cuney M., Gapais D., Lotout C., **Pourret O.**, Tartèse R. (2012) Caractérisation géochimique et géochronologique du gisement uranifère de Pen Ar Ran (Massif Armoricain) et de son environnement: du rôle respectif du granite de Guérande et des formations métamorphiques encaissantes dans la genèse de la minéralisation. *Réunion de la Société Géologique de France « Journées Uranium », 26-27 novembre 2012, Orsay, France.*

### **Communications par affichage**

1. Dia A., **Pourret O.**, Gruau G., Davranche M., et Hénin O. (2006) De la difficulté de contraindre le rôle des colloïdes organiques sur la distribution des éléments traces dans les eaux ... "Réseau Matières Organiques", *Carqueiranne, France.*
2. **Pourret O.**, Gruau G., Dia A., et Davranche M. (2008) Systematic, topography-related variability in the geochemistry of rare earth elements in shallow groundwaters. *Réunion des Sciences de la Terre (RST Conference), Nancy, France.*
3. Martinez R.E., et **Pourret O.** (2008) Modelling lanthanide binding sites on humic acid using linear programming model. *Réunion des Sciences de la Terre (RST Conference), Nancy, France.*
4. Ouattara Y., Obry F., Zouhri L., Lutz P. et **Pourret O.** (2010) Identification des caractéristiques physiques de l'aquifère de la craie: Approches géophysiques et

hydrogéologiques. *Réunion des Sciences de la Terre (RST Conference), Bordeaux, France. 25-29 Octobre. p. 225.*

5. Josso P., Dupouy M., Dutour E., Combaud A., Laurent-Charvet S. et **Pourret O.** (2011) Automatisation de l'analyse de corrélation entre un réseau hydrographique et les anisotropies linéaires. *SIG2011, conférence francophone ESRI, 5-6 Octobre 2011, Versailles, France.*
6. Hoang L.V., Trapy P.H., Acha V., Coste C., Marion R., et **Pourret O.** (2012) Traitement par ozone des lixiviats de décharge de sites pollués dans un pilote semi industriel. *20èmes Journées Information Eau, 25-27 Septembre 2012, Poitiers, France.*

## **Séminaires invités**

1. **Pourret O.** (2007) Géochimie des Terres Rares dans les eaux naturelles: modélisation du rôle de la matière organique. *16 janvier 2007, Hydrosciences Montpellier, France.*
2. **Pourret O.** (2007) Rare Earth Elements geochemistry in natural waters: experimental study and modelling of the role of organic matter. *1<sup>er</sup> mars 2007, Center for Ecology and Hydrology Lancaster et University of Lancaster, Royaume Uni.*
3. **Pourret O.** (2007) Modélisation de l'impact de la matière organique sur le comportement des terres rares en solution. *7 mars 2007, Institut de Physique du Globe Paris et Université Paris 7, France.*
4. **Pourret O.** (2007) Modélisation de la spéciation des terres rares aux interfaces eaux-roches: vision actuelle et développements futurs. *19 mars 2007, EOST Strasbourg, France.*
5. **Pourret O.** (2008) Rôle des colloïdes sur la composition chimique des eaux naturelles. *19 mars 2008, Séminaire interne Institut Polytechnique LaSalle Beauvais, France*
6. **Pourret O.** (2008) Rôle de la topographie sur le transfert des terres rares dans un aquifère de surface vu par la géochimie : un autre aspect de l'érosion... *28 mars 2008, 5<sup>èmes</sup> Journées de l'Environnement. Institut Polytechnique LaSalle Beauvais, France.*
7. **Pourret O.** (2008) Mobilité des métaux dans l'environnement. *28 novembre 2008, Journée Valorisation de la Recherche. Institut Polytechnique LaSalle Beauvais, France.*
8. **Pourret O.** (2010) Modélisation de la spéciation des terres rares aux interfaces eaux-roches et application à des études de sites. *27 janvier 2010, CEA-DAM, Bruyère-le-Châtel, France.*
9. **Pourret O.** (2011) Traitement des polluants organiques dans les lixiviats et terres brutes par ozonation. *29 septembre 2011, Journée dépollution des sols. Agence Régionale Innovation Picardie, Amiens, France.*

10. **Pourret O.** (2012) Traitement d'eaux polluées par procédés d'ozonation : Tests sur pilote semi-industriel. *1<sup>er</sup> décembre 2012, Table ronde Procédés d'oxydation avancée. Pollutec, Paris, France.*
11. **Pourret O.** (2012) Le cycle externe des terres rares revisité, vers de nouvelles ressources? *22 mars 2012, SEG Student Chapter LaSalle France, Beauvais, France.*
12. **Pourret O.** (2012) Reassessment of the rare earth elements external cycle in french watersheds. *16 juillet 2012, University of Freiburg, Allemagne.*
13. Acha V., Hoang L.V., Trapy P.H. et **Pourret O.** (2012) Traitement par ozonation des lixiviat de décharges - avancée des travaux de R&D. *19 septembre 2012, Journée dépollution des sites et sols. Agence Régionale Innovation Picardie, Amiens, France.*
14. **Pourret O.** (2013) Adsorption de terres rares sur oxydes de manganèse hydrogénés. *16 avril 2013, Ifremer, Brest, France.*

## Contrats publics et privés

### Programmes de recherche financés

1. 2009-2012 Programme Hubert-Curien – Volubilis: Les ressources en eau dans la région de Marrakech. Prospection, caractérisation, sources de pollution, périmètre de protection: apport de l'outil géophysique.

Porteur : Roger Guérin (UMR 7619 Sisyphe)

Partenaires : Lahcen Zouhri (correspondant LaSalle Beauvais), Lahoucine Hanich (Université Cadi Ayyad, Marrakech – Maroc)

Collaborateur : Olivier Pourret (géochimie)

2. 2010 Programme ioStipend : Caractérisation géochimique de l'altération de quatre différentes lithologies et transfert des éléments traces métalliques vers le réseau hydrographique - secteur de Malaval (Massif Central, France).

Porteur : Olivier Pourret

Partenaire : Marc Steinmann (UMR 6249 Chrono-Environnement - Université de Franche-Comté – Besançon)

3. 2011 Bonus Qualité Recherche – Université de Reims Champagne-Ardenne - Dossier Partenariat : Etude du comportement des éléments traces métalliques dans les sols d'un site fortement anthropisé : approche expérimentale et intercomparaison de modèles de spéciation géochimiques.

Porteur : Marie Ponthieu (GEGENAA – URCA)

Partenaire : Olivier Pourret (correspondant LaSalle Beauvais)

4. 2011-2014 Programme ANR Ecotech – Analyse Systémique des Terres Rares : Flux et Stocks.

Porteur : Johann Tuduri (brgm)

Partenaire : Olivier Pourret (correspondant LaSalle Beauvais)

5. 2012 Filipino-French Scientific Cooperation Program (FFSC): Phytogeography and biogeochemistry of flora from metalliferous soils in the Philippines: Implications in the phytoremediation and phytostabilization of soils contaminated by trace metals.

Porteur : Michel-Pierre Faucon (LaSalle Beauvais)

Collaborateur : Olivier Pourret (biogéochimie)

6. 2012-13 Projets de recherche SFR Condorcet : Caractérisation physico-chimique des sols d'un site fortement contaminé en éléments traces métalliques (CASICO).

Porteur : Béatrice Marin (GEGENAA – URCA)

Partenaire : Olivier Pourret (correspondant LaSalle Beauvais)

7. 2012-2013 NEEDS Projet Fédérateur « Ressources » : Caractérisation géochimique et géochronologique du gisement uranifère de Pen Ar Ran (Massif Armoricain) et de son environnement: du rôle respectif du granite de Guérande et des formations métamorphiques encaissantes dans la genèse de la minéralisation.

Porteur : Marc Poujol (Université de Rennes 1)

Partenaire : Jessica Bonhure (correspondant LaSalle Beauvais)

Collaborateur expert : Olivier Pourret (modélisation spéciation chimique U)

8. 2013 Projets de recherche SFR Condorcet : Spéciation des éléments traces métalliques dans les sols et leur accumulation dans la plante (SOLMETPLANT).

Porteur : Michel-Pierre Faucon (LaSalle Beauvais)

Partenaires : Benjamin Cancès (GEGENAA-URCA), Gilles Colinet (AgroBioTech Gembloix)

Collaborateur : Olivier Pourret (biogéochimie)

## **Programmes de recherche & développement financés**

1. 2010-2013 Programme Région Picardie/FEDER : Identification des critères physico-chimiques et morphologiques pour le choix des sables utilisés en fonderie automobile (ECOSABLE).

Porteur : Montupet SA

Partenaires: Sébastien Laurent-Charvet (LaSalle Beauvais), Patrick Goblet (Armines, Paris)

Collaborateur : Olivier Pourret (géochimie)

2. 2010-2013 Programme Acquisition en Connaissances Nouvelles ADEME : Optimisation des paramètres d'ozonation en phase liquide des polluants multiples de site pollué (OPOPOP).

Porteur : Olivier Pourret (LaSalle Beauvais)

## **Prestations industrielles**

1. **Pourret O.** (2007) Analyses minéralogiques sur fractions argileuses par diffractométrie des rayons X (lots LGV SEA et LYON TURIN CA) – Groupe J.
2. Laurent-Charvet S., **Pourret O.** et Gagnaison C. (2008) Analyses minéralogiques, caractérisations d'échantillons de sables – SIFRACO.
3. **Pourret O.** (2008) Analyses minéralogiques sur fractions argileuses par diffractométrie des rayons X - SPL.
4. **Pourret O.** (2008) Analyses minéralogiques sur fractions argileuses par diffractométrie des rayons X – Groupe J –Sous-traitance RFF.
5. **Pourret O.** (2008) Analyses minéralogiques sur fractions argileuses par diffractométrie des rayons X - UNISOL.
6. Tuduri J. et **Pourret O.** (2008) Analyses minéralogiques par diffractométrie des rayons X et par microscopie électronique à balayage – Imerys.
7. **Pourret O.** (2009) Analyses minéralogiques sur fractions argileuses par diffractométrie des rayons X - UNISOL.
8. **Pourret O.** (2009) Analyses minéralogiques sur roches totales par diffractométrie des rayons X – Silverlake Resources.
9. **Pourret O.** (2009) Analyses minéralogiques sur roches totales par diffractométrie des rayons X – Cominor CI – La Mancha.
10. Potel S. et **Pourret O.** (2009) Analyses minéralogiques sur roches totales et sur fractions argileuses par diffractométrie des rayons X – Toreador Energy.
11. Potel S. et **Pourret O.** (2010) Analyses minéralogiques sur roches totales et sur fractions argileuses par diffractométrie des rayons X – Toreador Energy.
12. **Pourret O.** (2013) Analyses géochimiques sur roches totales – Safege.

## **Collaborations**

### **Internes**

1. Michel-Pierre Faucon : écodynamique des éléments dans système sol-plante.
2. Petru Jitaru, Victor Acha et Le Vinh Hoang : écodynamique des éléments en solution.
3. Romain Armand et Claudia Cherubini: mobilité métaux sol, réseau hydrographique.
4. Sébastien Potel : caractérisation argiles.
5. Jessica Bonhoure : mobilité métaux roche.

### **Nationales**

1. UMR 6118 Géosciences Rennes – Université de Rennes 1 – Rennes, Mélanie Davranche, Aline Dia, Gérard Gruau: Modélisation du comportement des terres rares en solution ; Marc Poujol, Philippe Boulvais : Modélisation du comportement de l'uranium en solution.
2. UMR 6249 Chrono-Environnement - Université de Franche-Comté – Besançon Marc Steinmann: Transport et fractionnement des terres rares en solution.
3. ENAG-BRGM – Johann Tuduri, Eric Gloaguen: Fractionnement des terres rares dans les environnements géologiques de surface.
4. GEGENAA, Université de Reims Champagne-Ardenne : Beatrice Marin, Marie Ponthieu, Benjamin Cancès : Modélisation du fractionnement des éléments traces métalliques dans des environnements contaminés.

### **Internationales**

1. Institut für Geowissenschaften - Mineralogie, Geochemie – Freiburg University, Allemagne, Raul E. Martinez: Modélisation du comportement des éléments traces métalliques en solution.
2. Unité Système Sol Eau – Université de Liège, Gembloux AgroBiotech, Belgique, Gilles Colinet : Modélisation du fractionnement des éléments traces métalliques dans les sols.
3. Hiroshima University, Japon, Yoshio Takahashi : Modélisation du comportement des terres rares en solution.
4. Musée Royal de l'Afrique Centrale, Tervuren, Belgique, Sophie Decrée : Fractionnement des terres rares.

## **Responsabilités collectives et administratives**

Secrétaire (2001) et Président (2004) de Géocontact: association des étudiants, enseignants et chercheurs en sciences de la terre de l'Université de Rennes 1.

Membre élu (représentant doctorant) au Conseil de l'Ecole Doctorale Sciences de la Matière, Université de Rennes 1 (2005).

Membre nommé au Comité Scientifique de l'Institut Polytechnique LaSalle Beauvais (depuis 2007).

Responsable (fondateur) de l'Unité de Recherche HydrISE (depuis 2008).

Membre nommé au Conseil Scientifique de l'Institut Polytechnique LaSalle Beauvais (depuis 2008).

Délégué du personnel élu (suppléant de 2010 à 2013) et titulaire (depuis 2013) de l'Institut Polytechnique LaSalle Beauvais.

Membre nommé du Comité de Direction et du Conseil Scientifique de la SFR Condorcet (depuis 2012).

Membre de l'Editorial Board de Journal of Chemistry (depuis 2012).

Co-organisateur session «Rare Earths and Rare Metal Mineralization» à la Goldschmidt Conference 2013 (Florence, Italie).

## **Appartenance à des sociétés savantes**

1. American Chemical Society.
2. American Geophysical Union.
3. European Association for Geochemistry.
4. Geochemical Society.
5. Society of Economic Geologists (membre **Fellow** depuis 2011).

## **Expertises**

**Evaluations d'articles pour des revues de rang A:** Geochimica et Cosmochimica Acta (13), Journal of Colloid and Interface Science (9), Applied Geochemistry (8), Geochemical Journal (3), Naturwissenschaften (2), Analytica Chimica Acta (2), Colloids and Surfaces A (2), Chemical Geology (2), International Journal of Environmental Analytical Chemistry (1), Natural Resources Research (1), Environmental Earth Sciences (1), Earth Science Reviews (1), Gondwana Research (1), Science of the Total Environment (1).

**Evaluations de projets** pour American Chemical Society – Petroleum Research Fund, Fond National Suisse, Commission Européenne.

**Expert pour Prix Roberval** catégorie Enseignement Supérieur.

## Activités et responsabilités d'enseignement

Mon activité d'enseignement consiste en des missions variées tant sur leur contenu (de la géologie classique dont de la géologie de terrain à des enseignements plus pointus en géochimie de surface) que sur le niveau des étudiants ciblés (de la première année de Licence aux Masters 2). Cette expérience abordée en thèse (via un contrat d'allocataire moniteur) suivi par un demi-poste d'ATER se poursuit depuis septembre 2007 à LaSalle Beauvais et mon recrutement en tant qu'enseignant-chercheur en géochimie.

### **Moniteur (octobre 2003 à septembre 2006)**

| 2003-2004 : |                                     |      |               |
|-------------|-------------------------------------|------|---------------|
| Formation   | Matière                             | Type | Charge réelle |
| MSTU-BGG    | TGFA Terrain Géol. Fond. et Ap. ... | TD   | 12            |
| MSTU-BGG    | TPT Terrain Pétro-Tecto             | TD   | 24            |
| DEUG-SV2    | GEO2 Géologie 2 (UE14G)             | TP   | 24            |
| MAIT-BPE    | SCET Sciences de l'environnement... | TD   | 12            |

| 2004-2005 : |   |      |               |
|-------------|---|------|---------------|
| Formation   | Matière                                     | Type | Charge réelle |
| L3-ST       | 1-29 Levée d'une carte géologique           | TD   | 48            |
| M1-ENV      | 1FHT Fonctionnement et hydrochimie des sols | TD   | 6             |
| M1-ENV      | 1HST Hydrol. De surf. et systèmes aquifères | TD   | 6             |
| MSTU-BGG    | TPT Terrain Pétro-Tecto                     | TD   | 6             |

| 2005-2006 : |   |      |               |
|-------------|---|------|---------------|
| Formation   | Matière                                     | Type | Charge réelle |
| L3-ST       | 1-27 Atmosphère et hydroosphère             | TP   | 4             |
| M1-ENV      | 1FHS Fonctionnement et hydrochimie de sols  | TD   | 8             |
| M1-ENV      | 1FHT Fonctionnement et hydrochimie de sols  | TD   | 6             |
| M1-ENV      | 1HSA Hydrol. De surf. et systèmes aquifères | TP   | 18            |
| M1-ENV      | 1HST Hydrol. De surf. et systèmes aquifères | TD   | 6             |
| M1-ST       | 2CBG SPM Cycle hydrobiogéochimique          | TP   | 6             |
| L2-SVT      | G30 Matériaux Géologiques                   | TP   | 38            |

### **Attaché Temporaire d'Enseignement et de Recherche à l'Université de Rennes 1 (septembre 2006 à août 2007)**

| 2006-2007 |   |      |               |
|-----------|---|------|---------------|
| Formation | Matière                                     | Type | Charge réelle |
| L3-ST     | 235T Climats-sols-érosion – terrain         | TD   | 6             |
| M1-ENV    | 1FHS Fonctionnement et hydrochimie de sols  | TD   | 10            |
| M1-ENV    | 1FHT Fonctionnement et hydrochimie de sols  | TD   | 12            |
| M1-ENV    | 1HSA Hydrol. De surf. et systèmes aquifères | TD   | 8             |
| M1-ENV    | 2TER Terrain                                | TD   | 18            |
| M1-ST     | 2CBG SPM Cycle hydrobiogéochimique          | CM   | 4             |
| M1-ST     | 2CBG SPM Cycle hydrobiogéochimique          | TD   | 12            |
| M1-ST     | 2CBG SPM Cycle hydrobiogéochimique          | TP   | 18            |
| M1-GIBV   | IPE (SPM) de l'individu à la population     | TD   | 9             |
| M2-GIBV   | UE - Approche intégrée de terrain           | TD   | 6             |

## **Enseignant-chercheur à l’Institut Polytechnique LaSalle Beauvais (depuis septembre 2007)**

Responsable de modules d’enseignement de la formation Ingénieur en Géologie: Cristallochimie puis Minéralogie (L2), Bibliographie (L2), Géochimie 2 puis Mobilité des éléments (L3), Hydrochimie (M1), Eau et déchets puis Sites et Sols Pollués (M2) et Environnement industriel (M2).

Responsable du parcours fléché (M1) Aménagement et environnement de la formation Ingénieur en Géologie depuis septembre 2011.

Organisation et gestion d’intervention de professionnels extérieurs à LaSalle Beauvais (ADEME, Eurovia, veolia, brgm...).

### Missions développement échanges internationaux

- Mars 2009 Université du Québec à Chicoutimi et Université Laval, Canada.
- Avril 2009 Université Caddi Ayyad, Marrakech, Maroc.

Responsable métiers “Eau et environnement industriel”, relation avec le secteur professionnel « sites et sols pollués » et « environnement minier » - encadrement et suivi de stages en entreprise technicien et ingénieur.

### Missions relations entreprises

- Février 2009 PDAC Toronto (Canada) ;
- Décembre 2009 Pollutec Paris, représentant LaSalle Beauvais sur stand Région Picardie ;
- Mars 2010 PDAC Toronto (Canada), représentant LaSalle Beauvais sur stand UBI France ;
- Décembre 2010 Pollutec Lyon, représentant LaSalle Beauvais sur stand Région Picardie ;
- Décembre 2011 Pollutec Paris, représentant LaSalle Beauvais sur stand Région Picardie ;
- Novembre 2012 Pollutec Lyon, représentant LaSalle Beauvais sur stand Région Picardie.

### Recrutement

-Salon Etudiants Rennes (janvier 2008, 2009, 2010 & 2011), salon Etudiants Amiens (2012), entretiens de motivation.

Academic advisor student chapter SEG depuis 2011.

| 2007-2008 |  |      |               |  |
|-----------|--|------|---------------|--|
| Formation | Matière                                  | Type | Charge réelle |  |
| L1        | Excursion Terrain Bretagne               | TP   | 40            |  |
| L2        | Cristallochimie                          | CM   | 12            |  |
| L2        | Cristallochimie                          | TD   | 24            |  |
| L2        | Géodynamique interne                     | CM   | 24            |  |
| L2        | Ecole Terrain en cartographie            | TP   | 24            |  |
| L2        | Ecole Terrain en domaine magmatique      | TP   | 110           |  |
| L3        | Initiation aux techniques de laboratoire | TP   | 8             |  |
| M1        | Hydrochimie                              | CM   | 16            |  |
| M1        | Hydrochimie – Modélisation               | TP   | 8             |  |
| M1        | Metallogénie                             | CM   | 4             |  |
| M1        | Ecole Terrain Hydrogéologie              | TP   | 40            |  |

| <b>2008-2009</b> |  |      |               |
|------------------|--|------|---------------|
| Formation        | Matière                                  | Type | Charge réelle |
| L1               | Excursion Terrain Bretagne               | TP   | 40            |
| L2               | Cristallochimie                          | CM   | 10            |
| L2               | Cristallochimie                          | TD   | 24            |
| L2               | Bibliographie                            | CM   | 4             |
| L2               | Bibliographie                            | TD   | 6             |
| L2               | Ecole Terrain en cartographie            | TP   | 24            |
| L2               | Ecole Terrain en domaine magmatique      | TP   | 104           |
| L3 – Prepa       | Géologie générale                        | CM   | 4             |
| L3 - Prepa       | Petrographie                             | CM   | 4             |
| L3 - Tech        | Pollution-Dépollution                    | TD   | 16            |
| L3               | Initiation aux techniques de laboratoire | TP   | 6             |
| L3               | Géochimie 2                              | CM   | 24            |
| L3               | Géochimie 2                              | TD   | 24            |
| M1               | Hydrochimie                              | CM   | 16            |
| M1               | Hydrochimie – Modélisation               | TP   | 8             |
| M1               | Metallogénie                             | CM   | 2             |
| M1               | Ecole Terrain Hydrogéologie              | TD   | 40            |
| M2               | Environnement Industriel                 | TD   | 4             |
| M2               | Eau et Déchet                            | CM   | 6             |
| M2               | Transport de colloïdes - Modélisation    | CM   | 6             |

| <b>2009-2010</b> |  |      |               |
|------------------|--|------|---------------|
| Formation        | Matière                                  | Type | Charge réelle |
| L1               | Excursion Terrain Bretagne               | TP   | 40            |
| L2               | Cristallochimie                          | CM   | 10            |
| L2               | Cristallochimie                          | TD   | 24            |
| L2               | Bibliographie                            | CM   | 2             |
| L2               | Bibliographie                            | TD   | 12            |
| L2               | Ecole Terrain en cartographie            | TP   | 24            |
| L2               | Ecole Terrain en domaine magmatique      | TP   | 104           |
| L3 - Prepa       | Géologie générale                        | CM   | 6             |
| L3 - Tech        | Hydrogéologie appliquée                  | TD   | 16            |
| L3               | Initiation aux techniques de laboratoire | TP   | 4             |
| L3               | Géochimie 2                              | CM   | 24            |
| L3               | Géochimie 2                              | TD   | 36            |
| M1               | Hydrochimie                              | CM   | 16            |
| M1               | Hydrochimie – Modélisation               | TP   | 8             |
| M1               | Metallogénie                             | CM   | 2             |
| M2               | Transport de colloïdes - Modélisation    | CM   | 6             |
| M2               | Environnement Industriel                 | CM   | 4             |

| <b>2010-2011</b> |                                       |      |               |
|------------------|---------------------------------------|------|---------------|
| Formation        | Matière                               | Type | Charge réelle |
| L1               | Excursion Terrain Bretagne            | TP   | 40            |
| L1 - Tech        | Géologie de la France                 | CM   | 4             |
| L2               | Cristallochimie                       | CM   | 10            |
| L2               | Cristallochimie                       | TD   | 24            |
| L2               | Géochimie 1                           | CM   | 2             |
| L2               | Géochimie 1                           | TD   | 6             |
| L2               | Bibliographie                         | CM   | 2             |
| L2               | Bibliographie                         | TD   | 12            |
| L2               | Ecole Terrain en cartographie         | TP   | 24            |
| L2               | Ecole Terrain en domaine magmatique   | TP   | 104           |
| L3 – Prepa       | Géologie générale                     | CM   | 4             |
| L3 – Tech        | Hydrogéologie appliquée               | TD   | 6             |
| L3               | Géochimie 2                           | CM   | 16            |
| L3               | Géochimie 2                           | TD   | 24            |
| M1               | Hydrochimie                           | CM   | 16            |
| M1               | Hydrochimie – Modélisation            | TP   | 8             |
| M1               | Metallogénie                          | CM   | 2             |
| M2               | Transport de colloïdes - Modélisation | CM   | 6             |
| M2               | Eau et Déchets                        | CM   | 12            |

| <b>2011-2012</b> |                                       |      |               |
|------------------|---------------------------------------|------|---------------|
| Formation        | Matière                               | Type | Charge réelle |
| L1               | Excursion Terrain Bretagne            | TP   | 40            |
| L1 - Tech        | Géologie de la France                 | CM   | 4             |
| L1 - Tech        | Principes de datations - Isotopie     | CM   | 4             |
| L2               | Minéralogie                           | CM   | 10            |
| L2               | Minéralogie                           | TD   | 18            |
| L2               | Ecole Terrain en cartographie         | TP   | 24            |
| L2               | Ecole Terrain en domaine magmatique   | TP   | 104           |
| L2 - Tech        | Géochimie environnementale            | CM   | 12            |
| L3 - Prepa       | Géologie générale                     | CM   | 4             |
| L3               | Géochimie 2                           | CM   | 16            |
| L3               | Géochimie 2                           | TD   | 24            |
| M1               | Hydrochimie                           | CM   | 16            |
| M1               | Hydrochimie – Modélisation            | TP   | 8             |
| M2               | Transport de colloïdes - Modélisation | CM   | 6             |
| M2               | Sites et sols pollués                 | CM   | 6             |

| <b>2012-2013</b> |                                     |      |               |
|------------------|-------------------------------------|------|---------------|
| Formation        | Matière                             | Type | Charge réelle |
| L1               | Excursion Terrain Bretagne          | TP   | 40            |
| L2               | Minéralogie                         | CM   | 10            |
| L2               | Minéralogie                         | TD   | 18            |
| L2               | Ecole Terrain en cartographie       | TP   | 24            |
| L2               | Ecole Terrain en domaine magmatique | TP   | 104           |
| L2 - Tech        | Géochimie environnementale          | CM   | 12            |
| L3 - Prepa       | Géologie générale                   | CM   | 4             |
| L3               | Géochimie - Mobilité des éléments   | CM   | 6             |
| L3               | Géochimie – Mobilité des éléments   | TD   | 18            |
| M1               | Hydrochimie                         | CM   | 16            |
| M1               | Hydrochimie – Modélisation          | TP   | 8             |
| M2               | Environnement Industriel            | CM   | 6             |
| M2               | Sites et sols pollués               | CM   | 6             |

## **Mobilité Erasmus Enseignant**

Novembre 2012 Université de Liège, Gembloux AgroBioTech, Belgique.

## **Jury de mémoire de fin d'étude Ingénieur LaSalle Beauvais**

2007-08

Rapporteur interne : 7 dont 5 Président du Jury

2008-09

Rapporteur interne : 13 dont 7 Président du Jury

2009-10

Rapporteur interne : 13 dont 5 Président du Jury

2010-11

Rapporteur interne : 6 dont 3 Président du Jury

2011-12

Rapporteur interne : 9 dont 5 Président de Jury

**Jury de mémoire de master 2**

2008-09

Rapporteur externe (Université de Franche Comté) : 1

2010-11

Rapporteur externe (Université de Lille 1) : 1

## **Encadrement d'étudiants, doctorants et post-doctorants**

### **Doctorant à l'Université de Rennes 1 (2003 à 2006)**

1. Lucille Gouriou (Licence 3, Université de Rennes 1). Mai 2005 - Juin 2005: Validation de cellules d'ultrafiltration pour la caractérisation de la matière organique dissoute.
2. Dominique Gaertner (Master 1, ETH Zurich, Suisse). Octobre 2005 – Mars 2006: Compétition entre acides humiques et oxydes de manganèse vis à vis de la complexation/ adsorption des terres rares (co-encadrement Mélanie Davranche).
3. Dan Jin (Master 1, Université de Rennes 1). Avril 2006 - Juin 2006: Etude de la complexation compétitive des terres rares à la surface de matière organique et d'oxydes de manganèse (co-encadrement Mélanie Davranche).

### **ATER à l'Université de Rennes 1 (2006-2007)**

1. Jennifer Ponte (Licence 3, Ecole Centrale de Nantes). Avril 2007- Juillet 2007: Etude de la zétamétrie - Prise en main et élaboration d'un guide de fonctionnement de l'appareil Zetaphoremeter IV (co-encadrement Xavier Châtellier).

### **Enseignant-chercheur à l'Institut Polytechnique LaSalle Beauvais (depuis 2007)**

#### **Etudiants en licence 3 (projets d'initiation à la recherche)**

1. Marion Bourgès, Marie-Charlotte Brès et Mélanie Carillo (Institut Polytechnique LaSalle Beauvais). Septembre 2007 – Juin 2008: Les paléoaltérites: notion d'aquifère de socle - application à la prospection en eau (Lozères, France) (co-encadrement Johann Tuduri).
2. Thomas Deloges et Antoine Gielen (Institut Polytechnique LaSalle Beauvais). Septembre 2007 – Juin 2008: Bilan géologique et hydrogéologique de la zone de Bonneuil-en-Valois (Oise).
3. Alexandre Kinsman et Farah Nouari (Institut Polytechnique LaSalle Beauvais). Septembre 2007 – Juin 2008: Hydrogéologie de la nappe des Rocailles (Haute- Savoie, France).
4. François Grobel et Julien Trinel (Institut Polytechnique LaSalle Beauvais). Septembre 2007 – Juin 2008: Hydrogéologie de la nappe de Fillinge (Haute-Savoie, France).
5. François-André Duboin et Pierre-Alban Maistre (Institut Polytechnique LaSalle Beauvais). Septembre 2007 – Juin 2008: Hydrogéologie de la nappe du Vidourle (Gard, France).

6. Pierre Le Barbanchon et Pierre Revellin-Falcoz (Institut Polytechnique LaSalle Beauvais). Septembre 2008 – Juin 2009: Etude géochimique des craies sénoniennes de la région de Beauvais (Picardie) : approche minéralogique.
7. Florian Obry et Yaya Ouattara (Institut Polytechnique LaSalle Beauvais). Septembre 2008 – Juin 2009: Caractérisation géophysique de l'aquifère de la craie. Transect Le Gros Chêne - Le Thérain (méthodes électriques) (co-encadrement Lahcen Zouhri et Pascal Lutz).
8. Benjamin Groschaus et Elodie Laurent (Institut Polytechnique LaSalle Beauvais). Septembre 2008 – Juin 2009: Suivi hydrologique de la nappe de la Craie sur le site experimental du campus LaSalle Beauvais (co-encadrement Lahcen Zouhri).
9. Fanny Brulfert, Aurélie Fisne et Aladine Navarro (Institut Polytechnique LaSalle Beauvais). Janvier – Juin 2009: Caractérisation géochimique et pétrographique de roches magmatiques d'origines différentes : Exemple du Tianshan (NW Chine, Asie Centrale) (co-encadrement Sébastien Laurent-Charvet).
10. Thomas Routier et Ludovic Chaux (Institut Polytechnique LaSalle Beauvais). Septembre 2009 – Mai Juin 2010: Caractérisation des processus d'altération dans le bassin versant du Malaval (Massif Central).
11. Marianne Rousseau et Pauline Thévenet (Institut Polytechnique LaSalle Beauvais). Septembre 2009 – Juin 2010: Etude du réseau hydrographique à Meyrueis : Détermination et quantification des facteurs d'influence (co-encadrement Sébastien Laurent-Charvet).
12. Marie Sarre et Marie Targosz (Institut Polytechnique LaSalle Beauvais). Septembre 2009 – Juin 2010: Etude de différents paramètres influençant le réseau hydrographique de la région de Meyrueis (Cévennes, France) (co-encadrement Sébastien Laurent-Charvet).
13. Charlotte Catrouillet et Christelle De Bardon De Segonzac (Institut Polytechnique LaSalle Beauvais). Janvier 2010 – Juin 2010 : Etude du comportement des éléments majeurs et traces métalliques dans le ruisseau du Malaval (Massif Central).
14. Mélanie Mogicato et Natacha Ville (Institut Polytechnique LaSalle Beauvais). Septembre 2010 – Juin 2011 : Caractérisation de l'altération des roches métamorphiques ortho et para dérivées dans le bassin versant Sud de la Zone Axiale, Montagne Noire.
15. Alexandre Mopsus et Jérémie Brajou (Institut Polytechnique LaSalle Beauvais). Septembre 2010 – Juin 2011 : Comparaison de l'altération de gneiss sur deux versants opposés de la Montagne Noire (Massif Central français).
16. Pierre Josso et Etienne Dutour (Institut Polytechnique LaSalle Beauvais). Septembre 2010 – Juin 2011 : Etude des divers paramètres influençant le réseau hydrographique de la région de Roquebrun, versant sud de la Montagne Noire (Hérault, 34) (co-encadrement Sébastien Laurent-Charvet).

17. Maylis Dupouy et Arthur Du Peloux (Institut Polytechnique LaSalle Beauvais). Septembre 2010 – Juin 2011 : Etude du réseau hydrographique de la Montagne Noire: Influence des facteurs géologiques sur le réseau hydrographique (co-encadrement Sébastien Laurent-Charvet).
18. Sylvain Gaulmin et Géraldine Siboni (Institut Polytechnique LaSalle Beauvais). Septembre 2010 – Juin 2011 : Etude du gisement uranifère de Pen Ar Ran (Loire-Atlantique) (co-encadrement Jessica Bonhoure).
19. Clara Bellon, Xavier Cournot et Hadrien Descormes (Institut Polytechnique LaSalle Beauvais). Septembre 2010 – Juin 2011 : Etude géologique du gisement uranifère de Pen Ar Ran (Bretagne) (co-encadrement Jessica Bonhoure).
20. Maximilien Guillot et Christophe Marin (Institut Polytechnique LaSalle Beauvais). Janvier 2011 – Juin 2011 : Caractérisation des sables de fonderie - Projet Ecosable (co-encadrement Sébastien Laurent-Charvet et Sébastien Potel).
21. Alexandre Belin et Manuel Fedou (Institut Polytechnique LaSalle Beauvais) Etude de la mobilité des éléments métalliques dans le granite de Questembert (Morbihan) - Septembre 2011- Juin 2012.
22. Pierre Louis Junot et Robin Pelletier (Institut Polytechnique LaSalle Beauvais) Septembre 2011 – Juin 2012 : Caractérisation des sables de fonderie - Projet Ecosable (co-encadrement Sébastien Laurent-Charvet et Sébastien Potel).
23. Karine Charbonier et Adrien Moreau (Institut Polytechnique LaSalle Beauvais) Septembre 2011 – Juin 2012 : Caractérisation des sables de fonderie - Projet Ecosable (co-encadrement Sébastien Laurent-Charvet et Sébastien Potel).
24. Léo Thévenin et Baptiste Vincens (Institut Polytechnique LaSalle Beauvais) Septembre 2012 – Juin 2013 : Caractérisation minéralogique et géochimique des schistes ordoviciens du Grand Fougeray (Massif armoricain) - Projet ASTER (co-encadrement Sébastien Potel).
25. Artis Kensai et Alexandre Borniche (Institut Polytechnique LaSalle Beauvais) Septembre 2012 – Juin 2013 : Caractérisation minéralogique et géochimique des schistes ordoviciens du Grand Fougeray (Massif armoricain) - Projet ASTER (co-encadrement Sébastien Potel).
26. Faddy Nassif et Pierre-Marie Bastien (Institut Polytechnique LaSalle Beauvais) Septembre 2012 – Juin 2013 : Caractérisation minéralogique et géochimique des schistes ordoviciens du Grand Fougeray (Massif armoricain) - Projet ASTER (co-encadrement Sébastien Potel).
27. Charlotte Bohr, Cloé Delahaie et Arnaud Lhomme (Institut Polytechnique LaSalle Beauvais) Septembre 2012 – Juin 2013 : Référentiel sol au Katanga (Rep. Dem. Congo) (co-encadrement Romain Armand).

### **Etudiants en master 1 (initiation à la recherche)**

1. Alexandre Bevillard et Julien Leroy (Master 1, Institut Polytechnique LaSalle Beauvais). Décembre 2007- Juin 2008: *Miscanthus*, phytoremédiation et dépollution des sols.
2. Antoine Hincelin et Vincent Houvet (Master 1, Institut Polytechnique LaSalle Beauvais). Décembre 2007- Juin 2008: Phytoremédiation des métaux lourds par *Brassica Juncea*.
3. Ritesh Kumar (Master 1, Indian Institute of Technology, Inde). Mai 2010 – Juillet 2010. Modélisation de l'adsorption des terres rares par des oxydes de manganèse.
4. Camille Le Guillou, Marion Lemoine et Manon Le Couedic (Master 1, Institut Polytechnique LaSalle Beauvais). Décembre 2012- Juin 2013 : Disponibilité et accumulation du cobalt et du cuivre chez une métallophyte (co-encadrement Michel-Pierre Faucon et Bastien Lange).

### **Etudiants en master 2 (stage de fin d'études)**

1. Luc Fauvain (Master 2, Institut Polytechnique LaSalle-Beauvais). Janvier –Mars 2009: Optimisation de Model VI dans PHREEQC pour la modélisation de la spéciation des terres rares.
2. Alexandre Bak (Master 2, Université de Lille 1). Mars 2011- Septembre 2011 : Optimisation des paramètres d'ozonation en phase aqueuse pour la dépollution de lixiviats de décharges et de sites pollués – Projet OPOPOP (co-encadrement Victor Acha).
3. Pierre Henri Trapy (Master 2, Institut Polytechnique LaSalle Beauvais). Février 2012- Juillet 2012 : Optimisation des paramètres d'ozonation en phase aqueuse pour la dépollution de lixiviats de décharges et de sites pollués – Projet OPOPOP (co-encadrement Victor Acha).
4. Bastien Lange (Master 2, Institut Polytechnique LaSalle Beauvais). Février 2012- Juillet 2012 : Accumulation du cuivre et du cobalt chez des métallophytes du Katanga (Rep. Dem. Congo) (co-encadrement Michel-Pierre Faucon).
5. Pierre Josso (Master 2, Institut Polytechnique LaSalle Beauvais). Janvier 2013-Juillet 2013 : Analyses géochimiques par ICP-MS d'une collection d'échantillons représentant les grands types de minéralisation de mangénèse océaniques (co-encadrement Ewan Pelleter, Ifremer).

### **Doctorants**

1. Abdessamad Khalil (Univ. Cadi Ayyad, Marrakech, Maroc) depuis juin 2011 (2 mois par an à Beauvais): Cartographie de la pollution des sols par les rejets miniers acides en utilisant la géochimie et la télédétection hyperspectrale : Exemple de la mine abandonnée de Kettara (collaboration pour volet géochimie dans le cadre du projet financé Vollubilis).
2. Ellenita de Castro (De La Salle University Manila, Philippine) octobre-décembre 2012: Phytogeography and biogeochemistry of flora from metalliferous soils in the Philippines:

Implications in the phytoremediation and phytostabilization of soils contaminated by trace metals (co-encadrement avec Michel-Pierre Faucon dans le cadre du projet financé France - Philipines).

3. Bastien Lange (Univ. Libre de Bruxelles, Belgique) depuis octobre 2012: Tolérance et accumulation du cobalt chez les végétaux. Implication pour la phytoremediation des sols contaminés (collaboration pour volet géochimie).

### **Post-doctorants**

1. Le Vinh Hoang (LaSalle Beauvais) 2010-2012 - Optimisation des paramètres d'ozonation en phase aqueuse pour la dépollution de lixiviats de décharges et de sites pollués – Projet OPOPOP (co-encadrement Thierry Aussenac).
2. Florian Cobert (Université de Liège, AgroBioTech Gembloux, Belgique) depuis octobre 2012 - Apport des méthodes géochimiques et isotopiques à l'évaluation et la maîtrise de la mobilité des éléments nutritifs dans les agro-écosystèmes (co-encadrement Gilles Colinet).

## **Bilan de mes activités de recherche**



## Bilan de mes activités de recherche

### Avant-propos

Mes activités de recherche concernent de façon générale l'étude des interactions entre des éléments majeurs et traces et les phases minérales et organiques des eaux et des sols dans les cycles biogéochimiques. Mes travaux de thèse ont porté sur l'étude expérimentale et la modélisation de l'impact de la matière organique sur le comportement des terres rares en solution. Ce travail s'est poursuivi pendant mon contrat d'ATER par l'application des principaux résultats de ma thèse à des exemples de terrain pour lesquelles de nombreuses données étaient disponibles au laboratoire Géosciences Rennes dans le cadre de l'ORE AGHRYS. Depuis mon recrutement en tant qu'enseignant-chercheur à LaSalle Beauvais, outre l'utilisation des modèles développés précédemment, j'ai participé à la création de l'unité de recherche HydrISE (Hydrogéochimie et Interaction Sol-Environnement). Ces dernières années, j'ai initié la construction d'un projet de recherche collectif en parallèle de nouveau recrutement et de la création d'un parc analytique dédié aux analyses géochimiques (nouveaux investissements : ICP-MS et couplage HPLC, ICP-AES, AA...). J'ai défendu ce projet devant l'AERES en février 2011 ; ce projet a été validé par le conseil scientifique de LaSalle Beauvais en décembre 2011 et l'équipe reconnue officiellement par le Ministère de l'Agriculture (ministère de tutelle de l'établissement). Cela a permis à l'équipe d'intégrer la SFR Condorcet du PRES bi-régional UFECAp et d'être rattachée à l'école doctorale en Sciences, Technologies et Santé n°547. Dans le cadre de ce projet d'unité qui s'intéresse à l'écodynamique des éléments traces métalliques, mes activités de recherche portent plus particulièrement, sur le fractionnement et la mobilité des terres rares dans le système roche-eau-sol-plante. Pour répondre à ces questions, de nouveaux systèmes expérimentaux ont été développés (adsorption, oxydation...). Cette expérimentation est menée en parallèle avec le développement de la modélisation, qui consiste à utiliser, tester et adapter des modèles de spéciation en solution préexistants dans la littérature. Ce travail sur les terres rares me permet, en outre, d'avoir une reconnaissance dans ce domaine [nomination en janvier 2011 en tant que Fellow Member de la Society of Economic Geologist, participation à un projet ANR sur les terres rares et co-organisation d'une session sur le sujet à la prochaine Goldschmidt Conférence (Florence, Italie en août 2013)]. Cette approche sur les terres rares a été élargie et appliquée à d'autres éléments chimiques (Cu, Co, U) dans le cadre de recherches menées en parallèles et en collaboration avec mes collègues de l'unité HydrISE et des unités partenaires de GEGENAA (URCA) et Système Sol Eau (AgroBioTech Gembloux).

### Approches scientifiques

La démarche de ce travail s'est construite autour de trois axes complémentaires: (i) expérimentations en laboratoire, (ii) analyses d'échantillons naturels, (iii) modélisation.

#### I- Expérimentation en laboratoire

Quatre grands types d'expérimentation en laboratoire ont été menés : (i) adsorption (terres rares ou complexe organique de terres rares sur des oxydes de fer et de manganèse); (ii) complexation

(terres rares - matières organiques); (iii) complexation compétitive (terres rares - matières organiques - carbonates ou terres rares - matières organiques - oxydes de manganèse); (iv) adsorption-oxydation simultanée (terres rares et manganèse), et différents paramètres ont été testés (e.g., pH; concentrations en terres rares, matières organiques, carbonates, oxydes; rapport de concentrations; force ionique). La matière organique choisie est un acide humique standard commercial qui est une molécule organique modèle bien caractérisée. Les oxydes de fer et de manganèse ont été choisis pour leur ubiquité dans les sols et leurs propriétés oxydantes et adsorbantes. Les carbonates ont été choisis pour leur complexation préférentielle des terres rares lourdes à pH alcalins.

## II – Analyses d'échantillons naturels

Différents types d'échantillons naturels ont été analysés : (i) des eaux souterraines (analyses totales et fractionnement par ultrafiltration) ; (ii) des eaux de rivières (analyses totales et fractionnement par ultrafiltration) ; (iii) des roches et des profils d'altération (analyses totales et fractionnement par extractions séquentielles) ; et (iv) des sols (analyses totales et fractionnement par extractions séquentielles).

## III - Modélisation

Afin de mieux comprendre la spéciation des terres rares en contexte inorganique et organique, une phase de modélisation a été développée. Plusieurs modèles disponibles dans la littérature (WHAM, Visual Minteq, PHREEQC, PhreePlot...) ont été testés, validés (grâce à des travaux expérimentaux) et améliorés (par la détermination de nouvelles constantes) pour modéliser le comportement avec les matières organiques. Les bases de données de ces modèles ont été complétées afin d'intégrer les constantes de complexation inorganiques et organiques pour l'ensemble des terres rares et harmonisées, notamment les constantes de complexation des cations majeurs compétiteurs des terres rares (Ca, Fe, Al...). Les constantes de complexation des terres rares par la matière organique n'existant pas, celles-ci ont dans un premier temps été extrapolées et ensuite déterminées par modélisation inverse de données expérimentales. Un travail identique a été aussi réalisé concernant l'adsorption des terres rares par les oxydes de manganèse.

## Résultats scientifiques

---

Les recherches que je poursuit actuellement ont pour but de comprendre l'impact de la matière organique sur le comportement des terres rares en solution. A ce titre, ces travaux ont permis des avancées scientifiques significatives dans la compréhension des mécanismes responsables de la spéciation des terres rares dans les eaux naturelles riches en matière organique. Ces travaux ont permis de:

- (i) montrer pourquoi le développement d'anomalie de cérium négative dans des eaux organiques oxydantes ne se produit pas systématiquement;
- (ii) identifier le fractionnement des terres rares lors de complexation compétitive des terres rares à la surface d'acides humiques et d'oxydes de manganèse.

(iii) tester la capacité de deux modèles thermodynamiques spécifiques à la matière organique à prédire la distribution des terres rares dans les eaux organiques de manière fiable et précise;

(iv) fournir un jeu de constantes terres rares - acides humiques spécifiques à Model VI; et terres rares oxydes de manganèse spécifiques à PHREEQC ;

(v) tester l'impact des réactions de compétition entre des ligands organiques (acide humique) et inorganiques (carbonates) forts pour la complexation des terres rares sur leur distribution;

(vi) mettre en évidence un nouveau mécanisme capable de produire une anomalie négative de Ce dans les eaux organiques naturelles.

(vii) comprendre l'évolution de la spéciation des terres rares dans des eaux naturelles (souterraines, zones humides, rivières) ;

(viii) mettre en évidence le rôle majeur de la complexation organique des terres rares dans l'enrichissement en terres rares responsable de concentration à valeurs économiques.

Les principaux résultats obtenus sont résumés dans la synthèse qui suit.

## Introduction

Les terres rares (REE pour rare earth elements) ou lanthanides, forment une famille de 15 éléments chimiques (du La au Lu) du groupe IIIA dans la classification périodique des éléments, du numéro atomique 57 au 71. Conventionnellement, les REE légères (du La au Gd) sont distinguées des REE lourdes (du Tb au Lu). Les REE peuvent aussi être subdivisées en trois groupes les REE légères (du La au Nd), les REE intermédiaires (du Sm au Tb) et les REE lourdes (du Dy au Lu). Les REE sont caractérisées par une structure électronique de type  $[Xe]4f^n$  [ $0(La) < n < 14(Lu)$ ] et forment des composés qui présentent des liaisons à caractère ionique dominant. Le remplissage de la couche électronique 4f depuis le La jusqu'au Lu, génère une augmentation de l'attraction du noyau sur les électrons, ce qui entraîne une diminution des rayons ioniques et atomiques le long de la série, classiquement nommée contraction des lanthanides. Cette diminution reste cependant faible, ce qui explique les propriétés chimiques très voisines des lanthanides (Henderson, 1984). La chimie des REE est caractérisée par la prédominance du degré d'oxydation +III. Deux exceptions existent cependant: l'europium qui peut passer à l'état d'oxydation +II dans des conditions réductrices typiques de fluides hydrothermaux ou métamorphiques (e.g., Sverjensky, 1984; Bau, 1991), et le cérium qui peut être oxydé en Ce(IV) dans des conditions de pression et de température supergénères (e.g., De Baar et al., 1988; Elderfield, 1988). Cette oxydation peut se produire abiotiquement grâce à un mécanisme d'adsorption-oxydation (oxidation-scavenging en anglais) du Ce(III) à la surface de solides oxydants comme les oxydes de Mn ou de Fe (Koeppenkastrop et De Carlo, 1992; De Carlo et al., 1998; Bau, 1999; Ohta et Kawabe, 2001) mais ce mécanisme est cependant questionable (Bau et Koschinsky, 2009).

Les propriétés chimiques intrinsèques des REE ont permis d'utiliser leur abondance et leur fractionnement dans les roches comme traceurs des processus cosmochimiques, géodynamiques et pétrogénétiques (e.g., Henderson, 1984; Taylor et McLennan, 1985). Ces travaux ont permis de mieux contraindre les processus de différenciation et d'évolution chimique de la Terre. Ce n'est cependant que depuis une vingtaine d'années, grâce à la mise au point des techniques ICP-MS et à l'abaissement des limites de quantification, que les REE sont utilisées, et notamment leur fractionnement, dans les différents réservoirs de l'hydrosphère que sont les océans et les mers (Goldberg et al., 1963; Martin et al., 1976; Elderfield et Greaves, 1982; De Baar et al., 1983; Hoyle et al., 1984; De Baar et al., 1985; De Baar et al., 1988; Elderfield, 1988; Byrne et Kim, 1990; German et al., 1991; German et al., 1995; Bau et al., 1996; Byrne et Sholkovitz, 1996; Bau et al., 1997; Duncan et Shaw, 2004; Lawrence et Kamber, 2006), les fleuves et les rivières (Goldstein et Jacobsen, 1988; Elderfield et al., 1990; Sholkovitz, 1993; Sholkovitz, 1995; Bau et Dulski, 1996; Dupré et al., 1996; Gaillardet et al., 1997; Viers et al., 1997; Dupré et al., 1999; Elbaz-Poulichet et Dupuy, 1999; Tricca et al., 1999; Ingri et al., 2000; Deberdt et al., 2002; Shiller et al., 2002; Gerard et al., 2003; Gaillardet et al., 2003; Andersson et al., 2006 ; Steinmann et Stille, 2008), les lacs (Fee et al., 1992; Möller et Bau, 1993; Johannesson et Lyons, 1994; 1995; Johannesson et Zhou, 1999; De Carlo et Green, 2002; Gammons et al., 2003; Shacat et al., 2004) et les eaux souterraines (Smedley, 1991; Johannesson et al., 1995; 1996b; 1997; Viers et al., 1997; Braun et al., 1998; Johannesson et al., 1999; Dia et al., 2000; Johannesson et Hendry, 2000; Johannesson et al., 2000; Aubert et al., 2001; Janssen et Verweij, 2003; Duncan et Shaw, 2004; Gruau et al., 2004; Johannesson et al., 2004; Nelson et al., 2004). Dans ce cadre, les REE

sont utilisées pour tracer les circulations d'eau et de matière et/ou contraindre les mécanismes de l'altération.

De plus, les REE ont connus un regain d'intérêts ces dernières années pour leur intérêt économique, notamment quant à la grande demande en ces éléments et leur utilisation dans les nouvelles technologies dites vertes (aimants permanents, luminophores...). La croissance de la demande a engendré la réouverture des exploitations américaines et australiennes, permettant de commencer à contrebalancer le monopole chinois (Figure 1). Il est donc nécessaire de comprendre comment se forme un dépôt minéral à valeur économique de REE. Ainsi, White (1968) a défini quatre étapes indispensables (i) une zone source doit fournir les métaux; (ii) le minerai doit se dissoudre dans l'eau; (iii) les fluides doivent transporter les métaux en solution; (iv) le minerai doit précipiter sur le site de dépôt. De plus, selon la nomenclature de Kanazawa et Kamitani (2006), il existe trois grands types de gisements de REE: (i) les gisements ignées (i.e., hydrothermaux, carbonatites, granites et autre roches alcalines); (ii) les gisements sédimentaires (i.e., placers, conglomérats) et (iii) les gisements secondaires avec notamment les gisements d'altération de granite alcalin (e.g., argiles ioniques). A l'exception des premiers, les gisements sédimentaires et d'altération vont faire intervenir un facteur eau de surface, vecteur de mise en solution et de transport.

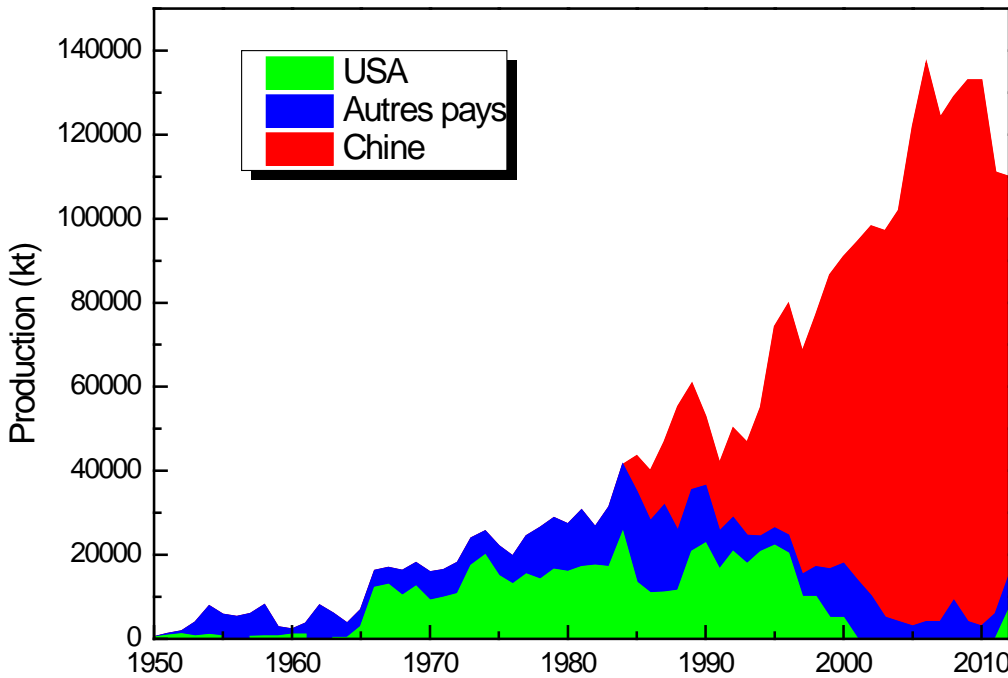


**Figure 1.** Evolution de la production d'oxyde de terres rares (kt)

Ainsi, les REE dans les eaux superficielles (vecteur de transport en solution) se distribuent entre deux composantes principales traditionnellement séparées par filtration à 0,2 µm. La

composante supérieure à 0,2 µm correspond à la fraction particulaire, tandis que la composante inférieure regroupe les fractions colloïdales (organiques et minérales) et le "dissous vrai" (Sholkovitz, 1995; Viers et al., 1997; Braun et al., 1998). Les REE liées aux colloïdes peuvent être distinguées des REE en solution grâce à des techniques d'ultrafiltration. Afin de corriger des variations d'abondances systématiques entre REE de numéros atomiques pairs et impairs, les teneurs en REE des eaux sont normalisées par rapport à celles de réservoirs de références et représentées sous forme de spectres. Les REE des eaux proviennent de l'altération des enveloppes superficielles de la Terre, de ce fait les réservoirs de référence utilisés sont des réservoirs "rocheux" de surface. Deux types de réservoirs sont généralement utilisé: (i) la croûte continentale supérieure et (ii) les "Shales" (Haskin et al., 1968; Taylor et McLennan, 1985; McLennan, 1989). La puissance des spectres de REE en tant que marqueur de mélange d'eau ou des processus d'altération tient de la diversité des spectres de REE rencontrés dans les eaux.

Les REE libres en solution sont peu abondantes, du fait de leur faible hydrosolubilité. De nombreuses études s'accordent pour attribuer un rôle majeur à la chimie des solutions et des interfaces dans le contrôle des concentrations en REE des eaux de surface, comparé à celui joué par les teneurs dans les roches mères (Goldstein et Jacobsen, 1988; Elderfield et al., 1990; Sholkovitz, 1995). La forme des spectres de REE des eaux et la teneur en REE en solution résultent de la conjonction d'un ensemble de processus susceptibles d'induire leur fractionnement. Ces processus sont eux-mêmes sous le contrôle d'un certains nombre de facteurs environnementaux (pH, température, potentiel redox, force ionique...). Parmi ces processus, quatre processus majeurs peuvent ainsi être distingués: (i) la complexation avec les anions inorganiques (e.g., carbonates, sulfates) et les anions organiques simples de bas poids moléculaire (e.g., acide acétique, acide lactique), (ii) la complexation avec les colloïdes organiques (e.g., substances humiques), (iii) les processus d'adsorption/désorption avec la surface des minéraux et les colloïdes inorganiques (e.g., oxyhydroxydes de Fe, Mn et Al, argiles) et (iv) les processus de précipitation (e.g., CeO<sub>2</sub>). Ainsi le spectre d'une eau filtrée correspondant au spectre du matériau source modifié des constantes de complexation/adsorption des REE vis à vis des particules, des colloïdes et des divers ligands en solution. Il en résulte une diversité de formes de spectres de REE, s'exprimant soit par des degrés d'enrichissement ou d'appauvrissement relatifs en REE lourdes variables, soit par la présence ou l'absence d'anomalies négatives en cérium.

Elderfield et al. (1990) classent les eaux continentales en deux groupes en fonction de leurs spectres de REE (Figure 2). Le premier correspond aux spectres qui montrent un enrichissement en REE légères et intermédiaires (Figure 2a). Le deuxième groupe est caractérisé par des spectres montrant un enrichissement continu du La au Lu (Figure 2b). Le premier type de spectre serait caractéristique des eaux à pH acide contenant de fortes concentrations en REE, tandis que le deuxième serait plutôt associé à des eaux présentant des pH alcalins et des teneurs en REE plus faibles. Ces auteurs expliquent le premier type de spectre par une complexation préférentielle des REE légères à intermédiaires par les colloïdes et le deuxième par une complexation préférentielle par des ligands inorganiques en solution des REE lourdes, associée à une adsorption préférentielle des REE légères sur la fraction particulaire. Goldstein et Jacobsen (1988) précisent que la présence de matière organique dans les eaux pourrait expliquer les spectres convexes observés, tandis que les spectres enrichis en REE lourdes seraient contrôlés par la formation de complexes carbonatés et hydroxylés. Sholkovitz (1995) propose un contrôle des concentrations en REE dans les eaux de rivières par les réactions avec les surfaces minérales. A la vue de ces interprétations, il semble important de comprendre la spéciation des REE en

solution. En effet, leur liaison à des colloïdes peut avoir un rôle prépondérant dans la mesure où la spéciation des REE peut dépendre des changements de propriétés. Il peut donc en résulter des différences d'adsorption, des variations de la chimie redox du Ce, des différences de transport et/ou de mélange.

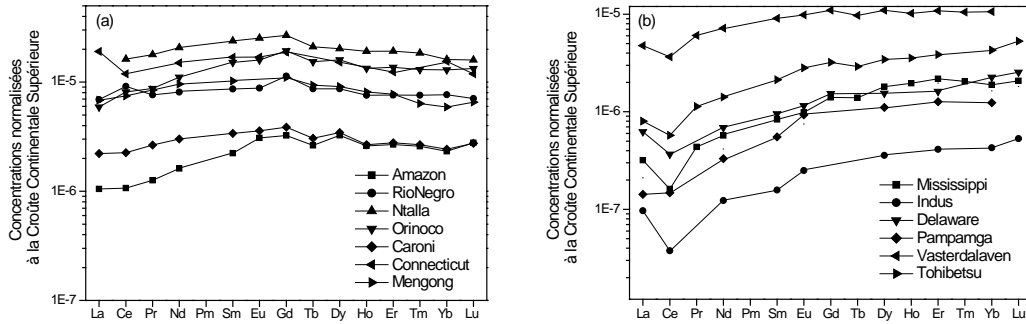


**Figure 2.** Spectres de REE normalisés à la Croûte Continentale Supérieure d'eaux de rivières montrant (a) un enrichissement en REE légères à intermédiaires et (b) un enrichissement en REE lourdes (Deberdt et al., 2002; Elderfield et al., 1990; Goldstein and Jacobsen, 1988; Sholkovitz, 1995).

La compréhension et la modélisation de l'information portée par la très large variété de spectres de REE rencontrée dans l'hydrosphère nécessite de connaître parfaitement les propriétés thermodynamiques des complexes aqueux de REE avec les ligands organiques simples (e.g., acide acétique) et inorganiques (e.g., sulfates, carbonates). Actuellement, comme l'ont souligné Wood (1990; 1993) et Byrne et Li (1995), les conditions expérimentales dans lesquelles les constantes de complexation ont été déterminées manquent de cohérence. Cependant, les constantes inorganiques proposées par Klungness et Byrne (2000), Luo et Byrne (2004) et Schijf et Byrne (2004) peuvent servir de base. Par ailleurs, le rôle des complexes organiques comme vecteur de mobilité des REE n'a été mis en évidence que depuis une quinzaine d'années (Dupré et al., 1996; Viers et al., 1997; Dia et al., 2000) dans des eaux continentales. Le manque de données expérimentales fiables concernant les complexes organiques de REE a suscité l'utilisation de codes de calculs théoriques ou empiriques (Wood, 1990; Lee et Byrne, 1992; Millero, 1992; Wood, 1993; Fairhurst et al., 1995; Tang et Johannesson, 2003). Néanmoins, l'acquisition de données expérimentales reste nécessaire afin de valider ces prédictions (Fairhurst et al., 1995; Lead et al., 1998; Tang et Johannesson, 2003). Il en est de même pour les oxyhydroxydes de Fe et de Mn où seules quelques études ont essayées de décrire l'adsorption des REE sur ses surfaces (e.g., Quinn et al., 2007). Ainsi cette étude s'attachera à étudier :

- (i) Impact des colloïdes sur le comportement des REE en solution ;
- (ii) Quantification des rôles respectifs de la matière organique et des oxydes de Fe et de Mn sur la spéciation des REE dans des eaux naturelles (eaux souterraines et de rivières) ;
- (iii) Utilisation du fractionnement des REE dans la compréhension de minéralisation.



## Partie I

# Impact des colloides sur le comportement des terres rares en solution

### Articles clés:

**Pourret O.**, Davranche M., Gruau G., Dia A. (2007) Rare Earth Elements complexation with humic acid. Chemical Geology 243, 128-141.

**Pourret O.**, Martinez R.E. (2009) Modeling lanthanide series binding sites on humic acid. Journal of Colloid and Interface Science 330, 45-50.

**Pourret O.**, Davranche M. (2013) Rare earth element sorption onto hydrous manganese oxide: A modeling study. Journal of Colloid And Interface Science 395, 18-23.



## I- Impact des colloides sur le comportement des terres rares en solution

Dans cette première partie la complexation inorganique et organique des REE a été étudiée, notamment comment la complexation influence le comportement des REE en solution et quelle rôle a t'elle sur l'inhibition sur d'autres réactions potentielles en compétition (e.g., oxydation). Cette étude est basée sur une démarche expérimentale couplant des expériences en laboratoire d'équilibre en réacteurs fermés et des calculs de spéciation à l'aide de programmes spécifiques aux calculs de spéciation avec des surfaces solides inorganiques, PHREEQC (Parkhurst et Appelo, 1999) et PhreePlot (Kinniburgh et Cooper, 2009) et à la matière organique, WHAM VI (Tipping, 1998).

### I.1. Expériences d'adsorption/oxydation sur oxydes de manganèse

Les oxydes de manganèse sont des complexants importants des REE dans les hydrosystèmes. Cependant, il est difficile d'inclure les oxydes de Mn dans les modèles de spéciation en raison de l'absence d'un ensemble complet des réactions de sorption en accord avec un modèle de complexation de surface), ainsi que des incohérences entre les données de sorption publiées et les prévisions en utilisant les modèles disponibles. Les réactions de complexation de surface pour un oxyde de manganèse hydraté ont été décrites en utilisant un modèle à deux sites de surface, et la double couche diffuse. La surface spécifique, densité de site surface, et le  $\text{pH}_{\text{zpc}}$  ont été fixés à  $746 \text{ m}^2/\text{g}$ ,  $2,1 \text{ mmol/g}$ , et  $2,2$ , respectivement, comme proposée par Tonkin et al. (2004). Deux types de sites ( $\equiv\text{XOH}$  et  $\equiv\text{YOH}$ ) ont également été utilisés avec des valeurs de  $\text{pKa}_2$  de  $2,35$  ( $\equiv\text{XOH}$ ) et de  $6,06$  ( $\equiv\text{YOH}$ ). La fraction des sites de haute affinité a été fixée à  $0,36$ . Des données sur la sorption des REE publiées ont ensuite été utilisées pour déterminer les constantes de complexation de surface à l'équilibre, tout en tenant compte de l'influence du pH, de la force ionique, et la concentration en métal (Figure 3). Les log K augmentent des REE légères aux REE lourdes et, plus particulièrement, développent un effet tétrade convexe (Figure 4). À faible concentration en métal, les sites de type  $\equiv\text{YOH}$  expriment fortement leur affinité pour les REE, alors que pour des concentrations en métal plus fortes, les sites de type  $\equiv\text{XOH}$  vont s'exprimer. Cette étude apporte ainsi la preuve de l'hétérogénéité dans la distribution des sites de complexation de surface des oxydes de manganèse envers les REE et une série de constantes capables de reproduire l'adsorption des REE en fonction du pH, le développement d'une anomalie de Ce et l'effet Tetrad. Cependant, le mécanisme d'adsorption-oxydation du Ce(III) à la surface des oxydes de Mn est toujours questionnable comme l'ont souligné Bau et Koschinsky (2009).

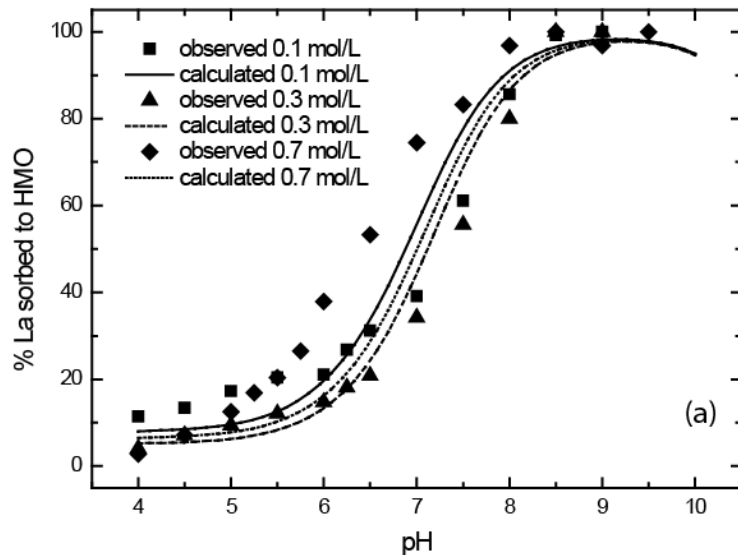


**Figure 3.** Comparaison entre %La adsorbé à la surface des oxydes de manganèses observés (points) et modélisés (traits pleins) obtenus avec les nouvelles constantes de stabilité.

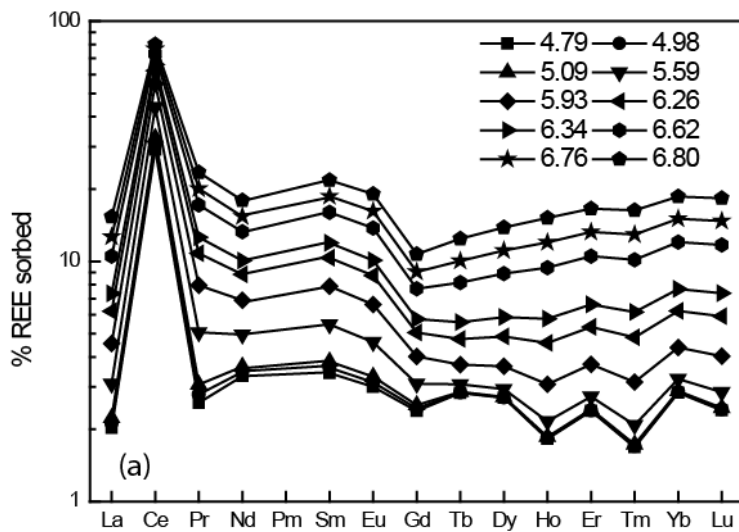


**Figure 4.** Spectres de REE modelisés (conditions expérimentales, Ohta et Kawabe, 2001).

## I.2. Complexation compétitive des terres rares à la surface d'acides humiques et d'oxydes de manganèse.

Des cinétiques d'adsorptions simultanées de REE sur des oxydes de manganèse et des acides humiques ont montrées que le taux d'adsorption des REE et d'oxydation du cérium variait dans le temps et en fonction du pH. Les REE libres sont immédiatement adsorbées par les acides humiques, une déstabilisation du complexe, due à la présence de l'oxyde de Mn qui se comporte comme un compétiteur, se produit au cours de l'expérience. Ce phénomène est marqué par le

développement d'une anomalie de Ce sur le spectre de REE qui reflète la compétition avec l'oxyde de manganèse. Un fractionnement entre les REE légères et lourdes est observé. L'ensemble de ces résultats suggère que plus le rapport matière organique/oxyde est faible et plus le pH est acide plus la compétition entre les oxydes et la matière organique est marquée. Des expériences d'adsorption des complexes REE-acides humiques à la surface d'oxyhydroxydes de fer et de manganèse ont montré que la complexation des REE par la matière organique inhibait à la fois, l'oxydation du Ce(III) en Ce(IV) et le développement d'un effet tetrad au niveau des spectres de REE des eaux. Cette inhibition est due au développement d'un écran organique entre les REE et les surfaces oxydantes/adsorbantes que représentent les oxydes de fer et de manganèse.

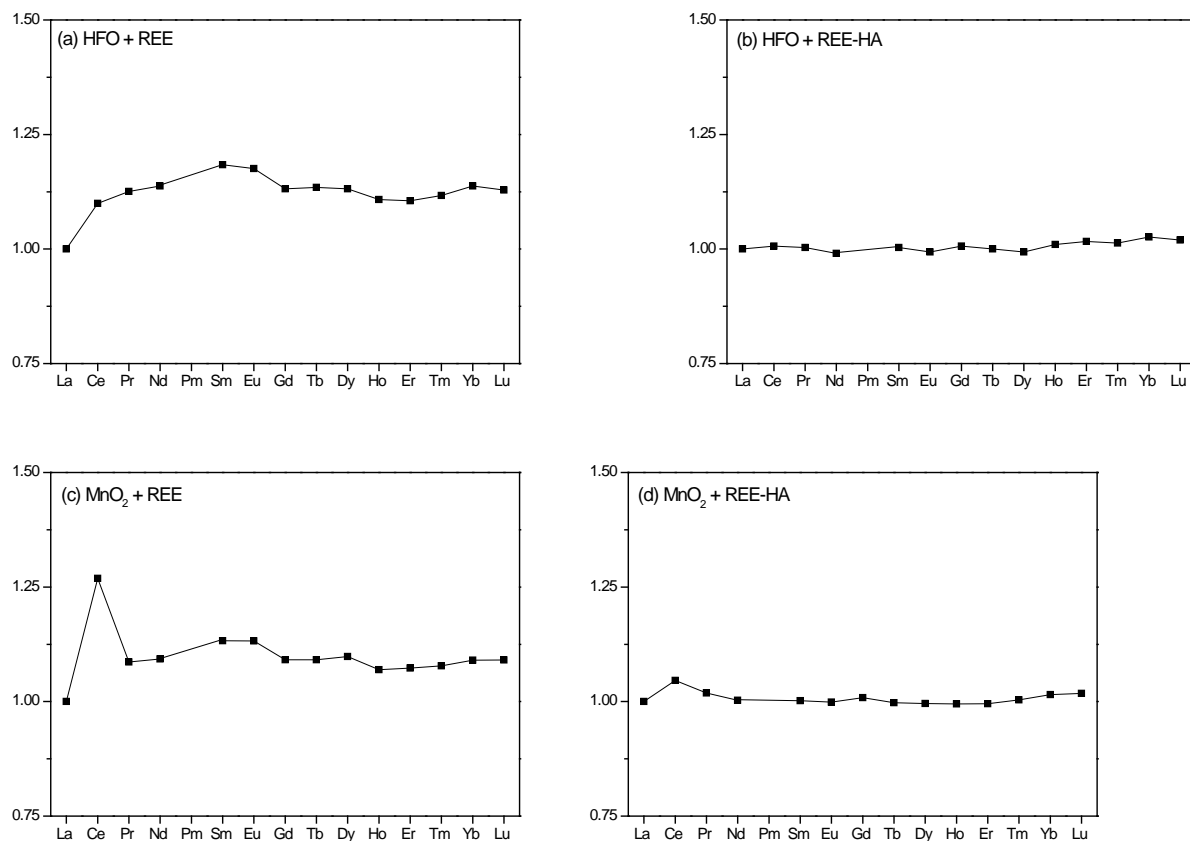


**Figure 5.** Spectres des coefficients de partage des REE (normalisation au La) adsorbées sur des oxydes de fer et de manganèse si les REE se trouvent sous forme (a et c) d'ions libre ou (b et d) de complexes organiques.

Les spectres obtenus (Figure 5), en conditions inorganiques, mettent en évidence le développement d'une anomalie de Ce, très faible pour HFO de l'ordre de 0,15 et importante pour  $\text{MnO}_2$  puisqu'elle atteint une valeur de 1,23 à l'équilibre. Des résultats similaires ont été obtenus par Ohta et Kawabe (2001) dans une étude de coprécipitation de  $\text{MnO}_2$  en présence de REE. Dans le cas des expériences organiques d'adsorption du complexe REE-acide humique, non seulement l'anomalie de Ce ne se développe plus mais, les spectres sont plats (Figure 6). Les valeurs de  $\log K_d$  chutent également de façon importante. Les  $\log K_d$  varient entre 3,3 et 4 pour

HFO et 3,2 et 4,2 pour  $\text{MnO}_2$  lorsque les REE sont introduites sous forme inorganique et entre 3 et 3,1 pour HFO et 3,2 et 3,4 pour  $\text{MnO}_2$  lorsque les REE sont introduites sous formes de complexe REE-acide humique. Ces résultats montrent, très clairement, que la complexation organique a, non seulement un effet sur le taux d'adsorption des REE mais aussi, sur leur comportement à la surface des oxyhydroxydes. Les  $\log K_d$  des REE et du COD à la surface de HFO ou  $\text{MnO}_2$  évoluent de façon conjointe (Figure 6).

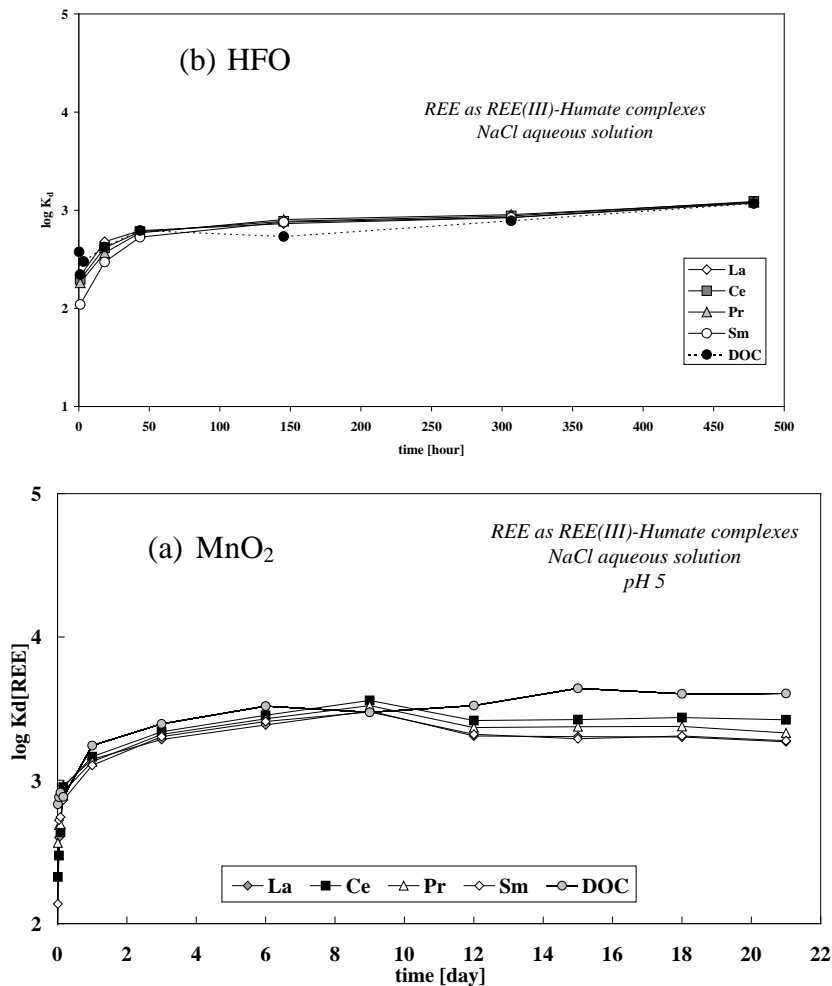
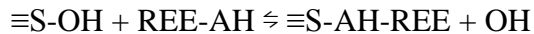


**Figure 6.** Evolution temporelle des  $\log K_d$  de La, Ce, Pr et du COD lors des expériences d'adsorption du complexe REE-acide humique à la surface de (a) HFO et (b)  $\text{MnO}_2$ .

Grâce à ces résultats, il a été possible de proposer un mécanisme permettant d'expliquer non seulement la disparition de l'anomalie de Ce, mais également la chute du taux d'adsorption des REE à la surface des solides lorsqu'elles sont sous forme de complexes organiques. L'anomalie de Ce ne se développe plus à la surface des solides oxydants parce que ceux-ci n'ont plus la possibilité d'oxyder le Ce(III) en Ce(IV). En effet, les REE restent liées aux acides humiques lors de leur adsorption. L'hypothèse est que ces derniers forment un écran organique entre le solide et les REE, le solide n'est plus en contact avec le Ce, la réaction d'oxydation de surface est impossible. La formation de l'anomalie de Ce est donc bloquée. De plus, toutes les

REE étant liées indifféremment à l'acide humique, il est impossible de différencier leur comportement. L'adsorption à la surface des solides est, en fait, une adsorption de type anionique qui se produit selon la réaction:



avec  $\equiv\text{S-OH}$  qui représente les fonctions de surface du solide : l'acide humique. Le complexe REE-acide humique s'adsorberait à la surface du solide par son côté ‘humique’ pour former un complexe ternaire de surface (Schindler, 1990; Nowack et Sigg, 1996). Cette réaction est favorisée par les conditions expérimentales de l'étude. Toutes les expériences ont été réalisées à un pH inférieur au  $\text{pH}_{zpc}$ . Une conséquence importante de ce mécanisme est le contrôle du taux d'adsorption des REE à la surface de l'oxyde par le taux d'adsorption des acides humiques. Il apparaît que dès 10 mg/L de COD initial, le log de  $K_d$  n'évolue plus et se stabilise à une valeur de 3,3 (Figure 7). La surface de  $\text{MnO}_2$  est saturée par les acides humiques. La valeur de saturation de 3,3 obtenue est très proche des valeurs obtenues dans les expériences d'adsorption organique de REE à la surface de  $\text{MnO}_2$  (condition expérimentale 10 mg/L de COD et 100 mg/L de  $\text{MnO}_2$ ). Cette valeur confirme le fait que le processus d'adsorption des REE dans les expériences organiques est totalement contrôlé par le comportement propre des acides humiques.

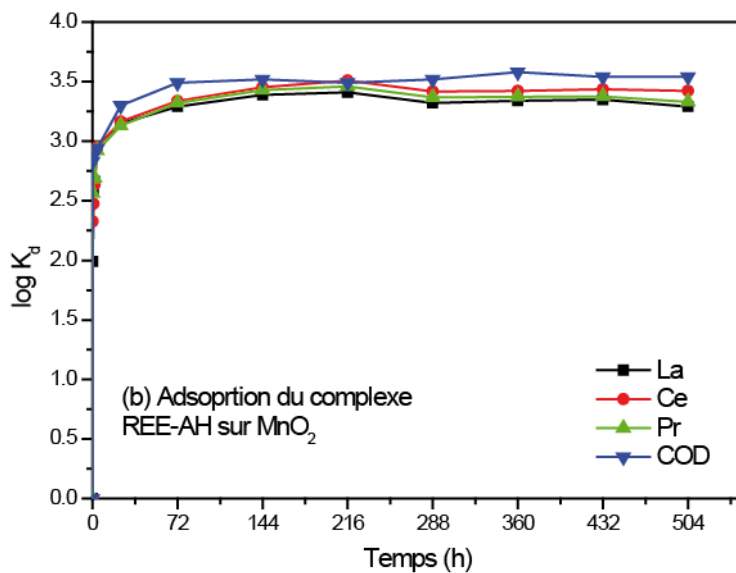


**Figure 7.** Evolution des log  $K_d$  COD/ $\text{MnO}_2$  en fonction de la concentration initiale en COD dans une suspension de 100 mg/L de  $\text{MnO}_2$ .

### I.3. Complexation des terres rares à la surface d'acides humiques

Des expériences de complexation REE - acides humiques ont montré une forte dépendance au pH. La proportion de complexe organique de REE augmente significativement avec les forts pH. Une complexation plus marquée des REE intermédiaires a également été

observée sur les différents spectres obtenus. Ces données ont été modélisées avec Model VI, ce qui a permis d'obtenir une série de constantes de complexation REE - acides humiques, spécifiques à ce modèle [ $\log K_{MA}$  (REE-HA)]. Les constantes obtenues pour Model VI montrent un fractionnement des REE similaire à celui obtenu avec des groupements carboxyliques simples comme les acides acétiques. La détermination de la spéciation des REE dans les eaux organiques par l'approche combinée de codes de calculs (SHM et Model VI) et d'une technique physique de fractionnement (i.e., ultrafiltration), a permis de caractériser la spéciation des REE dans des eaux de rivières et dans des eaux de nappes superficielles. Les calculs de spéciation, utilisant des constantes de complexation extrapolées, montrent une forte complexation des REE avec la matière organique (i.e., > 60 % pour  $5 < \text{pH} < 8,5$ ) dans les eaux de rivières moyennes mondiales.

L'étude précédente a montré l'influence de la complexation organique sur le comportement des REE à l'interface solide/liquide. Cette complexation est, à la fois, capable de modifier quantitativement (chute du taux d'adsorption), mais aussi qualitativement (modification de la forme des spectres de REE et suppression du développement de l'anomalie de Ce), la distribution des REE. Il est donc apparu indispensable d'évaluer quantitativement la complexation des REE par la matière organique. Le but de cette étude est de déterminer un jeu de constantes REE-acide humique et de les utiliser afin de prédire la spéciation des REE dans divers types d'eaux continentales oxydantes. Récemment, Tang et Johannesson (2003) ont effectué une étude dans ce sens. Cependant, leurs études sont basées sur un jeu de constantes estimées à partir des constantes de complexation d'acides organiques simples (acide acétique, acide lactique) avec d'autres métaux et spécifiques à Model V (Tipping, 1994). Plus récemment, Sonke et Salters (2006) et Sonke (2006) ont déterminé des constantes REE-acide humique pour l'ensemble du groupe et spécifique à Model V. Cependant, les constantes ont été déterminées une par une, pour chaque REE, par conséquent, elles ne tiennent pas compte de la compétition entre REE, compétition qui peut être importante puisque dans le milieu naturel, les REE interviennent toujours ensemble. Etant donné le rôle que peut jouer la complexation organique sur le comportement des REE, il est donc apparu indispensable de déterminer un jeu de constantes directement utilisable et fiable sur toute la gamme de pH des eaux naturelles afin de l'appliquer pour déterminer la spéciation des REE dans les eaux continentales. Les constantes ont été déterminées à partir d'expériences de complexation REE-acide humique en fonction du pH et de la concentration en acide humique. Les données expérimentales ont été ajustées à l'aide d'un modèle de complexation, spécifique à la matière organique, Model VI, introduit dans le code de calcul WHAM 6 (Tipping, 1998). Le jeu de constantes a, ensuite, été confronté aux constantes estimées de Tang et Johannesson (2003), ou à des jeux de constantes REE-acides organiques simples afin d'être validé puis utilisé. La figure 8 présente l'évolution en % de la complexation de La par l'acide humique (HA) en fonction du pH et de la concentration en HA. Le taux de complexation est dépendant à la fois de la concentration en acide humique et du pH. Ainsi, plus la concentration en acide humique est importante, plus la complexation à lieu à bas pH. De même, plus la valeur de pH est forte plus le pourcentage de La complexé augmente. A partir de pH 6, quelque soit la concentration en acide humique, 100 % du La est complexé à la matière organique.

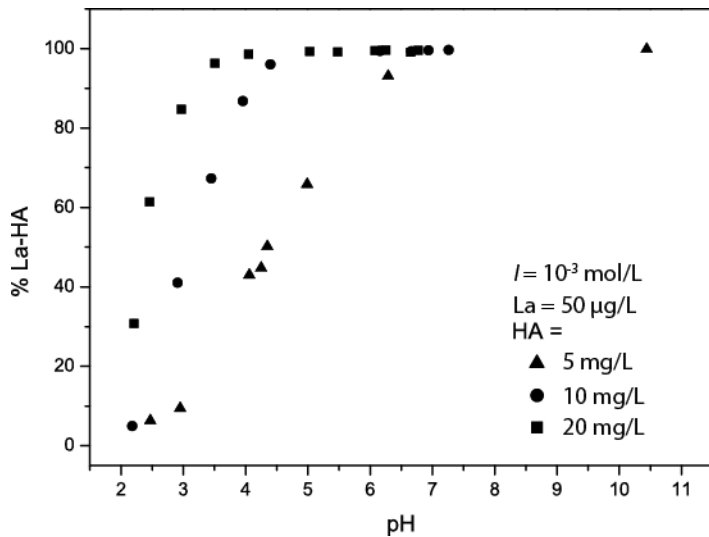


**Figure 8.** Pourcentage de La complexé aux acides humiques (HA) en fonction du pH et de la concentration en acide humique.

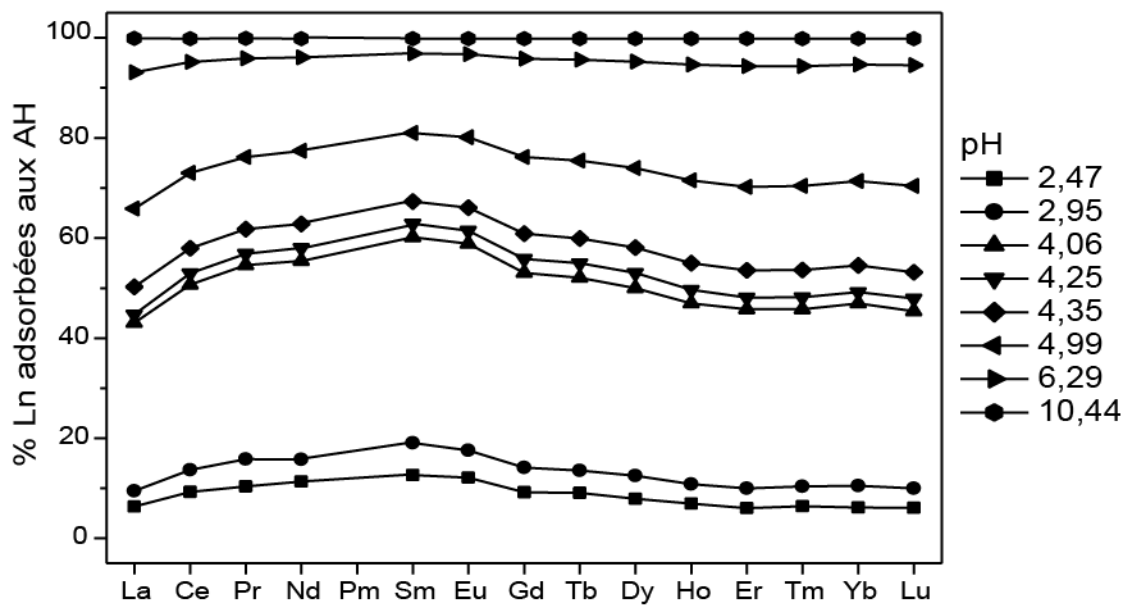


**Figure 9.** Spectres de REE de la solution inorganique en fonction du pH pour une concentration en acide humique de 5 mg/L.

Les spectres de REE (Figure 9) sont fractionnés et montrent un enrichissement en REE intermédiaires (du Sm au Tb). Ce fractionnement disparaît pour les fortes valeurs de pH dans la mesure où 100 % des REE sont complexés à l'acide humique.

Les constantes de complexation REE-acide humique spécifiques à Model VI ont été déterminées par calage (itérations manuelles) de façon à obtenir la meilleure adéquation entre

données expérimentales et calculées. Un jeu de données a été calculé pour chaque concentration en acide humique. La figure 10 illustre la bonne corrélation entre les données expérimentales et les données calculées à l'aide des constantes calées. Ces résultats démontrent le caractère réaliste des valeurs calculées des constantes tout en illustrant la capacité de Model VI à modéliser la complexation organique des REE.

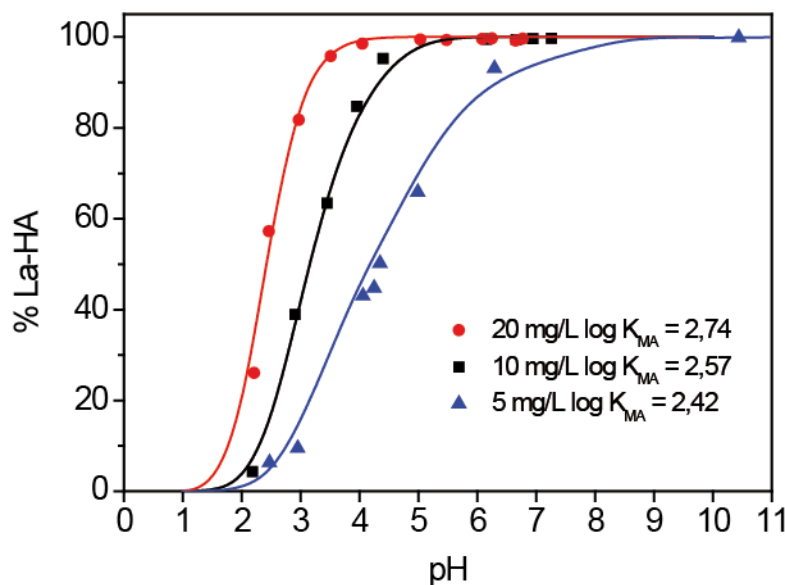


**Figure 10.** Données expérimentales et des données calculées à partir des constantes calées à l'aide de Model VI.

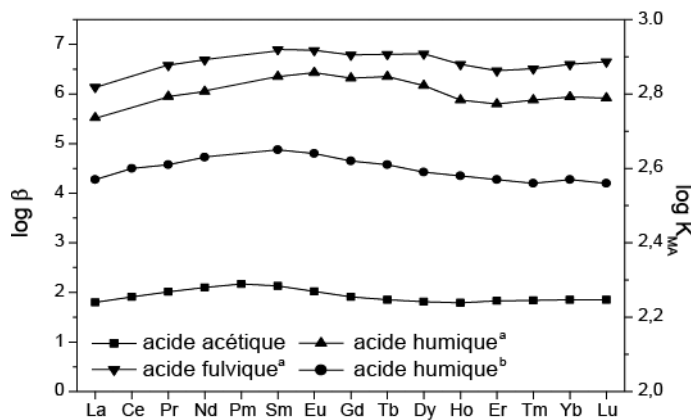


**Figure 11.** Distribution des  $\log \beta$  pour les complexes REE-acide acétique (Martell et Smith, 1998), (a) REE-acide fulvique (Yamamoto et al., 2005) et REE-acide humique (Suwannee river) (Yamamoto et al., 2006) et (b) des  $\log K_{MA}$  pour les complexe REE-acide humique (cette étude).

Ces valeurs de constantes ont également été validées par rapport à la littérature : la forme du spectre des constantes calculées ( $\log K_{MA}$ ) dans cette étude a été comparée à la forme du

spectre des constantes ( $\log \beta$ ) de complexation de REE à un acide acétique (Martell et Smith, 1998), un acide fulvique (Yamamoto et al., 2005) et un autre type d'acide humique (i.e., Suwannee River) (Yamamoto et al., 2006). L'acide acétique a été choisi car il représente le modèle des fonctions carboxyliques qui sont les sites les plus abondants à la surface des acides humiques (Figure 11). Les quatre spectres présentent la même distribution relative, à savoir un enrichissement en REE intermédiaires (de Sm à Tb) qui valident donc les résultats obtenus dans cette étude. Cette tendance se retrouve lorsque ces constantes sont comparées à une compilation des constantes de complexation des REE avec des ligands organiques (Figure 12). Enfin, comme pour les oxydes de mangénèse, la modélisation permet de confirmer que les liaisons MO-REE se produisent principalement grâce aux sites faibles (ca. 80%) et seulement 20% sont attribués aux sites forts. Le premier type de sites est attribué aux groupements carboxyliques, et le second aux groupements phénoliques. En outre, ceux-ci témoignent d'une hétérogénéité et engendre un fractionnement des REE (Figure 13).

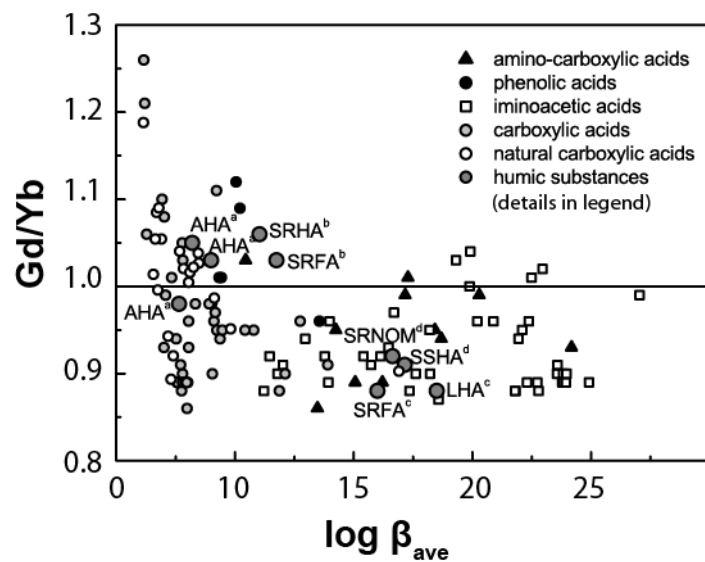


**Figure 12.** Compilation de constantes de complexation des REE avec ligands organiques extraites de la littérature.

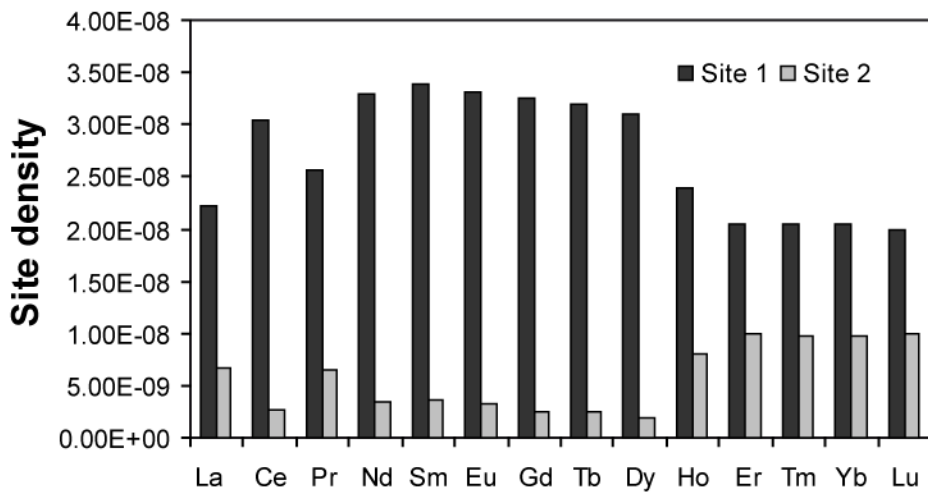


**Figure 13.** Distribution des densités de sites (mol Ln<sup>3+</sup>/mg HA).

#### I.4. Compétition acides humiques/carbonates

Des expériences de complexation compétitive carbonate/acide humique vis à vis des REE ont montré une forte dépendance au pH et à l'alcalinité. Aucune donnée ne permet d'identifier la formation de complexe ternaire de surface mettant en jeu des REE. Les calculs de spéciation avec Model VI reproduisent quantitativement les dépendances au pH et à la concentration en carbonates des résultats expérimentaux. Ces nouvelles données permettent de valider la série de constantes [log K<sub>MA</sub> (REE-HA)] déterminées précédemment, qui peut être utilisée avec confiance pour prédire la spéciation des REE dans des eaux alcalines. Ainsi, les modèles WHAM 6 et Model VI sont confortés dans leur capacité à calculer de manière fiable la spéciation des REE en milieu organique et alcalin.

Cette spéciation, dans un souci de validation non seulement des calculs mais aussi du jeu de constantes, a été comparée aux calculs réalisés par Tang et Johannesson (2003). Leurs calculs aboutissent à une spéciation différente des REE sur la gamme de pH considérée. Ainsi, REE-HM, l'espèce complexée aux substances humiques est dominante sur une gamme de pH plus restreinte et les pourcentages de complexation atteints sont beaucoup plus faibles. En fait, il apparaît que les espèces carbonatées sont plus compétitives vis-à-vis des substances humiques que dans nos propres calculs. Ceci est dû au fait que les valeurs des constantes estimées de Tang et Johannesson (2003) sont plus faibles que les valeurs des constantes déterminées expérimentalement dans cette étude. À la vue de cette différence, il nous est paru indispensable de réaliser une étude expérimentale de compétition entre acide humique et carbonate pour la complexation des REE en solution et de comparer les résultats expérimentaux aux résultats calculés avec Model VI à l'aide des constantes déterminées expérimentalement. Les expériences ont été réalisées entre pH 6,5 et 10,5, pour trois valeurs d'alcalinité (10<sup>-2</sup>, 5 10<sup>-3</sup> et 10<sup>-3</sup> mol/L). La solution organique (complexe REE-acide humique) a été séparée de la solution inorganique (REE-carbonate) par ultrafiltration à 5 kDa. Les résultats des expériences de compétition et des calculs de spéciation sont présentés sur la figure 14. Seuls les complexes REE-carbonate

expérimentaux et calculés sont représentés. Model VI, modifié par le jeu de constantes déterminées expérimentalement, reproduit bien les résultats expérimentaux sur tout le groupe des REE. Ces resultants permettent donc (i) de valider définitivement le jeu de constantes REE-acide humique obtenus dans ce travail, de (ii) valider la capacité de Model VI à modéliser le comportement des REE en milieu organique et enfin (iii) de valider la spéciation des REE calculée dans cette étude pour la World Average River Water.

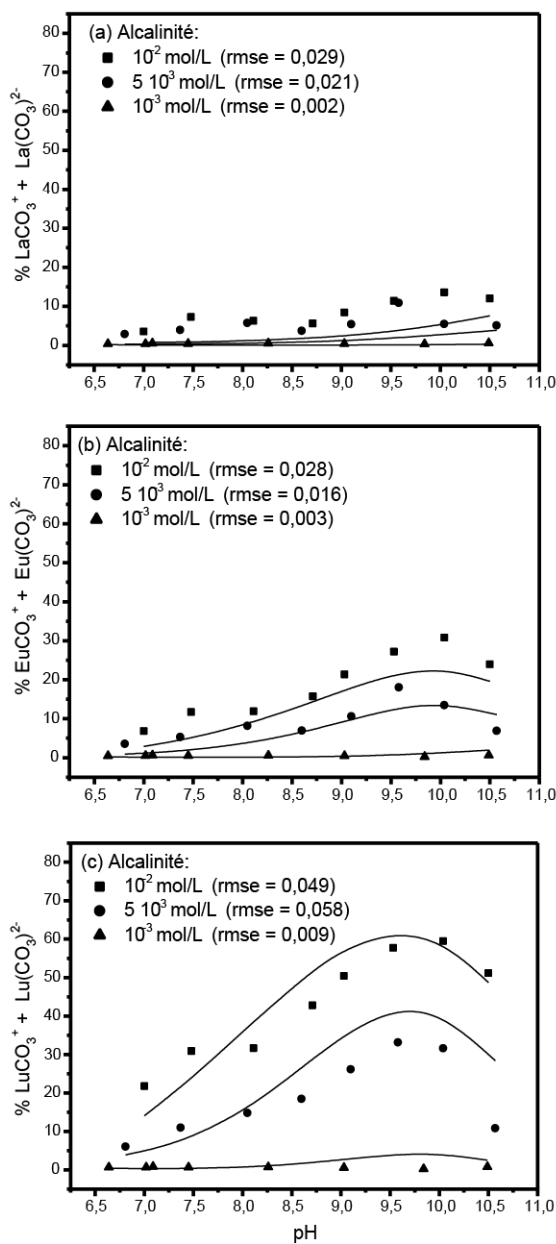


**Figure 14.** Pourcentage de REE complexées aux carbonates, mesurés (points) et calculés à l'aide de Model VI (lignes) dans les expériences de complexation compétitive entre carbonate et acide humique (10 mg/L).

## I.5. Nouveau processus de formation d'anomalie de cérium

Des expériences de compétition entre carbonates et acides humiques pour la complexation des REE ont également mis en évidence un fractionnement des REE entre ces complexants. En utilisant une méthode d'ultrafiltration, les phases complexées avec les acides humiques et les carbonates ont pu être séparées. Les résultats ont permis de mettre en évidence le développement d'une anomalie négative de Ce dans la fraction inorganique de la solution pour des pH supérieurs à 8, dont l'amplitude croît avec l'alcalinité. En vis-à-vis, une anomalie de Ce positive se développe sur les colloïdes organiques. Pour des pH > 8, le cérium s'oxyde sous forme Ce<sup>IV</sup> par formation d'un complexe carbonaté Ce<sup>IV</sup>(CO<sub>3</sub>)<sub>5</sub><sup>6-</sup>, qui peut être qualifié de précurseur. Une fois formé, ce complexe est déstructuré par les acides humiques de la solution. En effet, les constantes de complexation REE - acides humiques plus fortes que les constantes REE - pentacarbonate entraînent sa déstructuration au profit de la formation d'un complexe REE-HA. Le Ce<sup>IV</sup> ayant plus d'affinité pour les substances humiques que les autres REE trivalentes, celui-ci est préférentiellement adsorbé par les acides humiques de plus en plus électronégatifs. Il en résulte le développement d'une anomalie de Ce positive au sein de la fraction organique de la solution, et négative dans la fraction inorganique. La figure 15 illustre les spectres de distribution des taux de complexation des REE par les carbonates et les acides humiques, déterminés dans l'étude précédente. Une anomalie de Ce se développe pour les valeurs de pH supérieur à 9,1. Cette anomalie est positive pour la phase colloïdale organique et négative dans la solution carbonatée. Ce développement d'une anomalie de Ce est accompagné d'une diminution et d'une augmentation en REE, respectivement dans les solutions organique et inorganique. A partir de pH 8, cette évolution est représentative d'une forte augmentation de la complexation des REE par les carbonates au détriment de la complexation organique. Plus le pH augmente, plus la concentration des carbonates est importante et plus ils sont compétitifs des acides humiques.

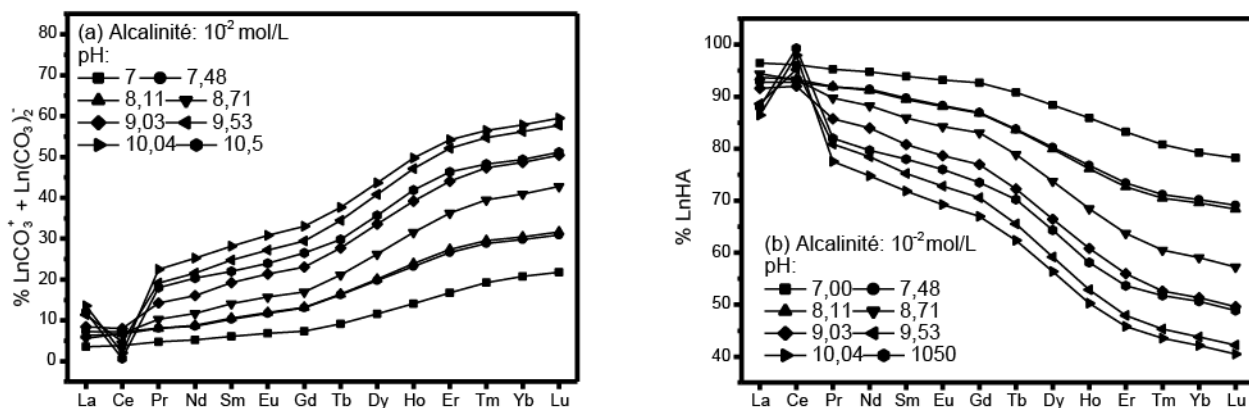


**Figure 15.** Spectre de répartition des REE correspondant respectivement, aux solutions inorganique (REE-carbonate) et organique (REE-acide humique) de l'expérience de complexation compétitive de l'acide humique et des carbonates pour REE.

Si l'évolution globale de la forme du spectre est facile à expliquer, il n'en est pas de même pour l'anomalie de Ce. Quel est le mécanisme responsable de son développement? La formation d'une anomalie de Ce est, comme nous l'avons vu précédemment, le fait d'une oxydation de Ce(III) en Ce(IV). Dans les eaux oxydantes rencontrées à la surface de la terre cette oxydation ne peut normalement avoir lieu ( $\text{pe}^0(\text{CeIII/CeIV}) = +29,47$  se trouve hors du domaine de potentiel de l'eau), si ce n'est en présence de surfaces oxydantes et/ou de bactéries spécifiques (Moffet, 1990; Koeppenkastrop et De Carlo, 1992; De Carlo et al., 1998; Bau, 1999; Ohta et Kawabe, 2001). Dans l'expérience de complexation compétitive des REE, l'un ou l'autre des ligands présents pourrait donc induire une chute du  $\text{pe}^0$  du couple redox Ce(IV)/Ce(III) est induire l'oxydation du Ce(III) en Ce(IV). Möller et Bau (1993) ont observé dans les eaux alcalines du lac Van (Turquie), la formation d'une anomalie positive de Ce. Ils l'ont expliquée par la formation d'un complexe pentacarbonaté de Ce(IV),  $\text{Ce}^{\text{IV}}(\text{CO}_3)_5^{6-}$ , permettant la stabilisation du Ce dans la solution par rapport aux autres REE et donc la formation d'une anomalie positive de Ce. La formation d'un tel complexe a également été mise en évidence par Doležal et Novák (1959), et Riglet-Martial et al. (1998) dans des études électrochimiques. Ils ont ainsi proposé la demi-équation de formation suivante:

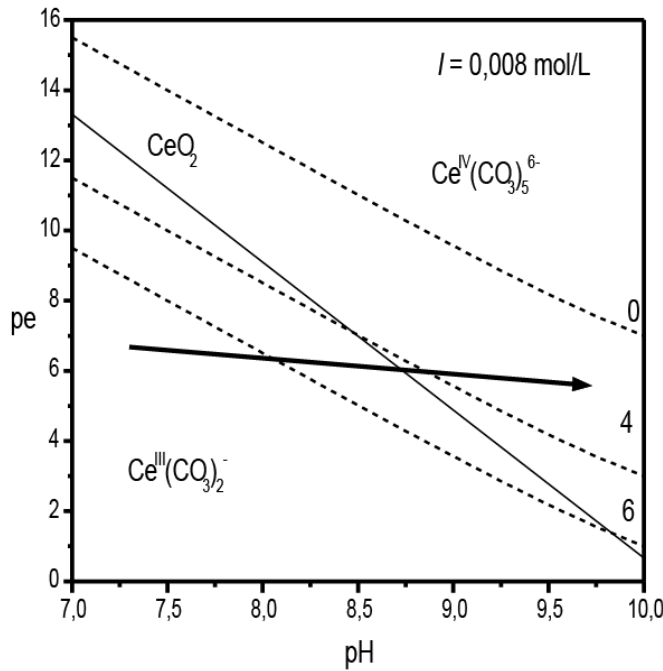
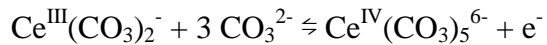
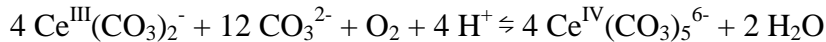
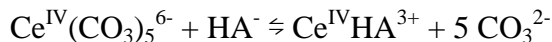


**Figure 16.** Diagramme pe-pH du système Ce-C-O-H retracé pour la force ionique de l'expérience de complexation compétitive des REE par l'acide humique et les carbonates. Les lignes noires représentent les réactions stables et les lignes en pointillées les réactions métastables. La flèche noire correspond aux conditions de pe et pH des expériences (données issues de Doležal et Novák, 1959; De Baar et al., 1988; Möller et Bau, 1993).

La question est maintenant de savoir si une telle réaction peut se produire dans les conditions expérimentales de l'expérience de complexation compétitive. Pour cela, un diagramme *pe-pH* du système Ce-C-O-H a été réalisé à la force ionique de nos expériences (données issues de Doležal et Novák, 1959; De Baar et al., 1988; Möller et Bau, 1993; Figure 16). Comme montré par Möller et Bau (1993), même si la valeur exacte du coefficient d'activité  $\gamma$  du complexe pentacarbonaté-Ce<sup>IV</sup> est inconnue, une valeur estimée de 6 peut être utilisée dans le calcul de la constante  $\log Q$  avec  $Q = \gamma(\text{Ce}^{\text{III}}(\text{CO}_3)_2^-) / \gamma(\text{Ce}^{\text{IV}}(\text{CO}_3)_5^{6-})$ . Pour des pH compris entre 8 et 9 et pour un *pe* de l'ordre de 7, il apparaît clairement que l'équilibre  $a(\text{Ce}^{\text{III}}(\text{CO}_3)_2^-)/a(\text{Ce}^{\text{IV}}(\text{CO}_3)_5^{6-})$  est atteint avant l'équilibre  $a(\text{Ce}^{\text{III}}(\text{CO}_3)_2^-)/a(\text{Ce}^{\text{IV}}\text{O}_2)$ . Ainsi, le Ce ne peut pas précipiter sous forme de  $\text{CeO}_2$  car il se complexe aux carbonates pour former le complexe soluble  $\text{Ce}^{\text{IV}}(\text{CO}_3)_5^{6-}$ . L'oxydation du Ce (III) en Ce(IV) est donc tout à fait possible du fait de la complexation par les carbonates. Etant données les conditions expérimentales et la composition de la solution lors de l'oxydation du Ce(III) en Ce(IV), l'équation de réduction correspondante est probablement la réduction de l'oxygène dissous ( $\text{pe}^0 = +20,75$  pour le couple  $\text{O}_2(\text{g})/\text{H}_2\text{O}$ ), selon la réaction :



Afin de connaître la faisabilité d'une telle réaction, la variation d'énergie libre de la réaction ( $\Delta G_R^0$ ) a été calculée. Les  $\Delta G_f^0$  des complexes  $\text{Ce}^{\text{III}}(\text{CO}_3)_2^-$  et  $\text{Ce}^{\text{IV}}(\text{CO}_3)_5^{6-}$  n'étant pas disponibles dans la littérature, ils ont été extrapolés à partir des constantes de formation de chaque complexe (Riglet-Martial et al., 1998) et recalculées pour une force ionique 0, grâce à l'équation de Davies. La variation d'énergie libre de la réaction est égale à -947,84 KJ/mol. Les  $\Delta G_R^0$  étant négatif, la réaction est donc spontanée. Dans le cas de la réaction décrite plus haut, l'oxydation du Ce(III) en Ce(IV) devrait aboutir à la formation d'une anomalie positive de Ce dans la solution inorganique, d'une manière équivalente à ce qui est décrit par Möller et Bau (1993). Or, ce sont les complexes organiques colloïdaux qui portent l'anomalie positive de Ce. Le Ce tétravalent a plus d'affinité pour les surfaces solides ou colloïdales que les REE trivalentes et sera donc plus adsorbé que les REE voisines qui elles restent trivalentes. Ainsi, Nash et Sullivan (1991) ont montré que la constante de complexation Ce(IV)-carboxylate est de 2 ordres de grandeur supérieurs à la constante Ce(III)-carboxylate. En considérant que les fonctions carboxyles sont les fonctions de surface les plus abondantes à la surface de l'acide humique, une fois le complexe  $\text{Ce}^{\text{IV}}(\text{CO}_3)_5^{6-}$  formé et donc le Ce oxydé en Ce(IV), le complexe est détruit par compétition avec l'acide humique selon la réaction :



Le complexe  $\text{Ce}^{\text{IV}}(\text{CO}_3)_5^{6-}$  joue donc le rôle de précurseur à l'adsorption de Ce(IV) par l'acide humique.

## Partie II

# Quantification des rôles respectifs de la matière organique et des oxydes de Fe et de Mn sur la spéciation des terres rares dans des eaux naturelles (eaux souterraines et de rivières)

### Articles clés:

**Pourret O.**, Davranche M., Gruau G., Dia A. (2007) Organic complexation of rare earth elements in natural waters: Evaluating model calculations from ultrafiltration data. *Geochimica et Cosmochimica Acta* 71, 2718-2735.

**Pourret O.**, Dia A., Davranche M., Gruau G., Hénin O., Angée M. (2007) Organo-colloidal control on major- and trace-element partitioning in shallow groundwaters: confronting ultrafiltration and modelling. *Applied Geochemistry* 22, 1568-1582.

**Pourret O.**, Gruau G., Dia A., Davranche M., Molénat J. (2010) Colloidal control on the distribution of rare earth elements in shallow groundwaters. *Aquatic Geochemistry*, 16: 31-59.



## **II - Quantification des rôles respectifs de la matière organique et des oxydes de Fe et de Mn sur la spéciation des terres rares dans des eaux naturelles (eaux souterraines et de rivières)**

### **II.1. Eaux souterraines de versant**

Le suivi temporel des concentrations et des formes de spectres de REE le long d'un transect d'un bassin versant expérimental a été effectué (Figure 17). Une grande stabilité des formes de spectres de REE a été observée au cours du temps alors qu'une variabilité spatiale a été observé le long du transect. Des ultrafiltrations ont été effectuées sur certains de ces échantillons et ont montré que la spéciation de ces échantillons était plus ou moins contrôlée par la matière organique dissoute (Figure 18). Ces échantillons présentent, en effet, des concentrations en carbone organique dissous croissantes d'amont en aval. Comme suggéré lors de différentes expérimentations, le spectre global de REE d'un échantillon d'eau naturelle représente la somme de différentes fractions organiques et inorganiques. Des calculs de spéciation ont été effectués sur ces mêmes échantillons et ceux-ci ont montré qu'il s'agissait d'un mélange entre une eau amont inorganique et une eau de versant organique (Figure 19). Une telle modélisation permet, en outre, de quantifier l'impact d'une variation de pH sur un tel mélange (Figure 20). En effet, les données révèlent que l'amplitude des anomalies Ce diminue avec la pente et correspond au changement de spéciation des REE ; les eaux souterraines en bas de versant ayant des REE principalement liés à des colloïdes organiques. Le suivi temporel montre que la source des colloïdes est située dans les horizons riches en matière organique du sol, et que l'introduction de colloïde se produit principalement quand la nappe phréatique monte lors des saisons humides. La topographie est, par conséquent, le facteur clé qui contrôle la variabilité spatiale de l'anomalie de Ce dans ces eaux souterraines peu profondes (Figure 21). Enfin, dans la fraction  $<0,2\text{ }\mu\text{m}$  la signature en REE vient de deux sources solides: la première est située dans le schiste profond, l'autre située dans l'horizon de sol riche en matière organique.

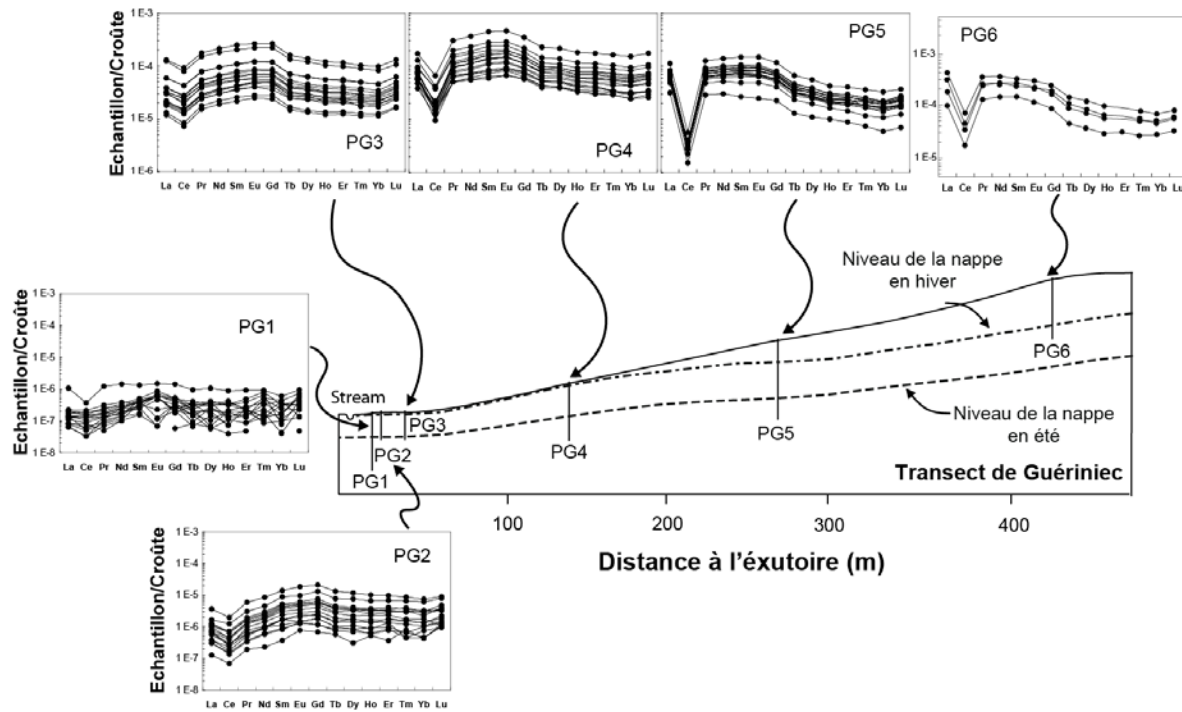


**Figure 17.** Evolution des spectres de REE normalisés à la crûte continentale supérieure en fonction de la pente, transect de Guériniec, Kervidy-Naizin (France).

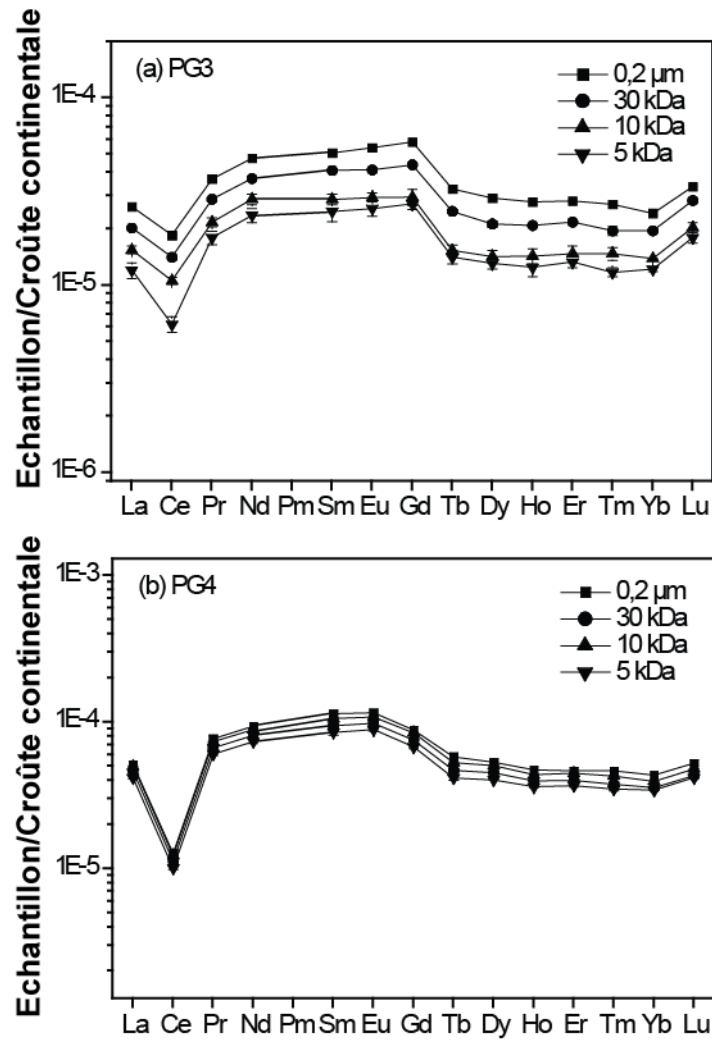


**Figure 18.** Spectres de REE normalisés à la crûte continentale supérieure après ultrafiltrations successives ( $0,2 \mu\text{m}$ , 30 kDa, 10 kDa et 5 kDa) pour les piézomètres (a) PG3 et (b) PG4.

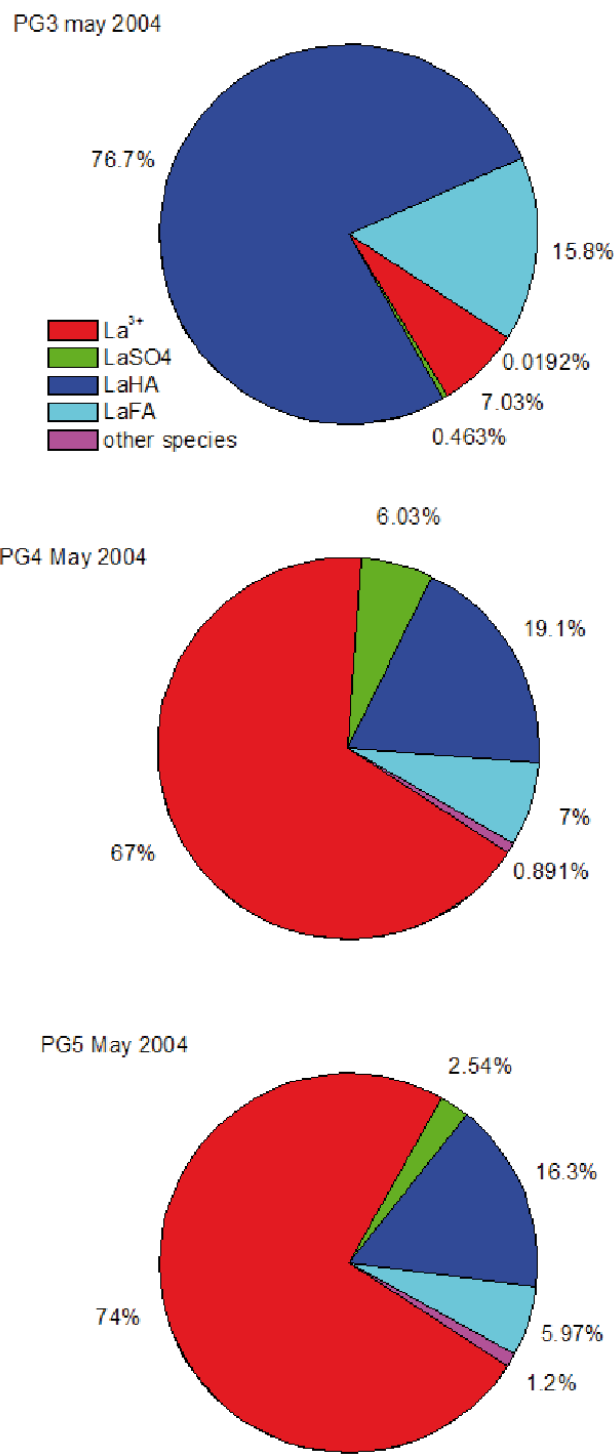


**Figure 19.** Résultats des calculs de spéciation en utilisant Model VI pour les eaux souterraines PG3, PG4 et PG5 en mai 2004.

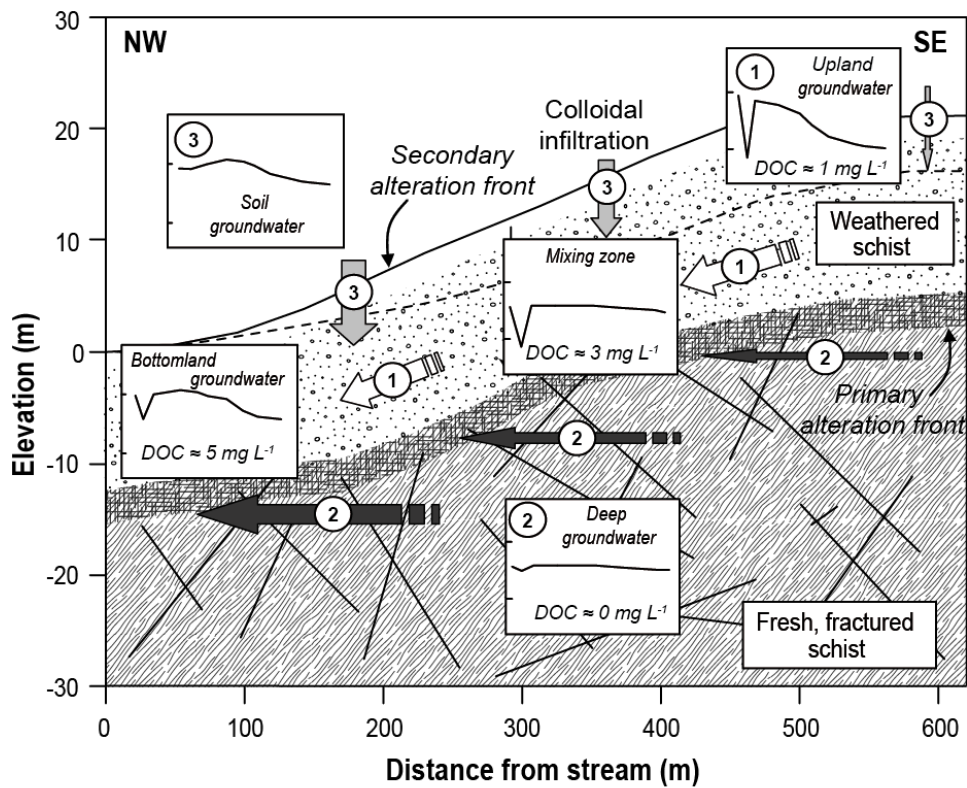


**Figure 20.** Scénario illustrant le fonctionnement du transect de Guériniec et la présence de trois flux expliquant la signature géochimique des eaux souterraines du bassin versant de Kervidy Naizin.

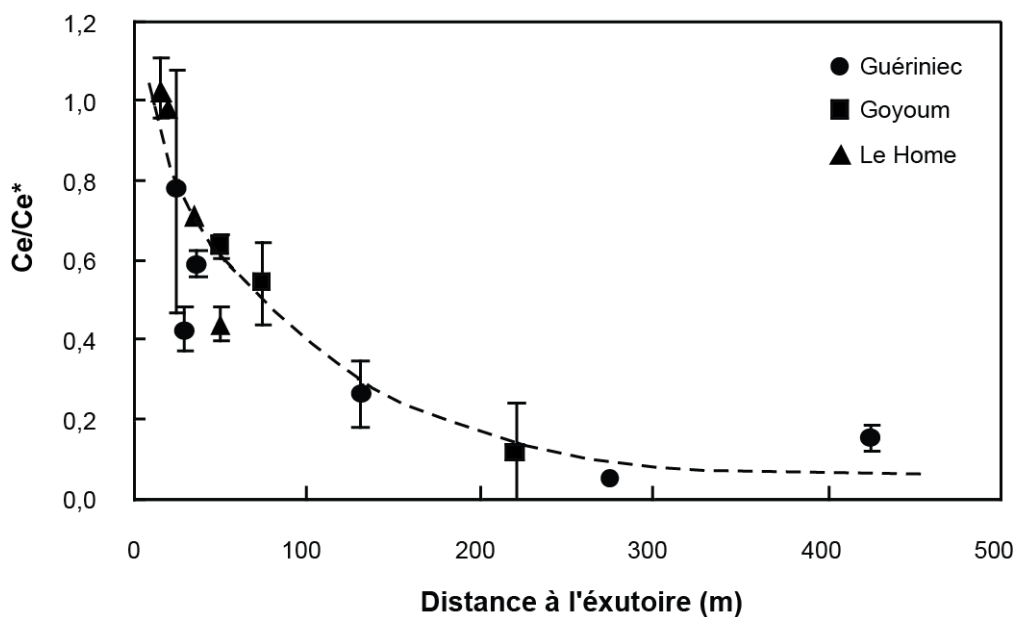


**Figure 21.** Evolution de l'anomalie de cérium en fonction de la distance à l'écoulement.

## II.2. Eaux souterraines de zone humide

De petites cellules d'ultrafiltration de seuils de coupure décroissants (30 kDa, 10 kDa et 5 kDa) ont été testées sur des eaux de zones humides, riches en matières organiques dissoutes (MOD), dans le but d'étudier les interactions MOD-métaux. Il s'agissait de distinguer la proportion de métaux traces présents à l'état libre de cations hydratés (correspondant à une fraction biodisponible), de la proportion de métaux complexés à de la matière colloïdale organique ou inorganique. Alors que les éléments alcalins, alcalino-terreux et le Ni semblent se comporter comme des éléments libres, non complexés par la MOD colloïdale, l'U, le Cu ou les REE semblent directement portés par la fraction colloïdale organique (Figure 22). Ces résultats sont en accord avec les calculs de spéciation réalisés avec Model VI (Figure 23). Dans la mesure où le piégeage et le transport des éléments traces liés à la matière organique doivent être mieux appréhendés pour comprendre le rôle fonctionnel joué par la matière organique à l'interface eau/sol quant à la dynamique des éléments traces métalliques, d'autres études dédiées aux variations conjointes des distributions de la MOD colloïdale et des éléments traces devront être entreprises dans des eaux provenant de différents environnements riches en MOD. Ces expériences d'ultrafiltration d'eau de sols riches en matières organiques ont montré un fractionnement des REE entre les différentes tailles de matières organiques (~ 90 %) et la phase inorganique (~ 10 %). Une relation linéaire est observée entre la concentration en REE et la concentration en carbone organique dissous.

Comme suggéré précédemment, le spectre global de REE d'un échantillon d'eau souterraine représente la somme de différentes fractions organiques et inorganiques. La comparaison d'expériences d'ultrafiltration sur deux échantillons d'eaux de sol riches en matières organiques (Figure 24), l'un en conditions réductrices et l'autre en conditions oxydantes, montre une variation de l'intensité de l'anomalie de Ce de la fraction inorganique (i.e., fraction < 5 kDa).

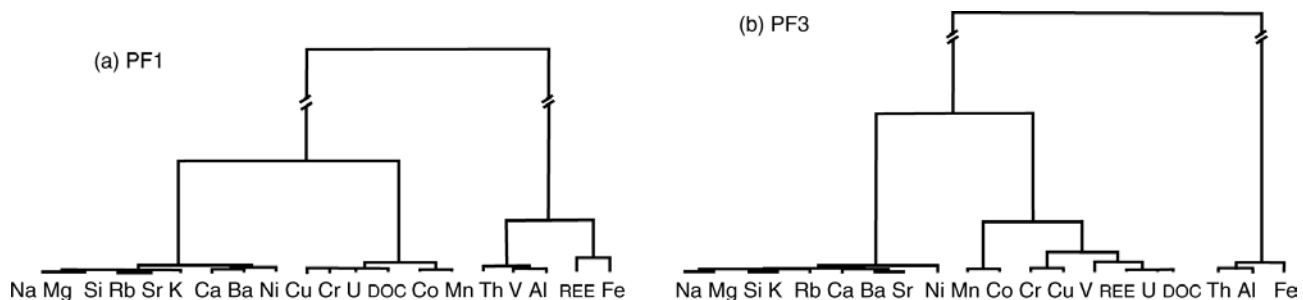


**Figure 22.** Classifications hiérarchiques ascendantes des eaux de zone humides (a) PF1 et (b) PF3.

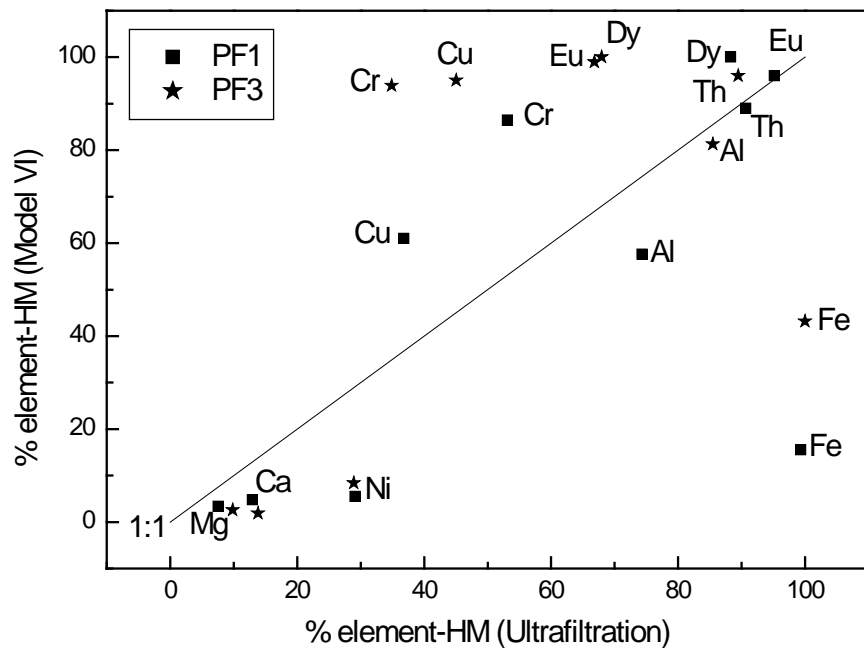


**Figure 23.** Pourcentage d'éléments complexés aux substances humiques calculé (avec Model VI) en fonction du pourcentage d'éléments complexés aux substances humiques observé (par ultrafiltration).

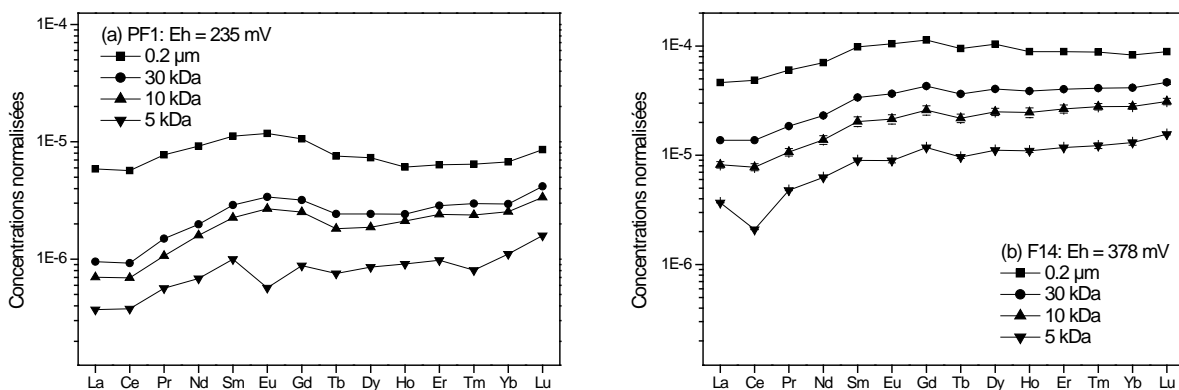


**Figure 24.** A Spectres de REE normalisés à la croûte continentale supérieure pour les différentes ultrafiltrations réalisées pour des échantillons d'eau de zones humides (a) en conditions réductrices ( $Eh = 235 \text{ mV}$ ) et (b) en conditions oxydantes ( $Eh = 378 \text{ mV}$ ).

## II.3 Eaux de rivières

### II.3.1. Spéciation des REE dans une eau de rivière de composition moyenne et oxydante

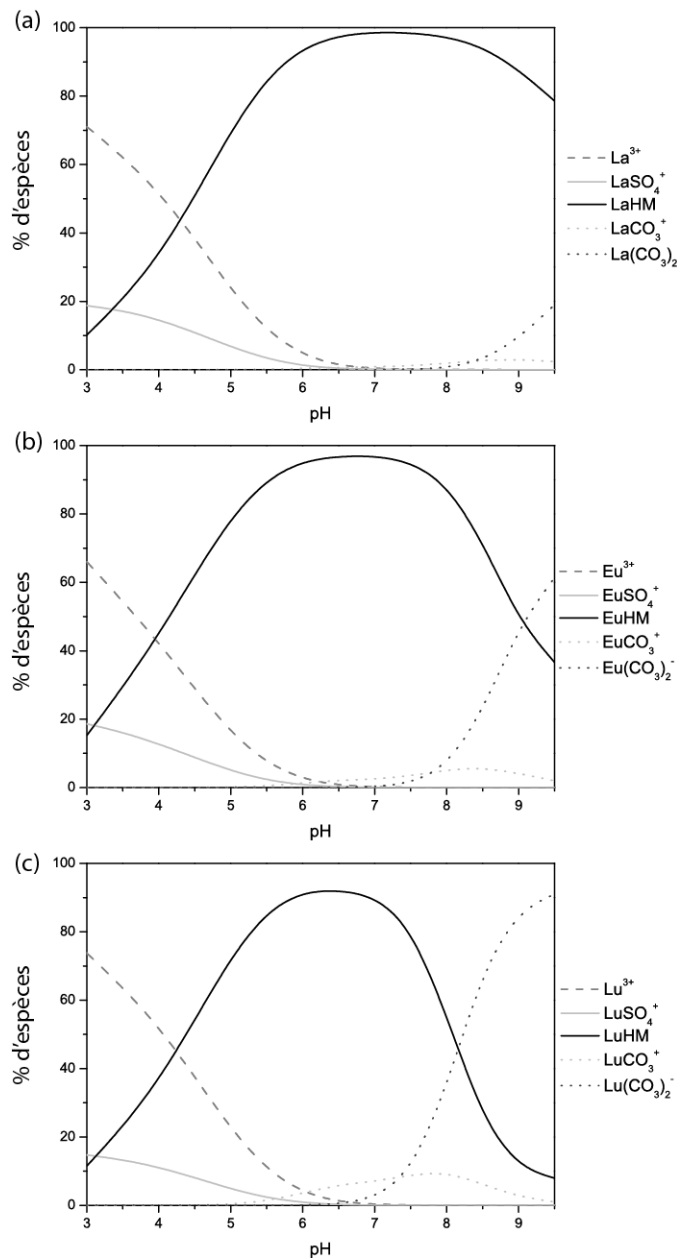


**Figure 25.** Spéciation calculée des La, Eu et Lu dans la World Average River Water à partir des log K<sub>MA</sub> expérimentaux spécifiques à Model VI (partie 1).

Le jeu de constantes précédemment déterminé (partie 1) a été utilisé afin de calculer la spéciation des REE dans une eau de rivière de composition moyenne, la ‘World Average River

Water'. Cette composition moyenne d'eau de rivière a été choisie de façon à comparer nos résultats à ceux obtenus par Tang et Johannesson (2003) pour la même eau, mais à l'aide de constantes estimées et de Model V. Les calculs ont donc été réalisés en utilisant les mêmes concentrations moyennes en ions majeurs, cations compétiteurs (i.e., Fe, Al), et COD (5 mg/L) que celles utilisées par Tang et Johannesson (2003). Dans ces calculs, les substances humiques sont supposées être constituées de 80 % d'acides humiques et de 20 % d'acides fulviques. De plus, les concentrations totales en éléments sont considérés comme invariantes sur la gamme de pH sauf pour les carbonates,  $\text{HCO}_3^-$  et  $\text{CO}_3^{2-}$ .

Le jeu de constantes introduit dans Model VI montre que les REE sont sous forme d'espèces libres  $\text{REE}^{3+}$  et sulfates à pH acide (Figure 25). Puis entre pH 5-5,5 et 7-8,5, l'espèce dominante est la forme complexée aux substances humiques ( $\text{REE-HM} \geq 60\%$ ). Au-delà de pH>8, la forme complexée aux carbonates devient prépondérante. Elle atteint ainsi un pourcentage de 80 % pour le Lu. Cette spéciation, dans un souci de validation non seulement des calculs mais aussi du jeu de constantes, a été comparée aux calculs réalisés par Tang et Johannesson (2003). Leurs calculs aboutissent à une spéciation différente des REE sur la gamme de pH considérée. Ainsi,  $\text{REE-HM}$ , l'espèce complexée aux substances humiques est dominante sur une gamme de pH plus restreinte et les pourcentages de complexation atteints sont beaucoup plus faibles. En fait, il apparaît que les espèces carbonatées sont plus compétitives vis-à-vis des substances humiques que dans nos propres calculs. Ceci est dû au fait que les valeurs des constantes estimées de Tang et Johannesson (2003) sont plus faibles que les valeurs des constantes déterminées expérimentalement dans cette étude.

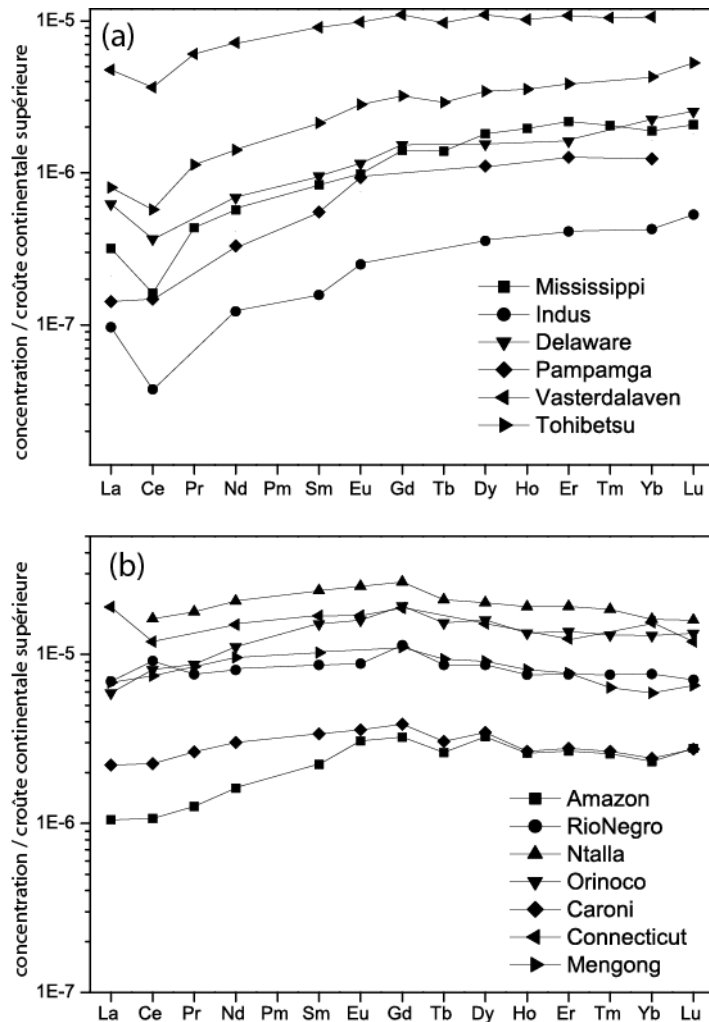


**Figure 26.** Spectres de REE d'eaux de rivières présentant (a) un enrichissement en REE lourdes (Taylor et McLennan, 1985), (b) un enrichissement en REE moyennes, spectres concaves (Goldstein et Jacobsen, 1988; Elderfield et al., 1990; Sholkovitz, 1995; Deberdt et al., 2002).

## **II.3.2 Les processus de transport et de fractionnement des terres rares dans l'eau des ruisseaux - dynamique**

Comme vu précédemment l'étude des REE est un outil puissant pour comprendre le comportement des métaux traces dans les eaux superficielles et souterraines. La distribution des REE est ainsi utilisée pour comprendre leur fractionnement et ainsi identifier les processus tels que la complexation de surface et les complexations en solution ou encore identifier la précipitation et la dissolution des phases minérales spécifiques (Gaillardet et al., 2003). Des études récentes ont montré que la fraction de REE  $<0,45$  ou  $<0,22 \mu\text{m}$  des eaux de surfaces et souterraines est principalement présente sous forme colloïdale plutôt que vraiment dissoute (Gaillardet et al., 2003). Les colloïdes organiques et/ou minéraux jouent un rôle majeur dans la mobilisation et la spéciation des éléments traces dans les eaux de rivières. Les paramètres physico-chimiques (pH, Eh, T, force ionique ...) sont les facteurs qui contrôlent la mobilisation colloïdale.

Récemment, Steinmann et Stille (2008) ont observé sur des échantillons d'eau filtrés à  $0,45 \mu\text{m}$  dans un cours d'eau du Massif Central français un appauvrissement croissant en REE légères d'amont en aval, sur une distance de moins de 10 km. Cette évolution est liée à l'indice de saturation (SI) des oxyhydroxydes de Fe. Les eaux des cours d'eau ont des spectres de REE semblables ceux de la roche basaltique en amont, où les échantillons sont fortement sursaturés par rapport aux oxyhydroxydes de Fe. Steinmann et Stille (2008) ont interprété cette évolution par la présence de colloïdes de Fe / Mn porteurs de REE qui se forment dans le flux d'eau et enfin précipitent sous forme de particules de Fe / Mn-oxyhydroxyde.

Pour confirmer ces hypothèses, des expériences d'ultrafiltration utilisant de petits dispositifs d'ultracentrifugation ont été effectuées (30 kDa, 10 kDa et 3 kDa) pour étudier le contrôle colloidal sur le fractionnement des éléments majeurs et traces dans ces cours d'eau. Six sites ont ainsi été échantillonnés dans le bassin versant du Malaval, d'amont en aval (Massif Central, France) au cours de deux campagnes d'échantillonnage (Septembre 2009 et Juin 2010) et analysés pour les éléments majeurs et traces, et le carbone organique. En plus de l'évolution spatiale, des mélanges entre deux confluences du Malaval ont été également étudiés. L'objectif principale de cette étude est de vérifier l'hypothèse de Steinmann et Stille (2008) par une analyse directe de la fraction colloïdale utilisant la procédure d'ultrafiltration décrite par Pourret et al. (2007b) pour séparer les colloïdes. Cette nouvelle méthode d'analyse a été complétée par des calculs de spéciation afin d'évaluer plus en détail la compétition entre les colloïdes organiques et inorganiques sur le transport des REE et le fractionnement dans l'eau du ruisseau. Les interactions avec les colloïdes organiques ont été décrites à l'aide de Model VI comme décrits par Pourret et al. (2007a) et intégré dans PHREEQC par Marsac et al. (2011) ; ceci a ainsi permis de considérer l'adsorption sur les oxyhydroxydes de Fe.

Les spectres de REE montrent une anomalie de Ce variable et un enrichissement en REE lourdes d'amont en aval (Figures 27 et 28). De plus, la plupart des éléments se comportent de manière cohérente dans le temps et leur spéciation évolue avec la distance à la source. Basé sur l'analyse en composantes principales et des classifications ascendantes hiérarchiques (Figure 29) effectuée sur l'ensemble des données d'ultrafiltration, trois groupes d'éléments ayant un comportement chimique spécifique peuvent être distingués: (i) un groupe dissous (Na, Mg, Si, K, Ca, Rb, Sr), (ii) un groupe réactif (Al, Fe, Y, Pb, Cu, Ni, As, U, Zr) et, (iii) un groupe

intermédiaire (Co). En regardant plus en détail chacun de ces groupes, les résultats suggèrent que (i) les alcalins et les alcalino-terreux sont présents sous forme d'espèces dissoutes, tandis que (ii) les REE et la plupart des autres éléments métalliques sont liés à la matière colloïdale. Enfin, (iii) quelques éléments, comme le cobalt, ont un comportement ambivalent: dans certains échantillons, ils se comportent comme le premier groupe et dans d'autres comme le deuxième groupe. Cependant, concernant le groupe colloidal, il est difficile de distinguer le rôle respectif des matières organiques et des oxyhydroxydes de Fe et Mn. Il est à noter que lors des ultrafiltrations une part importante (50 à 60%) des REE se trouve sous forme colloidale, et une faible part peut être interprétée comme organique (Figure 30). Ceci est confirmé par la modélisation qui montre qu'en amont la spéciation des REE est gouvernée par les matières organiques alors qu'en aval il y a une compétition entre phase carbonatée et phase organique (Figure 31).

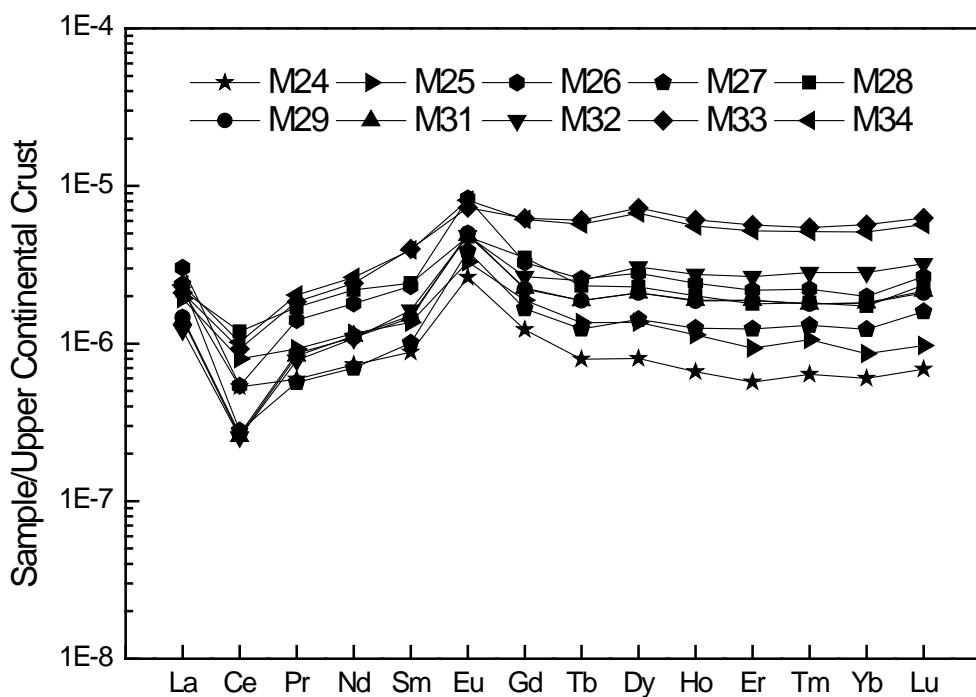


**Figure 27.** Spectres de REE normalisés à la croute continentale supérieure pour les échantillons du cours d'eau Malaval.

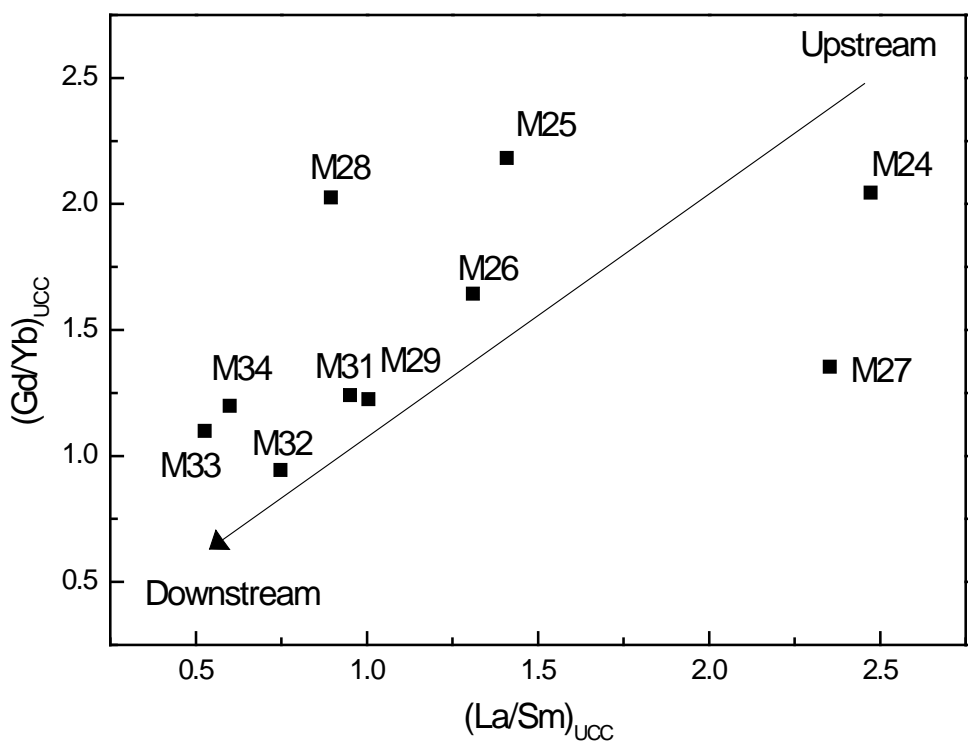


**Figure 28.** Evolution du fractionnement en REE d'amont en aval du cours d'eau Malaval.

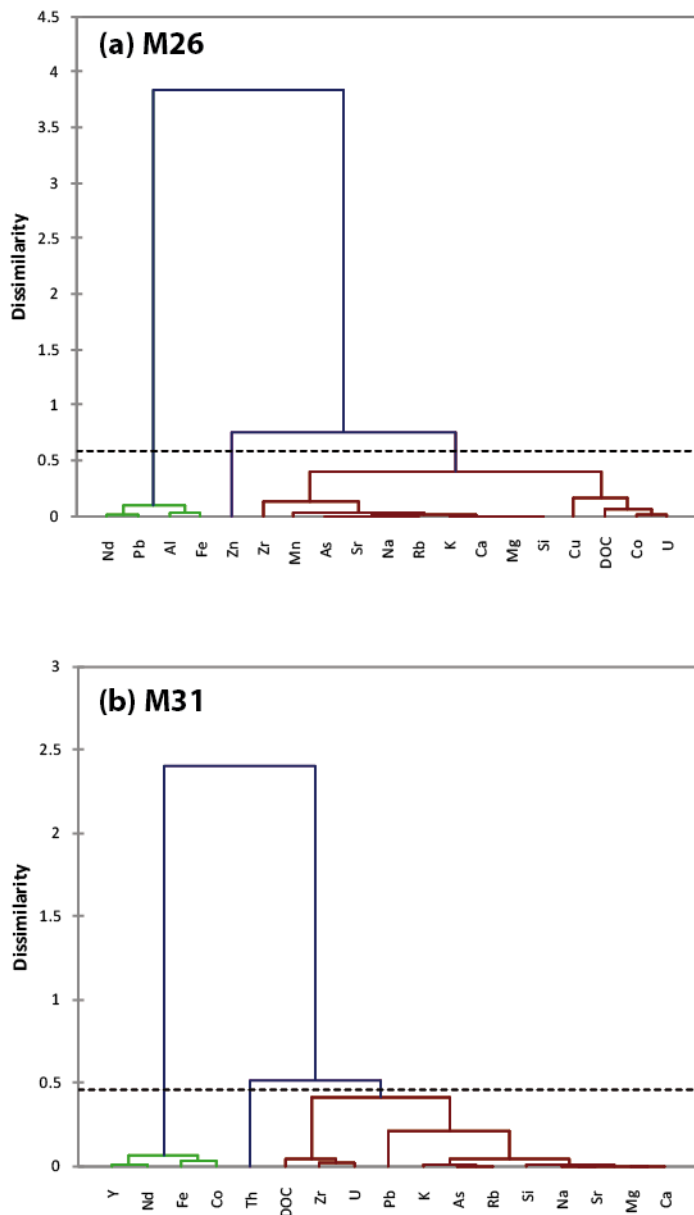


**Figure 29.** Classifications hierarchiques ascendantes des échantillons du cours d'eau Malaval (a) M26 et (b) M31.

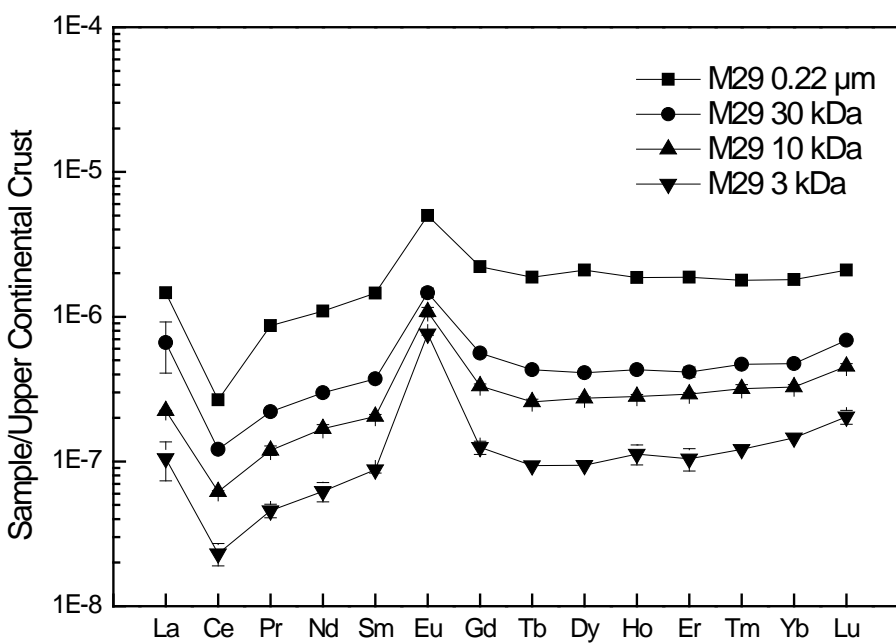
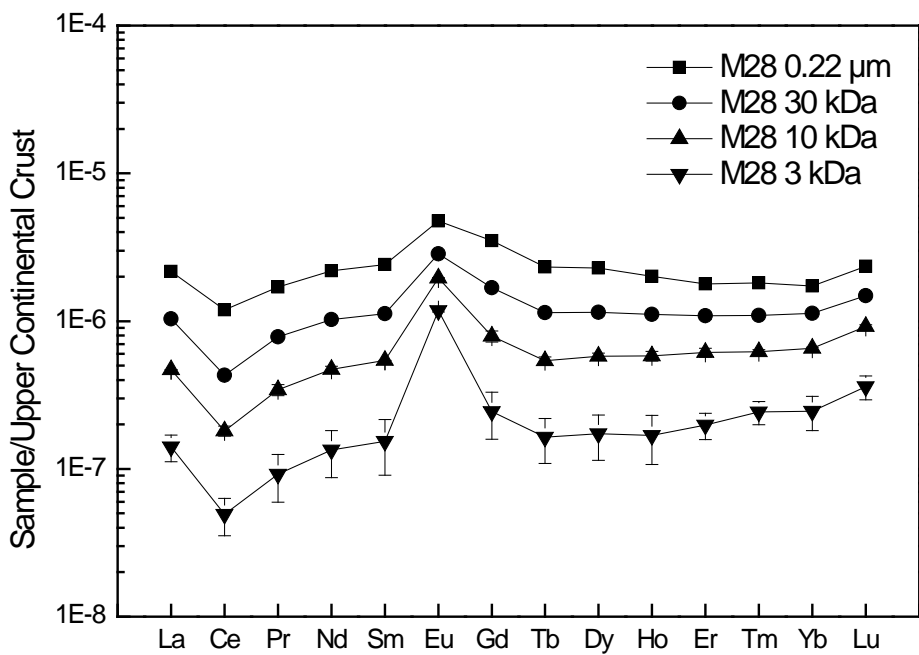


**Figure 30.** Spectres de REE normalisés à la crûte continentale supérieure après ultrafiltrations successives ( $0,2\text{ }\mu\text{m}$ ,  $30\text{ kDa}$ ,  $10\text{ kDa}$  et  $5\text{ kDa}$ ) pour les échantillons (a) M28 et (b) M29.

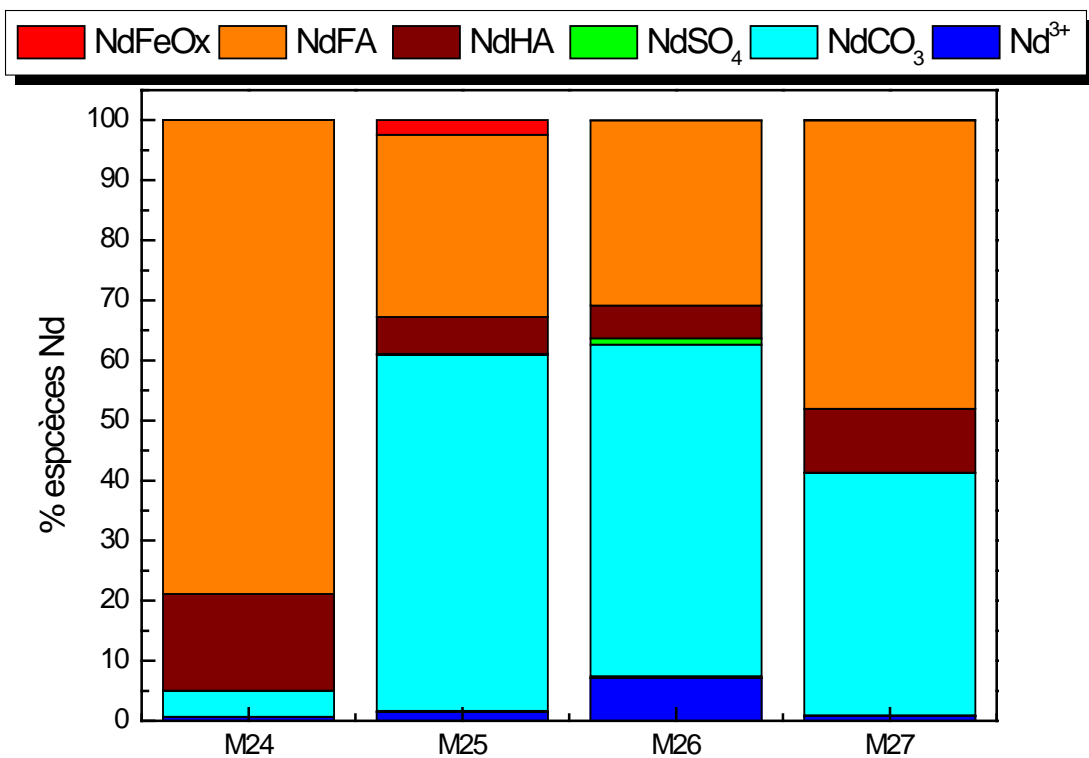


**Figure 31.** Résultats des calculs de spéciation en utilisant Model VI pour les eaux souterraines M24, M25, M26 et M27 en septembre 2009.

## Partie III

# Utilisation du fractionnement des terres rares dans la compréhension de minéralisations

### Articles clés:

Chaux L., Routier T., **Pourret O.**, Steinmann M., et Bontemps S. (2011) Mobility of Rare Earth Elements during Igneous Rocks Weathering and Associated Stream Water Transport (Malaval Catchment, Massif Central, France). *Mineralogical Magazine*, 75(3): 647.

**Pourret O.**, Tuduri J., Armand R., Bayon G., et Steinmann M. (2012) Reassessment of the rare earth elements external cycle in french watersheds - a high potential resource for the future. *Mineralogical Magazine*, 76(6): 2247.

Tuduri J., **Pourret O.**, Chauvet A., Barbanson L., Gaouzi A. et Ennaciri A. (2011) Rare earth elements as proxies of supergene alteration processes from the giant Imiter silver deposit (Morocco). In: Barra, F., Reich, M., Campos, E., and Tornos, F., eds., *Let's Talk ore deposits, Proceeding of the eleventh biennial SGA meeting*, 2: Antofagasta, Ediciones Universidad Católica del Norte, Antofagasta, Chile, p. 826-828.



### **III – Utilisation du fractionnement des terres rares dans la compréhension de minéralisations**

#### **III.1. Altération et mise en solution**

L'altération des roches, se produit au sein de la zone critique à l'interface entre l'atmosphère, la biosphère, l'hydroosphère et lithosphère. Il s'agit d'un processus majeur dans l'étude des cycles biogéochimiques globaux et contribue également à l'évolution des paysages (Gaillardet et al., 2003). L'altération chimique consiste à dissoudre partiellement ou complètement les minéraux des roches pour former des profils d'altération. Les ions dissous sont transportés par les eaux de ruissellement, de surface, souterraine, vers les océans. Afin d'établir un lien entre le mode de distribution des REE en solution et le substratum rocheux, une étude détaillée de la modification du socle granitique et gneissique ainsi que du basalte d'un petit bassin versant de montagne a été réalisé (bassin versant Malaval, Massif Central, France). La minéralogie des échantillons frais et altérés a été déterminée par microscopie et diffraction des rayons X. Les éléments majeurs et traces ont été déterminés par ICP-AES et ICP-MS. Une comparaison entre les spectres de REE des horizons les plus altérés de chaque profil et la fraction <0,22 µm du cours d'eau du Malaval a été réalisée. Les résultats suggèrent des mécanismes d'altération similaires pour le granite et le gneiss, qui est principalement contrôlée par la dissolution des plagioclases conduisant à des pertes en Na<sub>2</sub>O, CaO, SiO<sub>2</sub> et Al<sub>2</sub>O<sub>3</sub> (Figure 32). La mobilisation du K<sub>2</sub>O peut être liée à la fracturation des feldspaths alcalins, tandis que l'évolution des spectres de REE est principalement contrôlée par la distribution du zircon. Dans les profils d'altération sur basalte, l'olivine est le premier minéral à être oxydé conduisant à une mobilisation de MgO. La transformation des plagioclases en argiles est accompagnée par des pertes de Na<sub>2</sub>O et CaO. La chute des concentrations en fer est associée à la fracturation des pyroxènes.

Les spectres de REE normalisés du profil d'altération des basaltes montrent un léger appauvrissement tout en gardant les spectres des basaltes continentaux (Figure 33). Les différentes extractions séquentielles montrent que moins de 0,1% des REE sont mobiles et sont lessivables à l'eau ; les spectres de REE normalisés à la croûte continentale supérieure ont la même forme que les roches initiales (Figure 34). Si cette fraction est normalisée aux eaux des cours (i.e., Malaval, voir partie 2), les spectres sont plats (Figure 35). Ainsi, une comparaison entre les spectres de REE des horizons les plus altérés des profils d'altération suggère que la chimie de l'eau du Malaval adjacent est principalement contrôlée par l'altération chimique du basalte. Cette constatation est d'ailleurs confirmée par les extractions séquentielles effectuées sur des échantillons de basalte qui ont montré que la fraction hydrolisable donnait la signature à l'eau des ruisseaux (Figure 36).

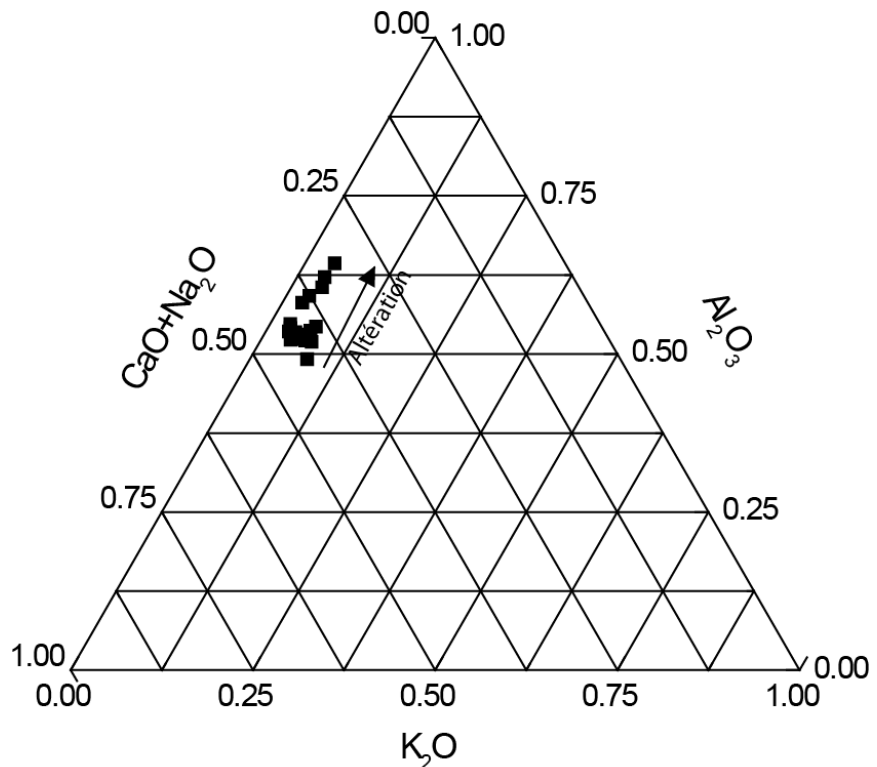


**Figure 32.** Diagramme ternaire  $\text{Al}_2\text{O}_3/\text{CaO}+\text{Na}_2\text{O}/\text{K}_2\text{O}$  illustrant le profil d'altération du basalte

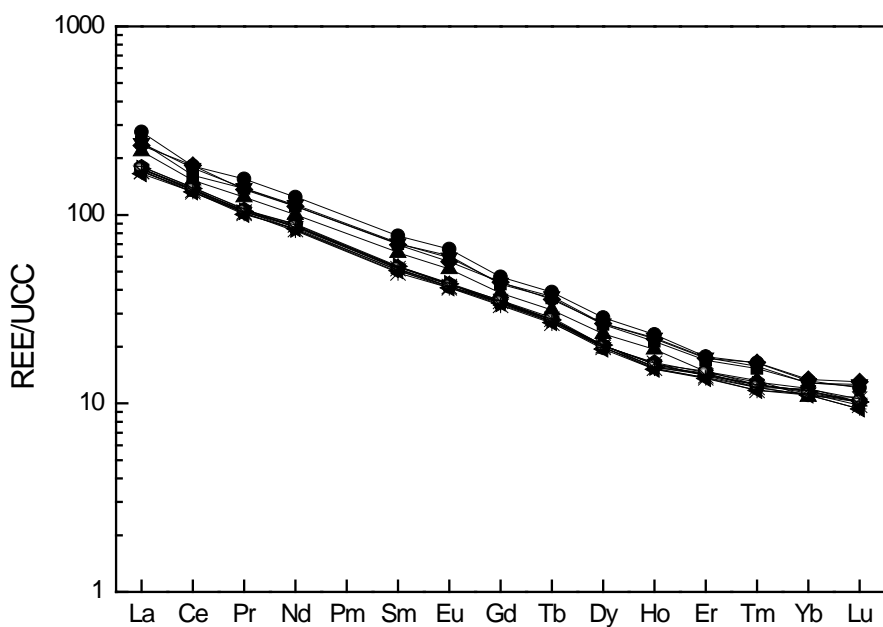


**Figure 33.** Spectres de REE normalisés à la crûte continentale supérieure des échantillons du profil d'altération des basaltes.

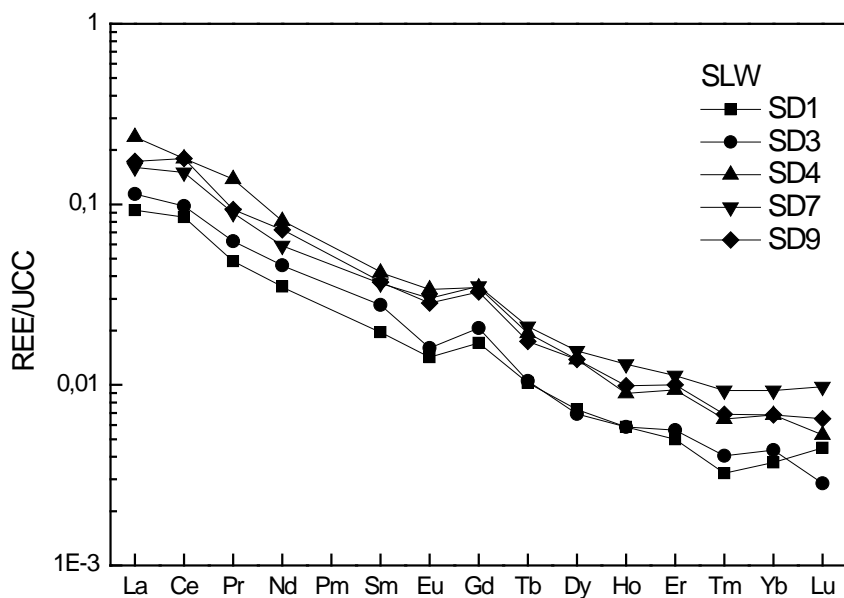


**Figure 34.** Spectres de REE normalisés à la crête continentale supérieure des fractions libres.

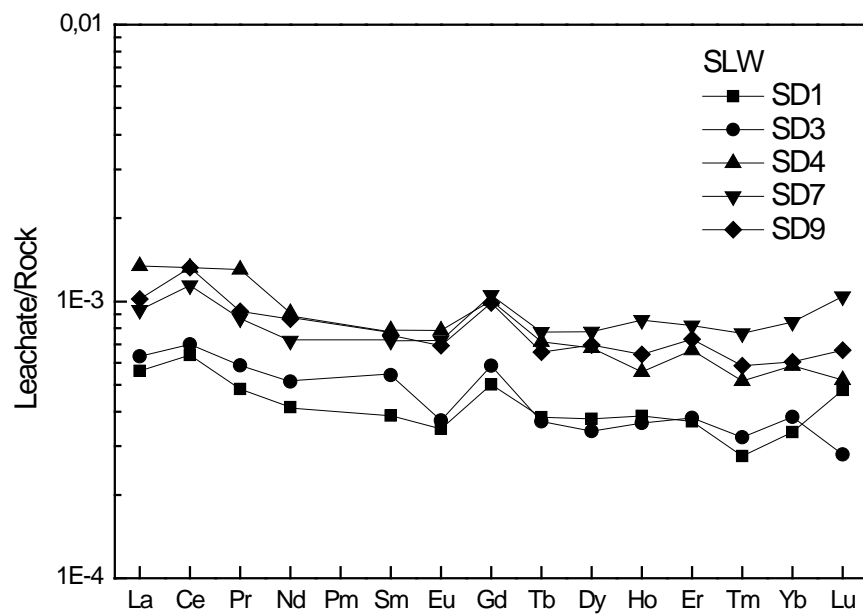


**Figure 35.** Spectres de REE normalisés à l'échantillon sain des fractions libres.

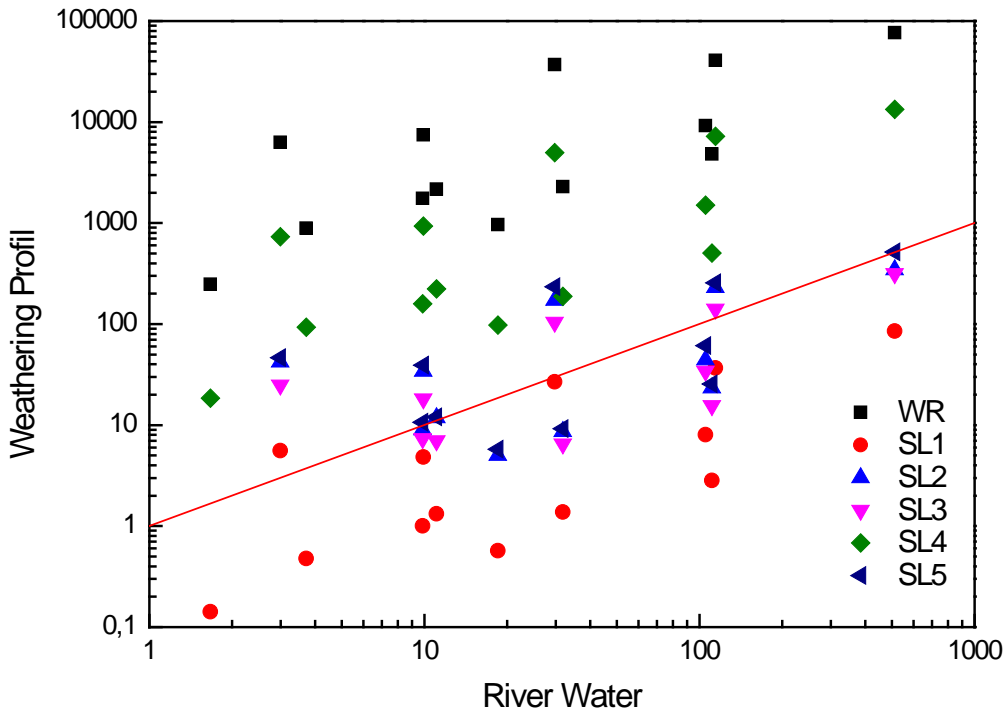


**Figure 36.** Relation entre les différentes fractions issues des extractions séquentielles et la signature chimique du cours d'eau du Malaval.

### III.2. Cycle externe des terres rares revisité

La combinaison de tous les résultats obtenus dans cette synthèse permet d'établir un schéma de formation des spectres des REE dans les eaux naturelles et d'expliquer la chute des concentrations en solution en REE depuis les eaux du sol jusqu'à l'océan. Une réinterprétation du cycle externe des REE est proposée et illustrée sur la Figure 37.

La chute de concentration en solution du Ce dans les océans et les rivières (développement d'une anomalie négative de Ce au niveau des spectres) a été attribuée à sa chimie redox (e.g., Elderfield, 1988). Toutefois les différents processus pouvant mener à cette chute sont mal identifiés. De façon plus générale concernant le fractionnement des REE dans leur globalité, le processus le plus souvent discuté est celui qui propose que le fractionnement ait lieu pendant le mélange estuaire favorisé par la réactivité extrêmement élevée de particules (par exemple,  $MnO_2$ ) et qui aboutit à un enrichissement en REE lourdes (Elderfield, 1988; Elderfield et al., 1990; Sholkovitz, 1995). La chute de concentration des REE pourrait également avoir lieu par coagulation du "pool" colloïdal de REE pendant les mélanges estuariens (Hoyle et al., 1984; Elderfield, 1988; Elderfield et al., 1990; Sholkovitz, 1995). Dans ce cas, le fractionnement des REE se produit par séparation des "pools" colloïdaux et "dissous vrai" qui présentent chacun des formes spécifiques de spectres de REE (Sholkovitz, 1992; Sholkovitz, 1995).

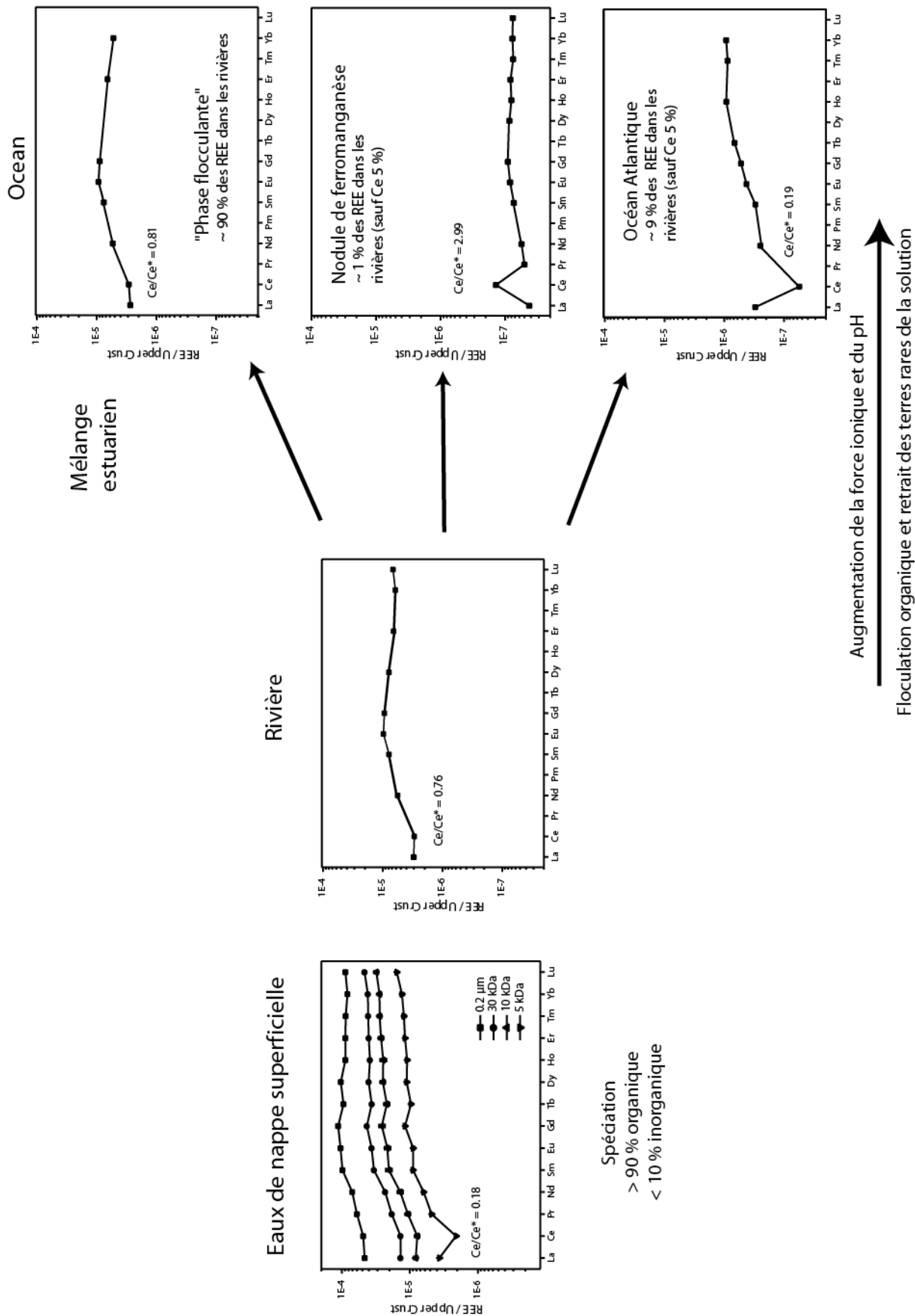
La compétition entre les acides humiques et les carbonates pour la complexation des REE peut mener au fractionnement des REE. Ainsi, la chute de concentration des REE peut être contrôlée par la coagulation du "pool" colloïdal de REE pendant les mélanges estuariens. Lorsque les deux phases sont physiquement séparées, elles présentent deux spectres de REE différents: (i) la phase organique montrant un spectre de REE relativement plat, (ii) la phase inorganique montre un spectre enrichi en REE lourdes proche de celui de l'eau de mer. Or, dans le milieu naturel, la séparation de la phase organique colloïdale du dissous peut tout à fait se produire lors d'une augmentation de salinité qui entraînerait la flocculation de colloïdes organiques. Des expériences d'ultrafiltration sur des eaux de nappe de sol riches en matières organiques indiquent qu'environ 90 % des REE sont présentes sous formes organiques. Environ 10 % du pool de REE des eaux de nappes superficielles est transféré vers les fleuves et rivières où la spéciation est ici considérée comme constante. Le transfert des fleuves vers les océans aboutit aux estuaires, où ont lieu des mélanges et où les phases organiques et inorganiques sont séparées. Environ 90 % des REE se retrouvent extraits de la solution par flocculation du matériel organique. Les REE inorganiques restant en solution peuvent également être fractionnées en contact avec des particules fortement réactives (comme les nodules de ferromanganèse) mais, cette proportion est minimale (1 % des REE par rapport au retrait de 90 % par flocculation organique). Ainsi, les spectres de REE des océans semblent refléter les spectres de REE de la fraction inorganique des eaux de rivières. Une telle information est donc masquée jusqu'à ce que les phases inorganiques et organiques soient séparées comme cela est le cas durant un mélange estuaire par exemple. Finalement, le plateau continental de l'Atlantique pourrait être considéré comme un piège potentiel à REE. Cette dernière hypothèse reste encore à tester en analysant différentes fractions (détritique, oxydes de Fe-Mn, composés organiques) de sédiments déposés dans les estuaires sur la marge de l'Atlantique Ouest.

Les résultats expérimentaux (partie 1) montrent que la compétition entre les acides humiques et les carbonates pour la complexation des REE peut mener au fractionnement des REE. Ces expériences illustrent et confirment le possible contrôle de la chute de concentration des REE par coagulation du "pool" colloïdal de REE pendant les mélanges estuariens (Elderfield et al, 1990; Sholkovitz, 1995). Lorsque les deux phases sont physiquement séparées, elles présentent deux spectres de REE différents: (i) la phase organique montrant un spectre de REE relativement plat, (ii) la phase inorganique montre un spectre enrichi en REE lourdes proche de celui de l'eau de mer. Or, dans le milieu naturel, la séparation de la phase organique colloïdale du dissous peut tout à fait se produire lors d'une augmentation de salinité qui entraînerait la flocculation de colloïdes organiques.

Les expériences d'ultrafiltration (partie 2) sur des eaux de nappe de sol riches en matières organiques indiquent qu'environ 90 % des REE sont présentes sous formes organiques. Environ 10 % du pool de REE des eaux de nappes superficielles est transféré vers les fleuves où la spéciation est ici considérée constante. Le transfert des fleuves vers les océans aboutit aux estuaires, où ont lieu des mélanges et où les phases organiques et inorganiques sont séparées. Environ 90 % des REE se retrouvent extraits de la solution par flocculation du matériel organique. Les REE inorganiques restant en solution peuvent également être fractionnées en contact avec des particules fortement réactives (comme les nodules de ferromanganèse) mais cette proportion est minimale (1 % des REE par rapport au retrait de 90 % par flocculation organique). Ainsi, les spectres de REE des océans semblent refléter les spectres de REE de la fraction inorganique des eaux de rivières. Une telle information est donc masquée jusqu'à ce que les phases inorganiques et organiques soient séparées comme pendant un mélange estuaire par exemple.

Ceci est illustré sur la carte de krigage du La dans les cours d'eaux en France (Figure 38). Si nous prenons l'exemple du bassin versant de la Dordogne, la source des REE se trouve dans le massif Central et son socle cristallin. Les REE sont essentiellement issues de l'altération de basalte et auront des spectres similaires à ceux du bassin versant de Malaval avec une anaomalie de Ce négative (Figure 39). Au cours du transport, les spectres de REE montrent un enrichissement en REE intermédiaires et une diminution de l'anomalie négative de Ce. L'anomalie de Ce est en effet corrélée avec la distance à l'éxutoire (Figure 40) : en effet plus la distance avec la source augmente plus les concentrations en REE et en MO augmentent (données non présentées). La spéciation des REE devient organique (voir partie 2).

**Figure 37.** Cycle des REE des eaux souterraines en passant par les rivières jusqu'aux océans. Les données sont extraites de De Barr et al. (1988), Elderfield et al (1990) et Pourret et al. (2007c).



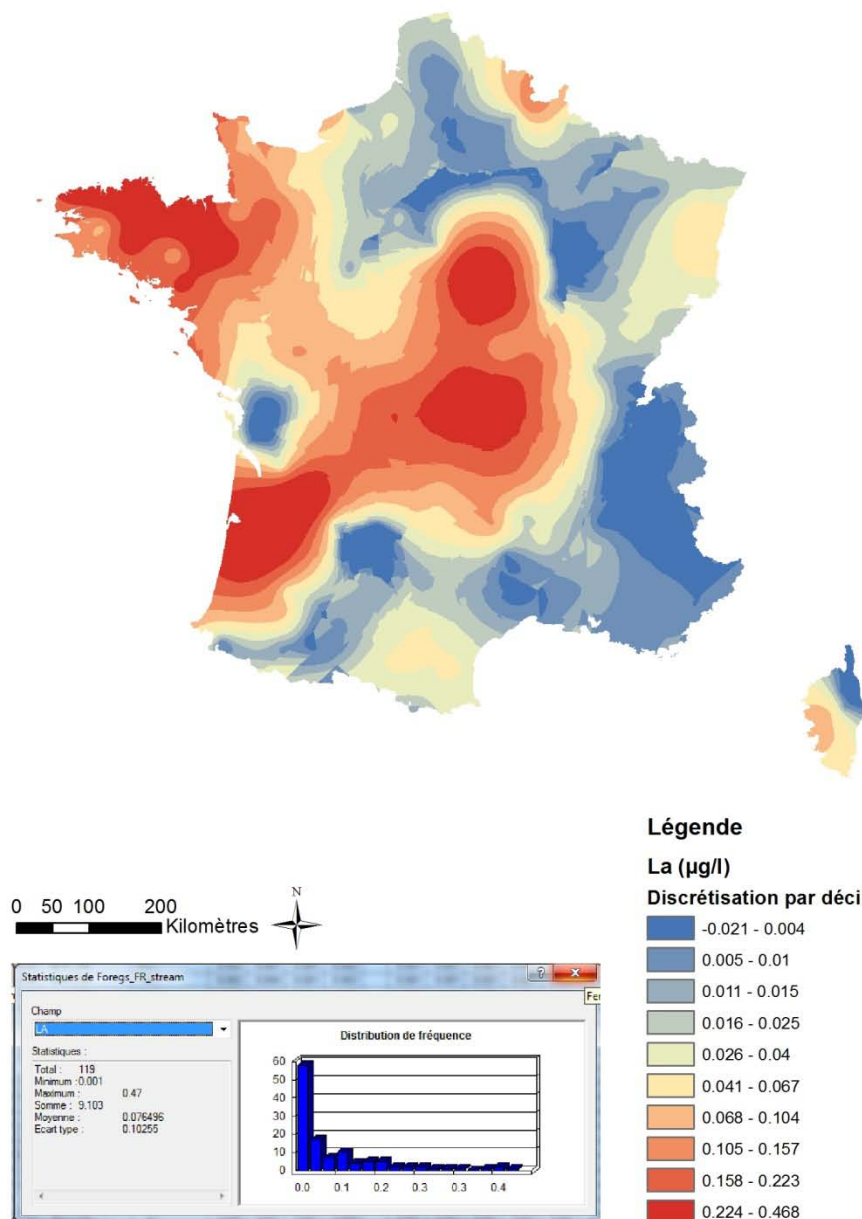


**Figure 38.** Carte de krigeage de la distribution du La dans les cours d'eaux en France (database FOREGS).

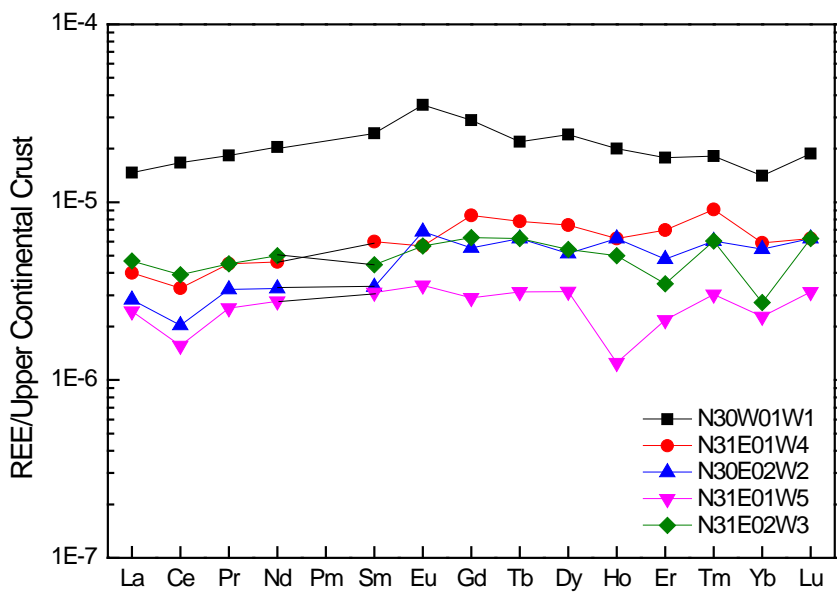


**Figure 39.** Spectres de REE normalisés à la croute continentale supérieure des échantillons du bassin versant de la Dordogne.

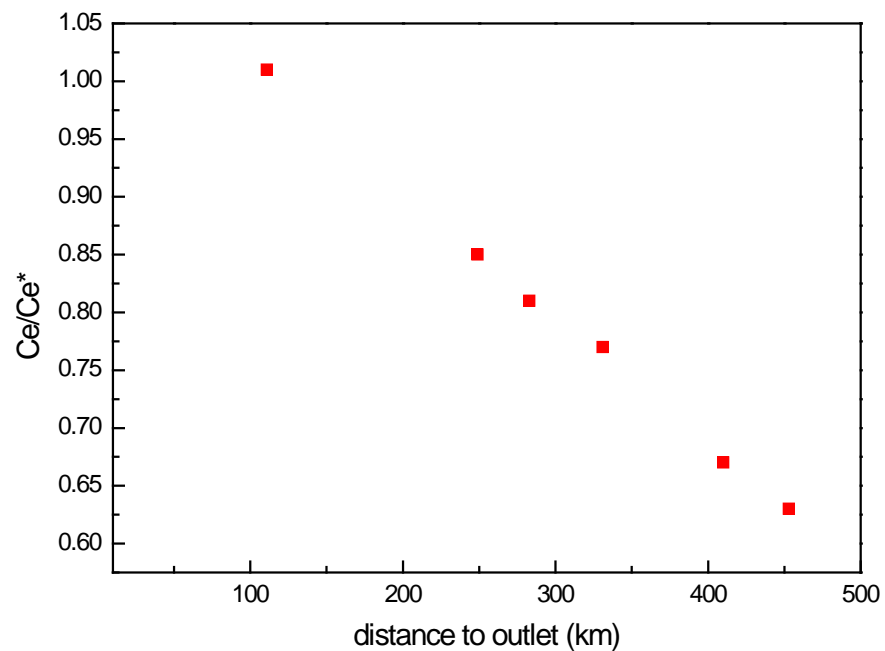


**Figure 40.** Evolution de l'anomalie de cérium en fonction de la distance à l'éxutoire.

### **III.3. Contrôle par matière organique**

La distribution des REE des cours d'eau, normalisée à la croûte continentale supérieure (UCC), a montré, de la source à l'exutoire du bassin versant, un fractionnement des spectres de REE, de spectres enrichis en REE lourdes vers des spectres plus plus plat, enrichi en REE intermédiaires. Une disparition progressive de l'anomalie Ce négative est aussi observée. En conséquence, Pourret et al. (2012) suggèrent que le plateau continental pourrait être considéré comme un piège à REE potentiel et donc que les roches sédimentaires du plateau, similaires aux sédiments profonds métallifères (Kato et al., 2011), représentent une ressource potentielle en REE et un guide pour leur exploration. La réévaluation du potentiel de REE de la France, nous a permis de discuter du comportement des REE, du plateau continental à la plaine du bassin, en utilisant les occurrences de monazite authigènes au sein des schistes ordoviciens du massif Armorican (France).

Les monazites grises (phosphates de REE enrichis en REE intermédiaires) de l'Ordovicien du massif Armorican ont été reconnues comme source des monazites présentes dans les placers du Grand Fougeray. L'étude pétrographique des schistes a mis en évidence la présence de quartz, de feldspath, de mica de type muscovite, de chlorite et de pyrophyllite. La matière organique caractérisée par pyrolyse montre une matière organique d'origine continentale. La présence de la monazite grise dans les schistes de l'Ordovicien peut s'expliquer par un enrichissement localisé dans ses schistes dans des niveaux riches en matière organique et biotite. Les grains de monazite (jusqu'à 2 mm de diamètre) sont principalement caractérisés par leur couleur grise, des inclusions minérales de schistes, leurs spectres de REE enrichis en REE intermédiaires (Figure 41), une concentration en Th et U, une absence de coeurs hérités, qui suggèrent fortement une cristallisation authigène au cours de la diagenèse. La composition chimique souligne des cristaux zonés avec des coeurs enrichis en REE intermédiaires (jusqu'à 10% en poids  $\text{Sm}_2\text{O}_3$ ; 1,3% en poids  $\text{Eu}_2\text{O}_3$  et 5% en poids  $\text{Gd}_2\text{O}_3$ ) et des bordures enrichies en REE légères. Ainsi les coeurs des grains sont caractérisés par des valeurs négatives et faibles en log  $[(\text{La}/\text{Sm})_{\text{UCC}}]$  et des valeurs élevées en Eu alors que les bordures sont légèrement négatives à positives en log  $[(\text{La}/\text{Sm})_{\text{UCC}}]$  avec de faibles concentrations en Eu (Figure 42). Les spectres de REE des monazites grises reflètent aussi l'abondance en REE des schistes. Il y a un enrichissement global en REE lorsque le rapport REE légères/REE lourdes augmente (Figure 43). En effet, lorsque les schistes sont dans l'anchizone ( $200^{\circ}\text{C} < T < 270^{\circ}\text{C}$ ), les monazites ont des spectres de REE enrichis en REE intermédiaires, directement liés à la matière organique, alors que lorsqu'ils sont dans l'épizone ( $T > 270^{\circ}\text{C}$ ), la spéciation des REE est principalement guidée par complexation avec des carbonates, ce qui entraîne la formation de monazites enrichies en REE légères (Figure 44). En effet, comme l'a montré Nakada et al. (2010) la décarboxylation va entraîner un fractionnement des REE et comme illustré par Pourret et Martinez (2009) il y aura enrichissement en REE légères associées aux groupements phénoliques. Cette dernière hypothèse sera encore testée et renforcée par l'analyse des fractions organiques des schistes et schistes noirs. Ce type de fractionnement est couramment admis pendant la diagenèse comme l'a montré Haley et al. (2004) et une telle hypothèse a été proposée par Lev et al. (1989) et Evans et Zalaziewics (1996) pour des environnements similaires de schistes à monazites enrichies en REE intermédiaires.

Comme, ces monazites ont de plus été concentrées dans des placers @ 2 kg / t et exploitées (Donnot et al., 1973), ce site nous permettra de proposer un modèle de gisement dans le cadre du projet ANR ASTER et de mieux comprendre le rôle des différents processus géologiques dans la genèse des minéralisations de REE.

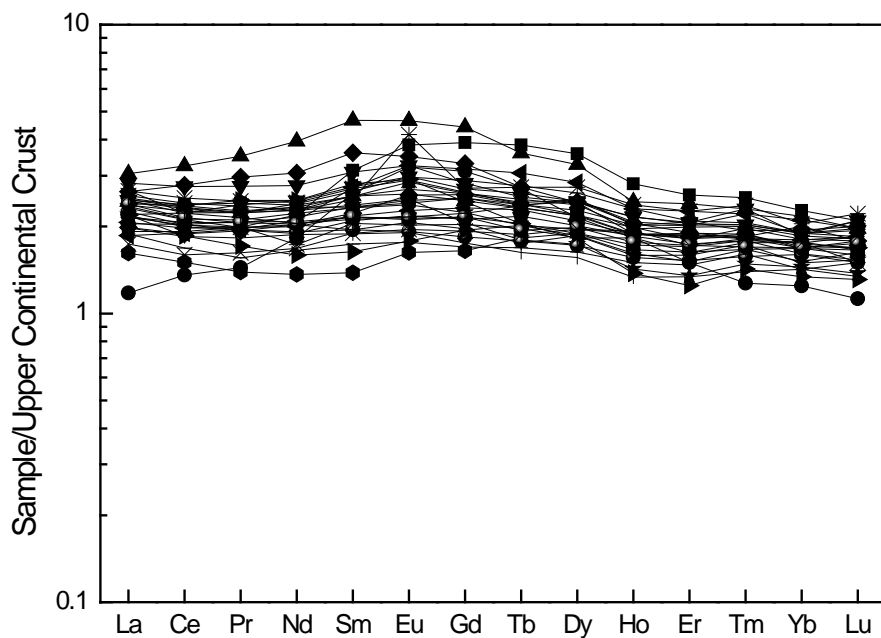


**Figure 41.** Spectres de REE normalisés à la croute continentale supérieure des schistes du Grand-Fougeray

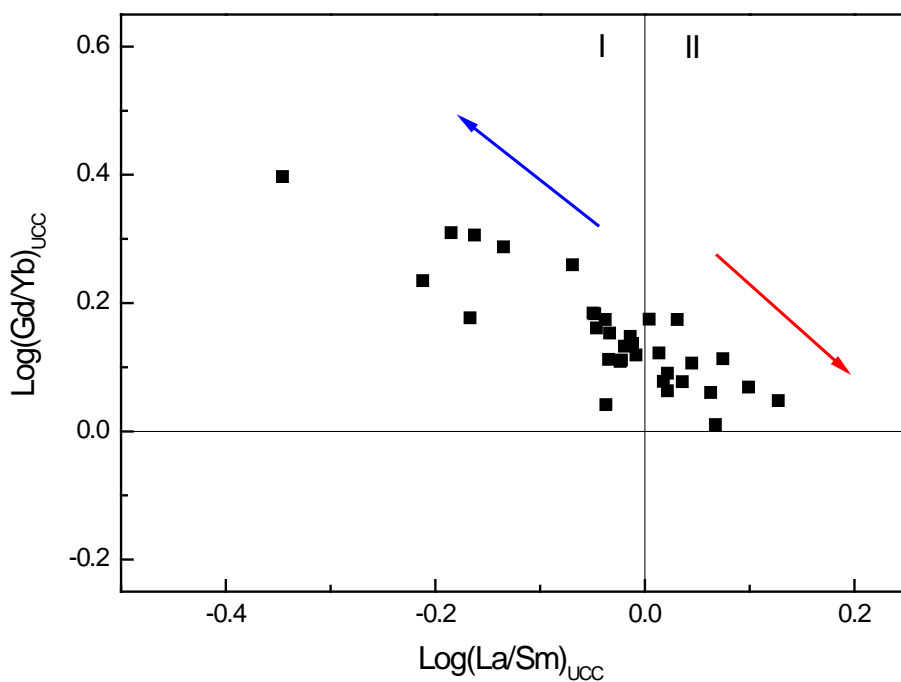


**Figure 42.** Evolution du rapport Gd/Yb en fonction du rapport La/Sm.

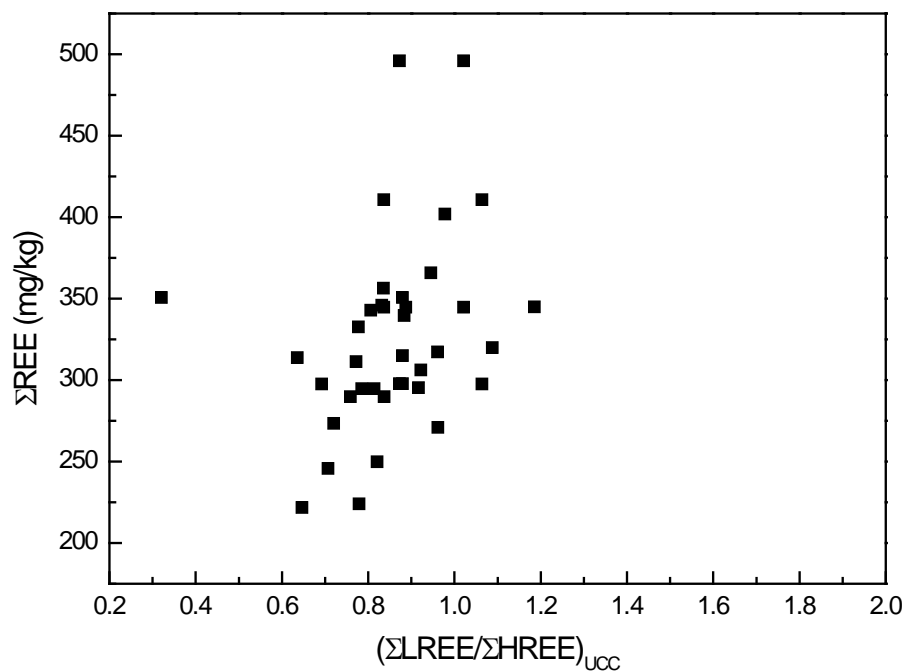


**Figure 43.** Evolution de la somme des REE en fonction du rapport REE légères/ REE lourdes.

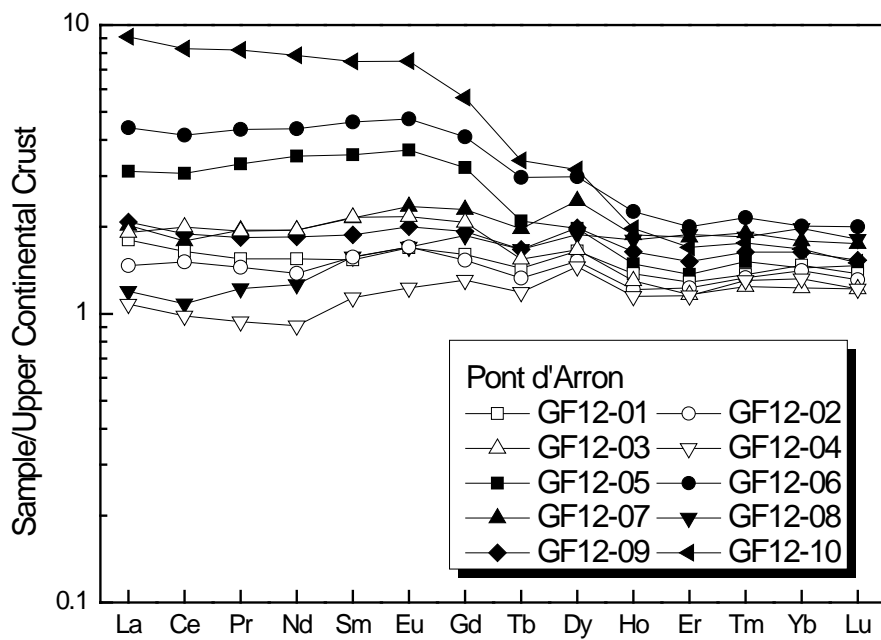
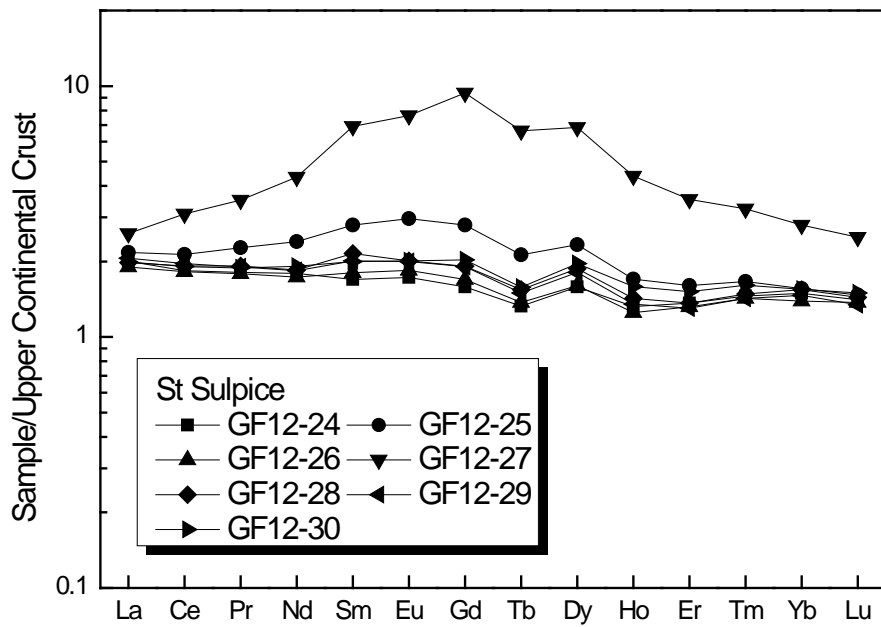


**Figure 44.** Spectres de REE normalisés à la croute continentale supérieure des schistes de deux localités autour du Grand Fougeray (a) St Sulpice et (b) Pont d'Arron.

### **III.4. Contrôle par oxydes de manganese et carbonates**

La Copperbelt katangaise (RD Congo) abrite près de la moitié des réserves mondiales en cobalt. L'hétérogénite ( $\text{CoOOH}$ ) est le mineraï de cobalt oxydé le plus abondant dans cette région. Il résulte de l'oxydation de la carrolite ( $\text{CuCo}_2\text{S}_4$ ) lors de processus d'altération supergène au Pliocène. Cela conduit à la formation d'une croute de surface enrichie en hétérogénite (Decrée et al. 2010). Cependant, les processus détaillés conduisant à la formation d'hétérogénite ne sont pas encore bien contraints. Ici, ces processus sont étudiés en considérant le fractionnement et la distribution des REE, qui est un outil peu exploré mais puissant pour comprendre la formation des oxyhydroxydes (Pourret et Davranche, 2013). En effet, étant donné que ces éléments se comportent comme un groupe cohérent, le fractionnement des REE peut être utilisé comme traceur des processus de mise en place. En première approche, l'étude des spectres de REE des hétérogénites ne permet pas d'identifier les différents types d'hétérogénites (Figure 45). Cependant, il est possible d'identifier différents comportements pour les hétérogénites de type 1 (Figure 46) : (i) le premier type est enrichi en REE intermédiaires, avec une anomalie de cérium négative et une relativement faible teneur en REE; (ii) le second est enrichi en REE légères, sans anomalie de cérium et avec une concentration en REE supérieure.

Les processus d'altération conduisant aux minéralisations d'hétérogénite consistent principalement en des l'équilibre eau-roche. À une forte activité de Co, l'hétérogénite précipite à un pH voisin de la neutralité simultanément aux oxydes de manganèse (i.e., pyrolusite). Les REE sont principalement fractionnées entre ces deux phases solides: les spectres de REE des hétérogénites sont clairement les complémentaires de ceux des oxydes de manganèse. L'anomalie de Ce variable pour le premier type dépend de la compétition entre Co, Cu, Fe et Mn (Figure 47). Comme l'activité du cobalt diminue, le champ de stabilité de l'hétérogénite se déplace vers des pH alcalins. Dans ces conditions, la spéciation des REE est principalement gouvernée par la complexation avec les carbonates, ce qui provoque la formation d'hétérogénite avec un spectre enrichi en REE légères (Figure 48).

Les deux types de signatures en REE sont conformes à la formation d'hétérogénite en considérant un modèle en deux étapes per descensum. Ainsi ce minéral (i) se forme en dépôts résiduels - similaires à des latérites - en association avec des oxydes de Mn, et ensuite (ii) se dépose à partir d'un fluide riche en carbonate.

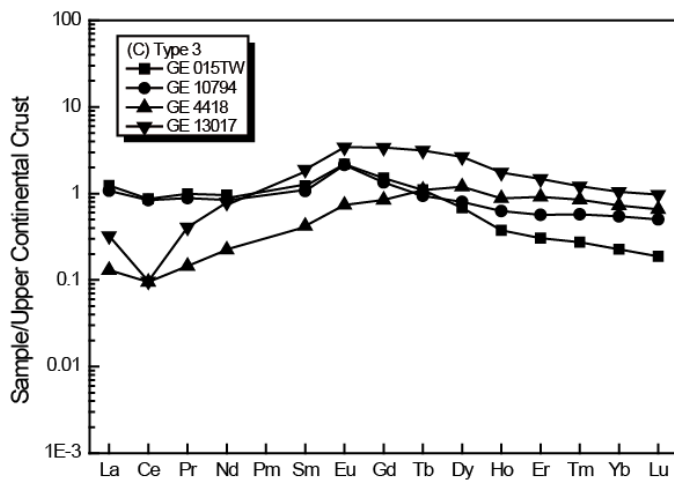
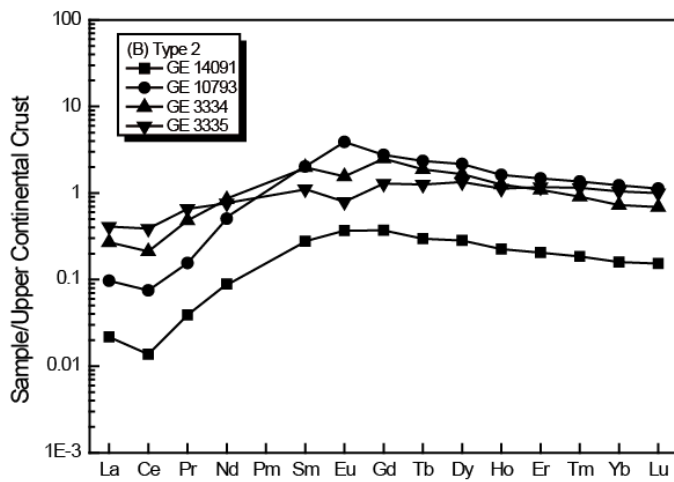
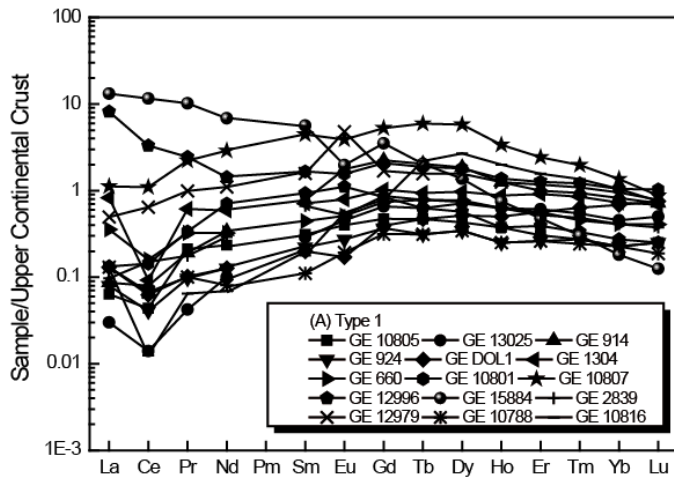


**Figure 45.** Spectres de REE normalisés à la croute continentale supérieure des hétérogenites de (A) type 1, (B) type 2 et (C) type 3.

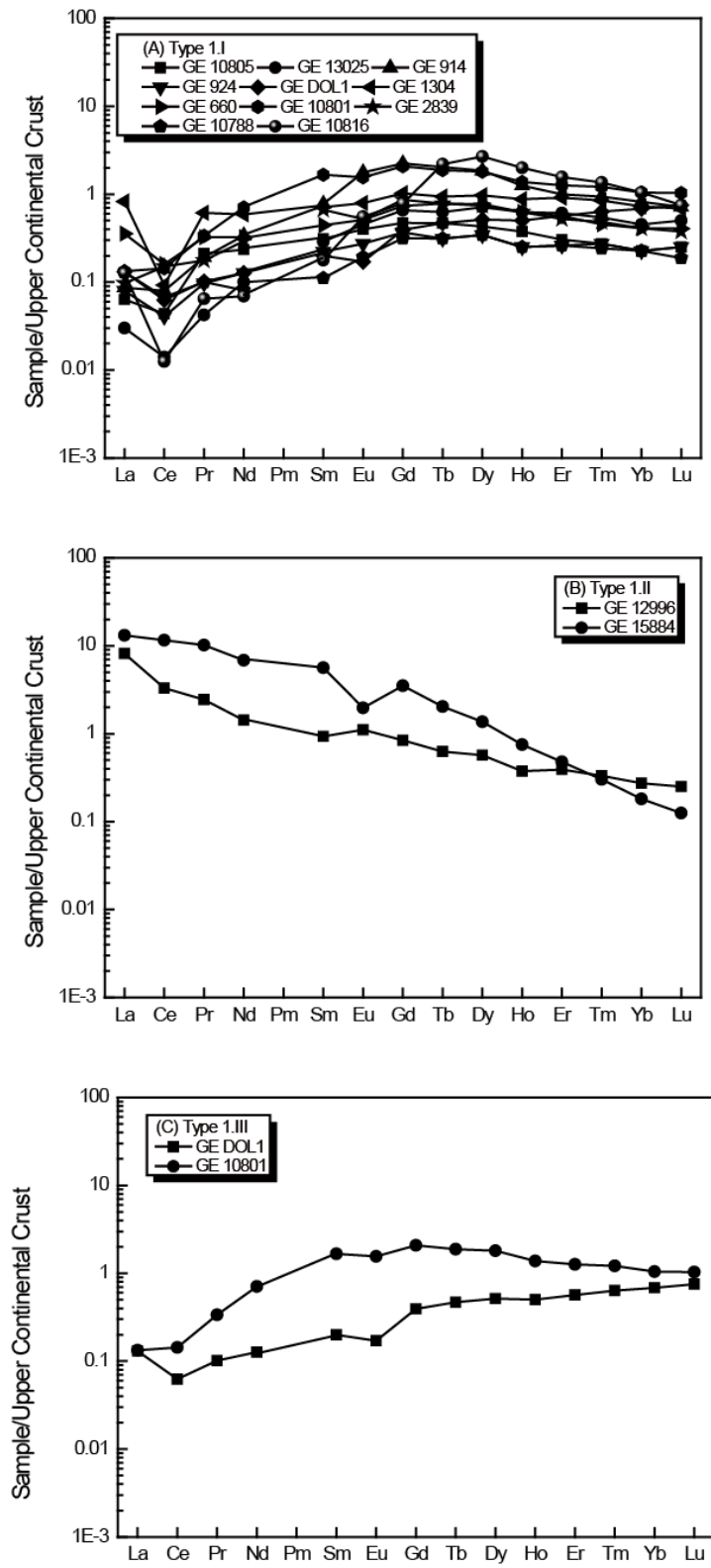


**Figure 46.** Spectres de REE normalisés à la croute continentale supérieure des hétérogenites de (A) type 1.1, (B) type 1.2 et (C) type 1.3.

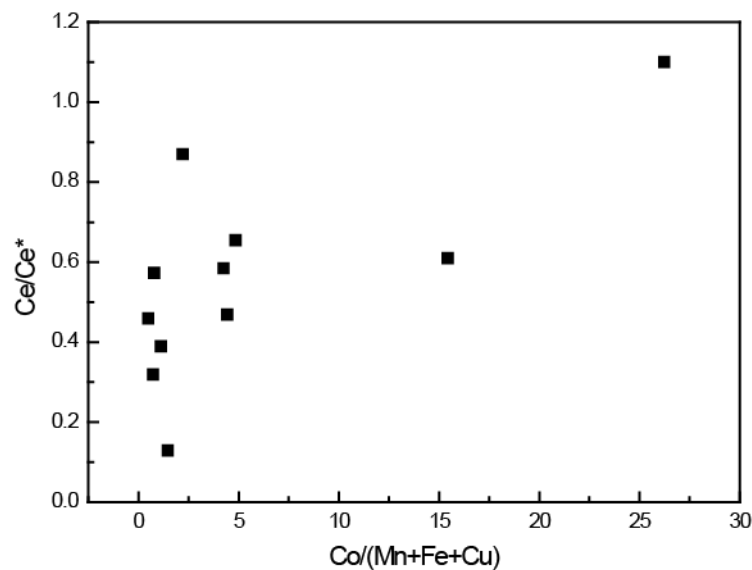


**Figure 47.** Evolution de l'anomalie de Ce en fonction du rapport Co/(Mn+Fe+Cu)

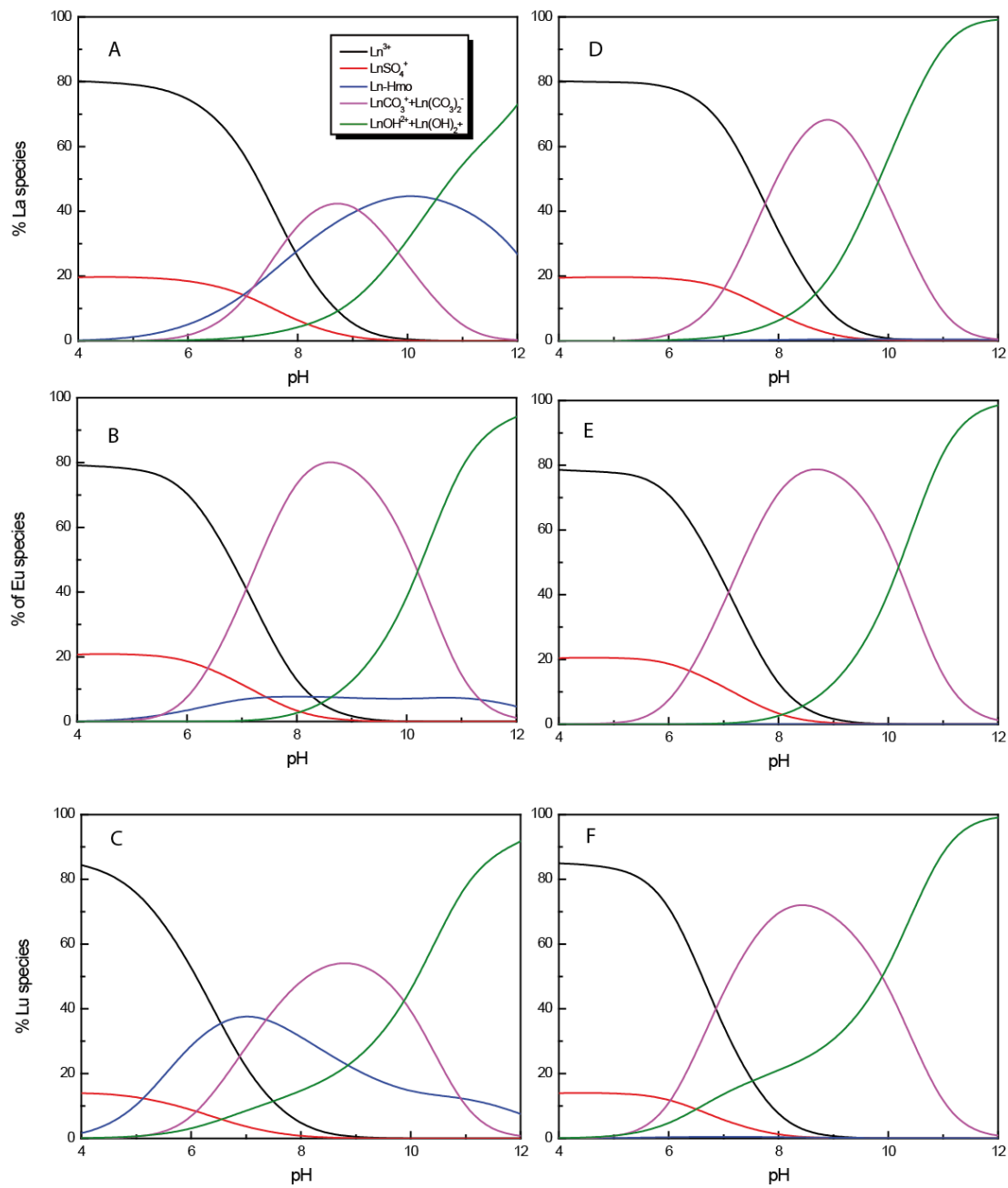


**Figure 48.** Modélisation de la spéciation d'une eau souterraine type (conditions dans Wood 1990) avec des oxydes de Mn (A, B, C)  $\text{Mn} 10^{-4} \text{ mol/L}$ ; et (D, E, F)  $10^{-5} \text{ mol/L}$ .

### III.5. Contrôle par matière organique, oxydes de Fe/Mn et fluide

La mine d'argent d'Imiter (de classe mondiale) a été étudié pour ses minéralisations hypogènes (Tuduri et al., 2006). Cependant, des processus supergènes ont remobilisés ses minéralisations primaires et engendrés un enrichissement en Ag. Cet enrichissement a été interprété comme étant la résultante d'une oxydation des minéralisations primaires. Le développement d'une telle minéralisation supergène suggère fortement la présence de conditions semi-arides. Le diagramme de mobilité des REE suggère une mise en solution par des chlorures et/ou des fluorures (appauvrissement) et une reprécipitation couplées avec oxydes de manganèse et matière organique (Figure 49). Comme vu précédemment, les processus d'altération donnent lieu à la mobilisation ainsi qu'à la redistribution des REE qui reprécipitent pour former des minéraux secondaires (e.g., les oxydes de Mn, fluorocarbonates). Dans le gisement d'argent d'Imiter (Maroc), une partie La présence de ligands aqueux, notamment les fluorures, les carbonates vont affecter fortement la solubilité des REE. De plus, la formation de minéraux secondaires de REE (e.g., synchisite ; Figure 50) peut indiquer les conditions de formation des minéraux (à valeurs économiques notamment) associés à ceux de REE. Ainsi, afin d'établir les conditions supergènes de la mise en place de minerai d'argent supergène, la spéciation des REE en solution a été calculée en considérant différents types de solution (eau de mer réduite et eaux souterraines enrichies en F). Les résultats montrent que (i) dans l'eau de mer réduite à pH proche de la neutralité, les REE existent sous forme ionique, carbonatée et chlorurée, (ii) dans l'eau souterraine enrichie en F, les REE existent sous forme ionique, carbonatée et fluorée. Bien qu'il n'y ait aucune indication de la présence de fluides alcalins, il existe des preuves de la présence de fluides enrichis en F. En effet, la précipitation de synchisite (fluorocarbonate de REE) suggère la présence de F et de CO<sub>2</sub> dans le fluide aqueux, le tout piégé par un niveau enrichi en matière organique.

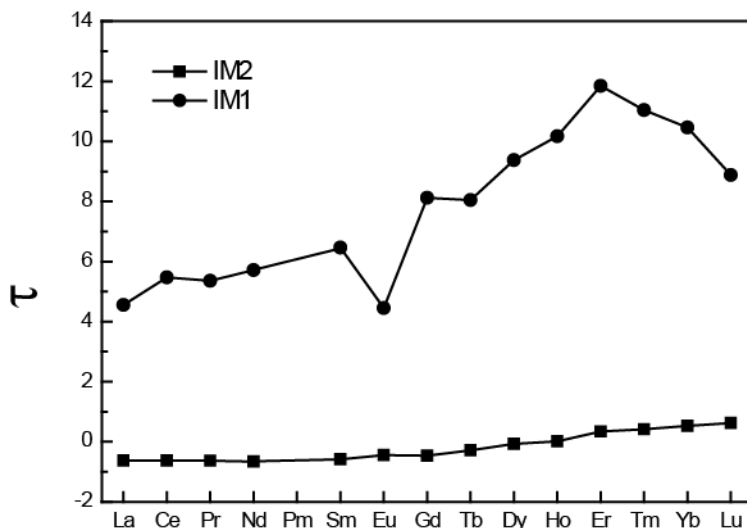


**Figure 49.** Mobilité des REE d'après Nesbitt (1979)

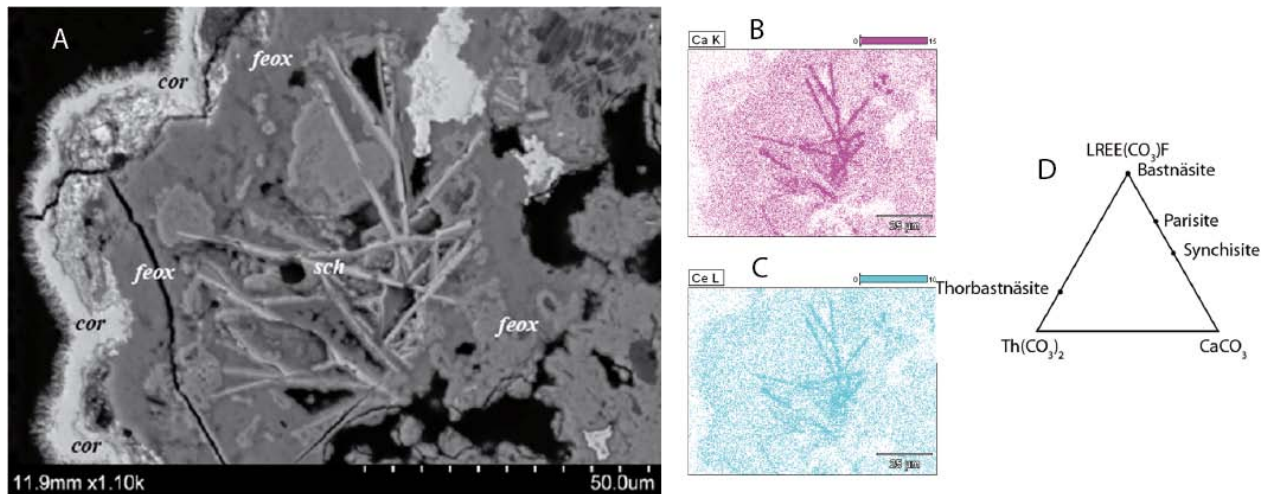


**Figure 50.** (A) Photographie par microscopie électronique à balayage d'un échantillon de coroandite, synchisite et oxyde de fer, (B) image élémentaire de la répartition du Ca, (C) image élémentaire de la répartition du Ce, (D) diagramme ternaire illustrant la solution solide de la synchisite.

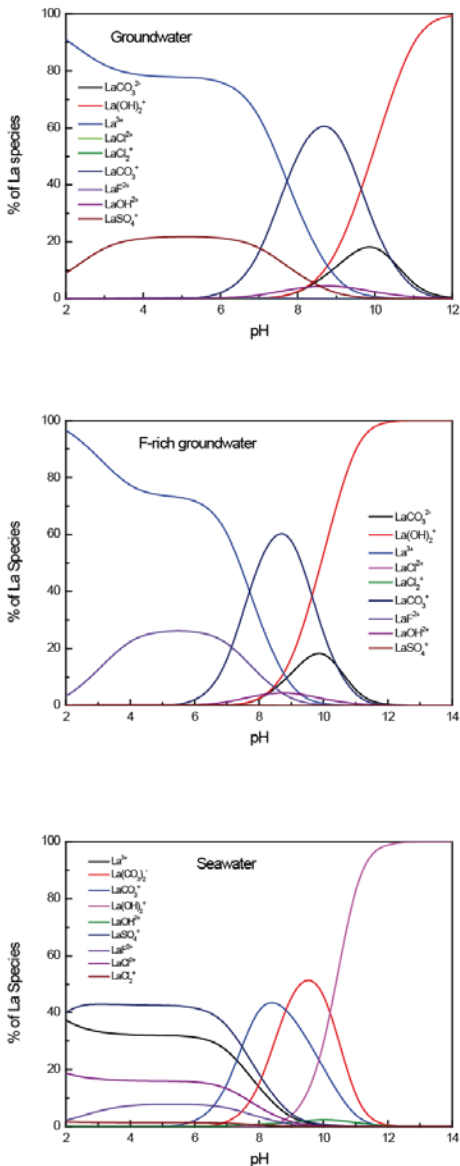


**Figure 51.** Modélisation de la spéciation (A) d'une eau souterraine type, (B) d'une eau souterraine enrichie en F et (C) d'une eau de mer (conditions dans Wood 1990).



## Bilan

---

Durant ces dernières années, mes activités de recherche axées sur l'étude des mécanismes aux interfaces solide/liquide dans les sols et les eaux et de leur impact sur la mobilité des REE a permis de mettre en exergue l'importance des éléments suivants:

- **le rôle de la complexation organique.** L'ensemble des travaux effectués a montré toute l'importance de la matière organique dans les processus de mobilisation et de transport des REE. Ainsi, la complexation par la matière organique influence la spéciation des REE en solution et peut contrôler leur précipitation. Elle doit donc être systématiquement prise en compte dans les études portant sur la composition des solutions naturelles et être intégrée au cours des modélisations. Pour ce dernier point, de nombreux programmes (e.g., PHREEQC) de spéciation devront être modifiés et améliorés de façon à modéliser plus en détail la matière organique ou même intégrer un module de complexation organique lorsque ces derniers n'en possèdent pas.
- **du rôle des oxyhydroxydes de manganèse.** Même si leur importance a été minimisée pour certains éléments, il apparaît que les oxyhydroxydes de Mn (et à un degré moindre de Fe) peuvent être les précurseurs de la mobilisation des REE en milieu oxydant. Ainsi, l'adsorption préférentielle des REE sur les oxyhydroxydes de Mn entraîne un fractionnement avec, notamment, le compartiment organique du sol ou de la solution. La signature des différents compartiments restant reflètera la différence entre la signature des oxyhydroxydes de Mn et le spectre global de la source (e.g., signatures hétérogénites supergénères dans les sols du Katanga). En effet, le contexte organique ou minéral d'un sol va jouer un rôle primordial sur le contrôle de la mobilité des minéraux précipités et la signature de la solution du sol et des eaux superficielles associées.

Enfin, ces travaux ont mis en évidence l'intérêt de coupler observations de terrain-expérimentation-modélisation dans la compréhension des systèmes naturels et la prédiction de leur évolution dans le temps et en fonction des conditions géologiques.



## Projet de recherche

Aux interfaces sol/solide/solution, il est souvent difficile d'identifier les paramètres les plus influents sur les réactions géochimiques. Les REE sont particulièrement intéressantes dans ce cas ; certaines réactions chimiques pouvant produire des spectres de REE caractéristiques. Les REE constituent donc un outil précieux et puissant pour la compréhension et l'identification des processus géochimiques aux interfaces sol/solide/solution. Cependant, les spectres de REE d'échantillons naturels résultent de la superposition de plusieurs processus de fractionnement. En effet, la forme des spectres est liée (i) à la nature et à l'abondance des phases solides mises en jeu dans les réactions d'adsorption, (ii) aux compétitions entre surfaces et ligands en solution et, (iii) aux paramètres physico-chimiques (e.g., pH, force ionique, alcalinité).

Les surfaces solides impliquées dans les réactions d'adsorption sont les oxyhydroxydes de Fe, Mn, les argiles, les sables, les matières organiques colloïdales ou particulières et les bactéries. A chaque nature de "solide" correspond un spectre spécifique de REE. D'une manière générale, l'impact des ligands inorganiques sur le fractionnement des REE a été plus souvent étudié. Cependant, peu d'études traitent de la compétition des ces ligands inorganiques avec les surfaces adsorbantes décrites précédemment.

Une étude intégrant l'ensemble de ces surfaces fournirait à la fois des spectres spécifiques aux réactions, mais également des données expérimentales nécessaires à la détermination de constantes thermodynamiques indispensables à la modélisation. Les spectres de REE obtenus représenteront la somme des différents processus chimiques impliqués. De plus, les modèles pourraient tenir compte de tous les équilibres chimiques permettant de modéliser l'ensemble des réactions de complexation (dont les réactions redox) pour mieux contraindre le cycle des éléments redox sensibles comme le Ce. Ces spectres de référence pourraient être confrontés aux spectres de REE de solutions naturelles et permettraient, après déconvolution, d'identifier et dans le même temps de hiérarchiser les paramètres physico-chimiques influents (potentiel redox, pH...) et les phases solides jouant un rôle majeur dans un sol ou un aquifère donné dans la mobilisation des REE. Les modèles plus globaux couplant les cycles d'éléments traces pourraient ainsi profiter d'une meilleure compréhension des interactions REE - colloïdes.

Pour comprendre le transfert de ces des REE dans les environnements de surface il est donc nécessaire d'examiner :

- (i) l'altération des roches et le transfert des REE de la roche vers l'eau et les sols ;
- (ii) le fractionnement et la spéciation des REE dans l'eau ;
- (iii) la rétention et la restitution des REE par les écosystèmes.

En effet, l'évaluation des risques chimiques et biologiques liés aux REE nécessite l'intégration de données concernant le transfert de ces REE dans le milieu, leur biodisponibilité, leur transformation, et leur impact potentiel sur les différentes composantes de l'écosystème. La complémentarité des REE associée à leurs mécanismes de fractionnements complexes, rend leur utilisation plus pertinente.

Si l'observation du milieu naturel a été et reste un pilier essentiel de la connaissance de l'état et de l'évolution des écosystèmes continentaux, elle doit être accompagnée du développement de nouveaux outils et démarches expérimentales originales. Les expérimentations

en laboratoire et en conditions naturelles, qu'elles soient conduites à court terme ou long terme, ne doivent pas être opposées car elles remplissent des fonctions différentes. Les essais de longue durée sont indispensables pour, d'une part, produire des données qui serviront à valider des modèles et, d'autre part, conserver des échantillons qui pourront être analysés avec de nouvelles techniques. Un couplage de ces observations avec des expérimentations aux interfaces eau/roche et eau/sol, et une modélisation des différents processus pouvant intervenir permettrait d'avoir une vision plus globale à l'échelle des grands cycles biogéochimiques.

Ce projet propose d'adopter la même démarche méthodologique que décrit précédemment (i.e., observation système naturel, expérience en laboratoire, modélisation) et, sera prioritairement réalisé dans le cadre du projet de l'équipe HydrISE, unité de recherche de l'Institut Polytechnique LaSalle Beauvais.

## Fractionnement et spéciation des terres rares en solution

---

Dans la continuité des travaux déjà développés sur le transport et le fractionnement des REE dans les eaux de surfaces (rivières et souterraines) où nous avons suggéré que le fractionnement des spectres de REE était dû à la compétition entre colloïdes d'oxyhydroxydes de Fe et de Mn et la matière organique, nous envisageons de développer des outils pour mieux comprendre le fractionnement et la spéciation des REE. Nous n'avons, pour l'instant, pas de preuve directe de la présence de colloïdes, qui sont de petites particules minérales ou organiques finement broyées ou des phases minérales ou organiques en cours de précipitation, responsables du fractionnement des REE en solution.

La méthode analytique donnant accès à la phase colloïdale est l'ultrafiltration. Le principe de cette méthode consiste à séparer plusieurs fractions colloïdales jusqu'à environ 1 nm à partir d'une eau préfiltrée à 0,22 ou 0,45 µm. Cependant, cette méthode ne permet pas de distinguer les colloïdes de tailles voisines entre eux. Pour cela, cette approche sera couplée à une technique spécifiquement dédiée à la détermination de la distribution des masses moléculaires ainsi que la conformation en solution des molécules, le fractionnement par flux-force (FFF). Cette technique sera utilisée en couplage avec un ICP-MS (e.g., Alasonati et al., 2010; Baalousha et al., 2011; Dubascoux et al., 2010). La séparation de la phase colloïdale est techniquement délicate et soumise à des artefacts analytiques, cependant de premiers résultats semblent prometteurs (e.g. Stolpe et al., 2013). C'est la raison pour laquelle des efforts considérables ont été fait pour intégrer l'interaction entre REE et phase colloïdale dans des modèles numériques. Ces modèles permettront d'affiner l'interprétation des données analytiques. Nous envisageons donc de continuer à modéliser l'interaction des REE avec la phase colloïdale et de comparer les résultats avec les données analytiques.

Le développement de cet axe de recherche s'appuiera sur les compétences en chimie analytique présentes au sein de l'unité HydrISE.

## **Ecodynamisme des terres rares**

---

L'étude des transferts des REE à l'interface sol-plante permettra, à la fois, de mieux comprendre l'impact de la végétation sur les cycles géochimiques de surface, de documenter les mécanismes de transfert des REE naturelles et anthropiques vers la biosphère, et de mieux évaluer les risques sanitaires et environnementaux associés à la dispersion de REE anthropiques (e.g., Brioschi et al., 2013).

Nous envisageons de quantifier la capacité de la végétation à stocker les REE et à fractionner leurs spectre ; ceci en fonction des espèces végétales. Ces données serviront de base pour intégrer la végétation dans des bilans quantitatifs des transferts des REE à l'échelle du bassin versant. L'objectif final de cette approche est de savoir dans quelle mesure les spectres de REE mesurés, dans l'écoulement de surface à la sortie d'un bassin versant, reflètent les échanges avec la végétation. Cette partie de l'étude sera entièrement basée sur des données de terrain.

Cette étude se focalisera aussi sur les mécanismes de transfert des REE à l'interface sol-plante et l'accumulation chez les plantes. Ce volet a pour but de comprendre les variations des spectres de distribution observés dans différents types de végétaux accumulant ou non spécifiquement d'autre métaux (e.g., Cu ou Co). Cette partie du projet sera à la fois basée sur des données acquises sur le terrain et sur des résultats expérimentaux obtenus en conditions contrôlées. Elle fournira une première caractérisation des paramètres susceptibles de favoriser l'accumulation des REE anthropiques ou non dans la végétation. La majorité des travaux antérieurs a ignoré le rôle de la végétation dans les transferts géochimiques et en tant que réservoir d'éléments chimiques au sein des cycles géochimiques externes. Ainsi, cette étude devrait contribuer à quantifier le rôle de la végétation en tant que réservoir de REE et permettre d'évaluer sa contribution au fractionnement des spectres de REE dans les systèmes eau-sol-plante.

Le développement de cet axe de recherche exige une approche pluridisciplinaire réunissant des compétences en pédologie/géochimie, en écologie et en chimie analytique présentes au sein de l'unité HydrISE et/ou de l'Institut Polytechnique LaSalle Beauvais.



## Bibliographie

- Alasonati, E., Slaveykova, V.I., Gallard, H., Croué, J.-P., Benedetti, M.F., 2010. Characterization of the colloidal organic matter from the Amazonian basin by asymmetrical flow field-flow fractionation and size exclusion chromatography. *Water Research*, 44, 223-231.
- Andersson, K., Dahlqvist, R., Turner, D., Stolpe, B., Larsson, T., Ingri, J., Andersson, P., 2006. Colloidal rare earth elements in a boreal river: Changing sources and distributions during the spring flood. *Geochimica et Cosmochimica Acta*, 70 (13), 3261-3274.
- Aubert, D., Stille, P., Probst, A., 2001. REE fractionation during granite weathering and removal by waters and suspended loads: Sr and Nd isotopic evidence. *Geochimica et Cosmochimica Acta*, 65, 387-406.
- Baalousha, M., Stolpe, B., Lead, J.R., 2011. Flow field-flow fractionation for the analysis and characterization of natural colloids and manufactured nanoparticles in environmental systems: A critical review. *Journal of Chromatography A*, 1218, 4078-4103.
- Bau, M., 1991. Rare-earth element mobility during hydrothermal and metamorphic fluid-rock interaction and the significance of the oxidation state of europium. *Chemical Geology*, 93, 219-230.
- Bau, M., 1996. Controls on the fractionation of isovalent trace elements in magmatic and aqueous systems: Evidence from Y/Ho, Zr/Hf, and lanthanide tetrad effect. *Contributions to Mineralogy and Petrology*, 123 (3), 323-333.
- Bau, M., 1999. Scavenging of dissolved yttrium and rare earths by precipitating iron oxyhydroxide: Experimental evidence for Ce oxidation, Y-Ho fractionation, and lanthanide tetrad effect. *Geochimica et Cosmochimica Acta*, 63, 67-77.
- Bau, M., Dulski, P., 1996. Anthropogenic origin of positive gadolinium anomalies in river waters. *Earth and Planetary Science Letters*, 143, 245-255.
- Bau, M., Koschinsky, A., 2009. Oxidative scavenging of cerium on hydrous Fe oxide: Evidence from the distribution of rare earth elements and yttrium between Fe oxides and Mn oxides in hydrogenetic ferromanganese crusts. *Geochemical Journal*, 43, 37-47.
- Bau, M., Möller, P., Dulski, P., 1997. Yttrium and lanthanides in eastern Mediterranean seawater and their fractionation during redox-cycling. *Marine Chemistry*, 56, 123-131.
- Braun, J.J., Viers, J., Dupré, B., Polvé, M., Ndam, J., Muller, J.P., 1998. Solid/liquid REE fractionation in the lateritic system of Goyoum, East Cameroon: the implication for the present dynamics of the soil covers of the humid tropical regions. *Geochimica et Cosmochimica Acta*, 62, 273-299.
- Brioschi, L., Steinmann, M., Lucot, E., Pierret, M., Stille, P., Prunier, J., Badot, P., 2013. Transfer of rare earth elements (REE) from natural soil to plant systems: implications for the environmental availability of anthropogenic REE. *Plant and Soil*, 366, 143-163.
- Byrne, R.H., Kim, K.-H., 1990. Rare earth element scavenging in seawater. *Geochimica et Cosmochimica Acta*, 54, 2645-2656.
- Byrne, R.H., Li, B., 1995. Comparative complexation behavior of the rare earths. *Geochimica et Cosmochimica Acta*, 59, 4575-4589.
- Byrne, R.H., Sholkovitz, E.R., 1996. Marine chemistry and geochemistry of the lanthanides. In: K.A. Gschneidner Jr. and L.R. Eyring (Editors), *Handbook on the Physics and Chemistry of Rare Earths*. Elsevier, Amsterdam, pp. 497-593.
- De Baar, H.J.W., Bacon, M.P., Brewer, P.G., 1983. Rare-earth distributions with a positive Ce anomaly in the Western North Atlantic Ocean. *Nature*, 301, 324-327.

- De Baar, H.J.W., Bacon, M.P., Brewer, P.G., Bruland, K.W., 1985. Rare earth elements in the Pacific and Atlantic Oceans. *Geochimica et Cosmochimica Acta*, 49, 1943-1959.
- De Baar, H.J.W., German, C.R., Elderfield, H., van Gaans, P., 1988. Rare earth element distributions in anoxic waters of the Cariaco Trench. *Geochimica et Cosmochimica Acta*, 52, 1203-1219.
- De Carlo, E.H., Green, W.J., 2002. Rare earth elements in the water column of Lake Vanda, McMurdo Dry Valleys, Antarctica. *Geochimica et Cosmochimica Acta*, 66, 1323-1333.
- De Carlo, E.H., Wen, X.-Y., Irving, M., 1998. The influence of redox reactions on the uptake of dissolved Ce by suspended Fe and Mn oxide particles. *Aquatic Geochemistry*, 3, 357-389.
- Deberdt, S., Viers, J., Dupré, B., 2002. New insights about the rare earth elements (REE) mobility in river waters. *Bulletin de la Société Géologique de France*, 173, 147-160.
- Decrée, S., Deloule, E., Ruffet, G., Dewaele, S., Mees, F., Marignac, C., Yans, J., De Putter, T., 2010. Geodynamic and climate controls in the formation of Mio-Pliocene world class oxidized cobalt and manganese ores in the Katanga province, DR Congo. *Mineralium Deposita*, 45, 621-629.
- Dia, A., Gruau, G., Olivié-Lauquet, G., Riou, C., Molénat, J., Curmi, P., 2000. The distribution of rare earth elements in groundwaters: assessing the role of source-rock composition, redox changes and colloidal particle. *Geochimica et Cosmochimica Acta*, 64, 4131-4151.
- Doležal, J., Novák, J., 1959. Beitrag zum polarographischen Verhalten von drei- und vierwertigem Cer. *Collection of Czechoslovak Chemical Communications*, 24, 2182-2189.
- Donnot, M., Guigues, J., Lulzac, Y., Magnien, A., Parfenoff, A., Picot, P.,  
ques de Bretagne. *Mineralium Deposita*, 8 (1), 7-18.
- Dubascoux, S., Le Hécho, I., Hassellöv, M., Von Der Kammer, F., Potin Gautier, M., Lespes, G., 2010. Field-flow fractionation and inductively coupled plasma mass spectrometer coupling: History, development and applications. *Journal of Analytical Atomic Spectrometry*, 25, 613-623.
- Duncan, T., Shaw, T.J., 2004. The mobility of rare earth elements and redox sensitive elements in the groundwater/seawater mixing zone of a shallow coastal aquifer. *Aquatic Geochemistry*, 9, 223-255.
- Dupré, B., Gaillardet, J., Rousseau, D., Allègre, C.J., 1996. Major and trace elements of river-borne material: The Congo Basin. *Geochimica et Cosmochimica Acta*, 60, 1301-1321.
- Dupré, B., Viers, J., Dandurand, J.-L., Polvé, M., Bénézeth, P., Vervier, P., Braun, J.-J., 1999. Major and trace elements associated with colloids in organic-rich river waters: ultrafiltration of natural and spiked solutions. *Chemical Geology*, 160, 63-80.
- Elbaz-Poulichet, F., Dupuy, C., 1999. Behaviour of rare earth elements at the freshwater-seawater interface of two acid mine rivers: the Tinto and Odiel (Andalucia, Spain). *Applied Geochemistry*, 14, 1063-1072.
- Elderfield, H., 1988. The oceanic chemistry of the rare earth elements in seawater. *Philosophical Transaction of the Royal Society of London*, A325, 105-126.
- Elderfield, H., Greaves, M.J., 1982. The rare earth elements in seawater. *Nature*, 296, 214-219.
- Elderfield, H., Upstill-Goddard, R., Sholkovitz, E.R., 1990. The rare earth elements in rivers, estuaries, and coastal seas and their significance to the composition of ocean waters. *Geochimica et Cosmochimica Acta*, 54, 971-991.

- Evans, J., Zalasiewicz, J., 1996. U-Pb, Pb-Pb and Sm-Nd dating of authigenic monazite: Implications for the diagenetic evolution of the Welsh Basin. *Earth and Planetary Science Letters*, 144 (3-4), 421-433.
- Fairhurst, A.J., Warwick, P., Richardson, S., 1995. The influence of humic acid on the adsorption of europium onto inorganic colloids as a function of pH. *Colloids and Surfaces A*, 99, 187-199.
- Fee, J.A., Gaudette, H.E., Lyons, W.B., Long, D.T., 1992. Rare-earth element distribution in Lake Tyrrell groundwaters, Victoria, Australia. *Chemical Geology*, 96, 67-93.
- Gaillardet, J., Dupré, B., Allègre, C.J., 1999. Geochemistry of large river suspended sediments: silicate weathering or recycling tracer? *Geochimica et Cosmochimica Acta*, 63 (23-24), 4037-4051.
- Gaillardet, J., Viers, J., Dupré, B., 2003. Elements in River Waters. In: E.D. Holland, Turekian, K.K. (Editor), *Treatise on Geochemistry*. Elsevier-Pergamon, pp. 225–263.
- Gammons, C.H., Wood, S.A., Ponas, J.P., Madison, J.P., 2003. Geochemistry of the rare-eath elements and uranium in the acidic Berkeley Pit Lake, Butte, Montana. *Chemical Geology*, 198, 269-288.
- Gerard, M., Seyler, P., Benedetti, M.F., Alves, V.P., Boaventura, G.R., Sondag, F., 2003. Rare earth elements in the Amazon basin. *Hydrological Processes*, 17, 1379-1392.
- German, C.R., Holiday, B.P., Elderfield, H., 1991. Redox cycling of rare earth elements in the suboxic zone of the Black Sea. *Geochimica et Cosmochimica Acta*, 55, 3553-3558.
- German, C.R., Masuzawa, T., Greaves, M.J., Elderfield, H., Edmond, J.M., 1995. Dissolved rare earth elements in the Southern Ocean: Cerium oxidation and the influence of hydrography. *Geochimica et Cosmochimica Acta*, 59, 1551-1558.
- Goldberg, E.D., Koide, M., Schmitt, R.A., Smith, R.H., 1963. Rare earth distribution in the marine environment. *Journal of Geophysical Research*, 68, 4209-4217.
- Goldstein, S.J., Jacobsen, S.B., 1988. Rare earth elements in river waters. *Earth and Planetary Science Letters*, 89, 35-47.
- Gruau, G., Dia, A., Olivié-Lauquet, G., Davranche, M., Pinay, G., 2004. Controls on the distribution of rare earth elements in shallow groundwaters. *Water Research*, 38, 3576-3586.
- Haskin, L.A., Haskin, M.A., Frey, F.A., Wilderman, T.R., 1968. Relative and absolute terrestrial abundances of the rare earths. In: A. L.H. (Editor), *Origin and distributions of the elements*, pp. 889-912.
- Henderson, P., 1984. *Rare earth element geochemistry*. Elsevier, Amsterdam.
- Hoyle, J., Elderfield, H., Gledhill, A., Greaves, M., 1984. The behaviour of rare earth elements during mixing of river and sea waters. *Geochimica et Cosmochimica Acta*, 48, 143-149.
- Ingri, J., Widerlund, A., Land, M., Gustafsson, Ö., Andersson, P., Öhlander, B., 2000. Temporal variations in the fractionation of the rare earth elements in a boreal river; the role of colloidal particles. *Chemical Geology*, 166, 23-45.
- Janssen, R.P.T., Verweij, W., 2003. Geochemistry of some rare earth elements in groundwater, Vierlingsbeek, The Netherlands. *Water Research*, 37, 1320-1350.
- Johannesson, K.H., Hendry, M.J., 2000. Rare earth element geochemistry of groundwaters from a thick till and clay-rich aquitard sequence, Saskatchewan, Canada. *Geochimica et Cosmochimica Acta*, 64, 1493-1509.
- Johannesson, K.H., Lyons, W.B., 1994. The rare earth element geochemistry of Mono Lake water and the importance of carbonate complexing. *Limnology and Oceanography*, 39, 1141-1154.

- Johannesson, K.H., Lyons, W.B., Stetzenbach, K.J., Byrne, R.H., 1995. The solubility control of rare earth elements in natural terrestrial waters and the significance of PO<sub>4</sub><sup>3-</sup> and CO<sub>3</sub><sup>2-</sup> in limiting dissolved rare earth concentrations: a review of recent information. *Chemical Geology*, 133, 125-144.
- Johannesson, K.H., Stetzenbach, K.J., Hodge, V.F., 1997. Rare earth elements as geochemical tracers of regional groundwater mixing. *Geochimica et Cosmochimica Acta*, 61, 3605-3618.
- Johannesson, K.H., Stetzenbach, K.J., Hodge, V.F., Lyons, W.B., 1996. Rare earth element complexation behavior in circumneutral pH groundwaters: Assessing the role of carbonate and phosphate ions. *Earth and Planetary Science Letters*, 139, 305-319.
- Johannesson, K.H., Tang, J., Daniels, J.M., Bounds, W.J., Burdige, D.J., 2004. Rare earth element concentrations and speciation in organic-rich blackwaters of the Great Dismal Swamp, Virginia, USA. *Chemical Geology*, 209, 271-294.
- Johannesson, K.H., Zhou, X., 1999. Origin of middle rare earth element enrichments in acid waters of a Canadian High Arctic lake. *Geochimica et Cosmochimica Acta*, 63, 153-165.
- Johannesson, K.H., Zhou, X., Guo, C., Stetzenbach, K.J., Hodge, V.F., 2000. Origin of rare earth element signatures in groundwaters of circumneutral pH from southern Nevada and eastern California, USA. *Chemical Geology*, 164, 239-257.
- Kanazawa, Y., Kamitani, M., 2006. Rare earth minerals and resources in the world. *Journal of Alloys and Compounds*, 408-412, 1339-1343.
- Kato, Y., Fujinaga, K., Nakamura, K., Takaya, Y., Kitamura, K., Ohta, J., Toda, R., Nakashima, T., Iwamori, H., 2011. Deep-sea mud in the Pacific Ocean as a potential resource for rare-earth elements. *Nature Geosci*, 4 (8), 535-539.
- Kinniburgh, D.G., Cooper, D.M., 2009. PhreePlot: Creating graphical output with PHREEQC. Available at: <http://www.phreeplot.org>, pp. 498.
- Klungness, G.D., Byrne, R.H., 2000. Comparative hydrolysis behavior of the rare earths and yttrium: the influence of temperature and ionic strength. *Polyhedron*, 19, 99-107.
- Koeppenkastrop, D., De Carlo, E.H., 1992. Sorption of rare-earth elements from seawater onto synthetic mineral particles: An experimental approach. *Chemical Geology*, 95 (3-4), 251-263.
- Lawrence, M.G., Kamber, B.S., 2006. The behaviour of the rare earth elements during estuarine mixing - revisited. *Marine Chemistry*, 100, 147-161.
- Lead, J.R., Hamilton-Taylor, J., Peters, A., Reiner, S., Tipping, E., 1998. Europium binding by fulvic acids. *Analytica Chimica Acta*, 369, 171-180.
- Lee, J.H., Byrne, R.H., 1992. Examination of comparative rare earth element complexation behavior using linear free-energy relationships. *Geochimica et Cosmochimica Acta*, 56, 1127-1137.
- Lev, S.M., McLennan, S.M., Meyers, W.J., Hanson, G.N., 1998. A petrographic approach for evaluating trace-element mobility in a black shale. *Journal of Sedimentary Research*, 68 (5), 970-980.
- Luo, Y.-R., Byrne, R.H., 2004. Carbonate complexation of yttrium and the rare earth elements in natural rivers. *Geochimica et Cosmochimica Acta*, 68, 691-699.
- Marsac, R., Davranche, M., Gruau, G., Bouhnik-Le Coz, M., Dia, A., 2011. An improved description of the interactions between rare earth elements and humic acids by modeling: PHREEQC-Model VI coupling. *Geochimica et Cosmochimica Acta*, 75 (19), 5625-5637.
- Martin, J.-M., Hogdahl, O., Philippot, J.C., 1976. Rare earth element supply to the ocean. *Journal of Geophysical Research*, 81, 3119-3124.

- McLennan, S.M., 1989. Rare earth element geochemistry in sedimentary rocks: influence of provenance and sedimentary processes. In: Lipin B.R. and Mc Kay G.A. (Editors), *Geochemistry and mineralogy of rare earth elements*, pp. 169-200.
- Millero, F.J., 1992. Stability constants for the formation of rare earth inorganic complexes as a function of ionic strength. *Geochimica et Cosmochimica Acta*, 56, 3123-3132.
- Moffett, J.W., 1990. Microbially mediated cerium oxidation in sea water. *Nature*, 345, 421-423.
- Möller, P., Bau, M., 1993. Rare-earth patterns with positive cerium anomaly in alkaline waters from Lake Van, Turkey. *Earth and Planetary Science Letters*, 117, 671-676.
- Nakada, R., Takahashi, Y., Zheng, G., Yamamoto, Y., Shimizu, H., 2010. Abundances of rare earth elements in crude oils and their partitions in water *Geochemical Journal*, 44, 411-418.
- Nash, K.L., Sullivan, J.C., 1991. Kinetics of complexation and redox reactions of the lanthanides in aqueous solutions. In: K.A. Gschneidner Jr. and L.R. Eyring (Editors), *Handbook on the Physics and Chemistry of Rare Earths*. Elsevier Sciences B.V., pp. 347-391.
- Nelson, B.J., Wood, S.A., Osiensky, J.L., 2004. Rare earth element geochemistry of groundwater in the Palouse Basin, northern Idaho-eastern Washington. *Geochemistry: Exploration, Environment, Analysis*, 4, 227-241.
- Nesbitt, H.W., 1979. Mobility and fractionation of rare earth elements during weathering of a granodiorite. *Nature*, 279, 206-210.
- Nowack, B., Sigg, L., 1996. Adsorption of EDTA and metal-EDTA complexes onto goethite. *Journal of Colloid and Interface Science*, 177, 106-121.
- Ohta, A., Kawabe, I., 2001. REE(III) adsorption onto Mn dioxide and Fe oxyhydroxide: Ce(III) oxidation by Mn dioxide. *Geochimica et Cosmochimica Acta*, 65, 695-703.
- Parkhurst, D.L., Appelo, C.A.J., 1999. User's guide to PHREEQC (Version 2) - A computer program for speciation, batch-reaction, one-dimensional transport, and inverse geochemical calculations. 99-4259, U.S. Geological Survey Water-Resources Investigations Report.
- Pourret, O., Davranche, M., 2013. Rare earth element sorption onto hydrous manganese oxide A modeling study. *Journal of Colloid and Interface Science*, 395, 18-23.
- Pourret, O., Davranche, M., Gruau, G., Dia, A., 2007a. Organic complexation of rare earth elements in natural waters: Evaluating model calculations from ultrafiltration data. *Geochimica et Cosmochimica Acta*, 71, 2718-2735.
- Pourret, O., Davranche, M., Gruau, G., Dia, A., 2007b. Rare Earth Elements complexation with humic acid. *Chemical Geology*, 243, 128-141.
- Pourret, O., Dia, A., Davranche, M., Gruau, G., Hénin, O., Angée, M., 2007c. Organo-colloidal control on major- and trace-element partitioning in shallow groundwaters: confronting ultrafiltration and modelling. *Applied Geochemistry*, 22, 1568-1582.
- Pourret, O., Martinez, R.E., 2009. Modeling lanthanide series binding sites on humic acid. *Journal of Colloid and Interface Science*, 330, 45-50.
- Pourret, O., Tuduri, J., Armand, R., Bayon, G., Steinmann, M., 2012. Reassessment of the rare earth elements external cycle in french watersheds - a high potential resource for the future. *Mineralogical Magazine*, 76 (6), 2247.
- Quinn, K.A., Byrne, R.H., Schijf, J., 2007. Sorption of yttrium and rare earth elements by amorphous ferric hydroxide: Influence of temperature. *Environmental Science & Technology*, 41, 541-546.
- Riglet-Martial, C., Vitorge, P., Calmon, V., 1998. Electrochemical characterisation of the Ce(IV) limiting carbonate complex. *Radiochimica Acta*, 82, 69-76.

- Schijf, J., Byrne, R.H., 2004. Determination of  $\text{SO}_4\beta_1$  for yttrium and the rare earth elements at  $I = 0.66 \text{ m}$  and  $t = 25^\circ\text{C}$ -Implications for YREE solution speciation in sulfate-rich waters. *Geochimica et Cosmochimica Acta*, 68, 2825-2837.
- Schindler, P.W., 1990. Co-adsorption of metal ions and organic ligands: formation of ternary surface complexes. In: M.F. Hochella and A.F. White (Editors), *Mineral-Water Interface Geochemistry*. Mineralogical Society of America, pp. 281-307.
- Shacat, J.A., Green, W.J., De Carlo, E.H., Newell, S., 2004. The geochemistry of Lake Joyce, McMurdo Dry Valleys, Antarctica. *Aquatic Geochemistry*, 10, 325-352.
- Shiller, A.M., 2002. Seasonality of dissolved rare earth elements in the Lower Mississippi River. *Geochemistry Geophysics Geosystems*, 3, 1068.
- Sholkovitz, E.R., 1992. Chemical evolution of rare earth elements: fractionation between colloidal and solution phases of filtered river water. *Earth and Planetary Science Letters*, 114, 77-84.
- Sholkovitz, E.R., 1993. The geochemistry of rare earth elements in the Amazon River estuary. *Geochimica et Cosmochimica Acta*, 57, 2181-2190.
- Sholkovitz, E.R., 1995. The aquatic chemistry of rare earth elements in rivers and estuaries. *Aquatic Geochemistry*, 1, 1-34.
- Smedley, P.L., 1991. The geochemistry of rare earth elements in groundwater from the Carnmenellis area, southwest England. *Geochimica et Cosmochimica Acta*, 55, 2767-2779.
- Sonke, J.E., 2006. Lanthanide-humic substances complexation. II. Calibration of Humic Ion-Binding Model V. *Environmental Science & Technology*, 40, 7481-7487.
- Sonke, J.E., Salters, V.J.M., 2006. Lanthanide-humic substances complexation. I. Experimental evidence for a lanthanide contraction effect. *Geochimica et Cosmochimica Acta*, 70, 1495-1506.
- Steinmann, M., Stille, P., 2008. Controls on transport and fractionation of the rare earth elements in stream water of a mixed basaltic-granitic catchment (Massif Central, France). *Chemical Geology*, 254, 1-18.
- Stolpe, B., Guo, L., Shiller, A.M., 2013. Binding and transport of rare earth elements by organic and iron-rich nanocolloids in Alaskan rivers, as revealed by field-flow fractionation and ICP-MS. *Geochimica et Cosmochimica Acta*, 106, 446-462.
- Sverjensky, D.A., 1984. Europium redox equilibria in aqueous solution. *Earth and Planetary Science Letters*, 67, 70-78.
- Tang, J., Johannesson, K.H., 2003. Speciation of rare earth elements in natural terrestrial waters: Assessing the role of dissolved organic matter from the modeling approach. *Geochimica et Cosmochimica Acta*, 67, 2321-2339.
- Taylor, S.R., McLennan, S.M., 1985. *The Continental Crust: Its composition and evolution*. Blackwell, Oxford, 312 pp.
- Tipping, E., 1994. WHAM - A chemical equilibrium model and computer code for waters, sediments, and soils incorporating a discrete site/electrostatic model of ion-binding by humic substances. *Computers & Geosciences*, 20, 973-1023.
- Tipping, E., 1998. Humic Ion-Binding Model VI: an improved description of the interactions of protons and metal ions with humic substances. *Aquatic Geochemistry*, 4, 3-48.
- Tonkin, J.W., Balistrieri, L.S., Murray, J.W., 2004. Modeling sorption of divalent metal cations on hydrous manganese oxide using the diffuse double layer model. *Applied Geochemistry*, 19, 29-53.

- Tricca, A., Stille, P., Steinmann, M., Kiefel, B., Samuel, J., Eikenberg, J., 1999. Rare earth elements and Sr and Nd isotopic compositions of dissolved and suspended loads from small river systems in the Vosges mountains (France), the river Rhine and groundwater. *Chemical Geology*, 160, 139-158.
- Tuduri, J., Chauvet, A., Ennaciri, A., Barbanson, L., 2006. Modèle de formation du gisement d'argent d'Imiter (Anti-Atlas oriental, Maroc). Nouveaux apports de l'analyse structurale et minéralogique. *Comptes Rendus Geoscience*, 338, 253-261.
- Viers, J., Dupré, B., Polvé, M., Schott, J., Dandurand, J.-L., Braun, J.J., 1997. Chemical weathering in the drainage basin of a tropical watershed (Nsimi-Zoetele site, Cameroon): comparison between organic-poor and organic-rich waters. *Chemical Geology*, 140, 181-206.
- White, D.E., 1968. Environments of generation of some base-metal ore deposits. *Economic Geology*, 63 (4), 301-335.
- Wood, S.A., 1990. The aqueous geochemistry of the rare-earth elements and yttrium. 1. Review of the available low-temperature data for inorganic complexes and inorganic REE speciation in natural waters. *Chemical Geology*, 82, 159-186.
- Wood, S.A., 1993. The aqueous geochemistry of the rare-earth elements: Critical stability constants for complexes with simple carboxylic acids at 25°C and 1 bar and their application to nuclear waste management. *Engineering Geology*, 34, 229-259.
- Yamamoto, Y., Takahashi, Y., Shimizu, H., 2005. Systematics of stability constants of fulvate complexes with rare earth ions. *Chemistry Letters*, 34, 880-881.
- Yamamoto, Y., Takahashi, Y., Shimizu, H., 2006. Interpretation of REE patterns in natural water based on the stability constants. *Geochimica et Cosmochimica Acta*, Supplement 1, A717.



# **Publications**

## Rare earth elements complexation with humic acid

Olivier Pourret\*, Mélanie Davranche, Gérard Gruau, Aline Dia

Géosciences Rennes, Université Rennes 1, CNRS Campus de Beaulieu 35042 Rennes Cedex, France

Received 2 May 2006; received in revised form 22 May 2007; accepted 24 May 2007

Editor: D. Rickard

### Abstract

The binding of rare earth elements (REE) to humic acid (HA) was studied by combining ultrafiltration and Inductively Coupled Plasma Mass Spectrometry techniques. REE–HA complexation experiments were performed at various pH conditions (ranging from 2 to 10.5) using a standard batch equilibration method. Results show that the amount of REE bound to HA strongly increases with increasing pH. Moreover, a Middle-REE (MREE) downward concavity is evidenced by REE distribution patterns at acidic pH. Modelling of the experimental data using Humic Ion Binding Model VI provided a set of  $\log K_{MA}$  values (i.e., the REE–HA complexation constants specific to Model VI) for the entire REE series. The  $\log K_{MA}$  pattern obtained displays a MREE downward concavity. Log  $K_{MA}$  values range from 2.42 to 2.79. These binding constants are in good agreement with the few existing datasets quantifying the binding of REE with humic substances but quite different from a recently published study which evidence a lanthanide contraction effect (i.e., continuous increase of the constant from La to Lu). The MREE downward concavity displayed by REE–HA complexation pattern determined in this study compares well with results from REE–fulvic acid (FA) and REE–acetic acid complexation studies. This similarity in the REE complexation pattern suggests that carboxylic groups are the main binding sites of REE in HA. This conclusion is further illustrated by a detailed review of published studies for natural, organic-rich, river- and ground-waters which show no evidence of a lanthanide contraction effect in REE pattern. Finally, application of Model VI using the new, experimentally determined  $\log K_{MA}$  values to World Average River Water confirms earlier suggestions that REE occur predominantly as organic complexes ( $\geq 60\%$ ) in the pH range between 5–5.5 and 7–8.5 (i.e., in circumneutral pH waters). The only significant difference as compared to earlier model predictions made using estimated  $\log K_{MA}$  values is that the experimentally determined  $\log K_{MA}$  values predict a significantly higher amount of Light-REE bound to organic matter under alkaline pH conditions.

© 2007 Elsevier B.V. All rights reserved.

**Keywords:** Rare earth elements; Humic acid; Binding; Speciation; Ultrafiltration; Model VI

### 1. Introduction

Rare Earth Elements (REE) are commonly used as tracers for geochemical processes in natural waters (Elderfield and Greaves, 1982; Henderson, 1984; Elderfield et al., 1990; Smedley, 1991; Sholkovitz,

1995; Johannesson et al., 1997; Johannesson et al., 2000). Ground- and river-waters do not exhibit uniform REE patterns (Goldstein and Jacobsen, 1988; Elderfield et al., 1990; Sholkovitz, 1995). Systematic variations in REE patterns occur which have been attributed, in part, to the presence of two REE pools – so-called “dissolved” and “colloidal” pools – having different REE fractionation pattern. For example, it is often suggested that REE patterns of rivers result from the

\* Corresponding author. Tel.: +33 2 23 23 60 42; fax: +33 2 23 23 60 90.

E-mail address: [olivier.pourret@univ-rennes1.fr](mailto:olivier.pourret@univ-rennes1.fr) (O. Pourret).

mixing between (i) a low REE concentration, dissolved pool, Light-REE (LREE) depleted, but Heavy-REE (HREE) enriched related to Upper Continental Crust (UCC) (Taylor and McLennan, 1985) and (ii) a REE-rich colloidal phase having a Middle-REE (MREE) downward concavity pattern, namely a pattern that exhibits both  $(\text{La}/\text{Sm})_{\text{UCC}}$  ratio below 1 and  $(\text{Gd}/\text{Yb})_{\text{UCC}}$  ratio above 1 (Goldstein and Jacobsen, 1988; Elderfield et al., 1990; Sholkovitz, 1995). Humic substances constitute a significant part of the colloidal phase in both ground- and river-waters (Thurman, 1985). Consequently, interpreting and understanding the significance of REE fractionation pattern variability in these waters rely, for a large part, on a better description of the binding of REE to humic materials (HM) and of the REE fractionation patterns that may occur during this binding.

Models based on thermodynamics principles offer an interesting perspective in order to predict the complexation of REE with HM and thus to explore the extent to which the shape of ground- and river-water REE patterns depends on REE fractionation by HM. Modelling calculations were already performed in seawater (Cantrell and Byrne, 1987; Byrne and Kim, 1990; De Baar et al., 1991) and ground-waters (Wood, 1990; Lee and Byrne, 1992; Johannesson et al., 1996b). They evidence that hydroxides and carbonates (Cantrell and Byrne, 1987; Lee and Byrne, 1993; Liu and Byrne, 1998; Luo and Byrne, 2004) are the major inorganic complexing ligands of REE. However, organic complexation is often not taken into account in these calculations. Studies on REE–dissolved organic material (DOM) interactions and in particular humic and fulvic acids (HA and FA) are sparse in all respect (Dupré et al., 1999; Tang and Johannesson, 2003; Johannesson et al., 2004). Natural organic molecules contain numerous and chemically different binding sites, and thus it is difficult to define discrete equilibrium constants for each complexation reaction (Crawford, 1996). Thus, addressing complexation with DOM in existing aqueous speciation models is not obvious. Until recently, REE–FA or –HA complexation constants were generally determined for a single REE (e.g., for HA: Sm–HA, Eu–HA, Tb–HA and Dy–HA) (Maes et al., 1988; Bidoglio et al., 1991; Moulin et al., 1992; Dierckx et al., 1994; Fairhurst et al., 1995; Franz et al., 1997; Lead et al., 1998; Lippold et al., 2005) or a set of REE (Ce, Eu, Gd, Tm and Lu) (Takahashi et al., 1997) while accurate stability constants are needed for the 14 naturally occurring REE to model speciation of natural water. Only two studies reporting REE–humate binding constants for the 14 naturally occurring REE have been

so far published. They have unfortunately yielded to somewhat different results. Yamamoto et al. (2005, 2006) studied complexation of REE with Suwannee River FA (SRFA) and Suwannee River HA (SRHA) using a solvent extraction method. Patterns of REE–FA and REE–HA complexation constants obtained by these authors show a general MREE downward concavity similar to that obtained for REE–diacetic acid complexation, sometimes superimposed to an overall increase of complexation constants from LREE to HREE. By contrast, Sonke and Salters (2006) studied complexation of REE with SRFA, Leonardite coal HA (LHA) and Elliot soil HA (EHA) using an EDTA-ligand competition method. Complexation patterns obtained by these authors are quite different from those reported by Yamamoto et al. (2005) exhibiting a lanthanide contraction effect, i.e., a regular and progressive increase of the constants from La to Lu. It must be added that experimental pH range is different in both of these studies ranging between 4 and 5.5 in Yamamoto et al. studies (2005, 2006) and 6 and 9 in Sonke and Salters' one (2006).

In this contribution, in order to further test pieces of evidence provided by both studies (Yamamoto et al., 2005; Sonke and Salters, 2006) and provide a more accurate REE–HA complexation dataset, experiments of REE–Aldrich HA (AHA) complexation were performed for the 14 naturally occurring REE simultaneously. This new dataset was obtained using a third experimental method which combines an ultrafiltration technique and the Inductively Coupled Plasma Mass Spectrometry method. Humic Ion Binding Model VI (hereafter denoted as Model VI) was used to model the experimental results (Tipping, 1998). Therefore, the constants reported are not intrinsic equilibrium constants but Model VI specific equilibrium constants (i.e.,  $\log K_{\text{MA}}$  values). Considering the key role played by organic colloids in natural terrestrial waters, the new results were also used to revisit the significance of REE patterns in organic-rich, ground- and river-waters. Finally, the new constants were input in Model VI to reinvestigate World Average River Water (Tang and Johannesson, 2003) and further constrain the speciation of REE in river-waters.

## 2. Materials and method

### 2.1. Experimental binding of rare earth elements by humic acid

All chemicals used in this study were of analytical grade, and all the experimental solutions used were

prepared with doubly deionized water (MilliQ system, Millipore<sup>TM</sup>). REE–HA complexes were prepared in polyethylene containers previously soaked in 10% Ultrapure HNO<sub>3</sub> for 48 h at 60 °C, then rinsed with MilliQ water for 24 h at 60 °C to remove all possible REE contamination sources. Synthetic REE solutions were prepared from nitrate REE standards (10 mg L<sup>-1</sup>, Accu Trace<sup>TM</sup> Reference Standard). All experiments were carried out at room temperature, i.e., 20 °C±2.

### 2.1.1. Humic acid

Purified humate, referred to below as HA (humic acid), was obtained from synthetic Aldrich<sup>TM</sup> humic acid (Aldrich<sup>TM</sup>, H1, 675-2) following the protocol described by Vermeer et al. (1998). HA sample was freeze-dried and stored in a glass container at room temperature. HA obtained was ash free and in its protonated form, with the following elemental composition (as mass fraction): C=55.8%, O=38.9%, H=4.6%, N=0.6%. REE concentrations in HA were below the detection limit of ICP-MS measurement (i.e., <1 ng L<sup>-1</sup>). HA has a mean molecular weight of 23 kDa (Vermeer et al., 1998). Prior to use, the freeze-dried humate was resuspended overnight in an 0.001 mol L<sup>-1</sup> NaCl electrolyte solution at pH=10, to ensure complete dissolution of the sample (Davranche et al., 2004; Davranche et al., 2005). Although AHA is sometimes criticized as a weak model for humic substances (HS), its ion-binding behavior and physico-chemical properties are rather similar to those of other HS (Avena et al., 1999; Milne et al., 2001, 2003; Saito et al., 2005).

### 2.1.2. Experimental set-up description

REE complexation with HA was investigated using a standard batch equilibration technique. REE (50 ppb of each REE) and HA (5, 10 and 20 mg L<sup>-1</sup>) were placed together in solution, at an ionic strength of 0.001 mol L<sup>-1</sup> and at pH values ranging from 2.18 to 10.44. Prior to addition of HA, pH-solution was about 4. The initial hydroxide and carbonate concentrations were thus negligible and concentrations of LnOH<sup>2+</sup> and LnCO<sub>3</sub><sup>2-</sup> were therefore also negligible. The pH was measured with a combined Radiometer Red Rod electrode. The electrode was calibrated with WTW standard solutions (pH 4, 7 and 10). The accuracy of the pH measurement was ±0.05 pH unit. Experimental solutions were stirred for 48 h (equilibrium time determined from preliminary kinetic experiments) to allow equilibration and partitioning of REE between the aqueous solution and the humate suspension. Solution aliquots of about 10 mL were sampled twice: first at the beginning of the experiment; then after 48 h at equilibrium state. REE complexed by the

HA were separated from the remaining inorganic REE by ultrafiltration. Ultrafiltrations were carried out by centrifugating the 10 mL solution samples through 15 mL centrifugal tubes equipped with permeable membranes of 5 kDa pore size (Millipore Amicon Ultra-15). All centrifugal filter devices used were washed and rinsed with 0.1 mol L<sup>-1</sup> HCl and MilliQ water two times before use in order to minimize contamination. Centrifugations were performed using a Jouan G4.12 centrifuge with swinging bucket rotor at 3000 g for 30 min. The centrifugal force allowed the REE–HA complexes to be quantitatively separated from inorganic REE species. The used membrane can retain the humic material, while permitting passage of smaller solutes. REE–HA complexes have a mean molecular weight of 23 kDa, and are therefore caught up by the 5 kDa membrane whereas inorganic REE species went through it. The filtrate contains only the free REE, while the retentate contains HA and associate bound REE. The amount of metal bound is determined by difference. The selectivity of the 5 kDa membrane regards to the REE–HA complexes was verified by monitoring the Dissolved Organic Carbon (DOC) contents of the ultrafiltrates. Results show that the latter were systematically lower or equal to blank values ( $\leq 0.1$  mg L<sup>-1</sup>). Even if the passage of small amounts of low molecular weight FA through the ultrafiltration membrane was previously described (Nordén et al., 1993) in such measurement of metal binding by HS, we considered that the purified HA (23 kDa) could not pass through the membrane (5 kDa) as illustrated by ultrafiltrate DOC values lower or equal to blank ones. Possible adsorption of inorganic REE species onto the membrane or onto cell walls was also monitored. Inorganic REE solutions of known REE concentration were ultrafiltered several times. Results showed that between 98.91 (for Ho) and 99.98% (for Yb) of the REE present in solution were recovered in the ultrafiltrates, demonstrating that no REE were adsorbed on the membranes or on the walls of the cell devices used.

In the following, REE complexation with HA is described by quantifying the amount of REE that remains into the <5 kDa ultrafiltrates after equilibration of the REE-bearing aqueous solutions with HA and by comparing this amount to the amount of REE which has been introduced initially into the experimental solutions. All the removed REE are assumed to have been complexed by the 23 kDa HA. REE concentrations were determined at Rennes 1 University using an Agilent Technologies<sup>TM</sup> HP4500 ICP-MS instrument. Quantitative analyses were performed using a conventional external calibration procedure. Three external standard solutions with REE concentrations similar to the analyzed samples were prepared from a

multi-REE standard solution (Accu Trace<sup>TM</sup> Reference, 10 mg L<sup>-1</sup>, USA). Indium was added to all samples as an internal standard at a concentration of 0.87 µmol L<sup>-1</sup> (100 µg L<sup>-1</sup>) to correct for instrumental drift and possible matrix effects. Indium was also added to the external standard solutions. Calibration curves were calculated from measured REE/indium intensity ratios. The accuracy on REE analysis in our laboratory as established from repeated analyses of multi-REE standard solution (Accu Trace<sup>TM</sup> Reference, USA) and of the SLRS-4 water standard is <±2.5% (Dia et al., 2000; Davranche et al., 2005). Chemical blanks of individual REE were all lower than detection limit (1 ng L<sup>-1</sup>), which is negligible since they are three to four orders of magnitude lower than the concentrations measured in the synthetic solutions used in the complexation experiments. DOC concentrations were determined at Rennes 1 University using a Shimadzu 5000 TOC analyzer. The accuracy of DOC concentration measurements is estimated at ±5% as determined by repeated analyses of freshly prepared standard solutions (potassium biphtalate). In order to check that no retention of REE occurs inside the membrane during ultrafiltration, mass balance calculations were performed. The initial concentration of each element is compared with the sum of each element concentration in the ultrafiltrate and in the retentate. In the presented experiments, mass balanced calculations show that >98% of the REE and DOC was recovered. Moreover, in order to verify that no precipitation occurs, samples were filtered at 0.2 µm before ultrafiltration. Concentrations of REE and HA were systematically identical within analytical uncertainties in the 0.2 µm filtrates and the raw samples.

## 2.2. Humic Ion Binding Model VI

Humic Ion Binding Model VI (Model VI) has been described in detail by Tipping (1998). The model is a discrete binding site model which takes into account electrostatic interactions. There is an empirical relation between net humic charge and an electrostatic interaction factor. The discrete binding sites are represented by two types of sites (types A and B), each comprising four different site subtypes present in equal amounts. Types A and B sites are described by intrinsic proton binding constants ( $pK_A$  and  $pK_B$ ) and spreads of the values ( $\Delta pK_A$  and  $\Delta pK_B$ ) within each type. There are  $n_A$  (mol g<sup>-1</sup>) Type A sites (associated with carboxylic type groups) and  $n_B = n_A / 2$  (mol g<sup>-1</sup>) Type B sites (often associated with phenolic type groups). Metal binding occurs at single proton binding sites (monodentate complexation) or by bidentate complexation between pairs of sites. A proximity factor is introduced that quantifies whether pairs of proton binding

groups are close enough to form bidentate sites. Type A and Type B sites have separate intrinsic binding constants ( $\log K_{MA}$  and  $\log K_{MB}$ ), together associated with a parameter,  $\Delta LK_1$ , defining the spreads of values around the medians. A further parameter,  $\Delta LK_2$ , takes into account a small number of stronger sites (bidentate and tridentate sites). For more details on whether mono-, bi- and tridentate sites may form see Tipping (1998). By considering results from many datasets, a universal average value of  $\Delta LK_1$  is obtained, and a correlation established between  $\log K_{MB}$  and  $\log K_{MA}$  (Tipping, 1998). Then, a single adjustable parameter ( $\log K_{MA}$ ) is necessary to fully describe metal complexation with HA in Model VI. Model VI parameters for HA are presented in Table 1. Model VI was preferentially selected because this model is a widely accepted metal-organic matter speciation code whose capability to model Eu complexation with HM has been already tested and proved to perform reasonably well (Lead et al., 1998). Binding of the first hydrolysis species REE (OH) to humics was not included in Model VI simulations.

## 3. Results

### 3.1. Experimental results

Experimental data are reported in Appendix A and illustrated for three REE (La, Eu, Lu) in Fig. 1. REE complexation by HA is examined by considering the proportion of REE-HA complexes formed as a function

Table 1  
Model VI parameters for humic acid (Tipping, 1998)

| Parameter     | Description   | Values                            |
|---------------|---|-----------------------------------|
| $n_A$         | Amount of type A sites (mol g <sup>-1</sup> )                                   | $3.3 \times 10^{-3}$              |
| $n_B$         | Amount of type B sites (mol g <sup>-1</sup> )                                   | $0.5 \times n_A$                  |
| $pK_A$        | Intrinsic proton dissociation constant for type A sites                         | 4.1                               |
| $pK_B$        | Intrinsic proton dissociation constant for type B sites                         | 8.8                               |
| $\Delta pK_A$ | Distribution terms that modifies $pK_A$   | 2.1                               |
| $\Delta pK_B$ | Distribution terms that modifies $pK_B$   | 3.6                               |
| $\log K_{MA}$ | Intrinsic equilibrium constant for metal binding at type A sites                | Fitted from experimental data     |
| $\log K_{MB}$ | Intrinsic equilibrium constant for metal binding at type B sites                | $3.39 \log K_{MA} - 1.15$         |
| $\Delta LK_1$ | Distribution term that modifies $\log K_{MA}$                                   | 2.8 (REE)                         |
| $\Delta LK_2$ | Distribution term that modifies the strengths of bidentate and tridentate sites | $0.55 \log K_{NH_3} + 0.29$ (REE) |
| $P$           | Electrostatic parameter   | -330                              |
| $K_{sel}$     | Selectivity coefficient for counterion accumulation                             | 1                                 |
| $M$           | Molecular weight  | 15,000 Da                         |
| $R$           | Molecular radius  | 1.72 nm                           |

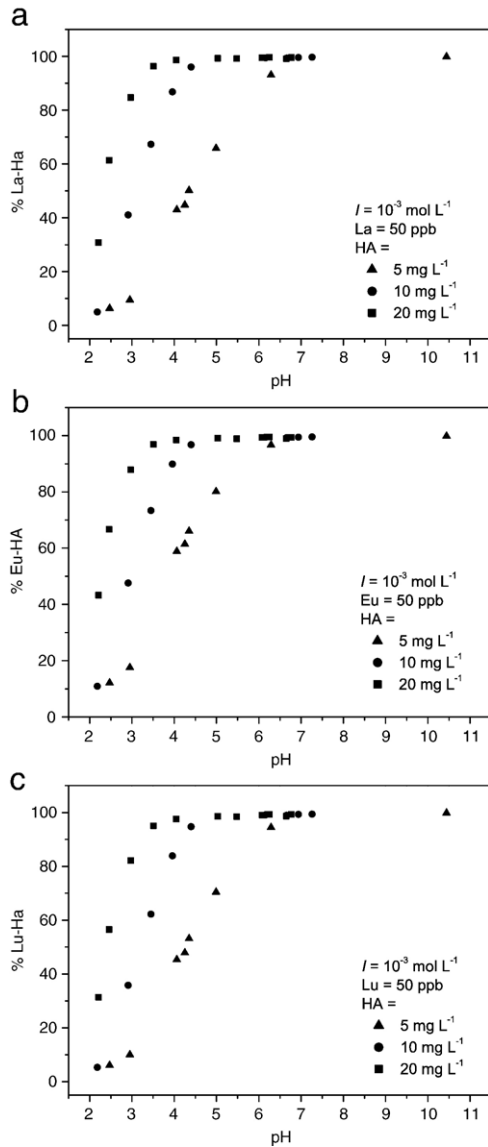


Fig. 1. Proportions of (a) La–HA, (b) Eu–HA and (c) Lu–HA complexes as a function of pH for various HA concentrations.

of pH. As shown in Fig. 1, the proportion of REE–HA complexes increases with increasing pH. It also depends on the HA concentration of the experimental solution. More specifically, the pH at which 100% of the REE are complexed by HA decreases with increasing HA concentration: pH ≈ 4, 5.5 and 7 for HA concentrations of 20, 10 and 5 mg L<sup>-1</sup>, respectively (see Fig. 1). These results are in good agreement with previously published data (Maes et al., 1988; Dierckx et al., 1994; Franz et al., 1997; Lippold et al., 2005). The observed pH dependence of REE complexation by HA can be explained by the deprotonation of the HA carboxylic and phenolic surface

groups at increasing pH, which is a classical feature of metal ion complexation by humic acid (Fairhurst et al., 1995; Lippold et al., 2005). Interestingly, patterns of the proportions of REE–HA exhibit a MREE downward concavity (i.e., (La–HA)/(Sm–HA) < 1 and (Gd–HA)/(Yb–HA) > 1) when the amount of REE complexed with HA is sufficiently low to evidence possible fractionation among the REE series (i.e., under acidic pH conditions; Fig. 2 and Appendix A). The same feature was already observed in complexation experiments of the REE with AHA using the dialysis method (Davranche et al., 2005).

### 3.2. Calculating log K<sub>MA</sub> values

Calculations were performed using the computer program WHAM 6 (Version 6.0.13) which includes Model VI. The three datasets corresponding to the three

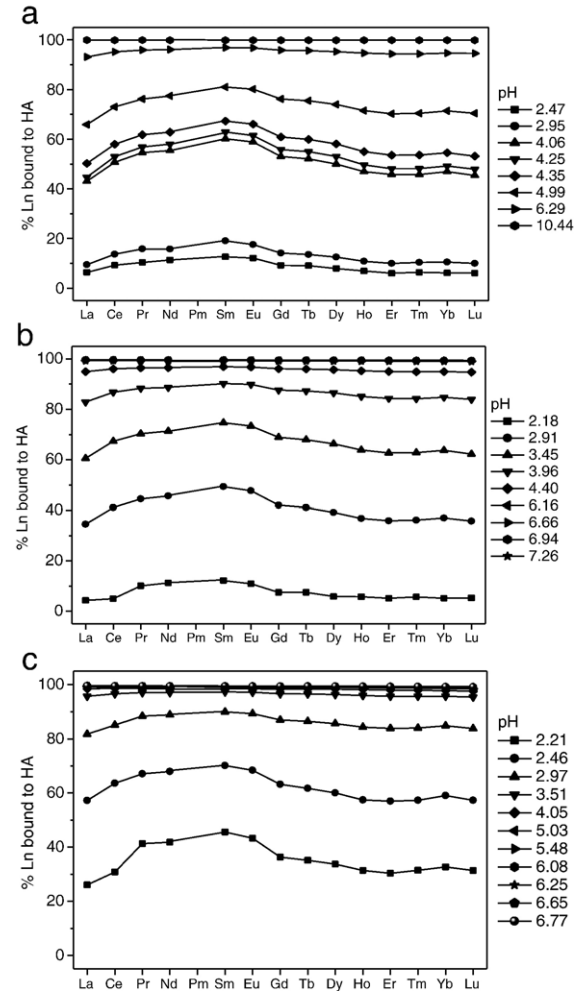


Fig. 2. Proportions of REE bound to HA as a function of pH for various HA concentrations of (a) 5 mg L<sup>-1</sup>, (b) 10 mg L<sup>-1</sup> and (c) 20 mg L<sup>-1</sup>.

different HA concentrations used were separately modelled. A classical strategy that consists in adjusting  $\log K_{MA}$  for each REE simultaneously until a reasonable fit is achieved was used. Values of  $[REE^{3+}]$  (i.e., the concentration of REE left in the <5 kDa ultrafiltrates) and  $v$  (moles of REE bound per gram of humic acid; i.e., the difference between the concentration of REE left in the <5 kDa ultrafiltrates and the concentration of REE initially present in the experimental solutions) are derived from the experimental data. The best fit is obtained when the root mean square error of the regression (rmse = sum of the squares of the differences between observed and calculated  $\log v$ ) is minimized. The three sets of optimized  $\log K_{MA}$  values thus obtained are reported in Table 2 for the 14 analyzed REE and illustrated in Fig. 3 for the case of La. As indicated by rmse values (<0.07), fits could be considered of good quality. The main characteristics of the REE–HA experiments to be reproduced by Model VI are a high proportion of REE–HA complexes at relatively low pH and a marked increase of this proportion with increasing pH.  $\log K_{MA}$  values increase with HA concentration of experimental solutions. The overall difference is of ca. 0.3 for all REE, which corresponds to a difference of ca. 12% on estimated  $\log K_{MA}$  values. As can be seen in Fig. 3, a 12% difference on  $\log K_{MA}$  values may result in a difference of up to 20% on the calculated proportion of REE–HA complex if the pH and the HA concentration are low. The default value is computed by taking the mean

Table 2  
Log  $K_{MA}$  values obtained for the three datasets using Model VI

| [HA]<br>(mg L <sup>-1</sup> ) | 5<br>(rmse) | 10<br>(rmse) | 20<br>(rmse) | mean | sd   |      |      |      |
|-------------------------------|-------------|--------------|--------------|------|------|------|------|------|
| La                            | 2.42        | 0.07         | 2.57         | 0.04 | 2.74 | 0.04 | 2.58 | 0.16 |
| Ce                            | 2.44        | 0.05         | 2.60         | 0.04 | 2.77 | 0.03 | 2.60 | 0.17 |
| Pr                            | 2.45        | 0.05         | 2.61         | 0.03 | 2.78 | 0.01 | 2.61 | 0.17 |
| Nd                            | 2.47        | 0.06         | 2.63         | 0.02 | 2.79 | 0.02 | 2.63 | 0.16 |
| Sm                            | 2.50        | 0.05         | 2.65         | 0.03 | 2.81 | 0.01 | 2.65 | 0.16 |
| Eu                            | 2.50        | 0.05         | 2.64         | 0.04 | 2.80 | 0.02 | 2.65 | 0.15 |
| Gd                            | 2.48        | 0.07         | 2.62         | 0.05 | 2.79 | 0.02 | 2.63 | 0.16 |
| Tb                            | 2.47        | 0.07         | 2.61         | 0.04 | 2.78 | 0.02 | 2.62 | 0.16 |
| Dy                            | 2.46        | 0.06         | 2.59         | 0.04 | 2.78 | 0.02 | 2.61 | 0.16 |
| Ho                            | 2.45        | 0.07         | 2.58         | 0.05 | 2.77 | 0.02 | 2.60 | 0.16 |
| Er                            | 2.45        | 0.07         | 2.57         | 0.02 | 2.77 | 0.02 | 2.60 | 0.16 |
| Tm                            | 2.44        | 0.07         | 2.56         | 0.02 | 2.76 | 0.02 | 2.59 | 0.16 |
| Yb                            | 2.45        | 0.06         | 2.57         | 0.01 | 2.77 | 0.03 | 2.60 | 0.16 |
| Lu                            | 2.44        | 0.07         | 2.56         | 0.04 | 2.76 | 0.02 | 2.59 | 0.16 |
| La/Sm                         | 0.97        |              | 0.97         |      | 0.98 |      | 0.97 |      |
| Gd/Yb                         | 1.01        |              | 1.02         |      | 1.01 |      | 1.01 |      |

rmse refers to root mean square error of the regression analysis (see text for details) while sd refers to standard deviation on the mean.

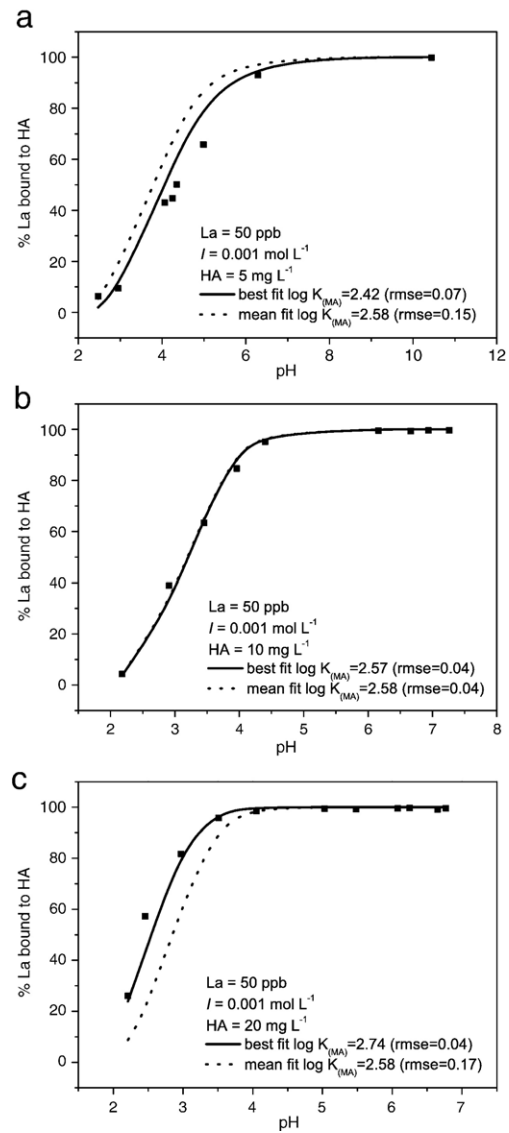


Fig. 3. Binding of La by HA. Dependence on pH of % La bound, measured by ultrafiltration; the solid line is the best fit and the dash line represents the calculated binding for the overall average  $\log K_{MA}$  (2.58) for various HA concentrations of (a) 5 mg L<sup>-1</sup>, (b) 10 mg L<sup>-1</sup>, and (c) 20 mg L<sup>-1</sup>.

between the three sets of values. This procedure means that equal weight is given to all the datasets obtained for different HA concentration levels. It implies that differences in  $\log K_{MA}$  for a given type of humic material are due to variations from one sample to another (Tipping, 1998). The adopted values are listed in Table 2. Log  $K_{MA}$  values increase from La (2.58) to Eu (2.65), then decrease from Gd (2.63) to Lu (2.59). It follows a  $\log K_{MA}$  pattern showing a MREE downward concavity.

## 4. Discussion

### 4.1. Comparison with published results

Data from previous studies (Moulin et al., 1992; Fairhurst et al., 1995; Lippold et al., 2005; Sonke and Salters, 2006) were modelled using Model VI to compare them with the newly obtained set of  $\log K_{\text{MA}}$ . Previous studies (Moulin et al., 1992; Fairhurst et al., 1995; Lippold et al., 2005) provide data for only a limited number of REE, namely Tb, Dy and Eu. Experimental conditions and fit results for these three studies are presented in Table 3. Modelled  $\log K_{\text{MA}}$  values for Tb (2.57) and Eu (2.73 and 2.77) are within the error range of the average  $\log K_{\text{MA}}$  values obtained here for these two REE ( $2.62 \pm 0.16$  and  $2.65 \pm 0.15$ , respectively; see Table 2). Only results for Dy are statistically different: 3.19 against  $2.61 \pm 0.16$  in the present study. The present results have also been compared to recently published results for the complexation of the 14 naturally occurring REE by Leonardite HA (LHA), a coal derived HA (Sonke and Salters, 2006). Complexation of the REE by LHA was experimentally studied at four different pH (6, 7, 8 and 9) using an EDTA-ligand competition method (Sonke and Salters, 2006). The corresponding modelled  $\log K_{\text{MA}}$  values are reported in Table 4. Even if  $\log K_{\text{MA}}$  values calculated for the LHA are of the same order of magnitude than  $\log K_{\text{MA}}$  values calculated for the AHA, a marked difference is noted in the REE fractionation pattern of  $\log K_{\text{MA}}$  values. REE-LHA complexation constants do not evidence the same MREE downward concavity as compared to that obtained with AHA, showing instead a progressive and continuous increase of  $\log K_{\text{MA}}$  values from La to Lu (i.e.,  $\log K_{\text{MA}}(\text{La-HA})/\log K_{\text{MA}}(\text{Sm-HA}) < 1$  and  $\log K_{\text{MA}}(\text{Gd-HA})/\log K_{\text{MA}}(\text{Yb-HA}) < 1$ ). This continuous increase of  $\log K_{\text{MA}}$  values from La to Lu as obtained for the LHA has been ascribed to a lanthanide contraction effect, and is quantified as the numerical difference between the Lu and La binding constants ( $\Delta_L \beta_{\text{Lu-La}}$  in Sonke and Salters, 2006). Such a feature (i.e., lanthanide contraction) has already been attributed to REE binding to coal derived HA (Takahashi et al., 1997).

The major difference between the results obtained here and the only dataset so far published for the 14 naturally

occurring REE with HA is thus in the shape of the  $\log K_{\text{MA}}$  values: MREE downward concavity here against linear increase from La to Lu for data published by Sonke and Salters (2006). They compared the constants they found for REE-LHA complexation with those found for 101 organic ligands (Byrne and Li, 1995). They further suggested that the lanthanide contraction effect they observed for LHA was in fact shared by a large number of organic ligands and could thus be a general feature of REE complexation by organic compounds. In addition to LHA, Sonke and Salters (2006) also determined REE complexation constants for two other HM sources – namely, fulvic acid from the Suwannee River and Elliot soil humic acid – using the same ligand-ligand technique as that used for LHA. They also evidenced a lanthanide contraction effect of their constant pattern. In the present study, no observation was found that a lanthanide contraction effect should exist in the complexation constants of REE by organic matter. Instead, the existing databank (Wood, 1993; Byrne and Li, 1995) points out that a MREE downward concavity of some constant pattern could occur, as obtained in the present study.

Complexation constants of REE with SRFA and SRHA were also determined by Yamamoto et al. (2005, 2006) using a solvent extraction technique (Fig. 4a; see also Fig. 1 in Yamamoto et al., 2005). Pattern of  $\log \beta$  (REE-FA) and  $\log \beta$  (REE-HA) looks very much like that found in the present study for REE-HA, being characterized by a MREE downward concavity shape (i.e.,  $\log K_{\text{MA}}(\text{La-HA})/\log K_{\text{MA}}(\text{Sm-HA}) < 1$  and  $\log K_{\text{MA}}(\text{Gd-HA})/\log K_{\text{MA}}(\text{Yb-HA}) > 1$ ). Binding of the REE to humic substances occurs mainly through carboxylic functions (Yamamoto et al., 2005). In this respect, simple organic compounds possessing carboxylic functional groups such as acetate can be regarded as analogue of complex organic matter, such as HA and FA (Wood, 1993). Thus,  $\log K_{\text{MA}}$  pattern of REE complexation with FA, HA and acetic acid can be together compared (Fig. 4) (Wood, 1993; Byrne and Li, 1995). As can be seen, patterns of  $\log K_{\text{MA}}$  values for acetic and diacetic acids do not evidence a lanthanide contraction effect: They are MREE downward concave, mimicking both those obtained by Yamamoto et al. (2005, 2006) for SRFA and SRHA and through this study for AHA. However, in some sample (particularly at pH 5.38)

Table 3  
Experimental conditions and fit of literature data (IE: ion exchange; S: spectrofluorometry)

| REE | [REE] ( $\mu\text{mol L}^{-1}$ ) | $I$ ( $\text{mol L}^{-1}$ ) | [HA] $\text{mg L}^{-1}$ | pH      | Technique | $\log K_{\text{MA}}$ | rmse | n  | References              |
|-----|----------------------------------|-----------------------------|-------------------------|---------|-----------|----------------------|------|----|-------------------------|
| Eu  | 0.001                            | 0.05                        | 10                      | 2 to 10 | IE        | 2.73                 | 0.01 | 7  | Fairhurst et al. (1995) |
| Eu  | 0.001                            | 0.05                        | 2                       | 2 to 10 | IE        | 2.77                 | 0.04 | 7  | Fairhurst et al. (1995) |
| Tb  | 0.100                            | 0.10                        | 5                       | 2 to 7  | IE        | 2.57                 | 0.06 | 7  | Lippold et al. (2005)   |
| Dy  | 2.000                            | 0.10                        | 0.5 to 9                | 5       | S         | 3.19                 | 0.03 | 13 | Moulin et al. (1992)    |

rmse corresponds to root mean square error of the regression analysis (see text for detail).

$\log \beta$ (REE–FA) shows both a MREE downward concavity superimposed on an overall increase in  $\log \beta$ (REE–FA) from LREE to HREE (Yamamoto et al., 2006).

The argument used by Sonke and Salters (2006) that a lanthanide contraction effect is observed in the constant pattern of many organic compounds is questionable. Indeed, their demonstration was built on the fact that a positive correlation exists when  $\Delta_L \beta_{Lu} - \beta_{La}$  of organic compounds is plotted against the average REE constant ( $\beta_{ave}$ ). REE stability constant is not always a simple function of atomic number. As suggested by Byrne and Li (1995), REE are best viewed as two series of elements corresponding to the LREE and HREE groups. The REE patterns of complexation constants with many organic ligands (Wood, 1993; Byrne and Li, 1995) or some inorganic ligands like  $\text{NO}_3^-$  (Wood, 1990; Millero, 1992) are characterized by a downward concavity centred on MREE. This shape corresponds to a (La/Sm) ratio below 1 and (Gd/Yb) ratio above 1 (Fig. 4a). Thus, such shapes are best viewed when REE are considered as two subgroups. Indeed, (La/Lu) ratio does not give an accurate description of the constants pattern. Let us for example consider a (La/Lu) ratio < 1. Such a value may actually reflect a pattern showing a continuous increase of the constant values from La to Lu, and thus a real lanthanide contraction effect. However, it may also reflect a REE pattern showing an increase of  $\log \beta$  values only from La to Sm or Eu and then constant values from Gd to Lu (no real HREE enrichment). It may even reflect a MREE downward concave pattern, the only required feature in that case being  $\log \beta_{La} < \log \beta_{Lu}$ . To test this possibility (Gd/Lu) ratios (i.e., shape of the MREE and HREE part of the constant pattern) for the same 101 organic compounds were

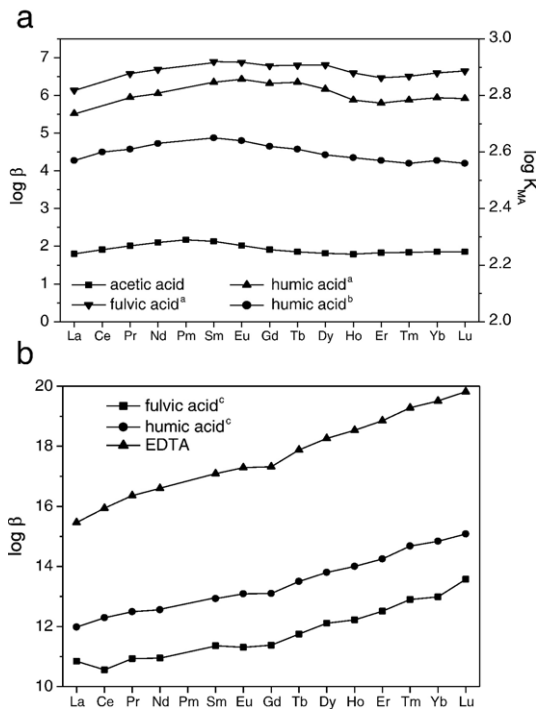


Fig. 4. REE patterns for (a)  $\log \beta$ (REE–acetic acid),  $\log \beta$ (REE–humic acid)<sup>a</sup>,  $\log \beta$ (REE–fulvic acid)<sup>a</sup> and  $\log K_{MA}$ (REE–humic acid)<sup>b</sup> and (b)  $\log \beta$ (REE–EDTA),  $\log \beta$ (REE–fulvic acid)<sup>c</sup> and  $\log \beta$ (REE–humic acid)<sup>c</sup>. <sup>a</sup>Yamamoto et al. (2006); <sup>b</sup>this study; <sup>c</sup>Sonke and Salters (2006).

calculated and compared with (Gd/Yb) ratios and  $\log \beta$  of these compounds. As shown in Fig. 5, the comparison shows that the positive correlation reported by Sonke and Salters (2006) when reporting (La/Lu) ratios of 101 compounds against their  $\beta_{ave}$  is lost when (Gd/Yb) is substituted to (La/Lu) ratios. For the purpose comparison Yamamoto et al. data for SRFA and SRHA (Yamamoto et al., 2005, 2006) and Sonke and Salters' data for SRFA and LHA (2006) were included in Fig. 5. In the present study, preliminary REE–HA constants calculations (not shown) give an order of magnitude for  $\log \beta$  values. While Yamamoto's  $\log \beta$  for SRFA and SRHA and our  $\log \beta$  for AHA are in the field of natural carboxylic and phenolic acids (Fig. 5), Sonke and Salters'  $\log \beta$  for SRFA and LHA are in the field of natural phenolic acids, natural amino-carboxylic acid and synthetic iminoacetic acids such as EDTA (Fig. 5). Observed differences between experiments presented in this study, and literature data (Takahashi et al., 1997; Yamamoto et al., 2005; Sonke, 2006; Sonke and Salters, 2006; Yamamoto et al., 2006) strongly suggest the heterogeneity of the complexing site (i.e., the coexistence of weak and strong binding sites) in the humic acid (Kubota et al., 2002). The main feature of our observations is that one can interpret differences as due to high concentration of weak sites (acetic-like sites) and low concentrations of strong

Table 4

Log  $K_{MA}$  values obtained for the four Sonke and Salters' datasets (2006) using Model VI (pH 6 to 9, 0.1 mol L<sup>-1</sup>  $\text{NaNO}_3$ , 100 nmol L<sup>-1</sup> REE, 10 mg L<sup>-1</sup> LHA and 500 nmol L<sup>-1</sup> EDTA)

| pH    | 6    | 7    | 8    | 9    |
|-------|------|------|------|------|
| La    | 2.57 | 2.44 | 2.22 | 2.16 |
| Ce    | 2.56 | 2.44 | 2.25 | 2.20 |
| Pr    | 2.53 | 2.44 | 2.26 | 2.23 |
| Nd    | 2.51 | 2.40 | 2.26 | 2.22 |
| Sm    | 2.52 | 2.42 | 2.30 | 2.28 |
| Eu    | 2.54 | 2.46 | 2.31 | 2.25 |
| Gd    | 2.54 | 2.45 | 2.31 | 2.23 |
| Tb    | 2.59 | 2.45 | 2.34 | 2.30 |
| Dy    | 2.59 | 2.48 | 2.37 | 2.37 |
| Ho    | 2.60 | 2.45 | 2.39 | 2.38 |
| Er    |      | 2.47 | 2.41 | 2.41 |
| Tm    | 2.64 | 2.51 | 2.46 | 2.46 |
| Yb    |      | 2.51 | 2.47 | 2.44 |
| Lu    | 2.67 | 2.54 | 2.50 | 2.48 |
| La/Sm | 1.02 | 1.01 | 0.97 | 0.95 |
| Gd/Yb |      | 0.98 | 0.94 | 0.91 |

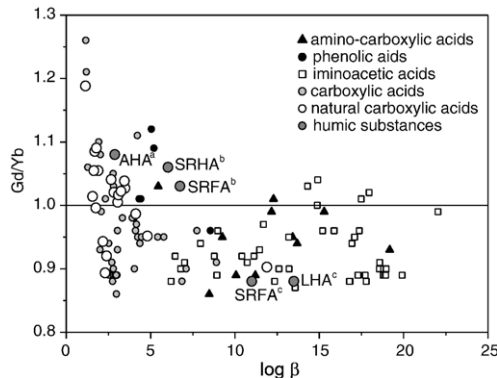


Fig. 5. Literature compilation of REE–organic ligand constants (re-calculated at  $I=0.1 \text{ mol L}^{-1}$  when necessary; Wood, 1993; Byrne and Li, 1995). Black triangles: amino-carboxylic acids; white squares: iminoacetic acids; black circles: phenolic acids; grey circles: carboxylic acids; white circles: natural carboxylic acids; dark grey circles: humic substances, Aldrich humic acid (AHA), Suwannee River fulvic acid (SRFA), Suwannee River humic acid (SRHA) and Leonardite humic acid (LHA) (<sup>a</sup>this study; <sup>b</sup>Yamamoto et al. (2006); <sup>c</sup>Sonke and Salters (2006)).

sites (EDTA-like sites). The weak sites determine the behavior of humic complexation at high metal concentrations, whereas the strong sites, although their concentration is only in the range of a few percent of the weak sites, determine the complexation strength of humic substances at trace metal concentrations (Hummel et al., 1995; Yamamoto et al., 2005). In our study, HS/Ln ratios are between 5 and 20, whereas in Yamamoto et al. (2005) experiments they are close to 80, in Sonke and Salters (2006) between 550 and 600 (in LHA experiments) and in Takahashi et al. (1997) as high as 100,000. Such a feature was already observed by Bidoglio et al. (1991) and Moulin et al. (1992) who evidenced that the REE concentration exerts a relatively great effect on the HM complexing capacity. This may be explained by a loading effect: At low loading, stronger sites will be favored whereas at large loadings, weaker sites will be involved in the complexation. This “HS/Ln ratio” effect is further marked by pH conditions: Phenolic sites are predominant at alkaline pH whereas carboxylic are dominant binding sites at acidic pH. Indeed, our study of pH spans a 2 to 10 range with an analytical window lied in the 2–6 range, whereas in Yamamoto et al. (2005, 2006) experiments pH varies between 4 and 5.5 and, in Sonke and Salters (2006) it varies between 6 and 9. Eventually, the understanding of this fractionation is not obvious and such a MREE downward concavity remains to be explained.

However, the similar MREE downward concavity patterns observed for REE complexation with HA (present study), with FA (Yamamoto et al., 2005) and with model molecule of carboxylic sites (acetic acid) (Wood, 1993), evidence that this type of fractionation could be expected in natural systems. Endly, the comparison of Sonke and

Salters (2006), Yamamoto et al. (2005), and present datasets allows validating the new  $\log K_{\text{MA}}$  (REE–HA) dataset presented in this study which could be then used to predict REE speciation in natural waters.

#### 4.2. REE speciation in natural river- and soil waters

Several authors confer a major role to the colloidal fraction in the transport of REE by rivers (Hoyle et al., 1984; Goldstein and Jacobsen, 1988; Cantrell and Byrne, 1987; Elderfield et al., 1990; Sholkovitz, 1992). Elderfield et al. (1990) proposed for example the existence of two REE compartments in river-waters (Fig. 6): (i) a “truly” dissolved pool, LREE depleted, but HREE enriched (Fig. 6a) and (ii) a “colloidal” pool LREE enriched and HREE flat, i.e., close to UCC (Fig. 6b) (Taylor and McLennan, 1985). Several studies have suggested that the HREE enrichment of the dissolved pool may be due to the greater solubility of HREE carbonate complexes as compared to LREE carbonate ones (Goldstein and Jacobsen, 1988; Elderfield et al., 1990; Sholkovitz, 1992). However, one of the characteristics of some river-waters is that  $(\text{La/Sm})_{\text{UCC}}$  and  $(\text{Gd/Yb})_{\text{UCC}}$  ratios are commonly lower than and higher than 1, respectively, producing a concave REE pattern (Fig. 6b) (Goldstein and Jacobsen, 1988; Elderfield et al., 1990; Sholkovitz, 1995; Viers et al., 1997; Deberdt et al., 2002). Such a characteristic is also well evidenced in organic-rich groundwaters (Viers et al., 1997; Dia et al., 2000; Deberdt et al., 2002; Gruau et al., 2004). As shown on Fig. 7,  $(\text{Gd/Yb})_{\text{UCC}}$  ratios increase while DOC content increases (Goldstein and Jacobsen, 1988; Elderfield et al., 1990; Sholkovitz, 1995; Viers et al., 1997; Deberdt et al., 2002). These features are further illustrated by ultrafiltration studies of organic-rich river- and ground-water samples. They indicate the absence of fractionation of HREE relative to LREE with decreasing pore-size cut-off (allowing colloidal separation) in the wide range of investigated pH (from 5.6 to 7.7) (Sholkovitz, 1995; Viers et al., 1997; Douglas et al., 1999; Dupré et al., 1999; Dia et al., 2000; Deberdt et al., 2002), they even evidence for some of them a MREE downward concavity fractionation (e.g., Fig. 15 in Sholkovitz, 1995). However, such a fractionation alone could not explain the whole REE pattern fractionation. Indeed, Johannesson et al. (1996a) suggested that MREE enrichment in hypersaline waters is the result of mineral weathering due to dissolution of MREE-enriched Fe- and Mn-rich particulates or surface coatings. Hannigan and Sholkovitz (2001) also proposed that MREE enrichment has to be related to the weathering of co-precipitated phosphates minerals. The present study demonstrates that organic substances play a major control onto REE speciation and thus onto REE fractionation pattern. Based on this ability of HA to preferentially complex

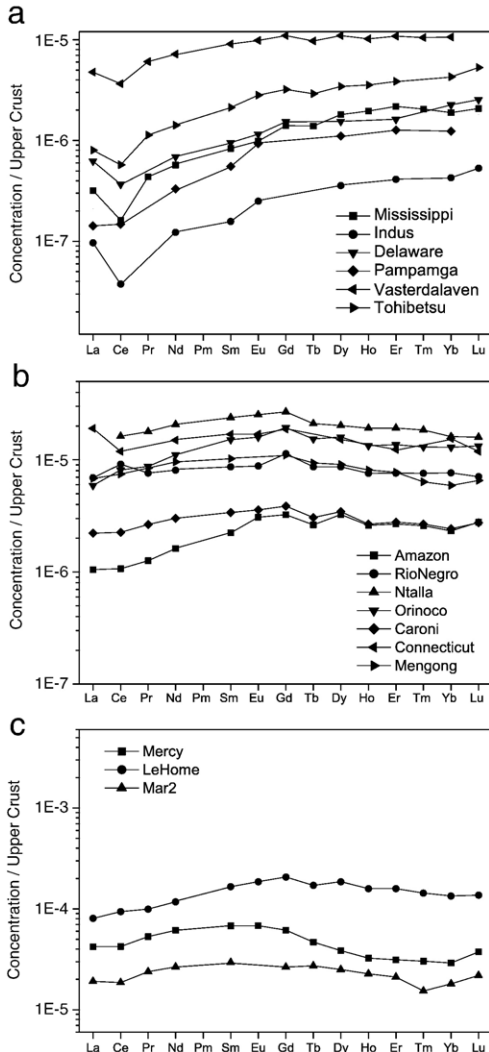


Fig. 6. REE normalized (to UCC) (Taylor and McLennan, 1985) patterns of river-waters showing (a) HREE enrichment and (b) MREE enrichment (Goldstein and Jacobsen, 1988; Elderfield et al., 1990; Sholkovitz, 1995; Deberdt et al., 2002), and (c) soil waters showing MREE enrichment (Viers et al., 1997; Dia et al., 2000; Gruau et al., 2004).

MREE, REE fractionation patterns at the Earth's surface can be revisited. DOC-rich river- and ground-waters REE patterns may reflect a mixing between (i) dissolved fraction of DOC-rich soil solutions, surface runoff and river-waters which display MREE downward concavity patterns (Viers et al., 1997; Dia et al., 2000; Deberdt et al., 2002; Gruau et al., 2004); and (ii) river suspended particles which are slightly LREE enriched inherited from preferential adsorption of LREE (Sholkovitz, 1995).

Up to now investigations of REE speciation in natural river- and soil waters were performed using Model V and Model VI with extrapolated constants obtained from Linear Free-Energy Relationships (LFER) (Tang and Johannesson, 2003; Pourret et al., 2007) and using Model V with constants fitted from experimental complexation between REE and HM (Sonke, 2006). Using the new determined  $\log K_{MA}$  dataset, REE speciation calculations – as a function of pH – were performed for the World Average River Water (Tang and Johannesson, 2003) in order to validate the results obtained with extrapolated constants. Major ions such as Fe and Al were adopted for re-calculating the REE speciation of the modelled World Average River Water (see Table 11 in Tang and Johannesson, 2003). We also followed their assumption that 80% of the active HM in this sample is present as FA and 20% as HA. Thus, the DOM content of World Average River Water is  $10 \text{ mg L}^{-1}$ , of which only  $5 \text{ mg L}^{-1}$  consists of HM able to complex with the REE, with  $4 \text{ mg L}^{-1}$  (80%) present as FA, and  $1 \text{ mg L}^{-1}$  (20%) as HA. Since pH is a key parameter to REE speciation, the REE speciation calculations were performed in the same way of these authors (op. cit.), i.e., holding the major solute composition constant (except carbonate alkalinity varying as a function of pH). Moreover, a fair degree of similarity between the model constants obtained for fulvic and humic acids exists as previously stated (Tipping and Hurley, 1992; Tipping, 1998) so  $\log K_{MA}(\text{FA})$  was calculated from  $\log K_{MA}(\text{HA})$ , obtained in Section 3, using Eq. (19) in Tipping (1998). Binding of REE(OH) species and Fe and Al oxyhydroxide precipitation was not considered in our calculation.

The obtained results are shown for La, Eu, and Lu in Fig. 8. The REE–HM species represent the proportion of each REE complexed with humic substances. The Model VI results are consistent with earlier investigations performed using Model V and Model VI with extrapolated constants from LFER (Tang and Johannesson, 2003; Sonke, 2006; Pourret et al., 2007). Model VI predicts that (i) REE occur predominantly as organic complexes ( $\text{REE-HM} \geq 60\%$ ) in the pH range between 5–5.5 and 7–8.5 (i.e.,

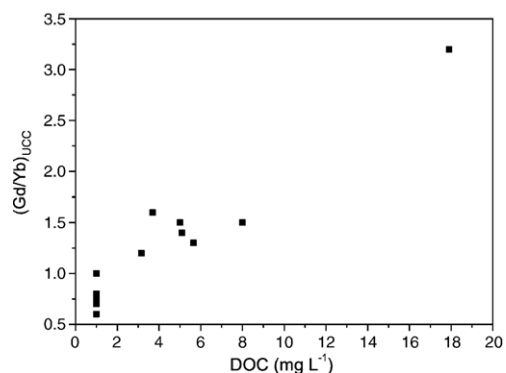


Fig. 7.  $(\text{Gd}/\text{Yb})_{\text{UCC}}$  ratios as a function of DOC concentrations; data are from river-waters presented in Fig. 6 (when no DOC concentrations available a concentration of 1 was assumed for comparison purpose (Thurman, 1985)).

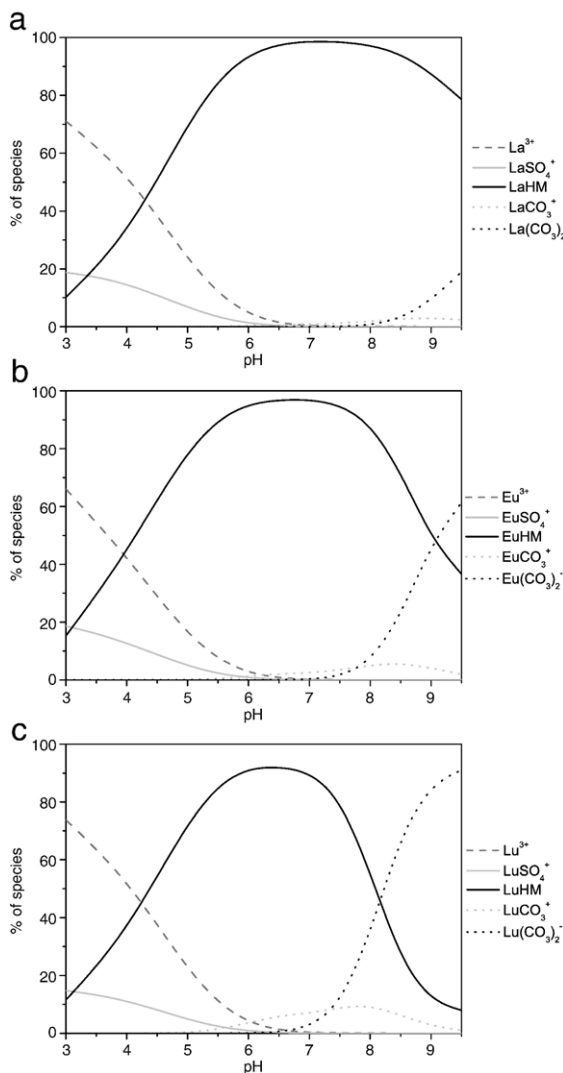


Fig. 8. Model VI speciation calculations for (a) La, (b) Eu and (c) Lu in World Average River Water as a function of pH.

circumneutral pH waters), (ii) REE–HM complexes become progressively less important with increasing atomic number across the REE series, and (iii) pH at which proportion of REE–HM species is maximum decreases from La to Lu. The only noticeable difference is that the new fitted constants allow Model VI to calculate significantly higher proportions of REE complexed with organic matter at high pH conditions than with extrapolated constants as already proposed by Sonke (2006) using Model V. As an example, with the fitted constants Model VI predicts La–HM ~85% at pH 9, while with extrapolated constants it only predicts 60% of La–HM. However, these new calculations are also a validation of the LFER method (Tang and Johannesson, 2003; Pourret et al., 2007). Moreover, these results are coherent with simple speciation calcu-

lations performed by Takahashi and co-workers (Takahashi et al., 1997, 1999) which led them to speculate that humate complexes should be the dominant species of REE(III) dissolved in natural aquifers where DOM occurs significantly.

## 5. Conclusions

Experimental studies of REE–HA binding were carried out using an ultrafiltration method. A strong pH dependence resulting in a significant increase in the proportion of REE–HA with increasing pH and a MREE downward concavity fractionation at acidic pH were observed. Moreover, modelling was performed using Humic Ion Binding Model VI. Experimental results were fitted to obtain a set of constants ( $\log K_{MA}$ ). The constants presented in our study are in good agreement with some literature constants. However, they are different from those published by Takahashi et al. (1997) and Sonke and Salters (2006) which evidence a lanthanide contraction effect. Model VI constants in this study indicate that REE–HA complexation involved a fractionation similar to the REE complexation with simple carboxylic groups such as acetates. The similar MREE downward concavity pattern observed for REE complexation with HA (this study), with FA (Yamamoto et al., 2005) and with simple organic acid such as acetic acid (Wood, 1993; Byrne and Li, 1995), illustrates that this type of fractionation could be expected in natural systems. All these observations allow validating the present  $\log K_{MA}$  (REE–HA) dataset that can be, therefore, used with confidence to predict REE speciation in natural waters. Essentially, experiments from this study coupled to observation made by Takahashi et al. (1997), Yamamoto et al. (2005, 2006) and Sonke and Salters (2006) allow covering a wide range of experimental conditions both in HS/Ln ratio and in pH range (from 2 to 10) and are thus complementary. Moreover, the results of the present study shed more light on the REE cycle at the Earth's surface. They confirm that organic REE speciation plays a major role onto REE fractionation in natural organic-rich river- and groundwaters. Dissolved fractions of DOC-rich soil solutions, surface runoff, and river-waters display MREE downward concavity patterns. The new  $\log K_{MA}$  were additionally introduced in WHAM 6 to predict speciation of the World Average River Water. REE occur predominantly as organic complexes (REE–HM  $\geq 60\%$ ) in circumneutral pH waters (pH range between 5–5.5 and 7.5–8). New fitted constants allow Model VI to calculate high proportions of LREE complexed with organic matter under alkaline pH conditions. Overall, the results of this study suggest that further considerations about organic matter should be taken into account to model and thus better understand global continent–ocean trace metal cycles.

## Acknowledgements

We thank the technical staff at Rennes (M. Le Coz-Bouhnik, O. Hénin and P. Petitjean) for their assistance during the experimental and analytical work. Dr. R. E. Martinez is acknowledged for useful discussions and English corrections. Dr. J.E. Sonke and an anonymous

reviewer are thanked for thorough and constructive comments of an earlier version of this paper. This research was supported by the CPER programs “Développement de la Recherche sur la Maîtrise de la Qualité de l'Eau en Bretagne” jointly funded by the French Government and the Council of Rennes Métropole.

## Appendix A

Proportion of REE-HA

| [HA]  | 5 mg L <sup>-1</sup>  |       |       |       |       |       |       |       |       |       |       |
|-------|-----------------------|-------|-------|-------|-------|-------|-------|-------|-------|-------|-------|
| pH    | 2.47                  | 2.95  | 4.06  | 4.25  | 4.35  | 4.99  | 6.29  | 10.44 |       |       |       |
| La    | 6.34                  | 9.44  | 43.01 | 44.74 | 50.20 | 65.83 | 93.05 | 99.86 |       |       |       |
| Ce    | 9.23                  | 13.66 | 50.65 | 52.92 | 57.97 | 72.98 | 95.15 | 99.83 |       |       |       |
| Pr    | 10.33                 | 15.83 | 54.59 | 56.81 | 61.77 | 76.13 | 95.89 | 99.85 |       |       |       |
| Nd    | 11.33                 | 15.77 | 55.44 | 57.98 | 62.81 | 77.37 | 96.08 | 99.84 |       |       |       |
| Sm    | 12.61                 | 19.05 | 60.12 | 62.84 | 67.27 | 80.96 | 96.86 | 99.84 |       |       |       |
| Eu    | 12.10                 | 17.55 | 58.86 | 61.45 | 66.06 | 80.13 | 96.70 | 99.83 |       |       |       |
| Gd    | 9.18                  | 14.12 | 53.04 | 55.78 | 60.87 | 76.16 | 95.80 | 99.83 |       |       |       |
| Tb    | 9.07                  | 13.52 | 52.01 | 54.94 | 59.90 | 75.47 | 95.58 | 99.83 |       |       |       |
| Dy    | 7.87                  | 12.48 | 49.95 | 52.99 | 58.07 | 73.94 | 95.22 | 99.83 |       |       |       |
| Ho    | 6.93                  | 10.79 | 46.92 | 49.66 | 54.99 | 71.50 | 94.60 | 99.83 |       |       |       |
| Er    | 5.99                  | 9.97  | 45.74 | 48.11 | 53.55 | 70.22 | 94.28 | 99.82 |       |       |       |
| Tm    | 6.39                  | 10.35 | 45.73 | 48.16 | 53.62 | 70.38 | 94.33 | 99.82 |       |       |       |
| Yb    | 6.16                  | 10.49 | 46.89 | 49.16 | 54.53 | 71.39 | 94.61 | 99.82 |       |       |       |
| Lu    | 6.07                  | 9.99  | 45.35 | 47.89 | 53.17 | 70.40 | 94.47 | 99.82 |       |       |       |
| La/Sm | 0.50                  | 0.50  | 0.72  | 0.71  | 0.75  | 0.81  | 0.96  | 1.00  |       |       |       |
| Gd/Yb | 1.49                  | 1.35  | 1.13  | 1.13  | 1.12  | 1.07  | 1.01  | 1.00  |       |       |       |
| [HA]  | 10 mg L <sup>-1</sup> |       |       |       |       |       |       |       |       |       |       |
| pH    | 2.18                  | 2.91  | 3.45  | 3.96  | 4.40  | 6.16  | 6.66  | 6.94  | 7.26  |       |       |
| La    | 4.31                  | 34.55 | 60.55 | 82.92 | 94.94 | 99.44 | 99.35 | 99.60 | 99.69 |       |       |
| Ce    | 5.00                  | 41.08 | 67.34 | 86.81 | 96.05 | 99.46 | 99.36 | 99.58 | 99.66 |       |       |
| Pr    | 10.12                 | 44.49 | 70.32 | 88.32 | 96.45 | 99.45 | 99.34 | 99.56 | 99.64 |       |       |
| Nd    | 11.27                 | 45.61 | 71.33 | 88.67 | 96.50 | 99.41 | 99.32 | 99.53 | 99.61 |       |       |
| Sm    | 12.20                 | 49.31 | 74.69 | 90.25 | 96.90 | 99.42 | 99.30 | 99.53 | 99.59 |       |       |
| Eu    | 10.95                 | 47.67 | 73.40 | 89.89 | 96.78 | 99.41 | 99.28 | 99.52 | 99.59 |       |       |
| Gd    | 7.52                  | 42.00 | 68.91 | 87.63 | 96.15 | 99.36 | 99.24 | 99.49 | 99.57 |       |       |
| Tb    | 7.50                  | 41.10 | 67.93 | 87.33 | 96.02 | 99.36 | 99.22 | 99.49 | 99.57 |       |       |
| Dy    | 5.91                  | 39.21 | 66.30 | 86.50 | 95.71 | 99.31 | 99.19 | 99.47 | 99.56 |       |       |
| Ho    | 5.79                  | 36.82 | 63.87 | 85.07 | 95.27 | 99.27 | 99.15 | 99.44 | 99.53 |       |       |
| Er    | 5.17                  | 35.88 | 62.69 | 84.33 | 95.01 | 99.22 | 99.10 | 99.41 | 99.51 |       |       |
| Tm    | 5.68                  | 36.13 | 62.77 | 84.22 | 94.87 | 99.18 | 99.08 | 99.38 | 99.48 |       |       |
| Yb    | 5.15                  | 37.02 | 63.70 | 84.75 | 94.97 | 99.17 | 99.07 | 99.36 | 99.47 |       |       |
| Lu    | 5.32                  | 35.77 | 62.21 | 83.92 | 94.77 | 99.15 | 99.05 | 99.34 | 99.45 |       |       |
| La/Sm | 0.35                  | 0.70  | 0.81  | 0.92  | 0.98  | 1.00  | 1.00  | 1.00  | 1.00  |       |       |
| Gd/Yb | 1.46                  | 1.13  | 1.08  | 1.03  | 1.01  | 1.00  | 1.00  | 1.00  | 1.00  |       |       |
| [HA]  | 20 mg L <sup>-1</sup> |       |       |       |       |       |       |       |       |       |       |
| pH    | 2.21                  | 2.46  | 2.97  | 3.51  | 4.05  | 5.03  | 5.48  | 6.08  | 6.25  | 6.65  | 6.77  |
| La    | 26.03                 | 57.24 | 81.73 | 95.76 | 98.52 | 99.44 | 99.28 | 99.57 | 99.67 | 99.16 | 99.60 |
| Ce    | 30.79                 | 63.60 | 85.09 | 96.65 | 98.62 | 99.38 | 99.19 | 99.52 | 99.63 | 99.11 | 99.57 |
| Pr    | 41.25                 | 67.06 | 88.39 | 97.06 | 98.58 | 99.31 | 99.10 | 99.47 | 99.59 | 99.08 | 99.54 |
| Nd    | 41.81                 | 67.94 | 88.83 | 97.06 | 98.49 | 99.22 | 99.01 | 99.41 | 99.54 | 99.01 | 99.50 |

(continued on next page)

## Appendix A (continued)

| [HA]  | 20 mg L <sup>-1</sup> |       |       |       |       |       |       |       |       |       |       |
|-------|-----------------------|-------|-------|-------|-------|-------|-------|-------|-------|-------|-------|
| Sm    | 45.53                 | 70.12 | 89.96 | 97.32 | 98.50 | 99.20 | 98.94 | 99.40 | 99.54 | 98.97 | 99.47 |
| Eu    | 43.31                 | 68.40 | 89.34 | 97.19 | 98.46 | 99.18 | 98.93 | 99.39 | 99.54 | 98.97 | 99.47 |
| Gd    | 36.32                 | 63.18 | 86.97 | 96.65 | 98.38 | 99.16 | 98.93 | 99.38 | 99.52 | 98.91 | 99.46 |
| Tb    | 35.14                 | 61.70 | 86.46 | 96.55 | 98.38 | 99.17 | 98.97 | 99.39 | 99.53 | 98.93 | 99.47 |
| Dy    | 33.68                 | 60.04 | 85.65 | 96.35 | 98.32 | 99.12 | 98.94 | 99.38 | 99.52 | 98.88 | 99.46 |
| Ho    | 31.34                 | 57.42 | 84.34 | 95.98 | 98.18 | 99.04 | 98.86 | 99.31 | 99.47 | 98.83 | 99.41 |
| Er    | 30.33                 | 56.94 | 83.87 | 95.74 | 98.02 | 98.96 | 98.77 | 99.25 | 99.42 | 98.77 | 99.36 |
| Tm    | 31.41                 | 57.32 | 84.02 | 95.70 | 97.91 | 98.87 | 98.69 | 99.21 | 99.37 | 98.73 | 99.34 |
| Yb    | 32.64                 | 59.02 | 84.81 | 95.76 | 97.80 | 98.81 | 98.59 | 99.16 | 99.35 | 98.73 | 99.32 |
| Lu    | 31.37                 | 57.32 | 83.81 | 95.41 | 97.63 | 98.70 | 98.48 | 99.07 | 99.27 | 98.62 | 99.26 |
| La/Sm | 0.57                  | 0.82  | 0.91  | 0.98  | 1.00  | 1.00  | 1.00  | 1.00  | 1.00  | 1.00  | 1.00  |
| Gd/Yb | 1.11                  | 1.07  | 1.03  | 1.01  | 1.01  | 1.00  | 1.00  | 1.00  | 1.00  | 1.00  | 1.00  |

## References

- Avena, M.J., Vermeer, A.W.P., Koopal, L.K., 1999. Volume and structure of humic acids studied by viscometry pH and electrolyte concentration effects. *Colloids and Surfaces A* 151, 213–224.
- Bidoglio, G., Grenthe, I., Qi, P., Robouch, P., Omenetto, N., 1991. Complexation of Eu and Tb with fulvic acids as studied by time-resolved laser induced fluorescence. *Talanta* 38, 999–1008.
- Byrne, R.H., Kim, K.H., 1990. Rare earth element scavenging in seawater. *Geochimica et Cosmochimica Acta* 54, 2645–2656.
- Byrne, R.H., Li, B., 1995. Comparative complexation behavior of the rare earths. *Geochimica et Cosmochimica Acta* 59, 4575–4589.
- Cantrell, K.J., Byrne, R.H., 1987. Rare earth element complexation by carbonate and oxalate ions. *Geochimica et Cosmochimica Acta* 51, 597–605.
- Crawford, M.B., 1996. PHREEQEV: the incorporation of a version of model V for organic complexation in aqueous solutions into the speciation code PHREEQE. *Computers & Geosciences* 22, 109–116.
- Davranche, M., Pourret, O., Gruau, G., Dia, A., 2004. Impact of humate complexation on the adsorption of REE onto Fe oxyhydroxide. *Journal of Colloid and Interface Science* 277, 271–279.
- Davranche, M., Pourret, O., Gruau, G., Dia, A., Le Coz-Bouhnik, M., 2005. Adsorption of REE(III)-humate complexes onto MnO<sub>2</sub>: experimental evidence for cerium anomaly and lanthanide tetrad effect suppression. *Geochimica et Cosmochimica Acta* 69, 4825–4835.
- De Baar, H.J.W., Schijf, J., Byrne, R.H., 1991. Solution chemistry of the rare earth elements in seawater. *European Journal of Solid State and Inorganic Chemistry* 28, 357–373.
- Deberdt, S., Viers, J., Dupré, B., 2002. New insights about the rare earth elements (REE) mobility in river waters. *Bulletin de la Société Géologique de France* 173, 147–160.
- Dia, A., Gruau, G., Olivié-Lauquet, G., Riou, C., Molénat, J., Curmi, P., 2000. The distribution of rare earth elements in groundwaters: assessing the role of source-rock composition, redox changes and colloidal particle. *Geochimica et Cosmochimica Acta* 64, 4131–4151.
- Dierckx, A., Maes, A., Vancluysen, J., 1994. Mixed complex formation of Eu<sup>3+</sup> with humic acid and a competing ligand. *Radiochimica Acta* 66/67, 149–156.
- Douglas, G.B., Hart, B.T., Beckett, R., Gray, C.M., Oliver, R.L., 1999. Geochemistry of suspended particulate matter (SPM) in the Murray–Darling River system: a conceptual isotopic/geochemical model for the fractionation of major, trace and rare earth elements. *Aquatic Geochemistry* 5, 167–194.
- Dupré, B., Viers, J., Dandurand, J.-L., Polvá, M., Bénézeth, P., Vervier, P., Braun, J.-J., 1999. Major and trace elements associated with colloids in organic-rich river waters: ultrafiltration of natural and spiked solutions. *Chemical Geology* 160, 63–80.
- Elderfield, H., Greaves, M.J., 1982. The rare earth elements in seawater. *Nature* 296, 214–219.
- Elderfield, H., Upstill-Goddard, R., Sholkovitz, E.R., 1990. The rare earth elements in rivers, estuaries, and coastal seas and their significance to the composition of ocean waters. *Geochimica et Cosmochimica Acta* 54, 971–991.
- Fairhurst, A.J., Warwick, P., Richardson, S., 1995. The influence of humic acid on the adsorption of europium onto inorganic colloids as a function of pH. *Colloids and Surfaces A* 99, 187–199.
- Franz, C., Herrmann, G., Trautmann, N., 1997. Complexation of samarium(III) and americium(III) with humic acid at very low metal concentrations. *Radiochimica Acta* 77, 177–181.
- Goldstein, S.J., Jacobsen, S.B., 1988. Rare earth elements in river waters. *Earth and Planetary Sciences Letters* 89, 35–47.
- Gruau, G., Dia, A., Olivié-Lauquet, G., Davranche, M., Pinay, G., 2004. Controls on the distribution of rare earth elements in shallow groundwaters. *Water Research* 38, 3576–3586.
- Hannigan, R.E., Sholkovitz, E.R., 2001. The development of middle rare earth element enrichments in freshwaters: weathering of phosphate minerals. *Chemical Geology* 175, 495–508.
- Henderson, P., 1984. Rare Earth Element Geochemistry. Elsevier, Amsterdam.
- Hoyle, J., Elderfield, H., Gledhill, A., Greaves, M., 1984. The behaviour of rare earth elements during mixing of river and sea waters. *Geochimica et Cosmochimica Acta* 48, 143–149.
- Hummel, W., Glaus, M., Van Loon, L.R., 1995. Binding of radionuclides by humic substances: the “conservative roof” approach. Proceeding of an NEA Workshop, 14–16 September 1994. OECD Documents, Bas Zurzach, Switzerland, pp. 251–262.
- Johannesson, K.H., Lyons, W.B., Yelken, M.A., Gaudette, H.E., Stetzenbach, K.J., 1996a. Geochemistry of the rare-earth elements in hypersaline and dilute acidic natural terrestrial waters: complexation behavior and middle rare-earth element enrichments. *Chemical Geology* 133, 125–144.
- Johannesson, K.H., Stetzenbach, K.J., Hodge, V.F., Lyons, W.B., 1996b. Rare earth element complexation behavior in circumneutral pH groundwaters: assessing the role of carbonate and phosphate ions. *Earth and Planetary Sciences Letters* 139, 305–319.
- Johannesson, K.H., Stetzenbach, K.J., Hodge, V.F., 1997. Rare earth elements as geochemical tracers of regional groundwater mixing. *Geochimica et Cosmochimica Acta* 61, 3605–3618.

- Johannesson, K.H., Zhou, X., Guo, C., Stetzenbach, K.J., Hodge, V.F., 2000. Origin of rare earth element signatures in groundwaters of circumneutral pH from southern Nevada and eastern California, USA. *Chemical Geology* 164, 239–257.
- Johannesson, K.H., Tang, J., Daniels, J.M., Bounds, W.J., Burdige, D.J., 2004. Rare earth element concentrations and speciation in organic-rich blackwaters of the Great Dismal Swamp, Virginia, USA. *Chemical Geology* 209, 271–294.
- Kubota, T., Tochiyama, O., Tanaka, K., Niibori, Y., 2002. Complex formation of Eu(III) with humic acid and polyacrylic acid. *Radiochimica Acta* 90, 569–574.
- Lead, J.R., Hamilton-Taylor, J., Peters, A., Reiner, S., Tipping, E., 1998. Europium binding by fulvic acids. *Analytica Chimica Acta* 369, 171–180.
- Lee, J.H., Byrne, R.H., 1992. Examination of comparative rare earth element complexation behavior using linear free-energy relationships. *Geochimica et Cosmochimica Acta* 56, 1127–1137.
- Lee, J.H., Byrne, R.H., 1993. Complexation of trivalent rare earth elements (Ce, Eu, Gd, Tb, Yb) by carbonate ions. *Geochimica et Cosmochimica Acta* 57, 295–302.
- Lippold, H., Müller, N., Kupsch, H., 2005. Effect of humic acid on the pH-dependent adsorption of terbium(III) onto geological materials. *Applied Geochemistry* 20, 1209–1217.
- Liu, X., Byrne, R.H., 1998. Comprehensive investigation of yttrium and rare earth element complexation by carbonate using ICP-Mass Spectrometry. *Journal of Solution Chemistry* 9, 803–815.
- Luo, Y.-R., Byrne, R.H., 2004. Carbonate complexation of yttrium and the rare earth elements in natural rivers. *Geochimica et Cosmochimica Acta* 68, 691–699.
- Maes, A., De Brabandere, J., Cremers, A., 1988. A modified Schubert method for the measurement of the stability of europium humic acid complexes in alkaline conditions. *Radiochimica Acta* 44/45, 51–57.
- Milne, C.J., Kinniburgh, D.G., Tipping, E., 2001. Generic NICA-DonnanModel parameters for proton binding by humic substances. *Environmental Science & Technology* 35, 2049–2059.
- Milne, C.J., Kinniburgh, D.G., Van Riemsdijk, W.H., Tipping, E., 2003. Generic NICA-Donnan Model parameters for metal-ion binding by humic substances. *Environmental Science & Technology* 37, 958–971.
- Millero, F.J., 1992. Stability constants for the formation of rare earth inorganic complexes as a function of ionic strength. *Geochimica et Cosmochimica Acta* 56, 3123–3132.
- Moulin, V., et al., 1992. Complexation behaviour of humic substances towards actinides and lanthanides studied by time-resolved laser-induced spectrofluometry. *Radiochimica Acta* 58/59, 121–128.
- Nordén, M., Ephraim, J.H., Allard, B., 1993. The binding of strontium and europium by an aquatic fulvic acid-ion exchange distribution and ultrafiltration studies. *Talanta* 40, 1425–1432.
- Pourret, O., Davranche, M., Gruau, G., Dia, A., 2007. Organic complexation of rare earth elements in natural waters: evaluating model calculations from ultrafiltration data. *Geochimica et Cosmochimica Acta* 71, 2718–2735.
- Saito, T., Nagasaki, S., Tanaka, S., Koopal, L.K., 2005. Electrostatic interactions model for ion binding to humic substances. *Colloids and Surfaces A* 265, 104–113.
- Sholkovitz, E.R., 1992. Chemical evolution of rare earth elements: fractionation between colloidal and solution phases of filtered river water. *Earth and Planetary Sciences Letters* 114, 77–84.
- Sholkovitz, E.R., 1995. The aquatic chemistry of rare earth elements in rivers and estuaries. *Aquatic Geochemistry* 1, 1–34.
- Smedley, P.L., 1991. The geochemistry of rare earth elements in groundwater from the Carnmenellis area, southwest England. *Geochimica et Cosmochimica Acta* 55, 2767–2779.
- Sonke, J.E., 2006. Lanthanide–humic substances complexation. II. Calibration of humic ion-binding model V. *Environmental Science & Technology* 40, 7481–7487.
- Sonke, J.E., Salters, V.J.M., 2006. Lanthanide–humic substances complexation. I. Experimental evidence for a lanthanide contraction effect. *Geochimica et Cosmochimica Acta* 70, 1495–1506.
- Takahashi, Y., Minai, Y., Ambe, S., Makide, Y., Ambe, F., Tominaga, T., 1997. Simultaneous determination of stability constants of humate complexes with various metal ions using multitracer technique. *The Science of the Total Environment* 198, 61–71.
- Takahashi, Y., Minai, Y., Ambe, S., Makide, Y., Ambe, F., 1999. Comparison of adsorption behavior of multiple inorganic ions on kaolinite and silica in the presence of humic acid using the multitracer technique. *Geochimica et Cosmochimica Acta* 63, 815–836.
- Tang, J., Johannesson, K.H., 2003. Speciation of rare earth elements in natural terrestrial waters: assessing the role of dissolved organic matter from the modeling approach. *Geochimica et Cosmochimica Acta* 67, 2321–2339.
- Taylor, S.R., McLennan, S.M., 1985. *The Continental Crust: Its Composition and Evolution*. Blackwell, Oxford, p. 312.
- Thurman, E.M., 1985. *Organic Geochemistry of Natural Waters*. Nijhoff/Junk Publishers, Dordrechtthe, Netherlands.
- Tipping, E., 1998. Humic ion-binding model VI: an improved description of the interactions of protons and metal ions with humic substances. *Aquatic Geochemistry* 4, 3–48.
- Tipping, E., Hurley, M.A., 1992. A unifying model of cation binding by humic substances. *Geochimica et Cosmochimica Acta* 56, 3627–3641.
- Vermeer, A.W.P., Van Riemsdijk, W.H., Koopal, L.K., 1998. Adsorption of humic acid to mineral particles. 1. Specific and electrostatic interactions. *Langmuir* 14, 2810–2819.
- Viers, J., Dupré, B., Polvé, M., Schott, J., Dandurand, J.-L., Braun, J.J., 1997. Chemical weathering in the drainage basin of a tropical watershed (Nsimi-Zoetele site, Cameroon): comparison between organic-poor and organic-rich waters. *Chemical Geology* 140, 181–206.
- Wood, S.A., 1990. The aqueous geochemistry of the rare-earth elements and yttrium. 1. Review of the available low-temperature data for inorganic complexes and inorganic REE speciation in natural waters. *Chemical Geology* 82, 159–186.
- Wood, S.A., 1993. The aqueous geochemistry of the rare-earth elements: critical stability constants for complexes with simple carboxylic acids at 25 °C and 1 bar and their application to nuclear waste management. *Engineering Geology* 34, 229–259.
- Yamamoto, Y., Takahashi, Y., Shimizu, H., 2005. Systematics of stability constants of fulvate complexes with rare earth ions. *Chemistry Letters* 34, 880–881.
- Yamamoto, Y., Takahashi, Y., Shimizu, H., 2006. Interpretation of REE patterns in natural water based on the stability constants. *Geochimica et Cosmochimica Acta*, Goldschmidt Conference Abstracts. doi:10.1016/j.gca.2006.06.1587.



## Modeling lanthanide series binding sites on humic acid

Olivier Pourret<sup>a,\*</sup>, Raul E. Martinez<sup>b,1</sup>

<sup>a</sup> Institut Polytechnique LaSalle-Beauvais, Département Géosciences, 19 rue Pierre Waguet, 60026 Beauvais Cedex, France

<sup>b</sup> Institut de Physique du Globe de Paris, Laboratoire Géobiosphère Actuelle et Primitive, 4 place Jussieu, 75252 Paris Cedex 05, France

---

### ARTICLE INFO

#### Article history:

Received 22 July 2008

Accepted 17 October 2008

Available online 13 November 2008

#### Keywords:

Rare earth elements

Humic acid

Binding

Speciation

LPM model

---

### ABSTRACT

Lanthanide (Ln) binding to humic acid (HA) has been investigated by combining ultrafiltration and ICP-MS techniques. A Langmuir-sorption-isotherm metal-complexation model was used in conjunction with a linear programming method (LPM) to fit experimental data representing various experimental conditions both in HA/Ln ratio (varying between 5 and 20) and in pH range (from 2 to 10) with an ionic strength of  $10^{-3}$  mol L<sup>-1</sup>. The LPM approach, not requiring prior knowledge of surface complexation parameters, was used to solve the existing discrepancies in Ln-HA binding constants and site densities. The application of the LPM to experimental data revealed the presence of two discrete metal binding sites at low humic acid concentrations (5 mg L<sup>-1</sup>), with log metal complexation constants ( $\log K_{S,j}$ ) of  $2.65 \pm 0.05$  and 7.00 (depending on Ln). The corresponding site densities were  $2.71 \pm 0.57 \times 10^{-8}$  and  $0.58 \pm 0.32 \times 10^{-8}$  mol of Ln<sup>3+</sup>/mg of HA (depending on Ln). Total site densities of  $3.28 \pm 0.28 \times 10^{-8}$ ,  $4.99 \pm 0.02 \times 10^{-8}$ , and  $5.01 \pm 0.01 \times 10^{-8}$  mol mg<sup>-1</sup> were obtained by LPM for humic acid, for humic acid concentrations of 5, 10, and 20 mg L<sup>-1</sup>, respectively. These results confirm that lanthanide binding occurs mainly at weak sites (i.e., ca. 80%) and second at strong sites (i.e., ca. 20%). The first group of discrete metal binding sites may be attributed to carboxylic groups (known to be the main binding sites of Ln in HA), and the second metal binding group to phenolic moieties. Moreover, this study evidences heterogeneity in the distribution of the binding sites among Ln. Eventually, the LPM approach produced feasible and reasonable results, but it was less sensitive to error and did not require an a priori assumption of the number and concentration of binding sites.

© 2008 Elsevier Inc. All rights reserved.

---

### 1. Introduction

The solution and mineral properties of lanthanides (Ln) make these trace elements excellent probes of low-temperature geochemical reactions. Interest in lanthanide geochemistry comes from their systematic variation in chemical properties, which often leads to fractionation in geochemical systems [1]. Ln form a coherent geochemical group of trace elements that generally occur in the trivalent oxidation state. The effective ionic radii of Ln systematically decrease when atomic number increases [2], producing characteristic regular features of normalized lanthanide patterns defining the CHARC and RADius-Controlled process (CHARAC) [3]. If a low-temperature geochemical system is characterized by CHARAC behavior, elements of similar charge and radius such as Ln are should display extremely coherent behavior. This behavior disappears when chemical processes are mainly driven by electronic external configuration, producing subpartition (non-CHARAC pro-

cesses). CHARAC behavior of Ln should thus generate smooth patterns, whereas irregular patterns (excepting redox-related anomalies) may indicate non-CHARAC behavior. By studying fractionation trends, it then becomes possible to quantify the underlying fractionation processes in the natural environment (e.g., [3,4]). In addition, quantification of lanthanide fractionation in natural geochemical systems is essential for the modeling of the immobilization and transport of radioactive elements, as Ln are often used as naturally occurring analogs for the trivalent actinides [5].

In aquatic geochemical systems, lanthanide fractionation occurs by complexation to organic or inorganic ligands or adsorption onto aquifer minerals. In natural waters, Ln may be associated with organic colloids that play a key role in complexing lanthanide elements and facilitate the fractionation of the lanthanide series (e.g., [6–10]). Dissolved organic matter (DOM), including humic acids (HA) and fulvic acids (FA), is abundant in surface water and groundwater systems [11]. HA are potent sorbents of dissolved metal cations such as lanthanide elements (e.g., [10]). These properties emphasize the importance of HA in regulating the speciation, transport, and subsequent fractionation of Ln in pristine and contaminated aquatic environments. The physicochemical quantification of lanthanide interaction with DOM in aquatic systems is

\* Corresponding author. Fax: +33 344 062 526.

E-mail address: olivier.pourret@lasalle-beauvais.fr (O. Pourret).

<sup>1</sup> Current address: Tübingen University, Center for Applied Geosciences, Sigwartstr. 10, 72076 Tübingen, Germany.

needed to predict lanthanide fractionation by organic metal complexation in aqueous systems. HA contain a large number of potential metal-complexing functional groups including carboxylic sites (e.g., [12]). Their chemical arrangement and conformation at the molecular level affects the ability of HA to complex lanthanide elements. For this reason, surface complexation modeling of LnHA acid interactions, using current surface complexation models such as FITEQL [13], WHAM and Model V and VI [14], or NICCA Donnan [15] may provide different discrete metal-binding constants for similar LnHA complexation reactions. Few studies have addressed LnHA interactions as a function of pH, ionic strength, and different lanthanide elements. Only a small number of single lanthanide complexation constants with HA (SmHA, EuHA, TbHA, and DyHA) have been evaluated [16–21]. Results from recent studies suggest that most of the LnHA complexation constants have to be measured or interpolated, especially for the whole lanthanide series [22,23]. In these studies LnHA interactions have been investigated using binding interactions that are based on one- and two-site conditional binding to discretized multisite (e.g., [24]) and continuous distribution models (e.g., [15]). Various electrostatic models have been developed to account for pH and *I* effects on ion binding (e.g., [24]). Sonke and Salters [25] adopted a monodentate (carboxylic) binding mechanism. The exact binding site nature, multidentism, and polyelectrolyte effects of HA are ignored in the monodentate binding concept and therefore implicitly included in the conditional binding constant, which consequently is only valid for a specific pH, *I*, and temperature. Sonke [26], Pourret et al. [27], and Stern et al. [28] further investigated this feature using Models V and VI. However, such modeling of LnHA complexation only considers specific constants and thus does not implicitly distinguish different binding sites.

The effects of HA on lanthanide fractionation was previously studied by monitoring the concentration of Ln as a function of increasing concentrations of HA [27]. The resultant sorption data were analyzed to assess multisite metal surface binding using linear programming regression methods (LPM) [29–31]. Most previous studies have investigated humic acid surface interactions with metals using single-site sorption isotherms that do not adequately describe the heterogeneity of humic acid surfaces [32]. Despite the previous application of LPM to describe metal binding to organic surfaces [29–31], this modeling approach has not yet been applied to study LnHA interactions.

## 2. Modeling of LnHA complexation data

The experimental data used in this study have been previously published by Pourret et al. [27]. Lanthanide complexation with HA was investigated using a standard batch equilibration technique. Ln (ranging from 360 to 286 nmol L<sup>-1</sup> depending on lanthanide) and Aldrich HA (5, 10, and 20 mg L<sup>-1</sup>) were placed together in solution at an ionic strength of 1 × 10<sup>-3</sup> mol L<sup>-1</sup> and at pH values ranging from 2.18 to 10.44. The present work will model lanthanide complexation to HA using a surface complexation modeling approach, the LPM method as described previously by Martinez and Ferris [30] and Martinez et al. [31], which does not require prior knowledge of log *K* or binding site concentrations. In order to describe Ln<sup>3+</sup> complexation to deprotonated humic acid sites, HA<sup>-</sup>, a competition reaction was assumed to take place in a 1:1 ratio,



where HHA<sub>j</sub> represents humic acid reactive sites. K<sub>S,j</sub> represents the concentration apparent equilibrium constant for the reaction in Eq. (1), conditional on ionic strength. For a *j*th deprotonated binding site at the *i*th step of the titration, K<sub>S,j</sub> can be defined as

$$K_{S,j} = \frac{[\text{LnHA}_j^{2+}]_i [\text{H}^+]_{\text{meas},i}}{[\text{HHA}_j]_i [\text{Ln}^{3+}]_{\text{meas},i}}, \quad (2)$$

where *i* = 1, ..., *n* are titrant additions and *j* = 1, ..., *m* binding sites. In the above expression, K<sub>S,j</sub> implicitly embodies electrostatic parameters and is a function of experimentally determined proton and metal concentrations, [H<sup>+</sup>]<sub>meas,i</sub> and [Ln<sup>3+</sup>]<sub>meas,i</sub>, and of the amount of Ln<sup>3+</sup> bound to the *j*th site at the *i*th step of the titration, [LnHA<sub>j</sub><sup>2+</sup>]<sub>*i*</sub>. The total bound metal at the *i*th titrant addition, [LnHA<sup>2+</sup>]<sub>T,i</sub>, and the total ligand concentration, [HA]<sub>T</sub>, can be expressed as

$$[\text{LnHA}^{2+}]_{T,i} = \sum_{j=1}^m [\text{LnHA}_j^{2+}]_i = [\text{Ln}^{3+}]_T - [\text{Ln}^{3+}]_{\text{meas},i} \quad (3)$$

and

$$[\text{HA}]_T = \sum_{j=1}^m [\text{HA}_j] = [\text{LnHA}_j^{2+}] + [\text{HA}_j^-] + [\text{HHA}_j], \quad (4)$$

where [HA<sub>j</sub><sup>-</sup>] refers to the individual site density for a particular surface functional group type. The total concentration of bound metal, [LnHA<sup>2+</sup>]<sub>T,i</sub>, can be expressed as a sum of complexed metal concentrations for each of the *j*th surface ligands at the *i*th step of the titration. However, experimental measurements of total, [Ln<sup>3+</sup>]<sub>T</sub>, and free metal concentrations, [Ln<sup>3+</sup>]<sub>meas,i</sub>, only allow direct determination of [LnHA<sup>2+</sup>]<sub>T,i</sub>, as indicated by Eq. (3).

The fraction of the total *j*th ligand concentration, bound by Ln<sup>3+</sup> at the *i*th step of the titration, α<sub>LnHA,ij</sub>, can be expressed as a function of the bound metal (i.e., Ln<sup>3+</sup>) at the *i*th titrant addition, [LnHA<sub>j</sub><sup>2+</sup>]<sub>*i*</sub>, and the *j*th ligand concentration, [HA<sub>j</sub><sup>-</sup>], as follows:

$$\alpha_{\text{LnHA},ij} = \frac{[\text{LnHA}_j^{2+}]_i}{[\text{HA}_j^-]} = \frac{[\text{LnHA}_j^{2+}]_i}{[\text{LnHA}_j^{2+}]_i + [\text{HHA}_j]_i}. \quad (5)$$

The protonated *j*th ligand concentration at the *i*th step of the titration, [HHA<sub>j</sub>]<sub>*i*</sub>, can in turn be expressed as a function of [LnHA<sub>j</sub><sup>2+</sup>]<sub>*i*</sub> by rearranging the expression for the equilibrium constant K<sub>S,j</sub> in Eq. (2). The calculated bound metal concentration at the *i*th titrant addition, [LnHA<sup>2+</sup>]<sub>T,calc,i</sub>, can then be determined as a function of measured ([H<sup>+</sup>]<sub>meas,i</sub> and [Ln<sup>3+</sup>]<sub>meas,i</sub>) and adjustable ([HA<sub>j</sub><sup>-</sup>]) parameters, as shown below:

$$[\text{LnHA}^{2+}]_{T,\text{calc},i} = \sum_{j=1}^m (\alpha_{\text{LnHA},ij} [\text{HA}_j^-]) = \sum_{j=1}^m \frac{[\text{Ln}^{3+}]_{\text{meas},i} K_{S,j}}{[\text{Ln}^{3+}]_{\text{meas},i} K_{S,j} + [\text{H}^+]_{\text{meas},i}} [\text{HA}_j^-]. \quad (6)$$

The linear programming approach to multisite metal sorption solves a matrix equation,  $b = A \cdot x$ , for  $x$ . Here  $A$  is an  $n \times m$  matrix of α<sub>LnHA,ij</sub> entries as defined in Eqs. (5) and (6). The  $b$  vector is an  $n \times 1$  vector of calculated bound metal concentrations for each titrant addition, [LnHA<sup>2+</sup>]<sub>T,calc,i</sub>, as defined in Eq. (6). The  $m \times 1$  vector  $x$  contains the adjustable parameters, [HA<sub>j</sub><sup>-</sup>], for each of the *m* binding sites. Numerical difficulties exist in attempting to fit the model in Eq. (6) because binding constants and site densities are correlated parameters. This problem is solved using a fixed interval grid of log K<sub>S,j</sub> values and writing the problem in matrix form, as described by Martinez et al. [31]. In addition, the nature of the matrices as described above makes this an *ill-posed* problem, meaning that more than one error minimum can be found from optimization for  $x$  as a solution to the equation  $b = A \cdot x$ , unless additional assumptions are made about the nature of the solution [31].

Linear programming regression minimizes the number of binding sites and the absolute error,  $e = |[\text{LnHA}^{2+}]_{T,\text{calc},i} - [\text{LnHA}^{2+}]_{T,i}|$ , using a simplex method [29]. This approach finds one global minimum for the error function, which emphasizes zero as a possible

solution and avoids convergence problems such as those found in FITEQL [30,31]. LPM optimizes parameters such as total binding site concentrations. Each site density,  $[HA_j^-]$ , is assigned a positive value where zero is a possible result. This generates a  $\log K_{S,j}$  spectrum where discrete metal-binding sites are determined by the number of  $\log K_{S,j}$  values, which have a corresponding nonzero metal-binding-site density. When  $[HA_j^-]$  values are added, their sum should approximate the total available ligand concentration on the sorbent surface,  $[HA]_T$ , for a maximum experimental pH value.

In our simulations, the binding of the Ln first hydrolysis product to HA was not considered. This choice is supported by the fact that (i) all but two data points (among 28) have  $pH < 7$ ; yet it is well established that the proportion of Ln-OH complexes and thus Ln-OH-HA complexes may become important only for water samples having  $pH > 8$  [17,33]; (ii) even for alkaline waters, recent model calculations show that lanthanide speciation can be reasonably well captured by considering only  $Ln^{3+}$  complexation with HA [34].

### 3. Results and discussion

**Tables 1 to 3** summarize LPM optimization results of  $\log K_{S,j}$ ,  $[HA_j^-]$ , and  $[HA]_T$  as defined by Eqs. (2) and (4), respectively, for experimental  $[Ln^{3+}]$  sorption by three different initial humic acid concentrations of 5 to 20 mg L<sup>-1</sup>, in the pH range of 2–10. **Tables 1 and 2** indicate the  $\log K_{S,j}$  and  $[HA]_T$  values for all lanthanide elements at the full range of humic acid concentrations, while **Table 3** shows  $[HA_j^-]$  for two sites (i.e.,  $j = 2$ ) at 5 mg L<sup>-1</sup> HA. LPM optimization of Eq. (6) finds an optimal solution set of binding site concentrations,  $[HA_j^-]$ , which are assigned to the corresponding  $\log K_{S,j}$  on a fixed interval grid. This procedure generates a discrete spectrum and by approximating the ideal condition  $e = |[LnHA^{2+}]_{T,calc,I} - [LnHA^{2+}]_{T,j}| = 0$ . LPM optimization should generate a unique binding site density corresponding to a single  $\log K_{S,j}$  on the grid. However, double peaks resulted for particular sites  $j$  (data not shown), because the true  $\log K_{S,j}$  of the sample falls at an intermediate position between two adjacent  $\log K_{S,j}$  on the grid [31]. Each doublet was converted to a single peak by averaging the two  $\log K_{S,j}$  values and computing the weighted average of  $[HA_j^-]$ . The averaged values, along with existing single peaks, in replicate spectra were used to calculate overall average  $\log K_{S,j}$  and  $[HA_j^-]$  values ( $\log K_{S,j(ave)}$  and  $[HA_j^-]_{(ave)}$ ).

The  $\log K_{S,j(ave)}$  and binding site densities obtained for the three humic acid concentrations are reported in **Tables 1 and 2** for the 14 analyzed lanthanide elements. The LPM fit results for Ln, as a function of pH, are illustrated in **Fig. 1** for  $La^{3+}$ . Sample  $\log K_{S,j}$  values for  $La^{3+}$  are  $2.65 \pm 0.21$  and 7, and  $3.00 \pm 0.14$  and  $3.85 \pm 0.07$  for  $[HA]_T = 5$ , 10, and 20 mg L<sup>-1</sup>, respectively. The main characteristics of the LnHA experiments, reproduced by LPM, are a low proportion of LnHA complexes at relatively low pH and a marked increase of this proportion with increasing pH. The  $\log K_{S,j}$  values increase with humic acid concentrations of experimental solutions (e.g., for La from 2.65 to 3.85 for humic acid concentrations of 5 and 20 mg L<sup>-1</sup>, respectively). Moreover,  $\log K_{S,j}$  values increase from La (2.65) to Pr (2.75), and then decrease from Eu (2.70) to Lu (2.60) for humic acid concentrations of 5 mg L<sup>-1</sup>. This feature is further marked for a higher humic acid concentration (i.e., 20 mg L<sup>-1</sup>) where  $\log K_{S,j}$  values increase from La (3.85) to Eu (4.15) and then decrease from Gd (4.06) to Lu (3.95). It follows a  $\log K_{S,j}$  pattern showing downward concavity of middle rare earth elements (MREE) (**Fig. 2**). As already proposed by Pourret et al. [27], literature compilation of REE–organic ligand constants as plotted against Gd/Yb ratio (**Fig. 3**) evidence that new calculated  $K_{S,j}$  values are in the field of natural carboxylic acids

**Table 1**  
 $\log K_{S,j}$  values.

| [HA] (mg L <sup>-1</sup> ) | 5               | 10   | 20              |                 |
|----------------------------|-----------------|------|-----------------|-----------------|
| La                         | $2.65 \pm 0.21$ | 7.00 | $3.00 \pm 0.14$ | $3.85 \pm 0.07$ |
| Ce                         | $2.60 \pm 0.21$ | 7.00 | $3.25 \pm 0.07$ | $3.95 \pm 0.07$ |
| Pr                         | $2.75 \pm 0.21$ | 7.00 | $3.15 \pm 0.21$ | $4.05 \pm 0.07$ |
| Nd                         | $2.60 \pm 0.21$ | 7.00 | $3.40 \pm 0.14$ | $4.10 \pm 0.07$ |
| Sm                         | $2.70 \pm 0.21$ | 7.00 | $3.35 \pm 0.07$ | $4.15 \pm 0.07$ |
| Eu                         | $2.70 \pm 0.21$ | 7.00 | $3.35 \pm 0.07$ | $4.15 \pm 0.07$ |
| Gd                         | $2.60 \pm 0.21$ | 7.00 | $3.25 \pm 0.07$ | $4.05 \pm 0.07$ |
| Tb                         | $2.60 \pm 0.21$ | 7.00 | $3.25 \pm 0.07$ | $3.95 \pm 0.07$ |
| Dy                         | $2.60 \pm 0.21$ | 7.00 | $3.10 \pm 0.14$ | $3.95 \pm 0.07$ |
| Ho                         | $2.65 \pm 0.21$ | 7.00 | $3.10 \pm 0.14$ | $3.95 \pm 0.07$ |
| Er                         | $2.65 \pm 0.21$ | 7.00 | $3.15 \pm 0.07$ | $3.95 \pm 0.07$ |
| Tm                         | $2.65 \pm 0.21$ | 7.00 | $3.15 \pm 0.07$ | $3.95 \pm 0.07$ |
| Yb                         | $2.65 \pm 0.21$ | 7.00 | $3.10 \pm 0.14$ | $3.95 \pm 0.07$ |
| Lu                         | $2.65 \pm 0.21$ | 7.00 | $3.15 \pm 0.07$ | $3.95 \pm 0.07$ |

**Table 2**  
Total site density (in mol of  $Ln^{3+}$ /mg of HA).

| [HA] (mg L <sup>-1</sup> ) | 5                     | 10                    | 20                    |
|----------------------------|-----------------------|-----------------------|-----------------------|
| La                         | $2.89 \times 10^{-8}$ | $5.05 \times 10^{-8}$ | $5.02 \times 10^{-8}$ |
| Ce                         | $3.31 \times 10^{-8}$ | $5.00 \times 10^{-8}$ | $5.02 \times 10^{-8}$ |
| Pr                         | $3.21 \times 10^{-8}$ | $4.99 \times 10^{-8}$ | $5.01 \times 10^{-8}$ |
| Nd                         | $3.65 \times 10^{-8}$ | $4.97 \times 10^{-8}$ | $5.00 \times 10^{-8}$ |
| Sm                         | $3.75 \times 10^{-8}$ | $4.98 \times 10^{-8}$ | $5.00 \times 10^{-8}$ |
| Eu                         | $3.65 \times 10^{-8}$ | $4.98 \times 10^{-8}$ | $5.01 \times 10^{-8}$ |
| Gd                         | $3.50 \times 10^{-8}$ | $4.99 \times 10^{-8}$ | $5.00 \times 10^{-8}$ |
| Tb                         | $3.44 \times 10^{-8}$ | $4.98 \times 10^{-8}$ | $5.01 \times 10^{-8}$ |
| Dy                         | $3.30 \times 10^{-8}$ | $4.98 \times 10^{-8}$ | $4.98 \times 10^{-8}$ |
| Ho                         | $3.20 \times 10^{-8}$ | $5.00 \times 10^{-8}$ | $5.02 \times 10^{-8}$ |
| Er                         | $3.04 \times 10^{-8}$ | $4.99 \times 10^{-8}$ | $5.01 \times 10^{-8}$ |
| Tm                         | $3.03 \times 10^{-8}$ | $4.98 \times 10^{-8}$ | $5.01 \times 10^{-8}$ |
| Yb                         | $3.01 \times 10^{-8}$ | $4.98 \times 10^{-8}$ | $5.00 \times 10^{-8}$ |
| Lu                         | $3.00 \times 10^{-8}$ | $4.98 \times 10^{-8}$ | $4.98 \times 10^{-8}$ |

**Table 3**  
Site density for both sites at a humic acid concentration of 5 mg L<sup>-1</sup> (in mol of  $Ln^{3+}$ /mg of HA).

|    | Site 1                | Site 2                |
|----|-----------------------|-----------------------|
| La | $2.22 \times 10^{-8}$ | $0.67 \times 10^{-8}$ |
| Ce | $3.05 \times 10^{-8}$ | $0.26 \times 10^{-8}$ |
| Pr | $2.56 \times 10^{-8}$ | $0.65 \times 10^{-8}$ |
| Nd | $3.30 \times 10^{-8}$ | $0.35 \times 10^{-8}$ |
| Sm | $3.38 \times 10^{-8}$ | $0.37 \times 10^{-8}$ |
| Eu | $3.32 \times 10^{-8}$ | $0.33 \times 10^{-8}$ |
| Gd | $3.25 \times 10^{-8}$ | $0.25 \times 10^{-8}$ |
| Tb | $3.20 \times 10^{-8}$ | $0.24 \times 10^{-8}$ |
| Dy | $3.10 \times 10^{-8}$ | $0.20 \times 10^{-8}$ |
| Ho | $2.40 \times 10^{-8}$ | $0.80 \times 10^{-8}$ |
| Er | $2.04 \times 10^{-8}$ | $1.00 \times 10^{-8}$ |
| Tm | $2.05 \times 10^{-8}$ | $0.98 \times 10^{-8}$ |
| Yb | $2.04 \times 10^{-8}$ | $0.97 \times 10^{-8}$ |
| Lu | $2.00 \times 10^{-8}$ | $1.00 \times 10^{-8}$ |

and phenolic acids. As the objective of this study was not to document fractionation among lanthanide series, differences between Sonke and Salters [25] and Pourret et al. [27] were not discussed (for that see discussions in [27,28]).

As evidenced in **Table 1**, two  $\log K_{S,j}$  values are proposed by LPM for a humic acid concentration of 5 mg L<sup>-1</sup>. This feature reflects the heterogeneity of humic acid binding sites, which are known to be composed from carboxylic groups varying from 3.2 to 4.8 meq g<sup>-1</sup> and phenolic ones from 1.4 to 3.4 meq g<sup>-1</sup> [35]. This latter characteristic is only evidenced by the first experimental condition, as it is the only one that spans up to a pH of 10, and thus only the conditions considering pHs greater than 7 can allow development of binding sites at alkaline pHs (i.e., phenolic or polycarboxylic ones). Indeed, the contribution of the second site by just doubling the concentration of HA from 5 to 10 mg L<sup>-1</sup>

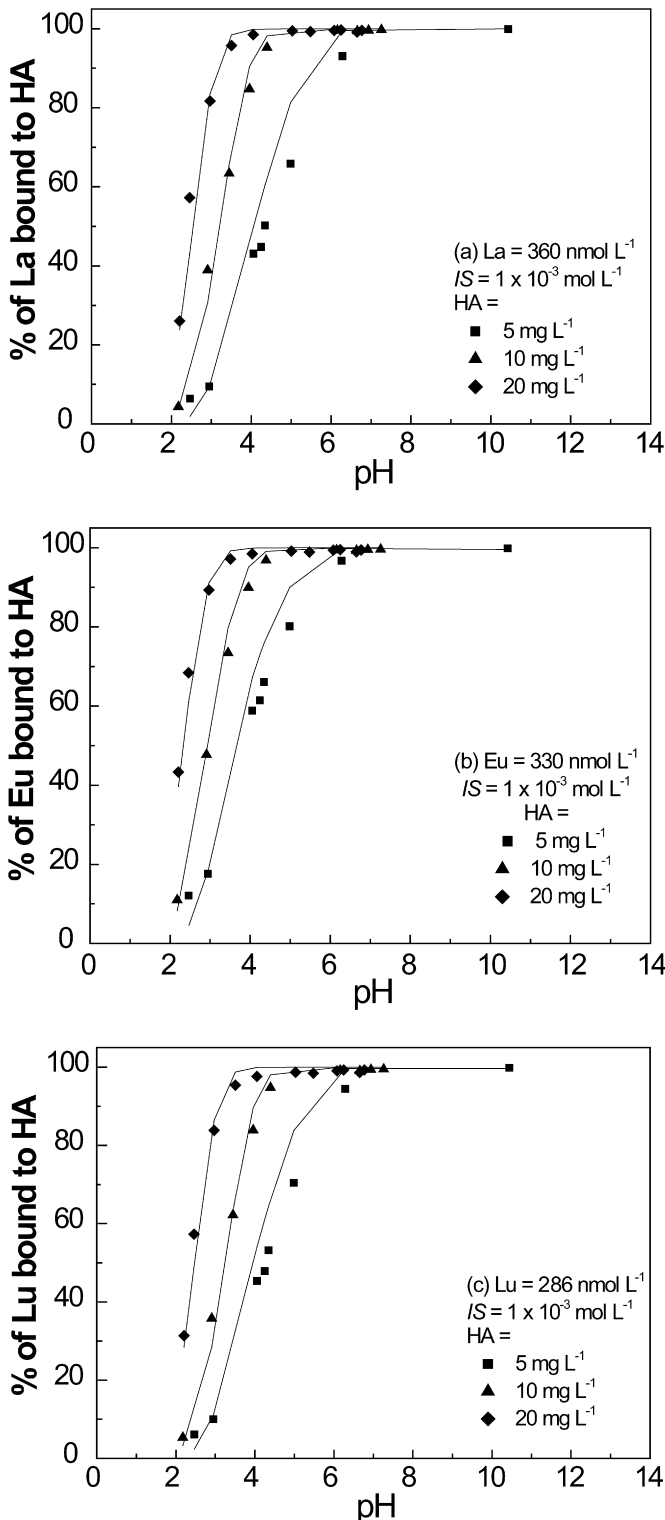


**Fig. 1.** Binding of (a) La, (b) Eu, and (c) Lu to HA for various humic acid concentrations (i.e., 5, 10, and 20 mg L<sup>-1</sup>) as a function of pH. Points correspond to experimental data [22], whereas solid lines correspond to LPM best fits, for which the absolute error  $\epsilon$  is minimal.

should still be expected at 10 and 20 mg L<sup>-1</sup>, since the contribution of the second site may reach up to 30% (i.e., from Er to Lu) at 5 mg L<sup>-1</sup>. However, the analytical window does not allow this latter feature to be expressed at both humic acid concentrations of 10 and 20 mg L<sup>-1</sup> (i.e., pH does not exceed pH values of 7.26 and 6.77, respectively) as phenolic functional groups are mostly expressed

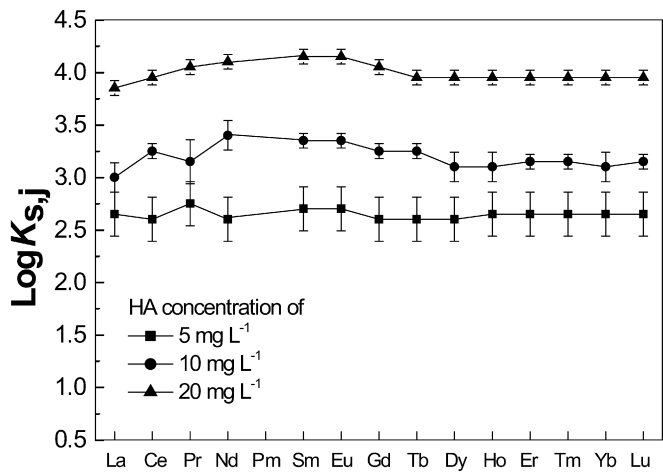


**Fig. 2.**  $\log K_{S,j}$  patterns for the 14 Ln.

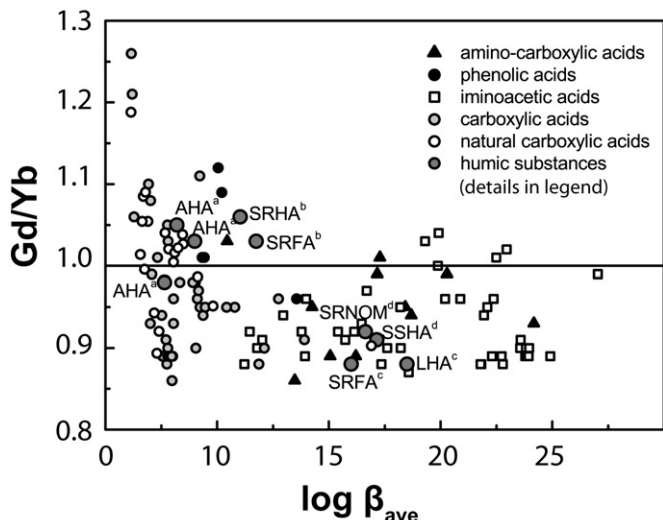


**Fig. 3.** Literature compilation of REE-organic ligand constants (recalculated at  $I = 0.1$  mol L<sup>-1</sup> when necessary [6,9]). Black triangles: amino-carboxylic acids; white squares: iminoacetic acids; black circles: phenolic acids; gray circles: carboxylic acids; white circles: natural carboxylic acids; dark gray circles: humic substances, Aldrich humic acid (AHA), Suwannee River fulvic acid (SRFA), Suwannee River humic acid (SRHA), Leonardite humic acid (LHA), Suwannee River natural organic matter (SRNOM), and Summit Hill soil humic acid (SSHA) (<sup>a</sup>this study; <sup>b</sup>Yamamoto et al. [42]; <sup>c</sup>Sonke and Salters [25]; <sup>d</sup>Stern et al. [28]).

from pH 8 to 10 [35]. This latter feature is also a verification of the results of Štamberg et al. [36], who previously studied Eu<sup>3+</sup> complexation to Aldrich HA and found that phenolic groups only occur, in lanthanide complexation, at alkaline pHs after neutralization of carboxylic groups. The corresponding total site densities ([HA]<sub>T</sub>) are  $2.89 \times 10^{-8}$ ,  $5.05 \times 10^{-8}$ , and  $5.02 \times 10^{-8}$  mol g<sup>-1</sup> of HA for 5, 10, and 20 mg L<sup>-1</sup> of HA, respectively, for La (Table 2). These latter total site densities only correspond to ca. 1% of the available sites on humic acid surfaces. Among these sites, as displayed in Table 3 for a humic acid concentration of 5 mg L<sup>-1</sup>, two types of sites may be considered. Weaker sites (i.e., sites with a mean  $\log K_{S,j}$  value of 2.65) are predominant and represent 67 to 94% of the active binding sites, whereas stronger sites (i.e., sites with a mean  $\log K_{S,j}$  value of 7.00) only represent 6 to 33% of the active binding sites. The corresponding site densities were  $2.71 \pm 0.57 \times 10^{-8}$  and  $0.58 \pm 0.32 \times 10^{-8}$  mol of Ln<sup>3+</sup>/mg of HA. As already observed, sites densities decrease with increasing  $\log K_{S,j}$  values [21].

Even if this study only considered monodentate sites, an interesting feature would be evidenced by the three humic acid

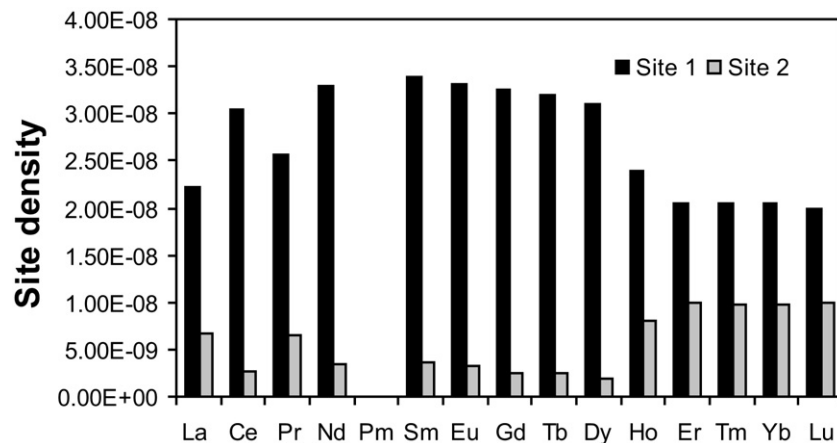


**Fig. 4.** Site density distribution (in mol of  $\text{Ln}^{3+}$ /mg of HA) for the 14 Ln (data are from Table 3).

concentrations. The binding of Ln by several separate complexing sites on HA may occur (i.e., carboxylic and phenolic binding sites), resulting in the fact that metal binding will depend upon the total humic acid concentration. In other words, two monodentate binding sites would result in lower total site densities available to complex Ln, as compared to a unique binding site. This lower total site density observed at the humic acid concentration of 5 mg L<sup>-1</sup>, for all 14 lanthanide elements, indicates a direct correlation between the amount of Ln sorbed on the external surface microenvironment of HA and the concentration of added HA. Moreover, this amount would increase with increasing humic acid concentration. This result confirms the results explained earlier, where the concentration of complexed metal is proportional to the concentration of added HA [37]. Oppositely, for the same conformation (i.e., one single monodentate site at a humic acid concentration of 10 or 20 mg L<sup>-1</sup>), there is no concentration dependence. Albeit not considered in this study, multidentate binding may also become increasingly important with increasing pH.

As evidenced by Table 3 and Fig. 4, site density distribution varies between Ln. Sites 1 are more predominant (i.e., represent >80–90% of the binding sites) for the MREE (i.e., from Nd to Dy), whereas for La or Lu they only represent 77% or 67% of the available binding sites. Complementarily, sites 2 in Table 3 are more present for binding La and Lu as regards MREE (i.e., 23% or 33% compared to <10–20%). This heterogeneity in the distribution of site types may thus reflect the competition among lanthanide elements, which is responsible for the fractionation of the lanthanide series. It must be noted that Ce does not follow this general trend, which may be ascribed to its redox behavior.  $\log K_{S,j}$  values for the lanthanide series are maximum for  $\text{Sm}^{3+}$ . Binding site densities display the same feature. It may be the result of the lanthanide coordination number change in the lanthanide complexes in solution from 9 to 8, which usually occurs in the  $\text{Eu}^{3+}$  to  $\text{Gd}^{3+}$  range. The number of water molecules about the inner lanthanide sphere is 9 from  $\text{La}^{3+}$  to  $\text{Nd}^{3+}$ , and 8 from  $\text{Tb}^{3+}$  to  $\text{Lu}^{3+}$  [38]. From a thermodynamic point of view the free energy of the lanthanide coordination number changes in the  $\text{Eu}^{3+}$  to  $\text{Gd}^{3+}$  range as a result of the sudden change of the coordination polyhedron type. Indeed, Choppin and Peterman [39] pointed out that Eu-acetate complexes occur as inner spheres and that as acetate represents a model molecule of simple carboxylic sites on complex organic matter such as HA [9], such a coordination number change must be expected in the  $\text{Eu}^{3+}$  to  $\text{Gd}^{3+}$  range. These processes are induced by variations of inter electronic repulsive potentials due to progressive filling of the 4f orbital during structural changes that especially involve inner coordination sphere of each lanthanide caused by an equilibrium ligand exchange reaction (e.g., organic phase–aqueous

phase equilibrium). Indeed, when processes involve lanthanide adsorption (or surface complexation) with an inner sphere mechanism, a non-CHARAC effect may take place. The complexation behavior of Ln thus does not depend exclusively on its ionic charge and radius, but is additionally controlled by its electron configuration and by the type of complexing ligand, since the latter two determine the character of the chemical bonding. Hence, aqueous systems are characterized by non-CHARAC trace element behavior [3], and electron structure must be considered as an additional parameter. However, this behavior needs to be further explored and refined.

As already discussed by Pourret et al. [27] and Stern et al. [28], observed differences between experiments presented by Takahashi et al. [40], Yamamoto et al. [41,42], Sonke and Salters [25], and both of these studies (i.e., [27] and [28]) strongly suggest the heterogeneity of the complexing sites in HS: high concentrations of weak carboxylic sites and low concentrations of strong phenolic sites [35]. The weak sites determine the behavior of humic complexation at high metal loading, whereas the strong sites determine the complexation strength of humic substances at trace metal concentrations [27,28], even when their concentration is only in the range of a few percent of the weak sites (i.e., 10 to 22% [35]). HS/Ln ratios considered in this study are between 5 and 20, whereas in Yamamoto et al. [41,42] they are close to 80, in Sonke and Salters [25] and Stern et al. [28] between 500 and 700, and in Takahashi et al. [40] as high as 100,000. At lower loadings, stronger sites are favored, whereas at higher loadings, weaker sites are involved in the complexation. Moreover, phenolic sites are predominant at alkaline pHs, whereas carboxylic sites are dominant binding sites at acidic pHs. Indeed, the pH range in this study spans from 2 to 10 with an analytical window in the 2–6 range, whereas in Yamamoto et al. [41,42], experimental pH varies between 4 and 5.5, and in Sonke and Salters [25] and Stern et al. [28], it varies between 6 and 10. The present study sheds more light on lanthanide loading by HA and needs to be extended to other HS by modeling existing data [25,28] with LPM to generalize this feature. In addition, all results, whether those of our study and Pourret et al. [27] or those of Sonke [26] and Stern et al. [28], suggest that the multifunctionality of the organic matter surface site should be taken into account differently in speciation studies and calculation codes. Indeed, whether Model V and VI, each of the models assumes the existence of two groups of surface sites that can form monodentate, bidentate (e.g., as in Model V [43]), and tridentate (e.g., as in Model VI [14]) complexes. However, their abundance and complexation constants are linked to one another by mathematical expressions and as regards lanthanide behavior (i.e., fractionation among lanthanide series as regards to binding

site affinities), and may be refined by considering the results obtained using LPM.

#### 4. Summary

Linear programming modeling was able to determine differences in lanthanide speciation as a function of increasing humic acid concentration. At low concentrations of dissolved organic matter, two lanthanide binding sites were found, whereas one site is obtained at higher amounts. Lanthanide binding occurs mainly at weak sites (i.e., ca. 80%; attributed to carboxylic groups) and second at strong sites (i.e., ca. 20%; attributed to phenolic moieties). However, heterogeneity in the distribution of the binding sites among Ln is evidenced, which could explain lanthanide fractionation patterns. Moreover, this study has been able to quantify LnHA interactions, including the determination of metal binding constants and site concentrations without the need for initial knowledge of these parameters, indicating the usefulness of the linear programming modeling approach to solving surface metal complexation in the presence of complex organic surfaces. Previous models including FITEQL have produced incomparable results, emphasizing the use of LPM as a tool for quantification of metal-ligand interactions, as previously suggested [29,31].

#### Acknowledgments

We thank the Biogeochemical Group from Géosciences Rennes for useful discussions when we were both in Rennes, and the Geologists Rock! Group in Beauvais when we were finalizing this project. Two anonymous reviewers are acknowledged for useful comments and Catherine Wilson and Genevieve Green are acknowledged for editorial handling.

#### References

- [1] P. Henderson, Rare Earth Element Geochemistry, Elsevier, Amsterdam, 1984.
- [2] R.D. Shannon, Acta Crystallogr. Sect. A 32 (1976) 751–767.
- [3] M. Bau, Contrib. Mineral. Petrol. 123 (1996) 323–333.
- [4] S.A. Wood, Chem. Geol. 82 (1990) 159–186.
- [5] K.B. Krauskopf, Chem. Geol. 55 (1986) 323–335.
- [6] R.H. Byrne, B. Li, Geochim. Cosmochim. Acta 59 (1995) 4575–4589.
- [7] A. Dia, G. Gruau, G. Olivière-Lauquet, C. Riou, J. Molénat, P. Curmi, Geochim. Cosmochim. Acta 64 (2000) 4131–4151.
- [8] B. Dupré, J. Viers, J.-L. Dandurand, M. Polvé, P. Bénézeth, P. Vervier, J.-J. Braun, Chem. Geol. 160 (1999) 63–80.
- [9] S.A. Wood, Eng. Geol. 34 (1993) 229–259.
- [10] J. Viers, B. Dupré, M. Polvé, J. Schott, J.-L. Dandurand, J.J. Braun, Chem. Geol. 140 (1997) 181–206.
- [11] E.M. Thurman, Organic Geochemistry of Natural Waters, Nijhoff/Junk, Dordrecht, 1985.
- [12] M. Plaschke, J. Rothe, M.A. Denecke, T. Fanghänel, J. Electron. Spectrosc. Relat. Phenom. 135 (2004) 53–62.
- [13] A.L. Herbelin, J.C. Westall, FITEQL, A computer program for determination of chemical equilibrium constants from experimental data, Report 99-01, Department of Chemistry, Oregon State University, Corvallis, 1999.
- [14] E. Tipping, Aquat. Geochem. 4 (1998) 3–48.
- [15] D.G. Kinniburgh, W.H. van Riemsdijk, L.K. Koopal, M. Borkovec, M.F. Benedetti, M.J. Avena, Colloids Surf. A 151 (1999) 147–166.
- [16] V. Moulin, J. Tits, C. Moulin, P. Decambox, P. Mauchien, O. de Ruty, Radiochim. Acta 58–59 (1992) 121–128.
- [17] A. Maes, J. De Brabandere, A. Cremers, Radiochim. Acta 44–45 (1988) 51–57.
- [18] C. Franz, G. Herrmann, N. Trautmann, Radiochim. Acta 77 (1997) 177–181.
- [19] G. Bidoglio, I. Grenthe, P. Qi, P. Robouch, N. Omenetto, Talanta 38 (1991) 999–1008.
- [20] J.R. Lead, J. Hamilton-Taylor, A. Peters, S. Reiner, E. Tipping, Anal. Chim. Acta 369 (1998) 171–180.
- [21] A. Dierckx, A. Maes, J. Vancluysen, Radiochim. Acta 66–67 (1994) 149–156.
- [22] J. Tang, K.H. Johannesson, Geochim. Cosmochim. Acta 67 (2003) 2321–2339.
- [23] O. Pourret, M. Davranche, G. Gruau, A. Dia, Geochim. Cosmochim. Acta 71 (2007) 2718–2735.
- [24] E. Tipping, M.A. Hurley, Geochim. Cosmochim. Acta 56 (1992) 3627–3641.
- [25] J.E. Sonke, V.J.M. Salters, Geochim. Cosmochim. Acta 70 (2006) 1495–1506.
- [26] J.E. Sonke, Environ. Sci. Technol. 40 (2006) 7481–7487.
- [27] O. Pourret, M. Davranche, G. Gruau, A. Dia, Chem. Geol. 243 (2007) 128–141.
- [28] J.C. Stern, J.E. Sonke, V.J.M. Salters, Chem. Geol. 246 (2007) 170–180.
- [29] P. Brassard, J.R. Kramer, P.V. Collins, Environ. Sci. Technol. 24 (1990) 195–201.
- [30] R.E. Martinez, F.G. Ferris, J. Colloid Interface Sci. 243 (2001) 73–80.
- [31] R.E. Martinez, K. Pedersen, F.G. Ferris, J. Colloid Interface Sci. 275 (2004) 82–89.
- [32] P. Zhou, H. Yan, B. Gu, Chemosphere 58 (2005) 1327–1337.
- [33] Y. Takahashi, Y. Minai, S. Ambe, Y. Makide, F. Ambe, Geochim. Cosmochim. Acta 63 (1999) 815–836.
- [34] O. Pourret, M. Davranche, G. Gruau, A. Dia, J. Colloid Interface Sci. 305 (2007) 25–31.
- [35] J.D. Ritchie, E.M. Perdue, Geochim. Cosmochim. Acta 67 (2003) 85–96.
- [36] K. Štamberk, P. Beneš, J. Mizera, J. Dolanský, D. Vopálka, K. Chalupská, J. Radíčová, Nucl. Chem. 258 (2003) 329–345.
- [37] E. Tipping, Cation Binding by Humic Substances, University Press, Cambridge, 2002.
- [38] D.G. Brookins, in: P.H. Ribbe (Ed.), Aqueous Geochemistry of Rare Earth Elements, The Mineralogical Society of America, Washington, 1989, pp. 201–225.
- [39] G.R. Choppin, D.R. Peterman, Coord. Chem. Rev. 174 (1998) 283–299.
- [40] Y. Takahashi, Y. Minai, S. Ambe, Y. Makide, F. Ambe, T. Tominaga, Sci. Total Environ. 198 (1997) 61–71.
- [41] Y. Yamamoto, Y. Takahashi, H. Shimizu, Chem. Lett. 34 (2005) 880–881.
- [42] Y. Yamamoto, Y. Takahashi, H. Shimizu, Geochim. Cosmochim. Acta Suppl. 1 (2006) A717.
- [43] E. Tipping, Comput. Geosci. 20 (1994) 973–1023.



## Rare earth element sorption onto hydrous manganese oxide: A modeling study

Olivier Pourret <sup>a,\*</sup>, Mélanie Davranche <sup>b</sup>

<sup>a</sup> HydrISE, Institut Polytechnique LaSalle Beauvais, 60026 Beauvais cedex, France

<sup>b</sup> Géosciences Rennes, Université Rennes 1, CNRS, 35042 Rennes cedex, France

### ARTICLE INFO

#### Article history:

Received 3 October 2012

Accepted 24 November 2012

Available online 5 December 2012

#### Keywords:

Rare earth elements

Manganese oxyhydroxides

Surface complexation modeling

Lanthanide

Manganese oxides

PHREEQC

PhreePlot

### ABSTRACT

Manganese oxides are important scavengers of rare earth elements (REE) in hydrosystems. However, it has been difficult to include Mn oxides in speciation models due to the lack of a comprehensive set of sorption reactions consistent with a given surface complexation model (SCM), as well as discrepancies between published sorption data and predictions using the available models. Surface complexation reactions for hydrous Mn oxide were described using a two surface site model and the diffuse double layer SCM. The specific surface area, surface side density, and  $pH_{zpc}$  were fixed to  $746 \text{ m}^2/\text{g}$ ,  $2.1 \text{ mmol/g}$ , and  $2.2$ , respectively. Two site types ( $\equiv\text{XOH}$  and  $\equiv\text{YOH}$ ) were also used with  $pK_{a2}$  values of  $2.35$  ( $\equiv\text{XOH}$ ) and  $6.06$  ( $\equiv\text{YOH}$ ). The fraction of the high affinity sites was fixed at  $0.36$ . Published REE sorption data were subsequently used to determine the equilibrium surface complexation constants, while considering the influence of pH, ionic strength, and metal loading.  $\log K$  increases from light REE to heavy REE and, more specifically, displays a convex tetrad effect. At low metal loading, the  $\equiv\text{YOH}$  site type strongly expresses its affinity toward REE, whereas at higher metal loading, the same is true for the  $\equiv\text{XOH}$  site type. This study thus provides evidence for heterogeneity in the distribution of the Mn oxide binding sites among REE.

© 2012 Elsevier Inc. All rights reserved.

## 1. Introduction

The distributions of rare earth elements (REEs) in natural waters have been intensively investigated for more than 40 years [1,2]. The absolute and relative concentrations of 14 stable REE have been determined in a variety of open ocean environments [3], estuaries [4], rivers [5], lakes [6], groundwaters [7], and hydrothermal fluids [8]. Although the complexation of hydrated trivalent REE with various inorganic anions (carbonate, hydroxide, sulfate, fluoride, and chloride) has been intensively studied [9], REE partitioning and fractionation between solution and relevant mineral surfaces are much less understood. To date, few studies have been dedicated to REE sorption onto mineral surfaces [10–15], and the most frequently used solids were Fe-oxyhydroxides [10,11,13–15]. REE sorption by amorphous ferric hydroxide was measured over a pH range of 3.5–9.0 and over a large ionic strength (IS) range. For a constant pH and individual REE, the magnitude of the estimated distribution coefficients differs by a factor of around 400. Although Mn-oxyhydroxides are as ubiquitous as Fe-oxyhydroxides and present high surface areas and a strong affinity for many elements [16], fewer studies have focused on REE adsorption by Mn-oxyhydroxides [10,13,17–19]. However, several studies have demonstrated that Mn-oxyhydroxides partly controlled REE

fractionation and mobility in natural water. Thereby, they provided the evidence that a negative Ce anomaly in solution is developed through the oxidation/scavenging of Ce(III) onto the  $\text{MnO}_2$  surface [10,17,19]. REE scavenging by ferromanganese nodules was also identified as a major process in controlling REE fractionation in seawater [8,20,21]. The lack of data for REE binding by Mn-oxyhydroxides may be attributed to the high variety of Mn-oxyhydroxide minerals and the heterogeneity of the published surface properties which complicate modeling studies. However, in order to accurately describe REE behavior, it is essential that REE binding to Mn-oxyhydroxides is quantitatively modeled. Many surface complexation models have been established to study and quantify cation sorption onto mineral surfaces. Each of them has their own solid–solution interface description, model parameters, and set of thermodynamic data, and many provide satisfactory fits to experimental data (e.g., [22]). Partially as a result of this model flexibility, ion sorption data on Mn-oxyhydroxides have been fit using a number of different surface complexation models (e.g., SCM). Thereby, a triple-layer SCM was used to evaluate and predict the surface complexation constants for hydrous manganese oxide (HMO) [23]. A variation on the constant capacitance model [24] was included in SCAMP to determine the model parameters for sorption on Mn-oxyhydroxides [25]. Crystallographic data were used as the basis for a new surface complexation model formulation [26]. More recently, Tonkin et al. [16] provided consistent surface complexation constants for several cations for a generic HMO

\* Corresponding author. Fax: +33 344 062 526.

E-mail address: [olivier.pourret@lasalle-beauvais.fr](mailto:olivier.pourret@lasalle-beauvais.fr) (O. Pourret).

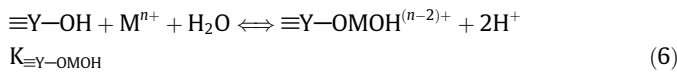
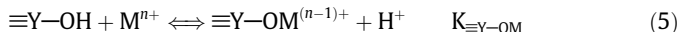
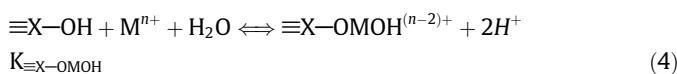
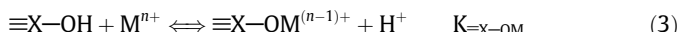
and a diffuse double layer SCM for a system in which HMO is an important scavenger.

In this study, a quantitative SCM model for REE sorption by HMO at low substrate loadings (from 1.6 to 100 mg/L) was proposed using the generic HMO surface parameters provided by Tonkin et al. [16]. The REE-HMO binding constant was extrapolated using the linear free energy relationship (LFER) methodology and by fitting experimental data sets with the PhreePlot program [27]. Published experimental data cover an ionic strength range from 0 to 0.7 mol/L and a relatively wide pH range from 4 to 9 [10]. This model was further used to discuss the nature and importance of REE sorption by manganese oxyhydroxides in the open ocean.

## 2. Materials and methods

### 2.1. Surface complexation model description

The diffuse double layer SCM describes the sorption of solutes onto oxide surfaces. This model is the central component of the generalized two-layer model used to compile the database of surface reactions for hydrous Fe(III) oxide (HFO) provided by Dzombak and Morel [28]. In this work, the SCM was chosen because of its relative simplicity and its success in describing cation sorption to HMO [16]. Surface equilibrium reactions are written as combination sorption reactions (Eqs. (1)–(6)) to specific hydroxyl sites on the oxide surface, to which a coulombic term that represents the electrochemical work of sorption is added. This coulombic term is calculated from the Gouy–Chapman electrical double layer theory and is included in the apparent equilibrium constants used by the model,  $P = \exp(-F\psi/RT)$ , where  $F$  is the Faraday constant,  $\psi$  is the electrostatic potential,  $r$  is the gas constant, and  $T$  is the absolute temperature.



The HMO surface properties (specific surface area (SSA), surface site density, and acidity constants), REE-HMO stability constants, and concentration of a non-specifically adsorbing electrolyte solution are required. Data for HMO were obtained from Tonkin et al. [16] (Table 1). The SSA value input to the model fixed at 746 m<sup>2</sup>/g is calculated and is therefore higher than the values determined by the BET-N<sub>2</sub> method, which range from 0.048 to 359 m<sup>2</sup>/g [29]. The total HMO concentration of the surface sites (mol/g) was divided into fractions for the two site types ( $\equiv XOH$  and  $\equiv YOH$ ), which present high and low affinity for REE binding, respectively.

**Table 1**  
SCM parameters for HMO [16].

| pK <sub>a1</sub> | pK <sub>a2</sub> | SSA<br>(m <sup>2</sup> /g) | Total site<br>density<br>(mmol/g) | 'Strong' site<br>density ( $\equiv XOH$ )<br>(mmol/g) | 'Weak' site<br>density ( $\equiv YOH$ )<br>(mmol/g) |
|------------------|------------------|----------------------------|-----------------------------------|---|---|
| 2.35             | 6.06             | 746                        | 2.1                               | 1.34  | 0.76  |

REE sorption onto HMO is therefore simulated assuming that two types of sites are available on the oxide surface (Table 1). Modeling calculations were performed with PHREEQC and PhreePlot [27,30]. Three keyword data blocks are required to define the surface complexation data for a simulation: (i) SURFACE\_MASTER\_SPECIES, (ii) SURFACE\_SPECIES, and (iii) SURFACE. The SURFACE\_MASTER\_SPECIES data block defines a binding site, named "Hmo" (HMO; [16]), with two binding sites, "Hmo\_w" and "Hmo\_s", for the "weak" and "strong" binding sites. Inorganic speciation was then performed; the Nagra/PSI database [31] was used and updated including the same well-accepted stability constants at infinite dilution (25 °C) for the REE inorganic complexes (hydroxide, sulfate, and carbonate; [32–34]). As Bau and Koschinsky [35] proposed, Ce(III) is oxidized after its sorption onto oxyhydroxide, and therefore, only REE(III) were considered in the proposed SCM.

### 2.2. REE-HMO sorption stability constants

#### 2.2.1. Extrapolation of the linear free energy relationship

The linear free energy relationship (LFER) or the correlation between the first hydrolysis constant for aqueous species and the corresponding surface complexation constant was used to estimate the sorption stability constant as has been previously done in numerous studies [16,28,36,37]. The LFER can be used to extend results from a limited data set to other metals. The REE-HMO stability constants were estimated by the same extrapolation method used by Tonkin et al. [16]. These authors observed that a LFER exists for HMO between  $\log K_{X-OMe}$ ,  $\log K_{X-OMOH}$ ,  $\log K_{Y-OMe}$  and  $\log K_{Y-OMOH}$  and the first hydrolysis (OH) constant for the metals ( $\log K_{MeOH}$ ).

However, Tonkin et al. [16] caution against assuming a LFER for all metals on HMO, notably with regard to the possible oxidation/scavenging mechanisms on the HMO surface. The estimated stability constant of REE binding to HMO is reported in Table 2. The first hydrolysis constant of REE,  $\log K_{REE-OH}$ , is taken from the NIST database [38]. The REE-HMO stability constants extrapolated from the LFER methodology are listed in Table 3 with the REE-OH stability constant used for the calculation.

#### 2.2.2. PhreePlot modeling

The pK<sub>a2</sub>,  $\alpha$  values, and published REE sorption data [10] were subsequently used to determine the equilibrium surface complexation constants for the whole REE series ([REE] = 125 µg/L; [HMO=δ-MnO<sub>2</sub>] = 10 mg/L; room temperature; IS fixed with NaNO<sub>3</sub>; no control of the CO<sub>2</sub> species). They were modeled using the computer program PhreePlot [27] and the Nagra/PSI database [31], which was modified to include the well-accepted infinite dilution (at 25 °C) of inorganic species [32,33]. Intrinsic constants for the surface complexation model were optimized by Powell's nonlinear least squares method using PhreePlot's fitting options. The REE-HMO stability constants are listed in Table 4. Only

**Table 2**

Stability constants used for the LFER established by Tonkin et al. [16].

|    | $\log K_{MeOH}$ | $\log K_{X-OMe}$ | $\log K_{X-OMOH}$ | $\log K_{Y-OMe}$ | $\log K_{Y-OMOH}$ |
|----|-----------------|------------------|-------------------|------------------|-------------------|
| Ba | 0.53            | 0.45             | –                 | –                | –                 |
| Ca | 1.15            | –1.5             | –                 | –                | –                 |
| Cd | 3.92            | –2.4             | –8                | –3.5             | –8.5              |
| Co | 4.35            | 1                | –3.9              | –                | –                 |
| Cu | 6.5             | 0.85             | –2.8              | 0.86             | –5.7              |
| Mg | 2.56            | –2.4             | –7.7              | –                | –                 |
| Mn | 3.41            | 1.2              | –2.7              | –                | –                 |
| Ni | 4.14            | –0.48            | –5                | –                | –                 |
| Pb | 6.29            | –                | –0.86             | 3.4              | –1.6              |
| Sr | 0.71            | –1.6             | –6.6              | –                | –                 |
| Zn | 5.04            | –0.01            | –4.4              | –                | –7.6              |

**Table 3**

REE-HMO stability constants extrapolated from the LFER established by Tonkin et al. [16].

|    | $\log K_{\text{MeOH}}$ | $\log K_{\text{XOMe}}$ | $\log K_{\text{XOMeOH}}$ | $\log K_{\text{YOMe}}$ | $\log K_{\text{YOMeOH}}$ |
|----|------------------------|------------------------|--------------------------|------------------------|--------------------------|
| La | 5.19                   | 0.05                   | -3.67                    | -0.58                  | -6.34                    |
| Ce | 5.66                   | 0.17                   | -3.23                    | 0.45                   | -5.41                    |
| Pr | 5.68                   | 0.18                   | -3.22                    | 0.50                   | -5.37                    |
| Nd | 5.82                   | 0.22                   | -3.09                    | 0.80                   | -5.10                    |
| Sm | 6.16                   | 0.31                   | -2.78                    | 1.55                   | -4.43                    |
| Eu | 6.24                   | 0.33                   | -2.70                    | 1.73                   | -4.27                    |
| Gd | 6.17                   | 0.31                   | -2.77                    | 1.57                   | -4.41                    |
| Tb | 6.36                   | 0.37                   | -2.59                    | 1.99                   | -4.03                    |
| Dy | 6.41                   | 0.38                   | -2.55                    | 2.10                   | -3.94                    |
| Ho | 6.44                   | 0.39                   | -2.52                    | 2.17                   | -3.88                    |
| Er | 6.48                   | 0.40                   | -2.48                    | 2.25                   | -3.80                    |
| Tm | 6.61                   | 0.43                   | -2.36                    | 2.54                   | -3.54                    |
| Yb | 6.76                   | 0.48                   | -2.23                    | 2.87                   | -3.25                    |
| Lu | 6.73                   | 0.47                   | -2.25                    | 2.80                   | -3.30                    |

**Table 4**

REE-HMO stability constants fitted with PhreePlot from De Carlo et al.'s [10] experimental data sets.

|    | $\log K_{\text{XOMe}}$ | $\log K_{\text{YOMe}}$ |
|----|------------------------|------------------------|
| La | -0.47                  | 2.50                   |
| Ce | 1.02                   | 3.73                   |
| Pr | -0.15                  | 2.51                   |
| Nd | -0.33                  | 2.70                   |
| Sm | -0.24                  | 2.70                   |
| Eu | -0.37                  | 2.65                   |
| Gd | -0.73                  | 2.58                   |
| Tb | -2.35                  | 2.69                   |
| Dy | -2.51                  | 2.67                   |
| Ho | -2.37                  | 2.49                   |
| Er | -1.79                  | 2.61                   |
| Tm | -1.55                  | 2.45                   |
| Yb | -3.86                  | 2.69                   |
| Lu | -1.49                  | 2.61                   |

$\log K_{\text{XOMe}}$  and  $\log K_{\text{YOMe}}$  were further considered because  $\log K_{\text{XOMeOH}}$  and  $\log K_{\text{YOMeOH}}$  are low and thus negligible.

### 3. Results and discussion

The speciation calculations presented below were performed using a diffuse double layer SCM in the PhreePlot program with the LFER extrapolated and PhreePlot fitted REE-HMO stability constants. The database was modified to integrate the extrapolated and fitted REE-HMO stability constant, as well as the infinite dilution (25 °C) stability constants for the REE inorganic (chloride and carbonate) complexes [32,33]. To test the validity of the extrapolated and fitted REE-HMO stability constant and the diffused double layer SCM, the modeling calculations were compared to the REE-HMO sorption experimental data sets [10,13,18,19].

#### 3.1. REE-HMO modeling with extrapolated stability constant

##### 3.1.1. LFER extrapolated stability constant

The data set for the extrapolated REE-HMO stability constants was subsequently used to calculate the distribution of La under various experimental conditions [10,13,18]. The comparison between the experimental and the calculated data provides evidence that the data set for the extrapolated REE-HMO stability constants cannot be used to reproduce the experimental distribution of REE onto HMO regardless of the pH, IS (Fig. 1; pH ranging from 4.0 to 9.5 and IS varying from 0.001 to 0.7 mol/L) and metal loading ([REE] varying from 5 µg/L to 0.2 mg/L and [HMO=δ-MnO<sub>2</sub>] ranging from 3.2 mg/L to 100 mg/L). The calculated proportion of bound

REE is strongly underestimated. Therefore, the data sets for the extrapolated constants were not used hereafter.

##### 3.1.2. PhreePlot fitted stability constants

The fitted stability constants were subsequently used to calculate the distribution of La, Eu, and Lu under De Carlo et al.'s [10] experimental conditions. Fig. 2 compares the experimental and calculated data sets. The model reproduces reasonably well the increasing light REE (LREE; illustrated by La) binding onto HMO with pH and IS. However, for heavy REE (HREE; illustrated by Lu), although the model predicts a decreasing binding strength, the experimental data show that 100% of REE are sorbed onto HMO. In Table 5, the rmse (root mean square errors) are reported between the experimental and modeling data for the three REE and IS conditions. The important rmse values for Eu and Lu at IS = 0.7 were expected with regards to the irregularity observed in the experimental data set [10]. Moreover, Fig. 2 shows that the discrepancy between the experimental and the calculated data also increases with pH, IS, and the REE atomic number. Lee and Byrne [39] demonstrated that REE binding by carbonate in solution increases with the REE atomic numbers. The most important difference observed for the heavy REE (HREE) therefore indicates that the model predicts larger concentrations of HREE bound to carbonate than in the experimental conditions.

### 3.2. PhreePlot modeling

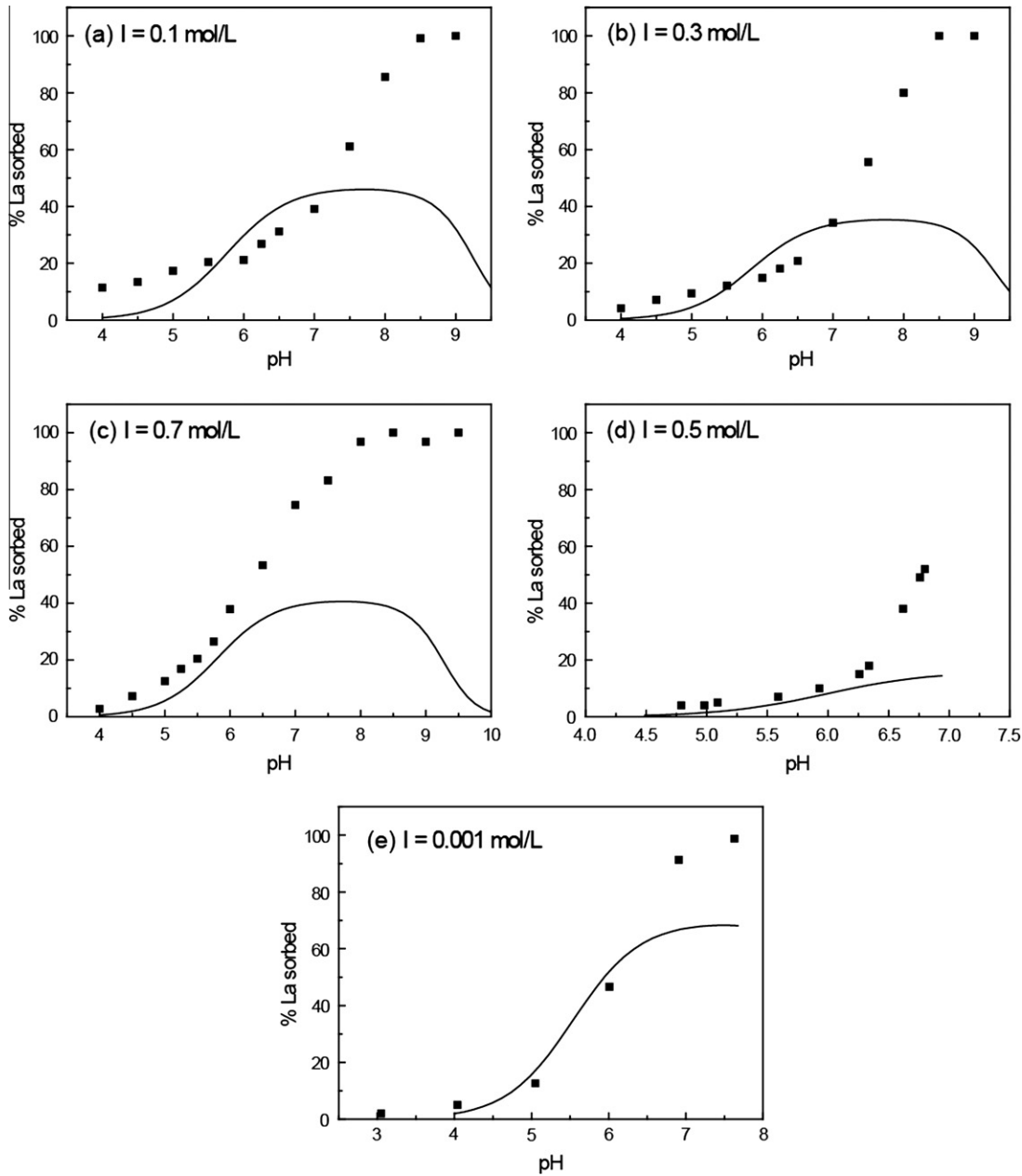
#### 3.2.1. pH dependence

Fig. 2 also compares the experimental and calculated data sets. The model reproduces reasonably well the increasing LREE binding onto HMO with pH and IS. However, the model predicts a decreasing binding strength at an alkaline pH for HREE. As already shown by De Carlo et al. [10], a large extent of the variability in the sorption efficiency is observed at low pH with the IS. This is generally evidenced by a shift in the adsorption edges toward an alkaline pH and reduced REE sorption with increasing IS, especially at an acidic pH. The differences appear more pronounced for LREE than HREE.

#### 3.2.2. REE patterns

The REE distribution between suspended HMO (at an IS of 0.5 mol/L) over the pH range from 4.79 to 6.80 [13] was further modeled using the previously described SCM procedure. The calculated REE patterns onto HMO are shown in Fig. 3a. The patterns exhibit extremely large positive Ce anomalies and a convex tetrad effect (well developed for the first two tetrads). These two features were already apparent in the experimental data sets of De Carlo et al. [10] and Ohta and Kawabe [13]. The same features occur for Davranche et al.'s [18] data set: the REE patterns exhibit large positive Ce anomalies (Fig. 3b), as well as convex tetrad curves. However, they are less developed. This discrepancy might be explained by the rather different experimental conditions used in Davranche et al. [18] as compared to those used in De Carlo et al. [10] from which the constants are derived.

Among these results, an interesting feature is that the modeling approach reproduces the strongly enhanced adsorption of Ce from acidic solution by HMO, relative to the other REE. The adsorption edge in the HMO suspension is therefore below pH 4 for Ce, whereas for strictly trivalent REE, it occurs near neutral pH. It should be noted that at ambient conditions and in the absence of strong ligands, tetravalent Ce is only stable in solid phase [40], or when it is derived from the oxidation/scavenging of Ce(III) onto the metal oxyhydroxide surface [35]. Thus, the Ce-HMO constant calculated in this study is a conditional constant, which considers the global oxidation-scavenging of the Ce(III, IV) mechanism onto the HMO surface.



**Fig. 1.** Proportion of La sorbed to HMO as a function of pH. The dots correspond to experimental data from the literature, and the solid line represents modeled data using extrapolated constants obtained from LFER (a) (b) (c) De Carlo et al. [10]; (d) Ohta and Kawabe [13]; (e) Davranche et al. [18].

### 3.2.3. Model validity and application

In order to check the validity of the model, calculations were performed with data from the literature [13,18]. Irrespective of the pH, IS (Fig. 1; pH ranging from 4.0 to 9.5 and IS varying from 0.001 to 0.7 mol/L) and metal loadings ([REE] varying from 5 µg/L to 0.2 mg/L and [HMO=δ-MnO<sub>2</sub>] ranging from 3.2 mg/L to 100 mg/L), the modeling is in agreement with the experimental results. In further detail, data from Ohta and Kawabe [13] for a high IS (i.e., 0.5 mol/L) are well reproduced, as were observed in De Carlo et al.'s [10] experimental conditions. However, data from Davranche et al. [18] for the lowest IS (i.e., 0.001 mol/L) are not well reproduced. The main differences between these experimental conditions, apart from the IS, are that different metal loadings are tested (i.e., 0.875 for Ohta and Kawabe [13]; 0.175 for De Carlo et al. [10]; 0.0007 for Davranche et al. [18,19]).

Unlike the various experimental conditions, differences between the experimental observations and the modeling are probably due to the generic parameters chosen to represent the Mn-oxyhydroxides. In fact, there are different Mn-oxyhydroxide varieties, and their properties are highly variable [29,41]. As an example, pH<sub>zpc</sub> values for HMO can vary from 2 to 9.6 [29]. Ohta and Kawabe [13] and De Carlo et al. [10] consider vernadite with a pH<sub>zpc</sub> of 2.25 [42], whereas Davranche et al. [18] consider pyrolusite with a pH<sub>zpc</sub> of 5.8.

Apart from these discrepancies, a faithful reproduction of the data from the literature constitutes an even better test of model's ability. While the conditional nature (IS, pH, and metal loading) of the determined stability constants would render such an exercise rather meaningless for a single element, the unique attributes of the REE series can be used to examine whole log K patterns. The

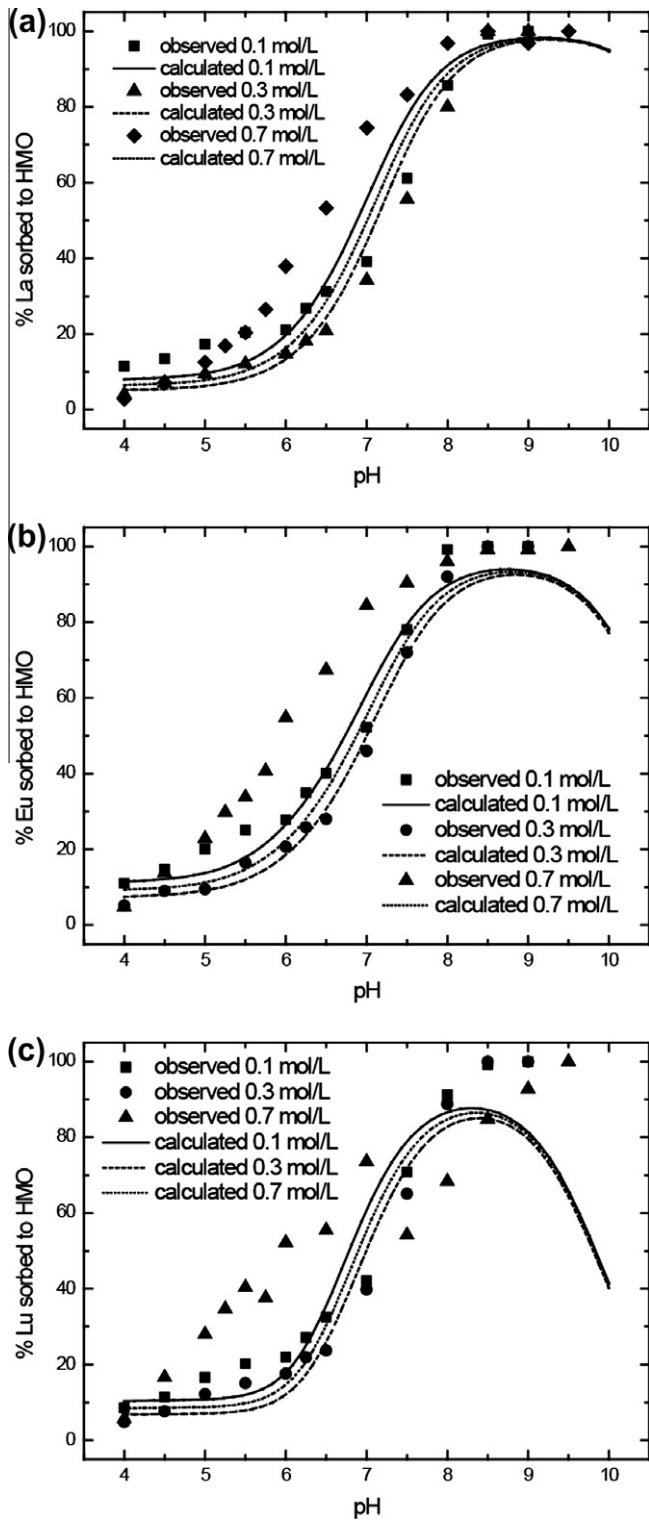


**Fig. 2.** A comparison between the experimental and calculated proportion of La, Eu and Lu bound to HMO using the fitted REE-HMO stability constants under the experimental condition's provided by De Carlo et al. [10]. The dots correspond to the displayed experimental data, and the solid line corresponds to the calculated data.

REE pattern shape (i.e., REE fractionation) is governed by the chemical properties of the REE and does not depend on the sorbent properties, which depend on its synthesis method which controls, for example, its crystallinity and specific surface area [43].

**Table 5**

Rmse (root mean square error) calculated between the experimental data sets [10] and the data sets calculated from the REE-HMO fitted stability constant.

|          | La   | Eu   | Lu   |
|----------|------|------|------|
| IS = 0.1 | 0.05 | 0.04 | 0.06 |
| IS = 0.3 | 0.04 | 0.03 | 0.35 |
| IS = 0.7 | 0.07 | 0.23 | 0.34 |

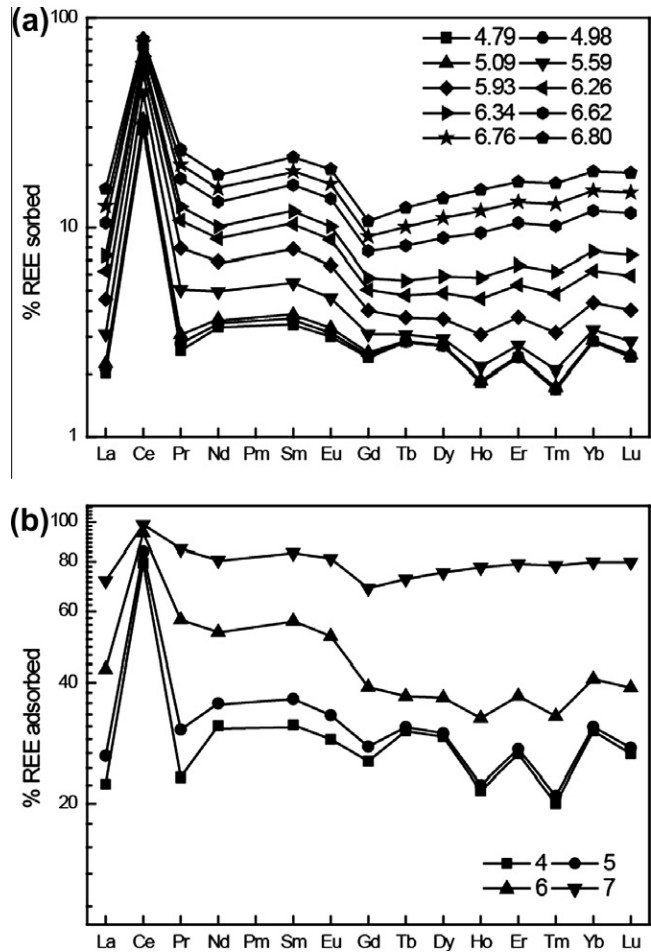


**Fig. 3.** Modeled versus experiments REE patterns showing Ce/Ce\* for the experimental conditions described in (a) Fig. 2 in Ohta and Kawabe [13], and (b) Fig. 4 in Davranche et al. [19] and Fig. 6 in Davranche et al. [18].

This type of SCM development can be used to improve the understanding of REE fractionation in seawater. Indeed, the experimental conditions are closed to those of marine system. Moreover, an interesting feature is that modeling approach can reproduce the high adsorption of Ce relative to the other REE under acidic conditions. This behavior is also observed in seawater when dissolved REE are scavenged by  $\delta\text{-MnO}_2$  [10]. The Ce anomaly is recognized as one of the fundamental features of lanthanide geochemistry due to its redox sensitivity [44]. Cerium is a prime proxy for ocean-atmosphere evolution over geological timescales [45]. The contribution of oxidative scavenging toward the removal of Ce from solution is most pronounced at acidic pH, where the strictly trivalent REE exhibit little propensity for sorption onto  $\delta\text{-MnO}_2$ . It has been suggested that the behavior of REE and Ce in the marine environment is more closely coupled to that of Mn than to that of Fe due to the oxidative scavenging of Ce by Mn-oxyhydroxides [44].

#### 4. Concluding remarks

Surface complexation modeling was used to test REE sorption onto HMO by considering LFER to determine  $\log K$ . However, this methodology does not allow experimental data to be reproduced. Therefore, these experimental data were further used to extrapolate equilibrium surface complexation constants by fitting them for a large data set [10]. The determined constants can reproduce pH dependence and REE fractionation over a wide variety of conditions (i.e., pH ranging from 4.0 to 9.5, IS varying from 0.001 to 0.7 mol/L, [REE] varying from 5 µg/L to 0.2 mg/L and [HMO=δ-MnO<sub>2</sub>] ranging from 3.2 mg/L to 100 mg/L). SCM development of this type can be used to improve the understanding of REE fractionation in seawater. However, these results emphasize the relevance of conducting further experiments and modeling for a better understanding of natural systems and have considerable implications for the assessment of REE mobility.

#### Acknowledgments

Dr. Atsuyuki Ohta is acknowledged for sharing the raw data used in this study. This research was funded by the French ANR, through the “Programme Jeunes Chercheuses – Jeunes Chercheurs: SURFREE (Rare earth elements partitioning at solid-water interface: Impact on REE geochemical behavior and tracing properties)”. Dr. Sara Mullin is acknowledged for post-editing the English content.

#### References

- [1] E.D. Goldberg, M. Koide, R.A. Schmitt, R.H. Smith, *J. Geophys. Res.* 68 (1963) 4209–4217.
- [2] P. Henderson, *Rare Earth Element Geochemistry*, Elsevier, Amsterdam, 1984.
- [3] H.J.W. De Baar, M.P. Bacon, P.G. Brewer, K.W. Bruland, *Geochim. Cosmochim. Acta* 49 (1985) 1943–1959.
- [4] E.R. Sholkovitz, H. Elderfield, *Global Biogeochem. Cy.* 2 (1988) 157–176.
- [5] S.J. Goldstein, S.B. Jacobsen, *Earth Planet. Sci. Lett.* 89 (1988) 35–47.
- [6] K.H. Johannesson, W.B. Lyons, D.A. Bird, *Geophys. Res. Lett.* 21 (1994) 773–776.
- [7] P.L. Smedley, *Geochim. Cosmochim. Acta* 55 (1991) 2767–2779.
- [8] M. Bau, *Contrib. Mineral. Petrol.* 123 (1996) 323–333.
- [9] S.A. Wood, *Chem. Geol.* 82 (1990) 159–186.
- [10] E.H. De Carlo, X.-Y. Wen, M. Irving, *Aquat. Geochem.* 3 (1998) 357–389.
- [11] M. Bau, *Geochim. Cosmochim. Acta* 63 (1999) 67–77.
- [12] A. Ohta, I. Kawabe, *Geochim. J.* 34 (2000) 439–454.
- [13] A. Ohta, I. Kawabe, *Geochim. Cosmochim. Acta* 65 (2001) 695–703.
- [14] K.A. Quinn, R.H. Byrne, J. Schijf, *Aquat. Geochem.* 10 (2004) 59–80.
- [15] J. Schijf, K.S. Marshall, *Mar. Chem.* 123 (2011) 32–43.
- [16] J.W. Tonkin, L.S. Balistrieri, J.W. Murray, *Appl. Geochem.* 19 (2004) 29–53.
- [17] D. Koeppenkastrop, E.H. De Carlo, *Chem. Geol.* 95 (1992) 251–263.
- [18] M. Davranche, O. Pourret, G. Gruau, A. Dia, D. Jin, D. Gaertner, *Chem. Geol.* 247 (2008) 154–170.
- [19] M. Davranche, O. Pourret, G. Gruau, A. Dia, M. Le Coz-Bouhnik, *Geochim. Cosmochim. Acta* 69 (2005) 4825–4835.
- [20] D.Z. Piper, *Geochim. Cosmochim. Acta* 38 (1974) 1007–1022.
- [21] H. Elderfield, C.J. Hawkesworth, M.J. Greaves, S.E. Calvert, *Geochim. Cosmochim. Acta* 45 (1981) 513–528.
- [22] P. Venema, T. Hiemstra, W.H. van Riemsdijk, *J. Colloid Interface Sci.* 181 (1996) 45–59.
- [23] R.W. Smith, E.A. Jenne, *Environ. Sci. Technol.* 25 (1991) 525–531.
- [24] P.W. Schindler, W. Stumm, in: W. Stumm (Ed.), *The Surface Chemistry of Oxides, Hydroxides and Oxide Minerals*, Wiley, 1987, pp. 83–110.
- [25] S. Lofts, E. Tipping, *Geochim. Cosmochim. Acta* 62 (1998) 2609–2625.
- [26] C.A.J. Appelo, D. Postma, *Geochim. Cosmochim. Acta* 63 (1999) 3039–3048.
- [27] D.G. Kinniburgh, D.M. Cooper, *PhreePlot: Creating graphical output with PHREEQC*, <<http://www.phreeplot.org/>>, 2009.
- [28] D.A. Dzombak, F.M.M. Morel, *Surface Complexation Modeling-Hydrous Ferric Oxide*, Wiley, New York, 1990.
- [29] M. Kosmulski, *Surface Charging and Points of Zero Charge*, CRC Press, Boca Raton, 2009.
- [30] D.L. Parkhurst, C.A.J. Appelo, *User's Guide to PHREEQC (Version 2) – A Computer Program for Speciation, Batch-Reaction, One-Dimensional Transport, and Inverse Geochemical Calculations*, 99-4259, U.S. Geological Survey Water-Resources Investigations Report, 1999, p. 309.
- [31] W. Hummel, U. Berner, E. Curti, F.J. Pearson, T. Thoenen, Nagra/PSI Chemical Thermodynamic Data Base 01/01, Universal Publishers, Parkland, Florida, 2002.
- [32] G.D. Klungness, R.H. Byrne, *Polyhedron* 19 (2000) 99–107.
- [33] Y.-R. Luo, R.H. Byrne, *Geochim. Cosmochim. Acta* 68 (2004) 691–699.
- [34] J. Schijf, R.H. Byrne, *Geochim. Cosmochim. Acta* 68 (2004) 2825–2837.
- [35] M. Bau, A. Koschinsky, *Geochim. J.* 43 (2009) 37–47.
- [36] J. Tang, K.H. Johannesson, *Geochim. Cosmochim. Acta* 67 (2003) 2321–2339.
- [37] O. Pourret, M. Davranche, G. Gruau, A. Dia, *Chem. Geol.* 243 (2007) 128–141.
- [38] A.E. Martell, R.M. Smith, R.J. Motekaitis, *NIST Critically Selected Stability Constants of Metal Complexes Database*, Version 8.0 for Windows, National Institute of Standards and Technology, Texas A&M University, 2008.
- [39] J.H. Lee, R.H. Byrne, *Geochim. Cosmochim. Acta* 56 (1992) 1127–1137.
- [40] D.G. Brookins, in: P.H. Ribbe (Ed.), *Aqueous Geochemistry of Rare Earth Elements*, The Mineralogical Society of America, Washington, 1989, pp. 201–225.
- [41] J.E. Post, *Proc. Natl. Acad. Sci. USA* 96 (1999) 3447–3454.
- [42] J.W. Murray, *J. Colloid Interface Sci.* 46 (1974) 357–371.
- [43] R.M. Cornell, U. Schwertmann, In the Iron Oxides, John Wiley & Sons, USA, 2003, p. 703.
- [44] H. Elderfield, *Philos. Trans. Roy. Soc. A* 325 (1988) 105–126.
- [45] K.M. Towe, *Palaeogeogr. Palaeocat.* 97 (1991) 113–123.

# Organic complexation of rare earth elements in natural waters: Evaluating model calculations from ultrafiltration data

Olivier Pourret <sup>\*</sup>, Mélanie Davranche, Gérard Gruau, Aline Dia

CAREN, Géosciences Rennes, UMR CNRS 6118, Campus de Beaulieu, 35042 Rennes Cedex, France

Received 13 April 2006; accepted in revised form 2 April 2007; available online 7 April 2007

---

## Abstract

The Stockholm Humic Model (SHM) and Humic Ion-Binding Models V and VI were compared for their ability to predict the role of dissolved organic matter (DOM) in the speciation of rare earth elements (REE) in natural waters. Unlike Models V and VI, SHM is part of a speciation code that also allows us to consider dissolution/precipitation, sorption/desorption and oxidation/reduction reactions. In this context, it is particularly interesting to test the performance of SHM. The REE specific equilibrium constants required by the speciation models were estimated using linear free-energy relationships (LFER) between the first hydrolysis constants and the stability constants for REE complexation with lactic and acetic acid. Three datasets were used for the purpose of comparison: (i) World Average River Water (Dissolved Organic Carbon (DOC) = 5 mg L<sup>-1</sup>), previously investigated using Model V, was reinvestigated using SHM and Model VI; (ii) two natural organic-rich waters (DOC = 18–24 mg L<sup>-1</sup>), whose REE speciation has already been determined with both Model V and ultrafiltration studies, were also reinvestigated using SHM and Model VI; finally, (iii) new ultrafiltration experiments were carried out on samples of circumneutral-pH (pH 6.2–7.1), organic-rich (DOC = 7–20 mg L<sup>-1</sup>) groundwaters from the Kervidy-Naizin and Petit-Hermitage catchments, western France. The results were then compared with speciation predictions provided by Model VI and SHM, successively. When applied to World Average River Water, both Model VI and SHM yield comparable results, confirming the earlier finding that a large fraction of the dissolved REE in rivers occurs as organic complexes. This implies that the two models are equally valid for calculating REE speciation in low-DOC waters at circumneutral-pH. The two models also successfully reproduced ultrafiltration results obtained for DOC-rich acidic groundwaters and river waters. By contrast, the two models yielded different results when compared to newly obtained ultrafiltration results for DOC-rich (DOC > 7 mg L<sup>-1</sup>) groundwaters at circumneutral-pH, with Model VI predictions being closer to the ultrafiltration data than SHM. Sensitivity analysis indicates that the “active DOM parameter” (i.e., the proportion of DOC that can effectively complex with REE) is a key parameter for both Model VI and SHM. However, a survey of ultrafiltration results allows the “active DOM parameter” to be precisely determined for the newly ultrafiltered waters studied here. Thus, the observed discrepancy between SHM predictions and ultrafiltration results cannot be explained by the use of inappropriate “active DOM parameter” values in this model. Save this unexplained discrepancy, the results presented in this study demonstrate that both Model VI and SHM can provide reliable estimates of REE speciation in organic-rich waters. However, it is essential to know the proportion of DOM that can actively complex REE before running these two speciation models.

© 2007 Elsevier Ltd. All rights reserved.

---

## 1. INTRODUCTION

The aquatic geochemistry of rare earth elements (REE) has been the subject of numerous studies over the past

two decades (Elderfield and Greaves, 1982; De Baar et al., 1988; Elderfield et al., 1990; De Baar et al., 1991; Smedley, 1991; Gosselin et al., 1992; Sholkovitz, 1995; Byrne and Sholkovitz, 1996; Johannesson et al., 1997, 2000; Johannesson and Hendry, 2000; Janssen and Verweij, 2003; Nelson et al., 2004). However, it is difficult to assess the extent to which REE patterns in natural waters are

\* Corresponding author. Fax: +33 2 23 23 60 90.  
E-mail address: [olivier.pourret@univ-rennes1.fr](mailto:olivier.pourret@univ-rennes1.fr) (O. Pourret).

controlled by the source rocks (Johannesson et al., 1999; Dia et al., 2000; Aubert et al., 2001). Processes such as REE complexation by inorganic ligands, or REE adsorption onto solid mineral phases, can fractionate the REE (e.g., Johannesson et al., 1999; Coppin et al., 2002). There is also some evidence that REE adsorption onto Fe- and Mn-oxides may lead to negative Ce anomalies in waters due to the oxidative scavenging of Ce onto these metallic oxides (Viers et al., 1997; Dupré et al., 1999; Dia et al., 2000; Davranche et al., 2004, 2005; Gruau et al., 2004). Above all, REE complexation with natural organic ligands may be of prime importance in controlling REE fractionation in natural waters, as inferred from recent ultrafiltration and electrochemical studies of organic-rich waters (Tanikazi et al., 1992; Viers et al., 1997; Dupré et al., 1999; Dia et al., 2000; Ingri et al., 2000; Johannesson et al., 2004).

Consequently, it is essential to develop models to predict the complexation of REE with dissolved organic matter (DOM). For that purpose, we require REE binding constants for REE-proton exchange with humic matter (HM). These constants can be experimentally determined, either for individual REE (e.g., Bidoglio et al., 1991; Moulin et al., 1992; Lead et al., 1998; Lippold et al., 2005) or for the whole REE series (Yamamoto et al., 2005; Sonke and Salters, 2006; Yamamoto et al., 2006). However, experimentally determined REE constants may be difficult to use because of differences in the pH and/or ionic strength conditions of the experiments (Bidoglio et al., 1991; Moulin et al., 1992; Lead et al., 1998; Lippold et al., 2005) or due to differences in the REE/HM ratio of the experimental solutions (Yamamoto et al., 2005; Sonke and Salters, 2006). An indirect method is to estimate the required Lanthanide-humic (LnHM) constants using the linear free-energy relationships (LFER) existing between metal-HM complexation and the stability constants for metal-lactic and metal-acetic acid complexation. These LnHM values can then be put into thermodynamic models aimed at predicting metal complexation with HM. The ability of the models to predict REE complexation with DOM can then be established by comparing model results with ultrafiltration data. The most successful attempt along these lines was made by Tang and Johannesson (2003), who applied the indirect method to test the ability of the well-known metal-HM speciation code Humic Ion-Binding Model V (Tipping, 1994) to predict REE complexation with DOM. Comparisons between model predictions and ultrafiltration results for six natural water samples were then used by these authors (op. cit.) to validate both the estimated LnHM and the model. Applying Model V to World Average River Water, Tang and Johannesson (2003) predicted that LnHM complexes are the principal carriers of REE in the dissolved (i.e., <0.2 µm) fraction of river waters.

However, Model V is exclusively a speciation model that does not take account of other reactions (i.e., dissolution/precipitation, adsorption/desorption, oxidation/reduction) that are also important in controlling the REE distribution in waters. In this study, we test the ability of the Stockholm Humic Model (SHM) to predict REE complexation by HM (Gustafsson, 2001a, 2003). This model was selected because

it is part of a full chemical equilibrium model that allows modelling of all the above reactions (Visual MINTEQ; Gustafsson, 2001b). The aim of our study is also to compare SHM with Model VI, which is the latest version of the Humic Ion-Binding Model (Tipping, 1998). REE constants were estimated using the above described indirect LFER method. For purposes of comparison, we used the following three-step approach: first, World Average River Water, previously investigated using Model V by Tang and Johannesson (2003), was reinvestigated successively using Model VI and SHM. Second, we used both SHM and Model VI to reinvestigate two of the six ultrafiltered organic-rich natural waters used by Tang and Johannesson (2003) to validate Model V. Finally, new ultrafiltration experiments were conducted using organic-rich (Dissolved Organic Carbon (DOC) 7–20 mg L<sup>-1</sup>) groundwaters with circumneutral-pH (pH 6.2–7.1) from the Kervidy-Naizin and Petit-Hermitage catchments, western France, and the results were compared with predictions from Model VI and SHM. Hence, the present study is also a new step in assessing the ability of the Humic Ion-Binding Model to predict REE complexation by organic matter in natural waters. So far, this model has been compared to only a limited number of ultrafiltration results (Tang and Johannesson, 2003).

## 2. MATERIALS AND METHODS

In this paper, we use the term *organic matter-bound REE solution complex* in the same way as in Tang and Johannesson (2003), namely, to include REE complexed to both low- and high-molecular weight (MW) organic matter.

### 2.1. Description of models

Humic Ion-Binding Model VI (here referred to as Model VI) is the latest version of a model developed by Tipping and co-workers in the early 1990s (Tipping and Hurley, 1992; Tipping, 1994, 1998). Model VI is a discrete site-electrostatic model for proton and metal ion interactions with fulvic (FA) and humic (HA) acids. The thermodynamic basis of the model has been presented and discussed in detail elsewhere (e.g., Tipping, 1998). Briefly, the model assumes that proton and metal complexation by organic matter involve two types of discrete sites (Type A and Type B) that have separate intrinsic binding constants for metals:  $\log K_{MA}$  and  $\log K_{MB}$ . By considering results from many datasets, we obtain a universal average value of  $\Delta LK_1$ , and can establish a correlation between  $\log K_{MB}$  and  $\log K_{MA}$  (Tipping, 1998). Thus, we only require one single adjustable parameter ( $\log K_{MA}$ ) to fully describe metal binding in Model VI. The parameters necessary to run the model are presented in Table EA1-Electronic Annex (based on Tipping, 1998). As shown by Tipping (1998) and Tipping et al. (2002), updating Model V to Model VI leads in many cases to an overall improvement of the predictive power of the model.

The Stockholm Humic Model (SHM) is an integral part of the chemical equilibrium model Visual MINTEQ (Gustafsson, 2001b), which enables modelling of solution

speciation along with adsorption/desorption, dissolution/precipitation and redox reactions. The principles of SHM have been fully presented and discussed elsewhere by Gustafsson (2001a) and Gustafsson et al. (2003). Where applicable, Gustafsson (2001a) gave the same symbols to denote SHM parameters as those used for corresponding parameters in Models VI, for sake of consistency. SHM is a discrete-ligand model in which the FA and HA are assumed to have eight proton-binding sites with distinct acid–base characteristics. In this model, seven adjustable parameters ( $n_A$ ,  $n_B$ ,  $\log K_A$ ,  $\log K_B$ ,  $\Delta pK_A$ ,  $\Delta pK_B$  and  $g_f$ ) are required to describe the proton dissociation reaction. Table EA2-Electronic Annex lists the fixed values that Gustafsson (2001a) derived for these seven parameters for FA and HA. In the present study, we select the generic values for these parameters listed in the “shmgeneric.mdb” database, since they are average values obtained from a large number of aquatic FA and HA samples (Gustafsson, 2001b). Three parameters are normally required with SHM to model the complexation of metals with organic matter, i.e., the monodentate complexation constant  $K_{Mm}$ , the bidentate complexation constant  $K_{Mb}$ , and the  $\Delta LK_2$  parameter, which determines the degree of binding site heterogeneity. Gustafsson (2001a) demonstrated that trivalent cation (e.g., Al) organic complexation is better fitted if only bidentate binding is involved. Therefore, in practice, only a single adjustable parameter ( $\log K_{Mb}$ ) is necessary to fully describe trivalent metal complexation by HM in natural waters (Gustafsson, 2001b).

However, results from both SHM and Model VI depend on the values of the  $\Delta LK_2$  parameter (i.e., the distribution term that modifies the strengths of complexation sites) which is input in models. Because SHM and Model VI are different in a number of respects, a  $\Delta LK_2$  value adopted from Model VI cannot be expected to yield similar good fits for SHM. In the following we use the  $\Delta LK_2$  values which were optimized by fitting published datasets (Milne et al., 2003) for SHM (namely 1.3; Gustafsson, 2001b) or from a correlation with the equilibrium constant for complexation of the metal with  $\text{NH}_3$  for Model VI (0.29; Lead et al., 1998; Tipping, 1998). The  $\Delta LK_2$  values are constrained to be identical for the whole REE series as REE are known for their chemical similarity.

Table 1

$\log K$  for metal complexation with lactic acid (LA), acetic acid (AA) and first hydrolysis (OH), as well as  $\log K_{MA}$  for HA and FA (from Tipping, 1998), used to obtain equations for LFER between  $\log K_{MA}$  and  $\log K$  for each ligand

| Metals           | $\log K(\text{LA})$ | $\log K(\text{AA})$ | $\log K(\text{MOH})$ | $\log K_{MA}(\text{HA})$ | $\log K_{MA}(\text{FA})$ | $\Delta LK_2$ |
|------------------|---------------------|---------------------|----------------------|--------------------------|--------------------------|---------------|
| $\text{Mg}^{2+}$ | 1.37                | 1.27                | 2.60                 | 0.70                     | 1.10                     | 0.12          |
| $\text{Ca}^{2+}$ | 1.45                | 1.18                | 1.30                 | 0.70                     | 1.30                     | 0.0           |
| $\text{Sr}^{2+}$ | 0.97                | 1.14                | 0.82                 | 1.11                     | 1.20                     | 0.0           |
| $\text{Mn}^{2+}$ | 1.43                | 1.4                 | 3.40                 | 0.60                     | 1.70                     | 0.58          |
| $\text{Co}^{2+}$ | 1.90                | 1.46                | 4.35                 | 1.10                     | 1.40                     | 1.22          |
| $\text{Ni}^{2+}$ | 2.22                | 1.43                | 4.14                 | 1.10                     | 1.40                     | 1.57          |
| $\text{Cu}^{2+}$ | 3.02                | 2.22                | 6.50                 | 2.00                     | 2.10                     | 2.34          |
| $\text{Zn}^{2+}$ | 2.22                | 1.57                | 5.00                 | 1.50                     | 1.60                     | 1.28          |
| $\text{Cd}^{2+}$ | 1.70                | 1.93                | 3.09                 | 1.30                     | 1.60                     | 1.48          |
| $\text{Pb}^{2+}$ | 2.78                | 2.68                | 6.40                 | 2.00                     | 2.20                     | 0.93          |
| $\text{Al}^{3+}$ | 3.30                | 2.57                | 9.00                 | 2.60                     | 2.50                     | 0.46          |

$\log K$  for AA, LA and OH are from NIST Database (Martell and Smith, 1998) for 25 °C and zero ionic strength conditions.

## 2.2. Estimating constant values for the REE

As pointed out in the introduction, we used the LFER method to estimate the specific binding constants necessary to run Model VI and SHM. The LFER method is based on Tipping’s observation (Tipping, 1994, 1998) that a LFER exists between  $\log K_{MA}$  and  $\log K$  for metal–lactic acid (LA) and metal–acetic acid (AA) complexation. Moreover, since this author (op. cit.) also notes a relation between  $\log K_{MA}$  and the first hydrolysis (OH) constants for metal (denoted here as  $\log K(\text{AA})$ ,  $\log K(\text{LA})$  and  $\log K(\text{OH})$ ), the LFER can be used to estimate  $\log K_{MA}(\text{REE})$  from published values of  $\log K(\text{REE-AA})$ ,  $\log K(\text{REE-LA})$  and  $\log K(\text{REE-OH})$ . The same approach can be used to estimate  $\log K_{Mb}(\text{REE})$ , the only difference being the assumption that the metal complexing capacity of one ligand with two functional groups (as expressed by  $K_{Mb}$ ) is similar to the metal complexing capacity of two ligands carrying only one functional group each (as expressed by  $K_2$ ).

Tables 1 and 2 list  $\log K_{MA}$  and  $\log K_{Mb}$  values describing the complexation of numerous metals with HA and FA (data from Tipping, 1998; Gustafsson, 2001b), along with published  $\log K(\text{AA})$ ,  $\log K(\text{LA})$ ,  $\log K(\text{OH})$ ,  $\log K_2(\text{AA})$ ,

Table 2

$\log K_2$  for metal complexation with lactic acid (LA), acetic acid (AA) and hydrolysis (OH), as well as  $\log K_{Mb}$  for HA and FA (from Gustafsson and van Schaik, 2003), used to obtain equations for LFER between  $\log K_{Mb}$  and  $\log K_2$  for each ligand

| Metals           | $\log K_2(\text{LA})$ | $\log K_2(\text{AA})$ | $\log K_2(\text{OH})$ | $\log K_{Mb}$ |
|------------------|-----------------------|-----------------------|-----------------------|---------------|
| $\text{Ca}^{2+}$ | 2.45                  | —                     | —                     | -11.30        |
| $\text{Mn}^{2+}$ | 2.10                  | —                     | 5.8                   | —             |
| $\text{Cu}^{2+}$ | 4.84                  | 3.63                  | 11.8                  | -5.80         |
| $\text{Zn}^{2+}$ | 3.75                  | 1.36                  | 10.2                  | -9.00         |
| $\text{Cd}^{2+}$ | 2.74                  | 2.86                  | 7.7                   | -9.30         |
| $\text{Pb}^{2+}$ | 3.61                  | 4.08                  | 10.9                  | -6.15         |
| $\text{Al}^{3+}$ | 5.97                  | 4.55                  | 17.9                  | -4.20         |
| $\text{Co}^{2+}$ | 3.07                  | 1.10                  | 9.2                   | -10.10        |

$\log K$  values for LA, AA and OH are taken from NIST Database (Martell and Smith, 1998) at 25 °C and zero ionic strength conditions.

$\log K_2(\text{LA})$  and  $\log K_2(\text{OH})$  for the same metals (values from NIST Database; Martell and Smith, 1998). Studentized residuals (i.e., the residual divided by its standard deviation; Ramsey, 1969) were used to detect and remove outlier cations (i.e., Cd and Th). The values of  $\log K_{\text{MA}}$

and  $\log K_{\text{Mb}}$  show good linear correlations with their hydrolysis constants, as well as the constants for LA and AA complexation (Figs. 1 and 2). The linear regression curves and correlation coefficients describing these relationships are as follows:

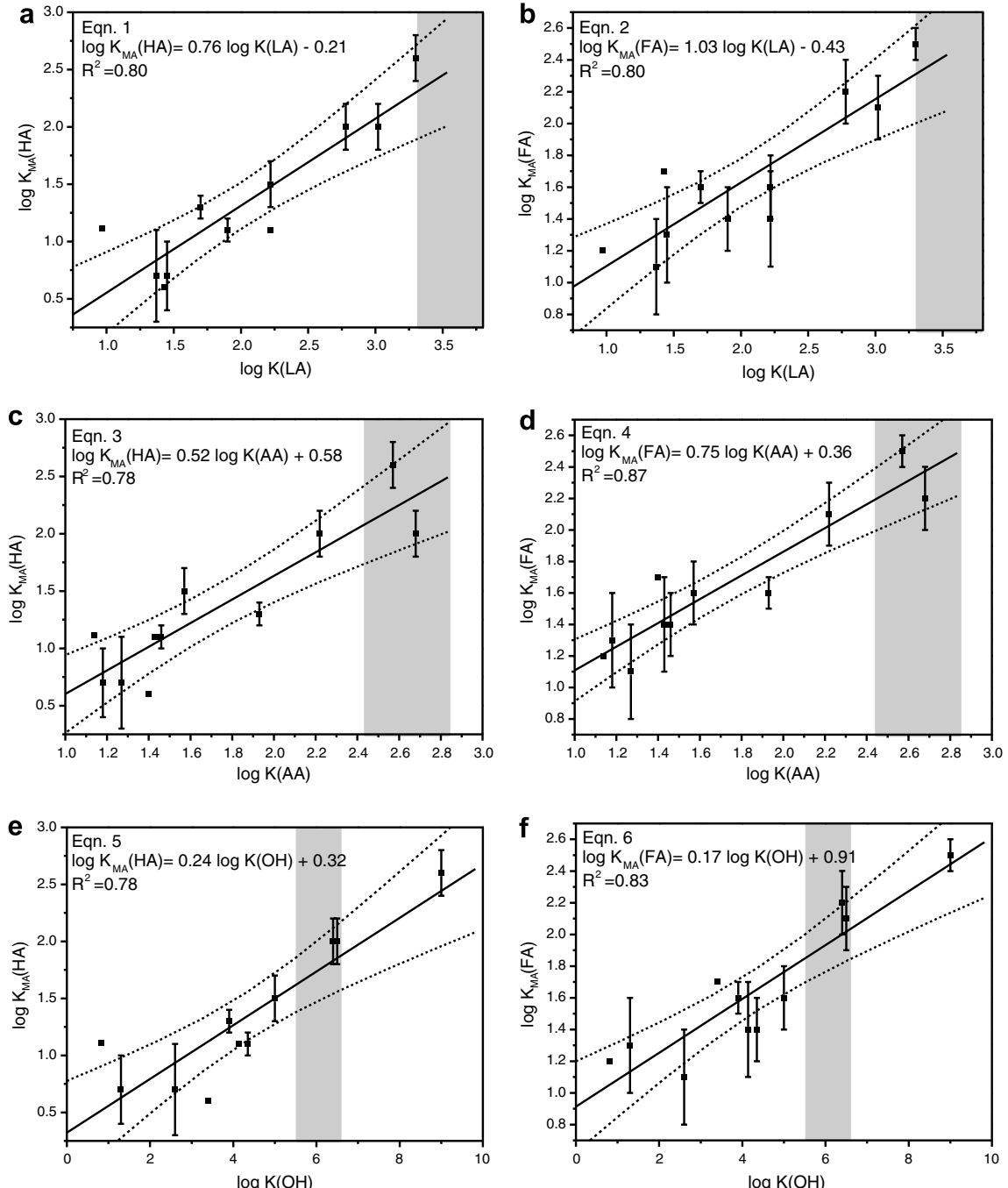


Fig. 1. Linear free-energy relationships between  $\log K_{\text{MA}}$  and (a, b, for HA and FA, respectively)  $\log K(\text{LA})$ , (c, d, for HA and FA, respectively)  $\log K(\text{AA})$  and (e, f, for HA and FA, respectively)  $\log K(\text{OH})$  listed in Table 2.  $\log K(\text{LA})$ ,  $\log K(\text{AA})$  and  $\log K(\text{OH})$  are from the NIST Database (Martell and Smith, 1998), whereas  $\log K_{\text{MA}}$  values are from Tipping (1998). Standard deviations are indicated where available. Dashed lines indicate 95% confidence intervals of linear fits. Shaded areas mark fields of available  $\log K(\text{LA})$ ,  $\log K(\text{AA})$  and  $\log K(\text{OH})$  data for REE.

$$\log K_{\text{MA}}(\text{HA}) = 0.76 \log K(\text{LA}) - 0.21, \quad R^2 = 0.80 \quad (1)$$

$$\log K_{\text{MA}}(\text{FA}) = 0.52 \log K(\text{LA}) + 0.58, \quad R^2 = 0.78 \quad (2)$$

$$\log K_{\text{MA}}(\text{HA}) = 1.03 \log K(\text{AA}) - 0.43, \quad R^2 = 0.80 \quad (3)$$

$$\log K_{\text{MA}}(\text{FA}) = 0.75 \log K(\text{AA}) + 0.36, \quad R^2 = 0.87 \quad (4)$$

$$\log K_{\text{MA}}(\text{HA}) = 0.24 \log K(\text{OH}) + 0.32, \quad R^2 = 0.78 \quad (5)$$

$$\log K_{\text{MA}}(\text{FA}) = 0.17 \log K(\text{OH}) + 0.91, \quad R^2 = 0.83 \quad (6)$$

$$\log K_{\text{Mb}} = 1.89 \log K_2(\text{LA}) - 15.13, \quad R^2 = 0.81 \quad (7)$$

$$\log K_{\text{Mb}} = 1.49 \log K_2(\text{AA}) - 11.80, \quad R^2 = 0.82 \quad (8)$$

$$\log K_{\text{Mb}} = 0.57 \log K_2(\text{OH}) - 13.86, \quad R^2 = 0.73 \quad (9)$$

These equations were subsequently employed to estimate  $\log K_{\text{MA}}$  (Table 3) and  $\log K_{\text{Mb}}$  (Table 4), using the  $\log K(\text{AA})$ ,  $\log K(\text{LA})$ ,  $\log K(\text{OH})$ ,  $\log K_2(\text{AA})$ ,  $\log K_2(\text{LA})$  and  $\log K_2(\text{OH})$  values listed for REE in the NIST Database (Martell and Smith, 1998; except  $\log K(\text{OH})$  listed in Klungness and Byrne, 2000; Figs. 1 and 2). However, as shown by Tables 3 and 4, the estimated values of  $\log K_{\text{MA}}$  and  $\log K_{\text{Mb}}$  vary depending on the equation used. To establish which sets of estimated values are more appropriate, we used the method of Tang and Johannesson (2003) to compare them with  $\log K_{\text{MA}}$  and  $\log K_{\text{Mb}}$ , which were determined by fitting Model VI and SHM to the available experimental data (Tipping, 1998; Gustafsson, 2001b). For purposes of comparison, we only considered “best-fit” values of  $\log K_{\text{MA}}$  and  $\log K_{\text{Mb}}$  (rms errors  $<0.1$ ), which limits the comparison solely to Eu and Dy (Tipping, 1998; Lead et al., 1998; Gustafsson, 2001b). It is clear that the  $\log K_{\text{MA}}$  values are too low when estimated from the LFER based on first hydrolysis constants (e.g.,  $\log K_{\text{MA}} = 1.79$  for Eu-HA complexation using Eq. (5), as against 2.10 using model fits). The same is true for Dy complexation by HA and FA (e.g.,  $\log K_{\text{MA}} = 1.83$  for Dy-HA complexation as obtained from Eq. (5), as against 2.9 using model fits). However, this does apply to the  $\log K_{\text{MA}}$  values estimated from Eqs. (1)–(4), where estimated values for Eu and Dy are close to the fitted experimental data (e.g., 2.47 and 2.44 for Eu-FA complexation using Eqs. (2) and (4), respectively, as against 2.36 from model fits). The  $\log K_{\text{MA}}$  estimates derived from the first hydrolysis constant LFER appear much too low. Whatever the reason, the observed discrepancy between estimates derived from Eqs. (5) and (6) and fits of experimental data leads us to eliminate these two equations from our procedure for estimating constants.

However,  $\log K_{\text{MA}}$  values estimated from Eqs. (1)–(4) are quite different for the HREE (on average, standard deviation are as high as 0.41). Recently published experimental results for REE complexation with FA and HA (Yamamoto et al., 2005, 2006) suggest that the  $\log K$  values for REE complexation with HM should vary across the REE series in an analogous way to the  $\log K$  values for AA. Moreover, Wood (1993) pointed out that AA likely represents a model system for simple carboxylic sites on more complex organic matter, such as HM. Carboxylic groups could thus be the major sites by which REE are bound to HM (Yamamoto et al., 2005, 2006).

$\log K_{\text{Mb}}$  values estimated using Eqs. (7)–(9) strongly differ from one another: by approximately two orders of magnitude for the LREE and by four orders of magnitude

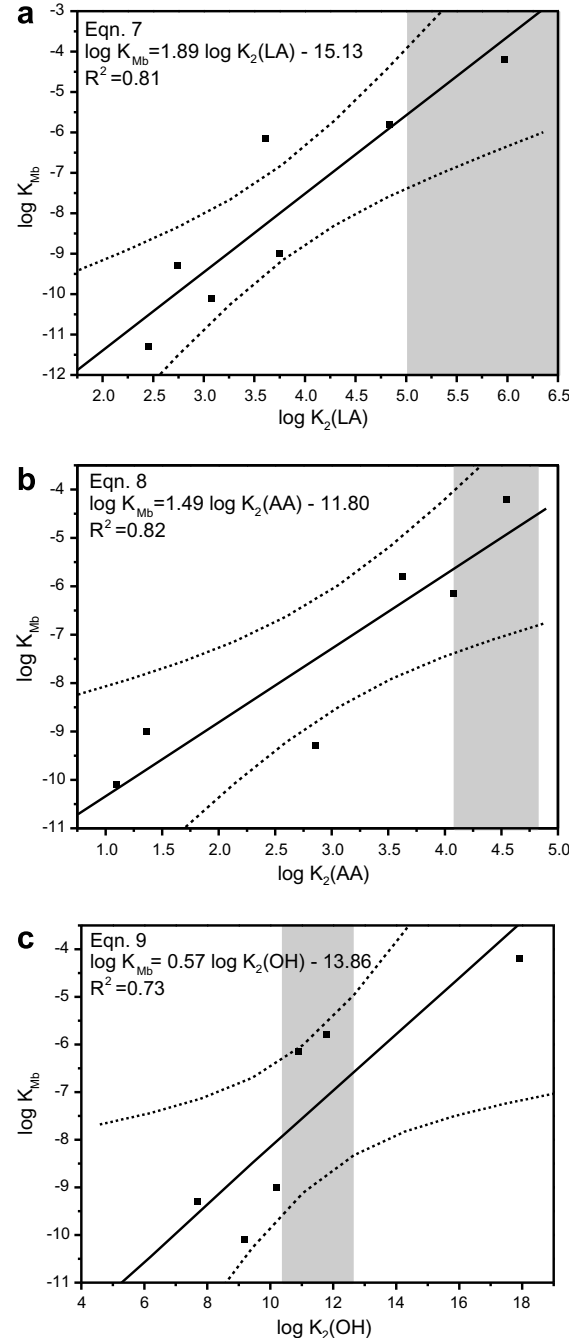


Fig. 2. Linear free-energy relationships between  $\log K_{\text{Mb}}$  and (a)  $\log K_2(\text{LA})$ , (b)  $\log K_2(\text{AA})$  and (c)  $\log K_2(\text{OH})$  listed in Table 5. The AA, LA and OH constants values are from the NIST Database (Martell and Smith, 1998), and the values of  $\log K_{\text{Mb}}$  are from the “shmgeneric” Database (Gustafsson, 2001b). Dashed lines indicate 95% confidence intervals of linear fits. Shaded areas mark fields of available  $\log K_2(\text{LA})$ ,  $\log K_2(\text{AA})$  and  $\log K_2(\text{OH})$  data for REE.

for the HREE (Table 4). As with the  $\log K_{\text{MA}}$  values,  $\log K_{\text{Mb}}$  can be estimated by comparing the values obtained for Eu with the  $\log K_{\text{Mb}}$  values determined by fitting SHM to Eu experimental results (Gustafsson, 2001b). By using the second hydrolysis constants, we obtain a  $\log K_{\text{Mb}}$  value

Table 3  
Summary of estimated  $\log K_{\text{MA}}$  for the REE

| REE | $\log K_{\text{MA}}(\text{HA})$ | From LA Eq. (1) | From AA Eq. (3) | From OH Eq. (5) | Adopted estimated values | $\log K_{\text{MA}}(\text{FA})$ |
|-----|---------------------------------|-----------------|-----------------|-----------------|--------------------------|---------------------------------|
| La  | 2.30                            | 2.20            | 1.54            | 2.20            | 2.20                     | 2.30                            |
| Ce  | 2.45                            | 2.25            | 1.66            | 2.25            | 2.40                     | 2.31                            |
| Pr  | 2.46                            | 2.30            | 1.66            | 2.30            | 2.40                     | 2.35                            |
| Nd  | 2.47                            | 2.32            | 1.69            | 2.32            | 2.41                     | 2.37                            |
| Sm  | 2.53                            | 2.50            | 1.77            | 2.50            | 2.45                     | 2.49                            |
| Eu  | 2.56                            | 2.42            | 1.79            | 2.42            | 2.47                     | 2.44                            |
| Gd  | 2.54                            | 2.31            | 1.78            | 2.31            | 2.46                     | 2.36                            |
| Tb  | 2.56                            | 2.20            | 1.82            | 2.20            | 2.47                     | 2.27                            |
| Dy  | 2.55                            | 2.13            | 1.83            | 2.13            | 2.47                     | 2.23                            |
| Ho  | 2.59                            | 2.09            | 1.84            | 2.09            | 2.49                     | 2.20                            |
| Er  | 2.60                            | 2.07            | 1.85            | 2.07            | 2.50                     | 2.18                            |
| Tm  | 2.62                            | 2.11            | 1.88            | 2.11            | 2.51                     | 2.21                            |
| Yb  | 2.64                            | 2.21            | 1.91            | 2.21            | 2.53                     | 2.28                            |
| Lu  | 2.72                            | 2.13            | 1.91            | 2.13            | 2.58                     | 2.23                            |

Table 4  
Summary of estimated  $\log K_{\text{Mb}}$  for the REE

| REE | $\log K_{\text{Mb}}$ | From LA Eq. (7) | From AA Eq. (8) | From OH Eq. (9) | Adopted estimated values |
|-----|----------------------|-----------------|-----------------|-----------------|--------------------------|
| La  | -5.74                | -5.66           | -7.82           | -5.66           | -5.66                    |
| Ce  | -5.02                | -5.60           | -7.65           | -5.60           | -5.60                    |
| Pr  | -4.68                | -5.13           | -7.59           | -5.13           | -5.13                    |
| Nd  | -4.55                | -5.04           | -7.53           | -5.04           | -5.04                    |
| Sm  | -4.32                | -4.65           | -7.36           | -4.65           | -4.65                    |
| Eu  | -4.15                | -4.79           | -7.36           | -4.79           | -4.79                    |
| Gd  | -4.41                | -5.04           | -7.25           | -5.04           | -5.04                    |
| Tb  | -4.11                | -5.40           | -7.19           | -5.40           | -5.40                    |
| Dy  | -3.83                | -5.50           | -7.13           | -5.50           | -5.50                    |
| Ho  | -3.70                | -5.57           | -7.08           | -5.57           | -5.57                    |
| Er  | -3.32                | -5.65           | -6.96           | -5.65           | -5.65                    |
| Tm  | -3.15                | -5.71           | -6.96           | -5.71           | -5.71                    |
| Yb  | -2.94                | -5.30           | -6.91           | -5.30           | -5.30                    |
| Lu  | -2.83                | -5.50           | -6.85           | -5.50           | -5.50                    |

of -7.36 for Eu that is dramatically low compared to -4.7 from the model fit (see Gustafsson, 2001b). By contrast, the  $\log K_{\text{Mb}}$  values estimated for Eu using Eqs. (7) and (8) (-4.15 and -4.79 from Eqs. (7) and (8), respectively) are closer to the fitted experimental data for this REE than the value of -4.65 derived from the model fit (Gustafsson, 2001b). However, as with the  $\log K_{\text{MA}}$  values, we note that the  $\log K_{\text{Mb}}$  values estimated using Eqs. (7) and (8) agree better with one another for the LREE and MREE than for the HREE (the standard deviation varies up to 1.89 for the latter). Bearing in mind that metal complexation with AA is probably a better analogy for REE complexation with HM than metal complexation with LA (see discussion above), in the following, we adopt the  $\log K_{\text{Mb}}$  values estimated from Eq. (8). To conclude, we should point out that, due to the smaller amount of experimental data, the AA LFER used to estimate  $\log K_{\text{Mb}}$  values is less well constrained than the AA LFER used to estimate  $\log K_{\text{MA}}$ . Thus, we can expect that modelling results derived from SHM are likely to be accompanied by larger uncertainties than Model VI predictions.

### 3. COMPARING THE PREDICTIVE ABILITY OF SHM AND MODELS V AND VI

SPECIATION calculations were performed using the computer programs WHAM 6 (Version 6.0.13) for Model VI, and Visual MINTEQ (Version 2.40) for SHM. Each model was modified by building a database that included our adopted  $\log K_{\text{MA}}$  and  $\log K_{\text{Mb}}$  values for REE complexation with HM, along with well-accepted infinite-dilution (25 °C) stability constants for REE inorganic complexes (hydroxide, sulphate and carbonate; Klungness and Byrne, 2000; Luo and Byrne, 2004; Schijf and Byrne, 2004). Up-to-date, default values of  $\log K_{\text{MA}}$ ,  $\log K_{\text{Mm}}$  and  $\log K_{\text{Mb}}$  were used for competing cations (Tipping, 1998; Gustafsson, 2001b). As oxyhydroxide precipitation reactions cannot be modelled by Model VI, they were not considered in SHM modelling. In our simulations, we do not take into account the binding of the first hydrolysis product to HM. This choice

is supported by the fact that (i) all the tested waters have  $\text{pH} < 7$ ; yet, it is well established that the proportion of  $\text{Ln}-\text{OH}$  complexes and thus  $\text{Ln}-\text{OH}-\text{HM}$  complexes may become important only for water having  $\text{pH} > 8$  (Maes et al., 1988); (ii) even for alkaline waters, recent model calculations show that REE speciation can be reasonably well captured by only considering  $\text{Ln}^{3+}$  complexation with HM (Pourret et al., 2007a).

In the speciation calculations presented here for World Average River Water, and Mengong and Mar2 samples, we follow the same assumptions as Tang and Johannesson (2003), i.e., (i) the DOM/DOC ratio of all samples is taken to be equal to 2; (ii) 50% of the DOM is considered to consist of HM able to complex the REE, the remaining 50% comprising simple organic acids that cannot form REE complexes. Thus, the active-DOM/DOC ratio (referred to here as the “active DOM parameter”) is taken as equal to unity for these samples.

### 3.1. World Average River Water

We applied the same DOC ( $5 \text{ mg L}^{-1}$ ), major ion, Fe and Al concentrations as those used by Tang and Johannesson (2003) in their earlier modelling of REE speciation in World Average River Water (see Table 11 in Tang and Johannesson, 2003). We also followed their assumption that 80% of the HM in this sample is present as FA and 20% as HA. Thus, the DOM content of World Average River Water is  $10 \text{ mg L}^{-1}$ , of which only  $5 \text{ mg L}^{-1}$  consist of HM able to complex with the REE, with  $4 \text{ mg L}^{-1}$  (80%) present as FA, and  $1 \text{ mg L}^{-1}$  (20%) as HA. Finally, because pH has a crucial influence on REE speciation, we also investigated the REE speciation of World Average River Water as a function of varying pH, while keeping the major solute composition constant (except carbonate alkalinity varying as a function of pH). Except for the slight modification of complexation constants, our model running procedure is thus entirely comparable to that used by Tang and Johannesson (2003).

The new modelling results are shown for La, Eu and Lu in Fig. 3 (Model VI) and 4 (SHM), respectively. Model VI calculations predict that REE occur as free species ( $\text{Ln}^{3+}$ ) and sulphate complexes ( $\text{LnSO}_4^{+}$ ) at acidic pH, and mainly as carbonate complexes ( $\text{LnCO}_3^{+}$  and  $\text{Ln}(\text{CO}_3)^{2-}$ ) at alkaline pH (Fig. 3). Based on these results, we also predict that, at circumneutral-pH conditions, the REE predominantly (i.e., >50%) occur in solution complexed with HM. More precisely, Model VI predicts that >50% of the LREE (e.g., La) occur in solution as organic complexes in the pH range between 5.2 and 9.5. For the MREE (e.g., Eu), the prediction is that >50% of the MREE occur as HM complexes in the pH range between 4.3 and 9.5. Finally, Model VI predicts that >50% of the HREE (e.g., Lu) occur as HM complexes in the pH range between 5.4 and 7. Another important result of the model is that the pH value at which the proportion of  $\text{LnHM}$  complexes reaches a maximum decreases across the REE series, from La (pH 7) to Lu (pH 6). Also, model results indicate that the proportion of REE forming HM complexes is higher for the LREE and MREE (up to 95% at pH 7) than for the HREE

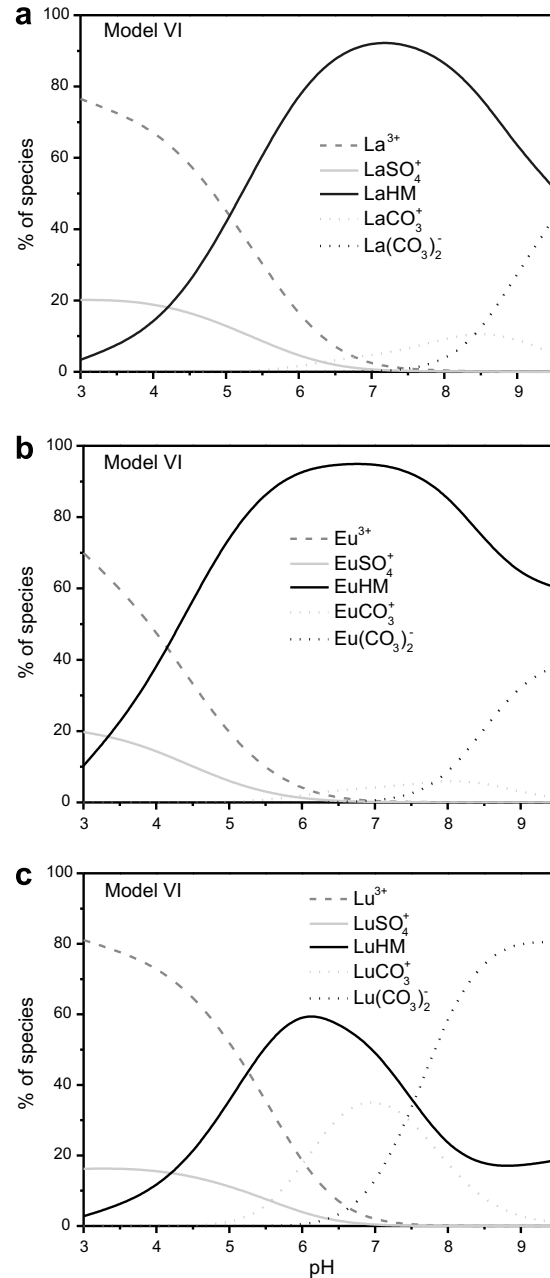


Fig. 3. Model VI speciation calculations for (a) La, (b) Eu and (c) Lu in World Average River Water as a function of pH. The proportion of active DOM complexing the REE is assumed to be 50% (i.e., active DOM content = DOC content).

(maximum of 60% at pH 6). All these features are consistent with Model V predictions reported previously by Tang and Johannesson (2003). The only noticeable difference is that Model VI calculates significantly higher proportions of REE complexed with organic matter under high pH conditions: for example, Model VI predicts  $\text{LaHM} \sim 60\%$  at pH 9, whereas Model V predicts only 10% of  $\text{LaHM}$  complexes at this pH value.

As with Models V and VI, SHM predicts that the LREE and MREE occur predominantly (i.e., >50%) in solution as HM complexes at circumneutral pH conditions. By

contrast, the prediction is lower for the HREE: maximum organic complexation  $\sim 40\%$ , against  $\sim 50\%$  with Model VI. As with Models V and VI, the pH value at which maximum REE complexation is predicted to occur also regularly decreases across the REE series, from 7.8 for La to 6.6 for Lu. However, we note three important differences with the Models V and VI results: (i) the pH at which there is a maximum proportion of REE organic complexes is about 0.75 pH unit higher with SHM (Fig. 4) than with Model VI (Fig. 3); (ii) the range of pH values over which

LnHM complexes are the predominant REE species is wider with Model VI than with SHM (e.g., LaHM  $>50\%$  for a range of 4.3 pH units with Model VI, as against only 3 pH units with SHM; see Figs. 3 and 4); finally, (iii) the proportion of LnHM species calculated at alkaline pH is higher with Models VI (e.g., for La,  $\sim 50\%$  at pH 9.5; see Fig. 3) than with SHM (e.g., for La,  $\sim 40\%$  at pH 9.5; see Fig. 4).

To sum up, predictions from Model VI and SHM confirm the two main conclusions proposed earlier by Tang and Johannesson (2003) from speciation modelling of World Average River Water, namely that (i) organic colloids are the principal REE carriers in the dissolved fraction (i.e.,  $<0.2 \mu\text{m}$ ); and (ii) dissolved organic ligand complexes of the REE are at least as important as carbonate complexes. The results of Model VI and SHM are clearly consistent for circumneutral-pH river waters, at least in broad outline. However, on the basis of the modelled data alone, it is difficult to determine whether Models V and VI or SHM gives the most accurate description of REE speciation in river waters. Only experimental studies involving direct measurement of the REE speciation in circumneutral-pH rivers will be able to decide which model is in better agreement with reality; for example, whether the proportion of LuHM complexes in these rivers is  $\geq 50\%$  as predicted by Models V and VI, or only  $\sim 40\%$  as predicted by SHM.

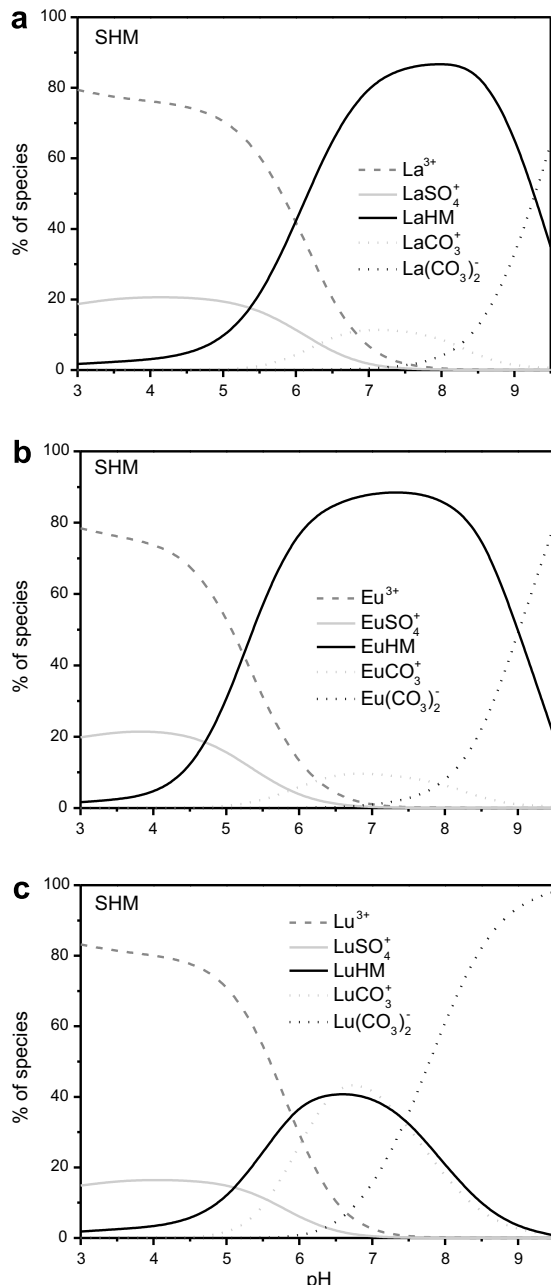


Fig. 4. SHM speciation calculations for (a) La, (b) Eu and (c) Lu in World Average River Water as a function of pH. The proportion of active DOM complexing the REE is assumed to be 50% (i.e., active DOM content = DOC content).

### 3.2. Mengong and Mar2 samples

Mengong and Mar2 are two samples of organic-rich (DOC = 23.8 and 18.1 mg L<sup>-1</sup>) acidic waters whose REE speciation was first investigated by ultrafiltration (Viers et al., 1997), and then modelled using Model V (Tang and Johannesson, 2003). Because the DOC of these waters is chiefly made up of the largest MW size fractions (Viers et al., 1997), Tang and Johannesson (2003) assumed that 85% of the DOC in these samples is composed of high MW HA, the remaining 15% containing low MW FA. The same assumption is used here. The values adopted for pH (Mengong = 4.6 and Mar2 = 5.5), as well as the major solute, DOC, Fe and Al concentrations, are those reported by Viers et al. (1997), being identical to the values used by Tang and Johannesson (2003). Table 5 lists the predicted proportions of LnHM complexes in these two water samples based on Model VI and SHM, as well as a comparison with the previous results obtained using Model V (Tang and Johannesson, 2003). Model VI predicts that between 46–90% (Mengong) and >98% (Mar2) of the REE occurring in the dissolved fraction (i.e.,  $<0.2 \mu\text{m}$ ) of these samples occurs as organic complexes, the remainder of each REE occurring as free species (Ln<sup>3+</sup>). Table 5 shows a good agreement between the Model VI and Model V predictions, the only noticeable difference being the slightly lower proportion of HREE organic complexes obtained with Model VI for the more acidic Mengong sample (Table 5; see also Table 8 in Tang and Johannesson, 2003). This difference is likely explained by our choice to use the log K<sub>MA</sub> values derived from the AA LFER rather than the log K<sub>MA</sub> values, which are averages of the estimates obtained using both the AA and LA LFER as described

Table 5

Proportions of LnHM complexes calculated with Model V (Tang and Johannesson, 2003), Model VI and SHM for Mengong and Mar2 water samples

|    | Mengong                   |                   |                    |               | Mar2                      |                   |                    |               |
|----|---------------------------|-------------------|--------------------|---------------|---------------------------|-------------------|--------------------|---------------|
|    | Ultrafiltration<br>% LnHM | Model V<br>% LnHM | Model VI<br>% LnHM | SHM<br>% LnHM | Ultrafiltration<br>% LnHM | Model V<br>% LnHM | Model VI<br>% LnHM | SHM<br>% LnHM |
| La | 86                        | 63                | 60                 | 39            | 94                        | 87                | 99                 | 95            |
| Ce | 86                        | 72                | 65                 | 40            | 94                        | 91                | 99                 | 95            |
| Pr | 87                        | 76                | 71                 | 55            | 96                        | 92                | 100                | 97            |
| Nd | 86                        | 77                | 74                 | 59            | 95                        | 93                | 100                | 98            |
| Sm | 100                       | 86                | 90                 | 71            | 100                       | 96                | 100                | 99            |
| Gd | 100                       | 80                | 73                 | 52            | 100                       | 94                | 100                | 98            |
| Tb | 100                       | 77                | 60                 | 46            | 100                       | 93                | 99                 | 95            |
| Dy | 100                       | 75                | 52                 | 43            | 100                       | 92                | 99                 | 94            |
| Ho | 100                       | 75                | 48                 | 41            | 100                       | 92                | 98                 | 93            |
| Er | 69                        | 75                | 46                 | 39            | 100                       | 93                | 98                 | 91            |
| Tm | 100                       | 77                | 50                 | 38            | 100                       | 93                | 98                 | 90            |
| Yb | 100                       | 78                | 61                 | 41            | 100                       | 93                | 99                 | 96            |
| Lu | 100                       | 81                | 52                 | 34            | 100                       | 95                | 99                 | 94            |

Fraction of LnHM complexes previously estimated for these two samples by ultrafiltration experiments are shown for comparison (Viers et al., 1997). The proportion of DOM active in complexing the REE is assumed to be 50% (i.e., active DOM content = DOC content).

in Tang and Johannesson (2003). As shown above in the case of the World Average River Water sample, this choice shifts the LnHM stability field slightly towards higher pH values (compare our Fig. 3 and Fig. 4 in Tang and Johannesson, 2003), thereby decreasing the proportion of REE complexed with organic matter in acidic waters as predicted by the Humic Ion-Binding Model.

SHM results are consistent with the predictions of Models V and VI for Mar2, while also indicating a predominance of LnHM complexes in this sample. The predicted complexation proportions based on SHM are equivalent to those predicted by Models V and VI (i.e., between 90% and 99% for SHM, compared with 98% and 100% for Model VI and 87% and 96% for Model V depending on the REE; see Table 5). By contrast, the results for Mengong are different. Indeed, SHM predicts that HM complexes should account for only 34–71% of each REE in solution, whereas Models VI and V predict higher complexation proportions, namely: between 46% and 90% (Table 5). For both the Mar2 and Mengong samples, the three tested models all indicate that the remainder of each REE occurs as free species ( $\text{Ln}^{3+}$ ). By comparing the model predictions to the ultrafiltration results (Table 5), we can see that Model VI and SHM yield comparable agreement with ultrafiltration data for Mar2 sample (less than 10% difference). However, for the more acidic Mengong water sample, the difference between model predictions and ultrafiltration results is higher when using SHM compared with Models V and VI, i.e., between 27% and 62%, as against between 10% and 52% (Table 5).

In summary, we confirm the suggestion made earlier by Tang and Johannesson (2003) that the Humic Ion-Binding Model is reasonably good representation of REE speciation in acidic DOC-rich waters. The differences between our predictions and those reported in Tang and Johannesson (2003) further demonstrate the sensitivity of models to the values of the stability constants that are introduced. As

regards SHM, the results presented above might suggest that this model is less accurate in predicting the speciation of the REE in low-pH, organic-rich natural waters. In the present study, however, we show that the ability of SHM to predict REE speciation in this type of water depends strongly on the value of the “active DOM parameter” that is introduced into the model. By changing this value to more appropriate values than those used by Tang and Johannesson (2003), we can drastically improve the agreement between SHM and Model VI predictions, and ultrafiltration data (see Section 4).

### 3.3. Kervidy-Naizin and Petit-Hermitage groundwater samples

#### 3.3.1. Ultrafiltration data

To further test the ability of SHM and Model VI to predict REE complexation with organic matter, we performed new ultrafiltration experiments on four circumneutral (pH 6.2–7.1), organic-rich ( $\text{DOC} = 7\text{--}20 \text{ mg L}^{-1}$ ) groundwater samples (PF1, PF3, F7 and F14). The samples were collected from two wetlands located in the Kervidy-Naizin and Petit-Hermitage catchments, in western France. These groundwaters have already been intensively studied for their DOC and REE chemistry (Dia et al., 2000; Olivie-Lauquet et al., 2001; Gruau et al., 2004). Appendix A gives details on the ultrafiltration procedure and chemical analysis of these samples.

Table EA3-Electronic Annex presents the concentrations of major anions and cations, as well as major and trace cations (including REE) and DOC in the  $0.2 \mu\text{m}$  filtrates, along with alkalinity and pH data. Concentrations of REE, Fe, Mn and DOC in the three ultrafiltered fractions (i.e.,  $<30 \text{ kDa}$  (Da = Dalton),  $<10 \text{ kDa}$  and  $<5 \text{ kDa}$ ) are presented in Table EA4-Electronic Annex (mean of two analyses). In Fig. 5, these results are plotted on  $\Sigma\text{REE}$  (Fe) vs. DOC variation diagrams.

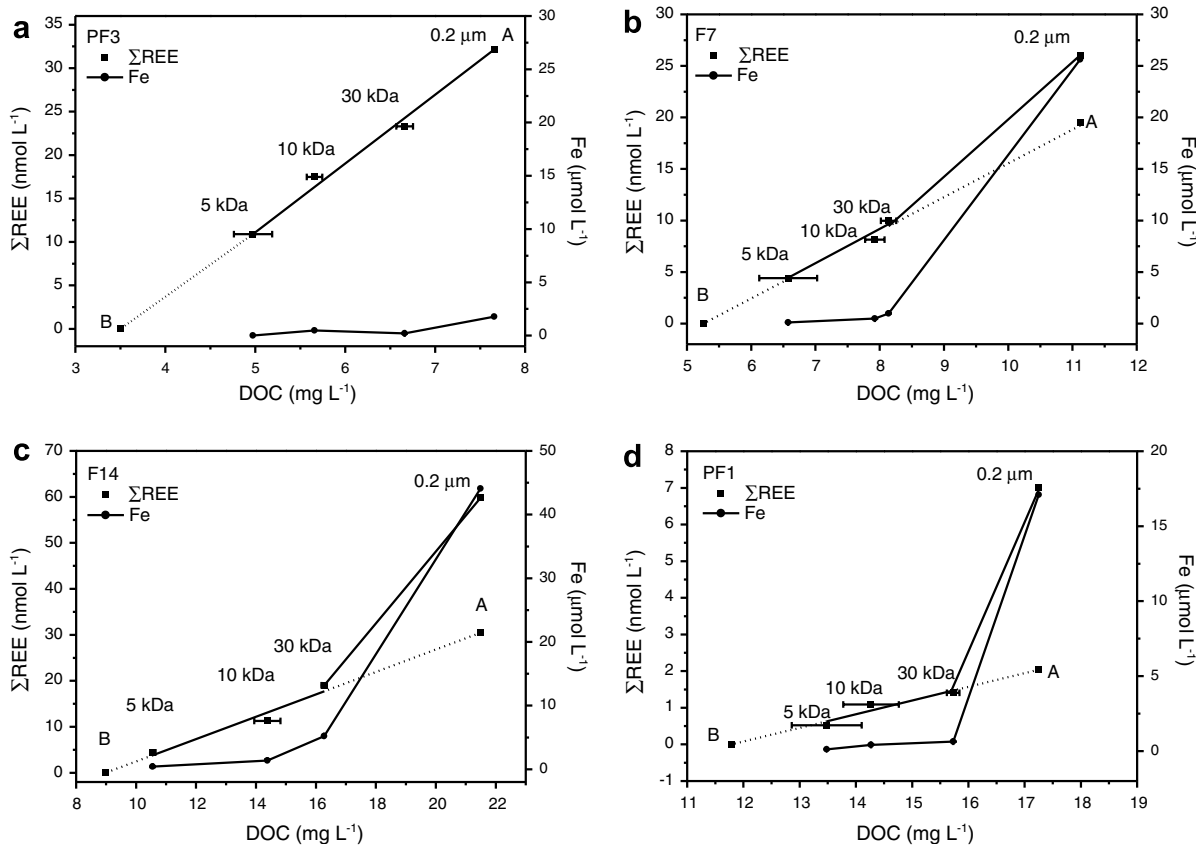


Fig. 5.  $\Sigma\text{REE}$  and Fe concentrations as a function of DOC concentrations in the successive filtrates ( $<0.2\ \mu\text{m}$ ,  $<30$ ,  $<10$  and  $<5\ \text{kDa}$ ) for (a) PF3, (b) F7, (c) F14 and (d) PF1 water samples. Error bars correspond to standard deviations for two replicates, with some error bars being smaller than the symbol size. Point A represents the extrapolated amount of REE thought to be bound to humic matter, whereas point B gives the DOC content extrapolated to a REE content equal to 0 (see text for further explanation).

Interpreting ultrafiltration data is not a trivial task and care must be taken to validate the speciation models before using this type of information. An inherent feature of ultrafiltration studies is the presence of mineral colloids (e.g., Fe and Mn oxyhydroxides) in the waters along with organic colloids. Some of these mineral colloids can be potentially strong competitors with organic matter for REE complexation (e.g., Fe oxyhydroxides; Bau, 1999; Dupré et al., 1999), and their presence may lead to an overestimation of the proportion of REE that are effectively complexed by HM. Thus, it is crucial to assess carefully whether the REE decrease associated with ultrafiltration of PF1, PF3, F7 and F14 waters (see Fig. 5) is accompanied solely by a decrease of the DOC content, or whether it is also correlated with a decrease in Fe concentration. It is clear that three of the four investigated water samples (i.e., PF1, F7 and F14) display a significant decrease in Fe content upon ultrafiltration (Fig. 5). However, the decrease in Fe content concerns only the 30 kDa ultrafiltration step. After this step, the Fe content is equally very low in all four samples, resulting in a marked change in the slope of the linear relationships otherwise shown on the REE vs. DOC variation diagrams (Fig. 5). This behaviour is particularly well illustrated by sample PF1, where ca. 80% of the REE and 96% of the Fe, but only 9% of the DOC, are removed during the first

ultrafiltration step. Moreover, the magnitude of the change in the slope of the REE–DOC linear relationship appears to be correlated with the  $\text{Fe}/\Sigma\text{REE}$  ratio of the waters. The  $\text{Fe}/\Sigma\text{REE}$  ratio of PF1 before ultrafiltration is 991, whereas the  $\text{Fe}/\Sigma\text{REE}$  ratios of F7, F14 and PF3 are 984, 737 and 55, respectively. Such relationships strongly suggest that the “colloidal” REE budget of samples PF1, F7 and F14 is partly controlled by REE-bearing Fe colloids. The Fe-colloid/organic-colloid ratio in these samples decreases in following order: PF1 > F7 > F14 ≫ PF3.

The REE colloidal pool of samples PF1, F7 and F14 was corrected for the contribution of the Fe-colloid fraction. The Fe colloid-free REE budget of these waters can be estimated by linearly extrapolating the relationship defined by the  $<5$ ,  $<10$  and  $<30\ \text{kDa}$  results to the DOC content of the  $<0.2\ \mu\text{m}$  fraction (point A in Fig. 5). The linear correlation defined by the DOC and REE contents of the four ultrafiltered fractions of PF3 (i.e., the water sample clearly depleted in Fe colloid) suggests that the organic fractions should yield a linear correlation in the  $\Sigma\text{REE}$  vs. DOC variation plots. This interpretation is supported by the fact that the  $\Sigma\text{REE}$  vs. DOC correlations defined by the three Fe colloid-bearing waters (i.e., PF1, F7 and F14) yield a slope that decreases with decreasing  $\text{Fe}/\Sigma\text{REE}$  ratio of the raw waters. This implies that the REE and

DOC contents are linearly correlated in Fe-free waters. Another problem arises during ultrafiltration studies of organic-rich waters when there is a negative  $y$ -axis intercept for the  $\Sigma$ REE vs. DOC correlation (Fig. 5). The likely interpretation for this is that (i) 100% of the REE present in the waters are bound to organic molecules and, more importantly (ii) the DOM is not composed solely of HM able to complex REE, but contains also a significant proportion of low MW organic molecules that do not complex these elements. In such waters, the key question is how to determine the amount of DOM that can complex the REE. In other words, we need to decide what value for the “active DOM parameter” should be introduced into the models. Considering the PF3 results, it is possible that this amount of active DOM could correspond to the  $y = 0$  intercept on the  $x$ -axis obtained by linearly extrapolating the  $\Sigma$ REE vs. DOC relationships (points B in Fig. 5). In so doing, we assume that all the REE are bound to HM, which is consistent with previously published ultrafiltration data (Tanikazi et al., 1992; Sholkovitz, 1995; Ingri et al., 2000). This assumption also agrees with recent observations by Johannesson et al. (2004) that all of the “dissolved” La in organic-rich waters from a swamp in south-eastern Virginia is “complexed” with organic ligands.

In the following, we assume that (i) 100% of the REE occurring in PF1, PF3, F7 and F14 waters are bound to HM; (ii) the REE remaining in the  $<5$  kDa fraction are complexed with the low molecular FA; and (iii) the amount of REE complexed with the HA fraction corresponds to the REE content of point A minus the  $<5$  kDa fraction. Table 6 reports the proportions of LnHA and LnFA complexes calculated in this way for the Kervidy-Naizin and Petit-Hermitage groundwater samples. The average proportions of LnHA are lower for PF3 and F7 (65% and 76%, respectively), but higher for PF1 and F14 (77% and 83%, respectively). Using these results, we estimated the LnFA/LnHA ratios of the four ultrafiltered samples as 0.30 for PF1, 0.54 for PF3, 0.31 for F7 and 0.21 for F14 (Table 6). The above calculations are strongly dependent on the validity of the correction/estimation procedures used to remove the contribution of Fe colloids and calculate the FA/HA ratio of the waters. The validity of this approach is tested below, by comparing the “corrected/estimated” ultrafiltration data with the modelled results. If the results of this test are positive—i.e., there is convergence between the modelling and ultrafiltration results—this confirms the ability of the models to predict LnHM speciation in the four investigated water samples, considering that the procedure for correction of the ultrafiltration data is independent of the modelling approach.

### 3.3.2. REE speciation modelling

The modelling of the Kervidy-Naizin and Petit-Hermitage samples is treated differently from the samples of World Average River Water, Mengong and Mar2, since the amount of active DOM is not taken as equivalent to a common empirical value of 50% of the total DOM content, but equal to individual values calculated following the method described above. The active DOM fractions obtained in this way are as follows: 32% for PF1, 55% for PF3, 53% for F7

and 59% for F14. Using the ultrafiltration results, we also calculated the HA and FA contents necessary to run both models. The HA contents are assumed to be equal to two times the difference between the DOC contents of the  $<0.2\text{ }\mu\text{m}$  and  $<5\text{ kDa}$  fractions. For FA, we take the value as two times the difference between the DOC content of the  $<5\text{ kDa}$  fraction and that corresponding to point B in Fig. 5. Hence, we assume that 65%, 76%, 83% and 77% and 35%, 24%, 17% and 23% of HM is made up of HA and FA, respectively, in PF3, F7, F14 and PF1. Finally, we should bear in mind that the REE content introduced into the models corresponds to point A in Fig. 5 and not the total REE content of the sample.

Table 6 presents the model results, which are compared with corrected ultrafiltration data. The “modelled” complexation proportions reported in Table 6 include the REE partitioning between the high MW HA fraction ( $>5\text{ kDa}$ ) and the low MW FA fraction ( $<5\text{ kDa}$ ). Table 6 shows a good convergence between Model VI and ultrafiltration results. LnHM proportions calculated with Model VI are all higher than 97%, indicating that this model also predicts that nearly all of the REE are complexed by HM in these samples. By contrast, the convergence is of poorer quality with SHM: LnHM proportions range from 43% to 100% depending on the samples, while the remainder of the REE occurs as carbonate, sulphate or free ion species (data not shown). The higher the pH and the smaller the Fe/ $\Sigma$ REE ratio are the better the agreement between SHM prediction and ultrafiltration data is (see PF3 sample as an example). Ultrafiltration results are independent of the modelling predictions. Therefore, the strong convergence between ultrafiltration results and Model VI predictions is considered highly significant, providing evidence that this model can accurately predict REE complexation by organic matter in natural waters.

## 4. DISCUSSION

The  $\log K_{\text{MA}}$  and  $\log K_{\text{Mb}}$  values adopted here appear to be the most reliable values derived so far using the LFER method. By confronting Model VI and SHM predictions with published results (Viers et al., 1997) and new ultrafiltration data, we can define the range of conditions under which these models will accurately predict the complexation of REE by organic matter in natural waters. To a first approximation, modelling of World Average River Water (Tang and Johannesson, 2003) suggests that Humic Ion-Binding Model and SHM could be equally valuable in modelling REE speciation in low-DOC river waters at circumneutral-pH. However, careful inspection of model results reveals that SHM predicts slightly lower organic complexation for the HREE than Models V and VI. Some disparities also occur for alkaline waters, with SHM predicting an out-competition of the organic complexes over the carbonate complexes, which is not predicted by Model VI. However, these disparities do not really cast doubt on the ability of SHM and Models V and VI to provide a reliable description of REE speciation in rivers, considering that most rivers worldwide are characterized by circumneutral-pH values (Brownlow, 1996). By confronting the model

Table 6

Comparison between the proportions of LnFA and LnHA complexes in PF1, PF3, F7 and F14 samples obtained by ultrafiltration experiments and modelling calculation using Model VI and SHM

|     | Ultrafiltration |        |        | SHM    |        |        | Model VI |        |        | Ultrafiltration |        |        | SHM    |        |        | Model VI |        |        |
|-----|-----------------|--------|--------|--------|--------|--------|----------|--------|--------|-----------------|--------|--------|--------|--------|--------|----------|--------|--------|
|     | % LnHA          | % LnFA | % LnHM | % LnHA | % LnFA | % LnHM | % LnHA   | % LnFA | % LnHM | % LnHA          | % LnFA | % LnHM | % LnHA | % LnFA | % LnHM | % LnHA   | % LnFA | % LnHM |
| PF3 |                 |        |        |        |        |        |          |        |        |                 |        |        |        |        |        |          |        |        |
| La  | 65              | 35     | 100    | 77     | 22     | 98     | 74       | 26     | 100    | 76              | 24     | 100    | 39     | 15     | 54     | 69       | 30     | 100    |
| Ce  | 69              | 31     | 100    | 76     | 22     | 99     | 74       | 26     | 100    | 79              | 21     | 100    | 40     | 16     | 56     | 71       | 29     | 100    |
| Pr  | 64              | 36     | 100    | 77     | 22     | 99     | 73       | 27     | 100    | 78              | 22     | 100    | 56     | 22     | 78     | 72       | 28     | 100    |
| Nd  | 63              | 37     | 100    | 77     | 23     | 100    | 74       | 26     | 100    | 76              | 24     | 100    | 58     | 22     | 81     | 73       | 26     | 100    |
| Sm  | 65              | 35     | 100    | 77     | 23     | 100    | 66       | 34     | 100    | 78              | 22     | 100    | 65     | 25     | 90     | 70       | 30     | 100    |
| Eu  | 67              | 33     | 100    | 77     | 23     | 100    | 71       | 29     | 100    | 87              | 13     | 100    | 63     | 24     | 87     | 73       | 27     | 100    |
| Gd  | 67              | 33     | 100    | 77     | 22     | 99     | 73       | 27     | 100    | 76              | 24     | 100    | 57     | 22     | 79     | 73       | 27     | 100    |
| Tb  | 69              | 31     | 100    | 76     | 22     | 98     | 72       | 27     | 99     | 76              | 24     | 100    | 45     | 17     | 62     | 69       | 31     | 99     |
| Dy  | 68              | 32     | 100    | 75     | 22     | 97     | 75       | 23     | 98     | 77              | 23     | 100    | 41     | 16     | 57     | 71       | 28     | 99     |
| Ho  | 66              | 34     | 100    | 75     | 22     | 97     | 74       | 23     | 98     | 76              | 24     | 100    | 38     | 15     | 53     | 70       | 28     | 98     |
| Er  | 63              | 37     | 100    | 74     | 22     | 96     | 73       | 24     | 97     | 75              | 25     | 100    | 34     | 13     | 47     | 68       | 30     | 98     |
| Tm  | 63              | 38     | 100    | 73     | 22     | 95     | 72       | 25     | 97     | 74              | 26     | 100    | 31     | 12     | 43     | 69       | 30     | 98     |
| Yb  | 61              | 39     | 100    | 70     | 21     | 90     | 71       | 27     | 98     | 71              | 29     | 100    | 45     | 17     | 62     | 69       | 30     | 99     |
| Lu  | 58              | 42     | 100    | 74     | 22     | 96     | 72       | 26     | 97     | 68              | 32     | 100    | 38     | 15     | 53     | 70       | 29     | 99     |
| F14 |                 |        |        |        |        |        |          |        |        |                 |        |        |        |        |        |          |        |        |
| La  | 83              | 17     | 100    | 72     | 7      | 79     | 61       | 38     | 100    | 73              | 27     | 100    | 67     | 13     | 79     | 80       | 20     | 100    |
| Ce  | 91              | 9      | 100    | 72     | 7      | 80     | 62       | 38     | 100    | 71              | 29     | 100    | 63     | 12     | 75     | 81       | 19     | 100    |
| Pr  | 83              | 17     | 100    | 83     | 8      | 92     | 62       | 38     | 100    | 75              | 25     | 100    | 73     | 14     | 87     | 81       | 19     | 100    |
| Nd  | 83              | 17     | 100    | 84     | 8      | 93     | 64       | 36     | 100    | 76              | 24     | 100    | 74     | 14     | 89     | 82       | 18     | 100    |
| Sm  | 83              | 17     | 100    | 88     | 9      | 97     | 57       | 43     | 100    | 75              | 25     | 100    | 78     | 20     | 98     | 78       | 22     | 100    |
| Eu  | 84              | 16     | 100    | 87     | 9      | 95     | 61       | 39     | 100    | 89              | 11     | 100    | 78     | 15     | 94     | 81       | 19     | 100    |
| Gd  | 82              | 18     | 100    | 84     | 8      | 92     | 63       | 37     | 100    | 81              | 19     | 100    | 73     | 14     | 87     | 81       | 18     | 100    |
| Tb  | 83              | 17     | 100    | 76     | 8      | 83     | 61       | 38     | 99     | 83              | 17     | 100    | 60     | 12     | 72     | 78       | 22     | 100    |
| Dy  | 83              | 17     | 100    | 72     | 7      | 79     | 64       | 35     | 99     | 75              | 25     | 100    | 53     | 10     | 64     | 80       | 20     | 99     |
| Ho  | 82              | 18     | 100    | 70     | 7      | 77     | 63       | 35     | 98     | 77              | 23     | 100    | 50     | 10     | 60     | 78       | 21     | 99     |
| Er  | 82              | 18     | 100    | 66     | 7      | 73     | 62       | 36     | 98     | 78              | 22     | 100    | 45     | 9      | 53     | 75       | 23     | 99     |
| Tm  | 81              | 19     | 100    | 62     | 6      | 68     | 62       | 37     | 98     | 82              | 18     | 100    | 39     | 8      | 47     | 75       | 24     | 99     |
| Yb  | 80              | 20     | 100    | 75     | 8      | 83     | 61       | 38     | 99     | 76              | 24     | 100    | 53     | 11     | 64     | 77       | 23     | 100    |
| Lu  | 79              | 21     | 100    | 76     | 7      | 77     | 63       | 36     | 99     | 64              | 36     | 100    | 46     | 9      | 55     | 74       | 25     | 99     |

Proportions of DOM active in complexing the REE were calculated from ultrafiltration results (see text for further explanation).

results with ultrafiltration studies, we obtain a somewhat different picture, suggesting that Model VI could be more accurate than SHM in DOC-rich acidic ground- and river waters at circumneutral-pH. This apparent poorer ability of SHM to accurately predict REE complexation with organic matter might be due to the different thermodynamic description of HM deprotonation by this model or competition effects between the REE and major dissolved cations such as Fe, Al or Ca. However, as shown below, the difference is more likely due to a higher sensitivity of SHM to the value of the “active DOM parameter”, which is required as input into metal–HM complexation models. In fact, careful evaluation of the effects of this parameter on some of the above results shows that, in most cases, SHM could be as accurate as Models V and VI for predicting REE speciation. However, we first need to evaluate the possible effects of differences in HM proton dissociation and major cation competition.

#### 4.1. Effect of HM proton dissociation

The main difference between SHM and Model VI is the electrostatic term. Model VI assumes that HM can be represented as rigid spheres of homogeneous size, carrying metal-humic binding sites on their surface with different binding strengths leading to of bidentate and tridentate binding configurations. In this model, electrostatic effects are corrected using equations based on the Debye-Hückel and Gouy-Chapman theories, assuming a homogeneous electrical double layer at the surface of each sphere (Tipping, 1998). In SHM, a discrete-site approach is employed involving eight sites of different acid strength. The bulk of the HM is considered to form gels, which are primarily treated as impermeable spheres. The electrostatic interactions on their surfaces are modelled using equations based on the Basic Stern Model (see Gustafsson (2001a) for further details).

Due to these differences in the thermodynamic description of electrostatic effects, the two models assume a different extent of proton dissociation of HM reactive sites at a given pH. As shown in Fig. 6, Model VI assumes more elec-

tronegative HA and FA surfaces at a given pH than SHM, so the density of surface sites available for REE complexation is proportionally higher in Model VI than in SHM. This may partly account for the observed differences in model predictions: (i) indeed, modelling of World Average River Water results shows there is a shift of about 0.75 pH unit between the maximum of LnHM predicted by Model VI and SHM, which is consistent with the difference in electrostatic correction (Figs. 3 and 4); (ii) the proportions of REE complexed with organic matter in Mengong (pH 4.6) sample are predicted to be slightly higher with Model VI than SHM, which is also consistent; (iii) calculations of REE speciation in three of the four organic-rich circumneutral-pH waters (i.e., PF1, F7 and F14) show differences between Model VI and SHM, with predicted values being at a maximum under acidic pH (i.e., F7 pH 6.19), which is also as expected from the difference in electrostatic correction.

#### 4.2. Effect of major competing cations (Fe, Al and Ca)

Fe, Al and Ca are known to complex strongly with HM (Dupré et al., 1999; Tipping et al., 2002), and can thus compete with REE in metal–HM complexing. As previously shown by Tang and Johannesson (2003), the presence of dissolved Fe and Al can decrease the amount of REE complexed with HM by ~10%. In the modelling calculations presented here, Fe, Al and Ca are present in solution, and the cation competitive effect is thus taken into account. The two models discussed here can be compared in terms of the relative importance of this effect by considering Table 7, which reports the proportions of Fe, Al and Ca humic complexes predicted by Model VI and SHM, as a function of pH. It can be seen that both SHM and Model VI predict roughly the same effect of Ca, which is by far the most abundant cation competing with REE in the three water samples considered here. However, the situation appears different for Fe and Al. We should note two important points: (i) the proportion of Al–HM complexes predicted to occur in circumneutral-pH waters is much

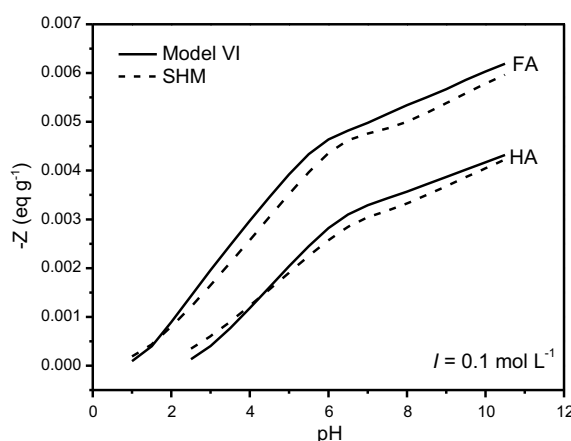


Fig. 6. Comparison of extent of proton dissociation for HA and FA calculated by Model VI and SHM as a function of pH.

Table 7  
Model VI and SHM speciation calculations for Fe, Al and Ca in World Average River Water as a function of pH

| pH  | % Fe–HM  |     | % Al–HM  |     | % Ca–HM  |     |
|-----|----------|-----|----------|-----|----------|-----|
|     | Model VI | SHM | Model VI | SHM | Model VI | SHM |
| 3   | 10       | 31  | 19       | 1   | 0        | 0   |
| 3.5 | 15       | 41  | 38       | 2   | 0        | 0   |
| 4   | 16       | 45  | 56       | 7   | 1        | 0   |
| 4.5 | 15       | 42  | 71       | 26  | 1        | 0   |
| 5   | 13       | 34  | 81       | 64  | 1        | 0   |
| 5.5 | 12       | 25  | 82       | 85  | 1        | 1   |
| 6   | 10       | 16  | 75       | 90  | 2        | 1   |
| 6.5 | 10       | 9   | 53       | 85  | 2        | 1   |
| 7   | 10       | 5   | 17       | 62  | 2        | 1   |
| 7.5 | 9        | 3   | 2        | 27  | 2        | 1   |
| 8   | 7        | 2   | 0        | 8   | 2        | 2   |
| 8.5 | 4        | 1   | 0        | 2   | 3        | 2   |
| 9   | 2        | 0   | 0        | 0   | 3        | 2   |
| 9.5 | 1        | 0   | 0        | 0   | 3        | 2   |

higher with SHM than with Model VI; (ii) SHM predicts a much higher competition of the REE with Fe for acidic waters than Model VI. To quantify the effects of the stronger Fe and Al competition imposed by SHM on REE complexation with HM, we re-investigated the four newly ultrafiltered circumneutral-pH water samples (i.e., PF1, PF3, F7 and F14) with this model, assuming no Al and Fe in solution. The results indicate that almost all of the REE are bound to HM ( $\sim 100\%$ ). On the other hand, when Fe and Al are included in the model, the LnHM species are predicted to account for 47–100% of each REE (depending on the sample; see Table 6). Consequently, SHM appears more sensitive to cation competition than Model VI. The reason for this difference is not clear, as the constants for Al, Fe and Ca used into the two models are derived from the same database (Tipping, 1998; Gustafsson and van Schaik, 2003).

#### 4.3. Effect of the “active DOM parameter” value

Apart from the deprotonation and cation competition effects described above, and despite the effects on the uncertainty of  $\log K_{MA}$  and  $\log K_{MB}$  values (see Tang and Johannesson, 2003 for a detailed discussion of the effect of constant uncertainty on Model V), differences in model predictions could result from the use of different values for the “active DOM parameter”. In the speciation calculations presented below for World Average River Water and the Mengong and Mar2 samples, we considered as Tang and Johannesson (2003) that the amount of active DOM in these samples is equal to the DOC content. Given that the DOM content of a water sample is approximately twice as high as its DOC concentration, this implies that only 50% of the DOM present in these samples can complex with the REE. In view of the ultrafiltration data reported by Viers et al. (1997), this hypothesis might not be valid for the Mengong and Mar2 samples. Indeed, as shown in Table 3 of Viers et al. (1997), the REE concentrations extrapolated to a zero DOC concentration are positive, rather than

negative as in the case of the newly ultrafiltered samples presented in our study. As shown above, calculated active DOM proportions range from 32% to 60% for the newly ultrafiltered samples, with a mean value of 50% fully in agreement with Tang and Johannesson’s assumption (2003). Evidently, the situation is quite different for the Mengong and Mar2 samples, where ultrafiltration data suggest that 100% of the DOM present in these samples could be active in complexing the REE.

To test the role of this parameter on model results, we performed sensitivity analysis on the Mengong and Mar2 samples. Model predictions using an “active DOM parameter” set equal to 50%, as suggested by Tang and Johannesson (2003), were compared with results predicted using an “active DOM parameter” of 100%, as indicated by ultrafiltration studies of these samples. We performed the same sensitivity analysis on World Average River Water. However, the newly ultrafiltered samples were not treated, given that ultrafiltration studies of these samples clearly imply that their “active DOM parameter” must be equal to about 50%. Table 8 shows the results for Mengong and Mar2 samples. Overall, Table 8 shows that raising the “active DOM parameter” from 50% to 100% strongly increases the proportion of REE that are predicted to be complexed with HM in these two samples. The predicted increase occurs in both Model VI and SHM. Moreover, SHM predictions become similar to Model VI results for Mar2 sample (i.e., LnHM > 98%) and to ultrafiltration data. However, SHM predictions are still lower than ultrafiltration results for the more acidic Mengong sample. Fig. 7 presents the results of the sensitivity analysis on World Average River Water for La, Eu and Lu. We note a strong difference compared with the predictions obtained for this sample when using an “active DOM parameter” of 50%. More specifically, both SHM and Model VI indicate that ca. 100% of the REE should occur as humate complexes at a pH higher than 6.5. The only remaining noticeable difference is that SHM continues to predict a slight deficit in LnHM species at low pH as compared to Model VI. This

Table 8

Model VI and SHM predictions of the proportion of REE occurring as humate complexes in Mengong and Mar2 waters, with the “active DOM parameter” assumed to be equal to 100%

| Mengong |                           |                    | Mar2          |                           |                    |     |
|---------|---------------------------|--------------------|---------------|---------------------------|--------------------|-----|
|         | Ultrafiltration<br>% LnHM | Model VI<br>% LnHM | SHM<br>% LnHM | Ultrafiltration<br>% LnHM | Model VI<br>% LnHM |     |
| La      | 86                        | 98                 | 85            | 94                        | 100                | 99  |
| Ce      | 86                        | 98                 | 86            | 94                        | 100                | 99  |
| Pr      | 87                        | 99                 | 92            | 96                        | 100                | 99  |
| Nd      | 86                        | 99                 | 94            | 95                        | 100                | 99  |
| Sm      | 100                       | 100                | 93            | 100                       | 100                | 100 |
| Gd      | 100                       | 99                 | 94            | 100                       | 100                | 99  |
| Tb      | 100                       | 98                 | 75            | 100                       | 100                | 98  |
| Dy      | 100                       | 97                 | 71            | 100                       | 100                | 98  |
| Ho      | 100                       | 96                 | 69            | 100                       | 100                | 98  |
| Er      | 69                        | 95                 | 66            | 100                       | 100                | 98  |
| Tm      | 100                       | 96                 | 64            | 100                       | 100                | 98  |
| Yb      | 100                       | 98                 | 78            | 100                       | 100                | 99  |
| Lu      | 100                       | 97                 | 71            | 100                       | 100                | 98  |

Ultrafiltration data shown for comparison are from Viers et al. (1997).

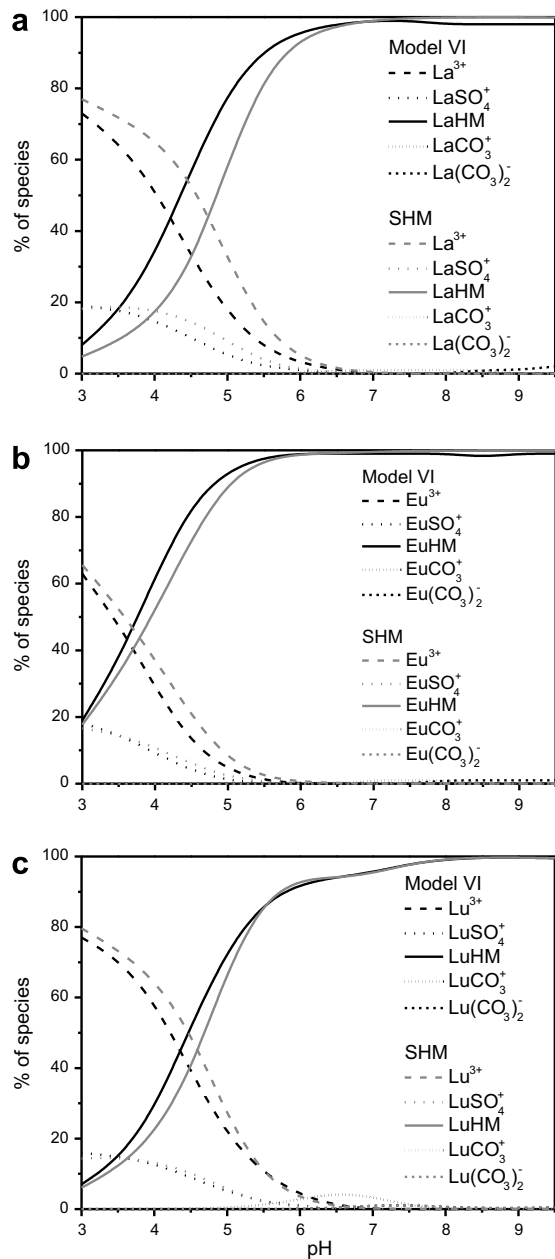


Fig. 7. Model VI and SHM speciation calculations for (a) La, (b) Eu and (c) Lu for World Average River Water illustrating the effects of setting a value of 100% for the “active DOM parameter” on the proportion of REE complexed with HM in this sample, as a function of pH (see Figs. 3 and 4, for comparison).

effect is known to be due to the lower extent of deprotonation of HM surfaces implied in SHM (see above).

Thus, raising the “active DOM parameter” from 50% to 100% leads to modifications in the modelling results that are far more important than those generated by differences in the electrostatic terms of the models or by uncertainties in the constant values for REE (see discussion in Tang and Johannesson, 2003) and/or competing cations. When the “active DOM parameter” is set to 100%, it is clearly not unexpected to observe a general increase in the proportion of the REE complexing with HM, as predicted both by

Model VI and SHM. This increase in the “active DOM parameter” value is equivalent to enhancing the abundance of organic ligands in sample solutions, which can then quantitatively scavenge all the dissolved REE. The other important key point is that the change in “active DOM parameter” value leads to a strong reduction of the disparities produced in model predictions for World Average River Water, and the Mengong and Mar2 samples (compare Figs. 3, 4 and 7, and Tables 5 and 8). Thus, by adopting an “active DOM parameter” of 100%, we obtain a fit between SHM and the ultrafiltration data for Mengong and Mar2 samples that is much better than previously established using a value of 50% for this parameter in SHM (see Tables 5 and 8).

Finally, two key questions arise from this study: what value should be adopted for the proportion of active DOM occurring in natural solutions (50% or 100%), and is this proportion constant from one natural solution to another? Considering the present ultrafiltration results and those obtained by Viers et al. (1997), it appears that the proportion of active DOM does not remain constant in waters, varying from 32% to 59% in the newly ultrafiltered samples, to 100% in the Mengong and Mar2 samples. A literature survey indicates that, in any case, this ratio could be significantly higher than the value of 50% used by Tang and Johannesson in their 2003 study. For example, a detailed study by Bryan et al. (2002) of the proportion of DOM that can complex metals (e.g., Cu and Al) in natural waters showed this amount to be ≈65% in most cases. This proportion is clearly lower than the value of 100% set in our sensitivity analysis, but significantly higher than the value of 50% used by Tang and Johannesson (2003).

To conclude, the above sensitivity analysis indicates that it is critical to have prior knowledge of the amount of active DOM in a water before making use of SHM or Model VI to predict the speciation of REE in waters. This implies that ultrafiltration experiments and/or other analytical techniques able to determine the REE complexing capacity of DOM must be performed on the samples that we wish to model.

## 5. CONCLUSION

The scope of this study was to increase our understanding of how to describe REE-organic complexation in equilibrium speciation models. For this purpose, we compared the ability of SHM and Models V and VI to assess the role of DOM in the speciation of REE in organic-rich ground- and river waters. We used REE specific equilibrium constants estimated by LFER, applying complexation constants for REE with acetic acid. The advantage of testing SHM is that this model is part of a wider equilibrium model (Visual MINTEQ) that also allows modelling of dissolution/precipitation, sorption/desorption and oxidation/reduction. Both Model VI and SHM yield comparable results for World Average River Water, confirming the earlier finding that a large fraction of the dissolved REE in rivers occurs as organic complexes. This also suggests that the two models could be equally valuable for calculating REE speciation in low-DOC waters at circumneutral-pH. The two

models also successfully reproduce ultrafiltration results obtained for acidic, DOC-rich ground- and river waters. However, the two models are found to yield slightly different results (depending on sample) when compared to newly obtained ultrafiltration results for organic-rich ( $\text{DOC} > 7 \text{ mg L}^{-1}$ ) groundwaters at circumneutral-pH, where Model VI predictions are in closer agreement with the ultrafiltration data than SHM. A survey of ultrafiltration results allows us to determine the “active DOM parameter” for the newly ultrafiltered water data. Thus, the observed discrepancy between SHM predictions and ultrafiltration results cannot be due to the input of inappropriate “active DOM parameter” values in this model. Clearly, SHM appears to need some improvements to become a REE speciation model of universal application (i.e., also usable under acidic pH conditions). Moreover, sensitivity analysis indicates that the “active DOM parameter” is a key parameter for both Model VI and SHM. Consideration of previously published speciation results based on Model V shows that great care should be taken in making use of these results because of the possible introduction of inappropriate values for this parameter. The results presented in this study show that, before running speciation models, it is essential to know the proportion of DOM that is active in complexing REE in a given water sample. This requirement could severely complicate the use of models to assess the role of DOM in controlling the speciation of REE in natural waters.

#### ACKNOWLEDGMENTS

We thank the technical staff at Rennes (M. Le Coz-Bouhnik, O. Hénin and P. Petitjean) for their assistance during the experimental and analytical work. Dr. M. S. N. Carpenter is acknowledged for English corrections. J. E. Sonke, K. H. Johannesson and several anonymous reviewers are thanked for thorough and constructive comments of an earlier version of this paper. This research was supported by the CPER programmes “Développement de la Recherche sur la Maîtrise de la Qualité de l’Eau en Bretagne” jointly funded by the French Government and the Council of Rennes Métropole.

#### APPENDIX A. ULTRAFILTRATION PROCEDURE AND CHEMICAL ANALYSES

Samples were collected in November 2004 from shallow piezometers (0.5–1.5 m deep). The pH was measured in the field with a combined Sentix 50 electrode. The accuracy of pH measurements is estimated at  $\pm 0.05$  pH unit. About 60 mL of each sample were immediately filtered on site, through 0.2  $\mu\text{m}$  cellulose acetate filter (Sartorius Minisart). An aliquot of 30 mL was acidified on site and subsequently used to measure major and trace cation concentrations. The remaining 30 mL were not acidified and used to measure alkalinity, major anions and DOC concentrations. For each sample, an extra 1 L aliquot was collected. This extra aliquot was filtered in the laboratory through 0.2  $\mu\text{m}$  cellulose acetate membrane using a Sartorius Teflon filtration unit. Thirty milliliters of the filtrate was acidified and used to re-measure major and trace cation concentrations (including REE), while 10 mL was used to re-measure the major anions and DOC content. Ultrafiltration experiments were

performed with the remaining filtrate. Ultrafiltrations were carried out with 15 mL centrifugal tubes equipped with permeable membranes of decreasing pore-size cut off (Millipore Amicon Ultra-15): 30, 10 and 5 kDa. Each centrifugal filter device was washed and rinsed with HCl 0.1 N and MilliQ water two times before use. Centrifugations were performed using a Jouan G4.12 centrifuge equipped with swinging bucket, at 3000g for between 20 (30 and 10 kDa) and 30 (5 kDa) min, depending on the pore-size cut off. Each of the four investigated samples (PF1, PF3, F7 and F14) was ultrafiltered in duplicate. All experiments were performed at room temperature:  $20 \pm 2^\circ\text{C}$ . Further information on the centrifugation procedure can be found in Pourret et al. (2007b).

Alkalinity was determined by potentiometric titration with an automatic titrator (794 Basic Titrino Methrom). Major anion ( $\text{Cl}^-$ ,  $\text{SO}_4^{2-}$  and  $\text{NO}_3^-$ ) concentrations were measured by ionic chromatography (Dionex DX-120). Major cation and trace element concentrations were determined by ICPMS (Agilent 4500), using indium as an internal standard. Dissolved organic carbon (DOC) was analysed on a total organic carbon analyzer (Shimadzu TOC-5050A). Typical uncertainties on anion and cation measurements, as established from repeated analyses of standard solutions (SLRS 4 geostandard water solution for cations; K-biphthalate solutions for DOC; Dionex seven anions standard solutions for anions), are estimated at  $<\pm 4\%$  for anions and at  $<\pm 5\%$  for all other measured species.

All procedures (sampling, filtration, storing and analysis) were carried out in order to minimize contamination. Samples were stored in acid-washed Nalgene polypropylene containers before analyses. Blank concentrations for DOC and REE were  $<0.5 \text{ mg L}^{-1}$  and  $<1 \text{ ng L}^{-1}$ , respectively. All reported DOC concentrations are blank corrected (maximum correction = 8%). For the REE, there was no need for blank corrections, since the sample concentrations were systematically two to three orders of magnitude higher than blank levels. The instrumental error on REE analysis in our laboratory as established from repeated analyses of multi-REE standard solution (Accu Trace™ Reference, USA) and of the SLRS-4 water standard is  $<\pm 2\%$  (Dia et al., 2000; Davranche et al., 2004, 2005; Gruau et al., 2004).

#### APPENDIX B. SUPPLEMENTARY DATA

Supplementary data associated with this article can be found, in the online version, at doi:10.1016/j.gca.2007.04.001.

#### REFERENCES

- Aubert D., Stille P., and Probst A. (2001) REE fractionation during granite weathering and removal by waters and suspended loads: Sr and Nd isotopic evidence. *Geochim. Cosmochim. Acta* **65**, 387–406.
- Bau M. (1999) Scavenging of dissolved yttrium and rare earths by precipitating iron oxyhydroxide: experimental evidence for Ce oxidation, Y-Ho fractionation, and lanthanide tetrad effect. *Geochim. Cosmochim. Acta* **63**, 67–77.

- Bidoglio G., Grenthe I., Qi P., Robouch P., and Omenetto N. (1991) Complexation of Eu and Tb with fulvic acids as studied by time-resolved laser induced fluorescence. *Talanta* **38**, 999–1008.
- Brownlow A. H. (1996) *Geochemistry*. Prentice Hall, Englewood Cliffs, NJ.
- Bryan S. E., Tipping E., and Hamilton-Taylor J. (2002) Comparison of measured and modelled copper binding by natural organic matter in freshwaters. *Comp. Biochem. Physiol. C* **133**, 37–49.
- Byrne R. H., and Sholkovitz E. R. (1996) Marine chemistry and geochemistry of the lanthanides. In *Handbook on the Physics and Chemistry of Rare Earths*, vol. 23 (eds. K. A. Gschneidner Jr. and L. R. Eyring), Elsevier Sciences B.V., pp. 497–593.
- Coppin F., Berger G., Bauer A., Castet S., and Loubet M. (2002) Sorption of lanthanides on smectite and kaolinite. *Chem. Geol.* **182**, 57–68.
- Davranche M., Pourret O., Gruau G., and Dia A. (2004) Impact of humate complexation on the adsorption of REE onto Fe oxyhydroxide. *J. Colloid Interface Sci.* **277**, 271–279.
- Davranche M., Pourret O., Gruau G., Dia A., and Le Coz-Bouhnik M. (2005) Adsorption of REE(III)-humate complexes onto MnO<sub>2</sub>: experimental evidence for cerium anomaly and lanthanide tetrad effect suppression. *Geochim. Cosmochim. Acta* **69**, 4825–4835.
- De Baar H. J. W., German C. R., Elderfield H., and van Gaans P. (1988) Rare earth element distributions in anoxic waters of the Cariaco Trench. *Geochim. Cosmochim. Acta* **52**, 1203–1219.
- De Baar H. J. W., Schijf J., and Byrne R. H. (1991) Solution chemistry of the rare earth elements in seawater. *Eur. J. Solid State Inorg. Chem.* **28**, 357–373.
- Dia A., Gruau G., Olivie-Lauquet G., Riou C., Molénat J., and Curmi P. (2000) The distribution of rare earth elements in groundwaters: assessing the role of source-rock composition, redox changes and colloidal particle. *Geochim. Cosmochim. Acta* **64**, 4131–4151.
- Dupré B., Viers J., Dandurand J.-L., Polvé M., Bénézeth P., Vervier P., and Braun J.-J. (1999) Major and trace elements associated with colloids in organic-rich river waters: ultrafiltration of natural and spiked solutions. *Chem. Geol.* **160**, 63–80.
- Elderfield H., and Greaves M. J. (1982) The rare earth elements in seawater. *Nature* **296**, 214–219.
- Elderfield H., Upstill-Goddard R., and Sholkovitz E. R. (1990) The rare earth elements in rivers, estuaries, and coastal seas and their significance to the composition of ocean waters. *Geochim. Cosmochim. Acta* **54**, 971–991.
- Gosselin D. C., Smith M. R., Lepel E. A., and Laul J. C. (1992) Rare earth elements in chloride-rich groundwater, Palo Duro Basin, Texas, USA. *Geochim. Cosmochim. Acta* **56**, 1495–1505.
- Gruau G., Dia A., Olivie-Lauquet G., Davranche M., and Pinay G. (2004) Controls on the distribution of rare earth elements in shallow groundwaters. *Water Res.* **38**, 3576–3586.
- Gustafsson J. P. (2001a) Modeling the acid-base properties and metal complexation of humic substances with the Stockholm Humic Model. *J. Colloid Interface Sci.* **244**, 102–112.
- Gustafsson J. P. (2001b) <http://www.lwr.kth.se/english/Our-Software/vminteq/index.htm>.
- Gustafsson J. P., Pechová P., and Berggren D. (2003) Modeling metal binding to soils: the role of natural organic matter. *Environ. Sci. Technol.* **37**, 2767–2774.
- Gustafsson J. P., and van Schaik J. W. J. (2003) Cation binding in a mor layer: batch experiments and modelling. *Eur. J. Soil Sci.* **54**, 295–310.
- Ingri J., Widerlund A., Land M., Gustafsson O., Andersson P., and Ohlander B. (2000) Temporal variations in the fractionation of the rare earth elements in a boreal river; the role of colloidal particles. *Chem. Geol.* **166**, 23–45.
- Janssen R. P. T., and Verweij W. (2003) Geochemistry of some rare earth elements in groundwater, Vierlingsbeek, The Netherlands. *Water Res.* **37**, 1320–1350.
- Johannesson K. H., Farnham I. M., Guo C., and Stetzenbach K. J. (1999) Rare earth element fractionation and concentration variations along a groundwater flow path within a shallow, basin-fill aquifer, southern Nevada, USA. *Geochim. Cosmochim. Acta* **63**, 2697–2708.
- Johannesson K. H., and Hendry M. J. (2000) Rare earth element geochemistry of groundwaters from a thick till and clay-rich aquitard sequence, Saskatchewan, Canada. *Geochim. Cosmochim. Acta* **64**, 1493–1509.
- Johannesson K. H., Stetzenbach K. J., and Hodge V. F. (1997) Rare earth elements as geochemical tracers of regional groundwater mixing. *Geochim. Cosmochim. Acta* **61**, 3605–3618.
- Johannesson K. H., Tang J., Daniels J. M., Bounds W. J., and Burdige D. J. (2004) Rare earth element concentrations and speciation in organic-rich blackwaters of the Great Dismal Swamp, Virginia, USA. *Chem. Geol.* **209**, 271–294.
- Johannesson K. H., Zhou X., Guo C., Stetzenbach K. J., and Hodge V. F. (2000) Origin of rare earth element signatures in groundwaters of circumneutral pH from southern Nevada and eastern California, USA. *Chem. Geol.* **164**, 239–257.
- Klungness G. D., and Byrne R. H. (2000) Comparative hydrolysis behavior of the rare earths and yttrium: the influence of temperature and ionic strength. *Polyhedron* **19**, 99–107.
- Lead J. R., Hamilton-Taylor J., Peters A., Reiner S., and Tipping E. (1998) Europium binding by fulvic acids. *Anal. Chim. Acta* **369**, 171–180.
- Lippold H., Müller N., and Kupsch H. (2005) Effect of humic acid on the pH-dependent adsorption of terbium(III) onto geological materials. *Appl. Geochem.* **20**, 1209–1217.
- Luo Y.-R., and Byrne R. H. (2004) Carbonate complexation of Yttrium and the rare earth elements in natural rivers. *Geochim. Cosmochim. Acta* **68**, 691–699.
- Maes A., De Brabandere J., and Cremers A. (1988) A modified Schubert method for the measurement of the stability of europium humic acid complexes in alkaline conditions. *Radiochim. Acta* **44/45**, 51–57.
- Martell A. E., and Smith R. M. (1998) *NIST Critical Selected Stability Constants of Metal Complexes Database*. Available at: <http://www.nist.gov/srd/nist46.htm>.
- Milne C. J., Kinniburgh D. G., Van Riemsdijk W. H., and Tipping E. (2003) Generic NICA-Donnan model parameters for Metal-Ion binding by humic substances. *Environ. Sci. Technol.* **37**, 958–971.
- Moulin V., Tits J., Moulin C., Decambox P., Mauchien P., and de Ruty O. (1992) Complexation behaviour of humic substances towards actinides and lanthanides studied by Time-Resolved Laser-Induced Spectrofluometry. *Radiochim. Acta* **58/59**, 121–128.
- Nelson B. J., Wood S. A., and Osiensky J. L. (2004) Rare earth element geochemistry of groundwater in the Palouse Basin, northern Idaho-eastern Washington. *Geochim. Exploration Environ. Anal.* **4**, 227–241.
- Olivie-Lauquet G., Gruau G., Dia A., Riou C., Jaffrezic A., and Henin O. (2001) Release of trace elements in wetlands: role of seasonal variability. *Water Res.* **35**, 943–952.
- Pourret O., Davranche M., Gruau G., and Dia A. (2007a) Competition between humic acid and carbonates for rare earth elements complexation. *J. Colloid Interface Sci.* **305**, 25–31.
- Pourret O., Dia A., Davranche M., Gruau G., Hénin O., and Angée M. (2007b) Organo-colloidal control on major- and trace-element partitioning in shallow groundwaters: confronting ultrafiltration and modelling. *Appl. Geochem.* doi:10.1016/j.apgeochem.2007.02.007.

- Ramsey J. B. (1969) Tests for specification errors in classical linear least-squares regression analysis. *J. R. Stat. Soc. Ser. B XXXI*(Part 2), 350.
- Schijf J., and Byrne R. H. (2004) Determination of  $\text{SO}_4\beta_1$  for yttrium and the rare earth elements at  $I = 0.66 \text{ m}$  and  $t = 25^\circ\text{C}$ : Implications for YREE solution speciation in sulfate-rich waters. *Geochim. Cosmochim. Acta* **68**, 2825–2837.
- Sholkovitz E. R. (1995) The aquatic chemistry of rare earth elements in rivers and estuaries. *Aquat. Geochem.* **1**, 1–34.
- Smedley P. L. (1991) The geochemistry of rare earth elements in groundwater from the Carnmenellis area, southwest England. *Geochim. Cosmochim. Acta* **55**, 2767–2779.
- Sonke J. E., and Salters V. J. M. (2006) Lanthanide-humic substances complexation. I. Experimental evidence for a lanthanide contraction effect. *Geochim. Cosmochim. Acta* **70**, 1495–1506.
- Tang J., and Johannesson K. H. (2003) Speciation of rare earth elements in natural terrestrial waters: assessing the role of dissolved organic matter from the modeling approach. *Geochim. Cosmochim. Acta* **67**, 2321–2339.
- Tanikazi Y., Shimokawa T., and Nakamura M. (1992) Physicochemical speciation of trace elements in river waters by size fractionation. *Environ. Sci. Technol.* **26**, 1433–1444.
- Tipping E. (1994) WHAM – A chemical equilibrium model and computer code for waters, sediments, and soils incorporating a discrete site/electrostatic model of ion-binding by humic substances. *Comput. Geosci.* **20**, 973–1023.
- Tipping E. (1998) Humic Ion-Binding Model VI: an improved description of the interactions of protons and metal ions with humic substances. *Aquat. Geochem.* **4**, 3–48.
- Tipping E., and Hurley M. A. (1992) A unifying model of cation binding by humic substances. *Geochim. Cosmochim. Acta* **56**, 3627–3641.
- Tipping E., Rey-Castro C., Bryan S. E., and Hamilton-Taylor J. (2002) Al(III) and Fe(III) binding by humic substances in freshwaters, and implication for trace metal speciation. *Geochim. Cosmochim. Acta* **66**, 3211–3224.
- Viers J., Dupré B., Polvé M., Schott J., Dandurand J.-L., and Braun J.-J. (1997) Chemical weathering in the drainage basin of a tropical watershed (Nsimi-Zoetele site, Cameroon): comparison between organic-poor and organic-rich waters. *Chem. Geol.* **140**, 181–206.
- Wood S. A. (1993) The aqueous geochemistry of the rare-earth elements: Critical stability constants for complexes with simple carboxylic acids at  $25^\circ\text{C}$  and 1 bar and their application to nuclear waste management. *Eng. Geol.* **34**, 229–259.
- Yamamoto Y., Takahashi Y., and Shimizu H. (2005) Systematics of stability constants of fulvate complexes with rare earth ions. *Chem. Lett.* **34**, 880–881.
- Yamamoto Y., Takahashi Y., and Shimizu H. (2006) Interpretation of REE patterns in natural water based on the stability constants. *Geochim. Cosmochim. Acta*. Goldschmidt Conference Abstracts, doi:10.1016/j.gca.2006.06.1587.

Associate editor: Robert H. Byrne



# Organo-colloidal control on major- and trace-element partitioning in shallow groundwaters: Confronting ultrafiltration and modelling

Olivier Pourret <sup>\*</sup>, Aline Dia, Mélanie Davranche, Gérard Gruau,  
Odile Hénin, Maxime Angée

CNRS, UMR 6118, Géosciences Rennes, Université Rennes 1, Campus Beaulieu, 35042 Rennes Cedex, France

Available online 21 March 2007

---

## Abstract

Ultrafiltration experiments using new small ultracentrifugal filter devices were performed at different pore size cut-offs to allow the study of organo-colloidal control on metal partitioning in water samples. Two shallow, circumneutral pH waters from the Mercy site wetland (western France) were sampled: one dissolved organic carbon (DOC)- and Fe-rich and a second DOC-rich and Fe-poor. Major- and trace-element cations and DOC concentrations were analysed and data treated using an ascendant hierarchical classification method. This reveals the presence of three groups: (i) a “truly” dissolved group (Na, K, Rb, Ca, Mg, Ba, Sr, Si and Ni); (ii) an inorganic colloidal group carrying Fe, Al and Th; and (iii) an organic colloidal group enriched in Cr, Mn, Co, Cu and U. However, REE and V have an ambivalent behaviour, being alternatively in the organic pool and in the inorganic pool depending on sample. Moreover, organic speciation calculation using Model VI were performed on both samples for elements for which binding constants were available (Ca, Mg, Ni, Fe, Al, Th, Cr, Cu, Dy, Eu). Calculation shows relatively the same partitioning of these elements as ultrafiltration does. However, some limitations appear such as (i) a direct use of ultrafiltration results which tends to overestimate the fraction of elements bound to humic material in the inorganic pool as regards to model calculations as well as, (ii) a direct use of speciation calculation results which tends to overestimate the fraction of elements bound to humic material in the organic pool with regard to ultrafiltration results. Beside these limitations, one can consider that both techniques, ultrafiltration and speciation calculation, give complementary information, especially for more complex samples where inorganic and organic colloids compete.

© 2007 Elsevier Ltd. All rights reserved.

---

## 1. Introduction

Dissolved organic matter (DOM) is ubiquitous in aquatic and terrestrial environments and plays a key role in the geochemistry of major and trace elements (Stumm and Morgan, 1996). While

DOM represents only a small proportion of the global C reservoir, it is instrumental in many reactions and influences environmental chemistry far beyond its mass contribution (Macalady, 1998). DOM acts as a major carrier for many elements through complexation, sorption and dissolution reactions (Buffle, 1988; Cabaniss and Shuman, 1988; Benedetti et al., 1996; Buerge-Weirich et al., 2003).

---

<sup>\*</sup> Corresponding author.

E-mail address: olivier.pourret@univ-rennes1.fr (O. Pourret).

Since DOM may compete with rock surfaces because of their high sorption capacities (Iler, 1979), sorption and/or complexation of cations onto DOM are major controlling processes for element migration and removal in weathering and aquifer systems (McCarthy et al., 1998; Tosiani et al., 2004; Braun et al., 2005). Moreover, speciation, bioavailability and mobility of major and trace elements can be strongly influenced by DOM (Wells and Goldberg, 1991; Tipping and Hurley, 1992; Dahlqvist et al., 2004). Since in natural aquatic systems, metal ions are rarely present as free hydrated ions, DOM provides binding sites influencing both their bioavailability and general transport behaviour. It also interacts with mineral phases modifying the exchange rates with solutions and constrains part of elemental mobility (Bennett and Siegel, 1987; Christensen et al., 1996; Schmitt et al., 2003).

Colloids, ubiquitous in natural waters, either organic or inorganic, are microscopic particles with size in the range 1 µm to 1 nm (Stumm and Morgan, 1996). Because of their small size, they tend not to settle out of suspensions, being influenced by Brownian motion and minor currents in the bulk solutions. The solid-water interface established by these microparticles plays a key role in regulating the concentrations of most reactive elements and of many pollutants in soils and natural waters (Stumm and Morgan, 1996). They adsorb heavy metal ions and waterborne pollutants governing, via their movements in aqueous systems, the fates of reactive elements and/or pollutants.

Recent studies coupled or not with speciation calculations suggested that a large fraction of trace elements are closely associated with DOM including colloidal organic matter in many natural waters (Tanizaki et al., 1992; Viers et al., 1997; Dupré et al., 1999; Dia et al., 2000; Ingri et al., 2000; Gruau et al., 2004; Johannesson et al., 2004). Moreover, redox conditions do control the dynamics and fate of some toxic and/or redox sensitive elements at the soil/water interface. The true respective roles of DOM and Fe–Mn oxyhydroxides as elemental carriers are still poorly understood. As Fe–Mn oxyhydroxides are redox sensitive (Stumm and Morgan, 1996), it is not clear whether trace metals are directly bound to the oxyhydroxides and complexed by DOM when the oxyhydroxides are dissolved during reduction, or whether they are directly bound to DOM and controlled by the organic matter dynamics throughout the entire redox cycle.

Considering that the respective contribution of organic and inorganic element carriers still remains a matter of debate, this work is dedicated to (i) investigate trends in trace element partitioning in size fractionated samples of well water using small ultracentrifugal devices and (ii) compare this field data to geochemical modelling calculations.

## 2. Samples

### 2.1. Sample location

The Kervidy/Coët-Dan catchment ( $5 \text{ km}^2$ ) is located in the Coët-Dan drainage basin, about 100 km SW of Rennes in Central Brittany, France (Fig. 1). The bedrock is made of fissured and fractured upper Proterozoic schists (Dabard et al., 1996). The soils, developed into a loamy material derived from bedrock weathering and eolian Quaternary deposits, exhibit facies variations, which are locally, dominated by silt, clay or sandstone materials (Pellerin and Van Vliet-Lanoë, 1998). The mineralogical composition of schist was determined from drill cutting analysis and includes (in decreasing relative proportion): quartz, muscovite, chlorite, K-feldspar and plagioclase (Pauwels et al., 1998). The soil horizons comprise a large number of secondary mineral phases including illite, smectite, kaolinite, various Fe-oxides and Fe-oxyhydroxides (hematite, goethite, etc.) and Mn oxides (Curmi et al., 1995; Pauwels et al., 1998).

Previous hydrochemical studies (Durand and Juan Torres, 1996; Jaffrézic, 1997; Dia et al., 2000; Molénat et al., 2002) showed that the Kervidy/Coët-Dan groundwater can be summarized by the contrast of two spatially-distributed chemical domains. These include: (i) the uppermost part of the groundwater, sampled below the hillslope, and which is colourless, slightly acidic, always oxidized and  $\text{NO}_3^-$ -contaminated (up to  $200 \text{ mg L}^{-1} \text{ NO}_3^-$ ) (Molénat et al., 2002), (ii) the shallow groundwater domain located in the wetlands where the water table reaches the organic-rich upper soil horizons. This second groundwater component is coloured, DOC-rich and exhibits variable  $\text{NO}_3^-$  concentrations (Durand and Juan Torres, 1996; Jaffrézic, 1997). In addition, these waters are characterized by the development of periodic reducing conditions mostly in late winter and spring, which is a direct consequence of the waterlogging of the uppermost soil horizon (Jaffrézic, 1997).

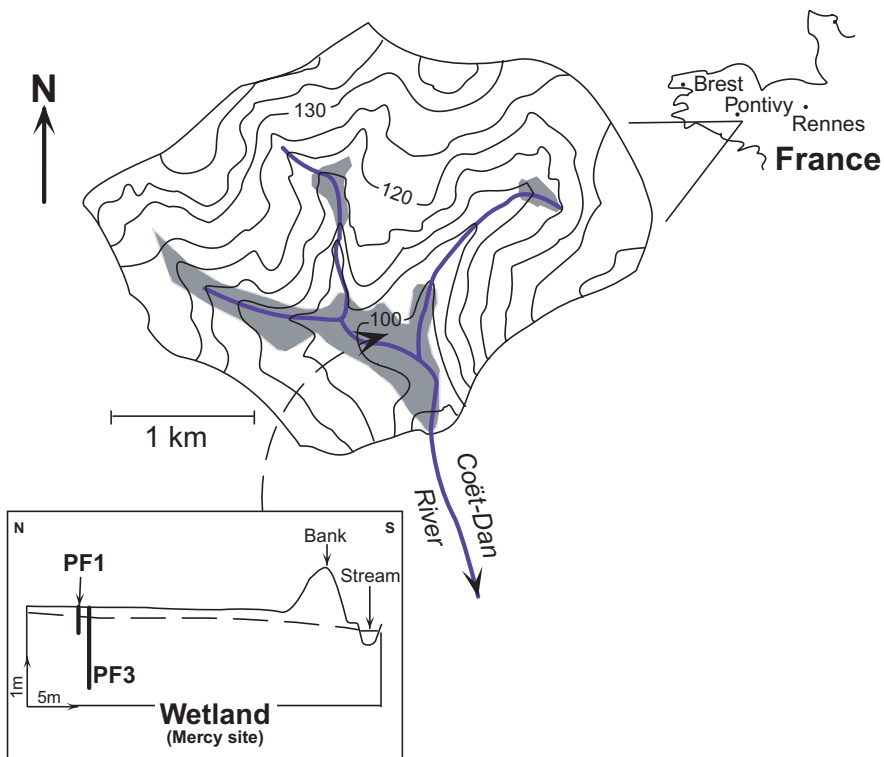


Fig. 1. Sketch showing topography, channel network geometry and geographical location of the Kervidy-Coët Dan subcatchment, and sampling point locations. Discontinuous patterned areas located close to the channel network indicate the location of wetland zones.

## 2.2. Sampling procedure

Two organic-rich groundwater samples were collected from shallow wells (PF1, 0.5 m- and PF3, 0.8-m-deep) located in the Mercy wetland (Fig. 1) in November 2004. Physicochemical parameters (pH and temperature) were measured directly in the field. The pH was measured with a combined Sentix 50 electrode after a calibration performed with WTW standard solutions (pH 4.01 and 7.00 at 25 °C). The accuracy of the pH measurement is  $\pm 0.05$  pH units. Samples used for determination of dissolved (<0.2 µm) major-, trace-element and DOC concentrations were pumped using Teflon tubing connected to a polyethylene syringe. The collected waters (about 1 L) were immediately filtered on site using 0.2 µm cellulose acetate filter capsule (polyether sulfone membrane Sartorius Minisart), and stored in pre-cleaned, acid-washed polyethylene bottles. About 30 mL were used to measure alkalinity, major anions and DOC concentrations. The remaining solution was used to measure major and trace cation concentrations and was then suc-

cessively filtered through ultracentrifugal devices with decreasing pore size cut-offs in order to allow separation of colloids from “truly” dissolved forms.

## 3. Experimental

### 3.1. Ultrafiltration set-up description and chemical analyses

To separate the colloidal bound elements from the non colloid-borne elements ultrafiltration experiments were performed on these samples using 15 mL centrifugal tubes (Millipore Amicon Ultra-15) equipped with permeable membranes of decreasing pore sizes (30 kDa, 10 kDa, and 5 kDa with  $1 \text{ Da} = 1 \text{ g mol}^{-1}$ ). Metal-colloid complexes are retained by the ultrafiltration membrane while free ions and smaller complexes pass into ultrafiltrate. The degree of metal-colloid complexation is usually determined from the metal concentration in the ultrafiltrate relative to the original solution. Each centrifugal filter device was washed and rinsed with HCl 0.1 mol L<sup>-1</sup> and MilliQ water twice before

use. The starting filtrate had been passed through a 0.2 µm filter, and then aliquots of these filtrates were passed through membranes of smaller sizes. All ultrafiltrations of the 0.2 µm filtrates were done in parallel. The centrifugations were performed using a Jouan G4.12 centrifuge equipped with swinging bucket at about 3000g for 20 min and 30 min, for 30 kDa, 10 kDa and 5 kDa devices, respectively (centrifugation times determined from preliminary experiments, not shown). All experiments were carried out at room temperature:  $20 \pm 2^\circ\text{C}$ .

Major cations and trace elements concentrations were determined at Rennes 1 University using an Agilent Technologies™ HP4500 ICP-MS instrument. Quantitative analyses were performed using a conventional external calibration procedure. Three external standard solutions with major and trace element concentrations similar to the analyzed samples were prepared from mono- and multi-elements standard solutions (Accu Trace™ Reference, USA). Indium was added to all samples as an internal standard at a concentration of  $0.87 \mu\text{mol L}^{-1}$  ( $100 \mu\text{g L}^{-1}$ ) to correct for instrumental drift and possible matrix effects. Indium was also added to the external standard solutions. Calibration curves were calculated from measured major cations and trace elements/In intensity ratios. The instrumental error on major cations and trace elements analysis in the laboratory as established from repeated analyses of the SLRS-4 water standard is  $<\pm 2\%$ . DOC concentrations were determined at Rennes 1 University using a Shimadzu 5000 TOC analyzer. The accuracy of DOC concentration measurements is estimated at  $\pm 5\%$  as determined by repeated analyses of freshly prepared standard solutions (potassium biphtalate). Total alkalinity was determined by potentiometric titration with an automatic titrating device (794 Basic Titrino Methrom). Major anion ( $\text{Cl}^-$ ,  $\text{SO}_4^{2-}$  and  $\text{NO}_3^-$ ) concentrations were measured by ionic chromatography (Dionex DX-120): the uncertainty is below  $\pm 4\%$ .

The same material was used for all filtrations, molecular size exclusion rather than adsorption onto membranes should control the colloid distributions between ultrafiltrates. The selectivity of the 10 and 5 kDa membranes with regard to Aldrich Humic Acid, with a mean molecular weight of 23 kDa, was verified by monitoring the DOC contents of the ultrafiltrates (preliminary experiments, not shown). Results show that the latter were systematically lower or equal to blank values ( $<0.5 \text{ mg L}^{-1}$ ). Possible adsorption of inorganic

major and trace element species onto the membrane or onto cell walls was also monitored. Inorganic multi-elements solutions of known concentration were ultrafiltrated several times. Results showed that 100% of the major and trace elements present in solution was recovered in the ultrafiltrates, demonstrating that no major or trace elements were adsorbed on either the membranes or on the walls of the cell devices used. All ultrafiltrations were performed in duplicate. Good reproducibility is observed for DOC and major and trace element concentrations. Duplicates are better than 5% for most elements except for some trace elements in the lower pore size cut-off fraction (i.e., in the  $<5 \text{ kDa}$  fraction, about 10%).

All procedures (sampling, filtration, storing and analysis) were carried out in order to minimize contamination. Samples were stored in acid-washed Nalgene polypropylene containers before analyses. Chemical blank concentrations of individual major cations and trace elements were all better than 2% for all studied elements except for DOC, Al and Cu (<8%, 10% and 11%, respectively).

### 3.2. Speciation calculation

The aqueous speciation of some major (Al, Ca, Fe, Mg) and trace elements (Cu, Eu, Dy, Th) was calculated using the computer program WHAM 6 (Version 6.0.13). It includes Model VI which has been described in detail by [Tipping \(1998\)](#). The model is a discrete binding site model in which binding is modified by electrostatic interactions. There is an empirical relation between net humic charge and an electrostatic interaction factor. In this study the computation is performed using only the default parameters values and the generic log  $K_{\text{MA}}$  values (see [Tipping, 1998](#)). Humic substances were the only colloidal phases considered in this calculation, none colloidal oxide phase was considered.

### 3.3. Data treatment

The ascending hierarchical classification using the Ward criterion was performed through SPAD 4.5 routines (DECISIA, France) so as to implement sample classification ([Dillon and Goldstein, 1984](#)). This method is based on squared Euclidian distances between individuals in the space formed by the available variables. The initial sample is partitioned into several classes of individuals so as to maximise interclass inertia (i.e., to maximise

variability between groups) and minimise intraclass inertia (i.e., to maximise homogeneity in each group). As for factor analysis, the raw data matrix was introduced in principal component analysis, without any rotation. The input data are the whole set of ultrafiltrates after each cut-off for all considered elements.

## 4. Results

### 4.1. Ultrafiltration

In the following sections the behaviour of major, trace and DOC concentrations obtained for successive ultrafiltrations will be discussed. Major, trace element and DOC concentrations are reported in **Table 1**. Major anions are not considered in this part of the study. Ultrafiltration data are presented following the hierarchical classification described in the above “data treatment” paragraph. The results of cluster analysis are presented as a dendrogram, where the similarity of two elements is conversely proportional to the linkage distance (**Fig. 2**). This graph reveals three clusters: (i) cluster I includes alkalis (Na, K, Rb), alkaline earth metals (Ca, Mg, Ba, Sr) as well as Si and Ni; (ii) cluster II contains Cr, Mn, Co, Cu and U; and (iii) cluster III includes Al, Fe and Th. REE and V are either in cluster II or in cluster III for PF1 and PF3 samples, respectively.

As stated previously, colloids span a wide range from about 1 nm to a few  $\mu\text{m}$ ; in successive ultrafiltrations through decreasing pore size membranes, DOC concentrations decrease in the ultrafiltrates (**Fig. 3**). These successive ultrafiltrations allow further consideration about various molecular weight humic substances. To determine whether metals are bound or not to humic substances, metal concentrations will be systematically plotted as a function of DOC concentrations.

#### 4.1.1. Common elemental distribution in the two samples

##### (i) Cluster I: “truly” dissolved behaviour

Concentrations of Rb and other alkalis such as Na and K, are not affected by ultrafiltrations since no fractionation occurs when following the decreasing pore sizes or the DOC concentrations (**Fig. 4a**). Alkaline elements behave as “truly” dissolved in the form of inorganic species as often reported in the liter-

ature (Pokrovsky and Schott, 2002, and references therein). Major and trace alkaline earth (Ca, Mg, Sr and Ba) concentrations do not change significantly during filtration except for the smallest pore size (5 kDa). The small drop between 5 kDa and 10 kDa filtrates (**Fig. 4b**) can suggest that part of these elements (about 10%) could be associated with low-molecular weight organic colloids as reported elsewhere where complexes of Ca and Mg with natural fulvic acids have been identified (Shapiro, 1964). Silicon concentrations display no significant variations in the successive filtrates. This suggests that aqueous silica is not trapped by organic colloids (Pokrovski and Schott, 1998) and/or by small-size clay minerals or phytolites. Nickel concentrations do not exhibit large variations through the different decreasing pore size cut-offs suggesting that this transition metal has to be mostly present as “truly” dissolved species or small size inorganic complexes.

##### (ii) Cluster II: organic colloidal pool-borne elements

Both Cu and U concentrations display extremely regular linear relationships as reported versus DOC concentrations for both samples (**Fig. 5a** and b ; **Table 1**). The linear relationships suggest that these two trace elements are strongly bound to organic matter and probably complexed to very low molecular weight organic ligands such as extracellular ligands as well as, larger size colloids such as fulvic and/or humic acids, cell fragments or bacteria as reported elsewhere (Xue et al., 1995; Sigg et al., 2000). Since Cu and U concentrations tend to zero before DOC does, one can suggest that no fraction of Cu and U occurs as free species in solutions and that a fraction of DOM is unable to complex these two elements. However, organic matter remains the major carrier of Cu and U as often previously stated (Stumm and Morgan, 1996). Chromium, Mn and Co concentrations (**Table 1**) also display linear positive correlations when reported versus DOC concentrations for both samples. Organic matter is thus also a major carrier of these elements.

##### (iii) Cluster III: inorganic colloidal pool-borne elements

Aluminium and Fe concentration variations through successive filtrations (**Fig. 6a** and b)

Table 1

Ultrafiltration results, all concentrations are expressed in  $\mu\text{g L}^{-1}$ , except  $\text{Cl}^-$ ,  $\text{NO}_3^-$ ,  $\text{SO}_4^{2-}$  and DOC in  $\text{mg L}^{-1}$ , and alkalinity in  $\mu\text{mol L}^{-1}$ 

|                          | PF1               |        |        |        |        |        |        | PF3               |        |        |        |        |        |        |
|--------------------------|-------------------|--------|--------|--------|--------|--------|--------|-------------------|--------|--------|--------|--------|--------|--------|
|                          | 0.2 $\mu\text{m}$ | 30 kDa | 30 kDa | 10 kDa | 10 kDa | 5 kDa  | 5 kDa  | 0.2 $\mu\text{m}$ | 30 kDa | 30 kDa | 10 kDa | 10 kDa | 5 kDa  | 5 kDa  |
| T ( $^{\circ}\text{C}$ ) | 10.6              |        |        |        |        |        |        | 10.7              |        |        |        |        |        |        |
| pH                       | 7.08              |        |        |        |        |        |        | 6.93              |        |        |        |        |        |        |
| Cl                       | 47                |        |        |        |        |        |        | 37                |        |        |        |        |        |        |
| $\text{SO}_4$            | 10                |        |        |        |        |        |        | 9                 |        |        |        |        |        |        |
| $\text{NO}_3$            | 2                 |        |        |        |        |        |        | 46                |        |        |        |        |        |        |
| Alkalinity               | 1867              |        |        |        |        |        |        | 385               |        |        |        |        |        |        |
| DOC                      | 17.3              | 15.7   | 15.8   | 13.9   | 14.6   | 13.9   | 13.0   | 7.66              | 6.73   | 6.60   | 5.60   | 5.72   | 5.13   | 4.82   |
| Na                       | 17,130            | 17,480 | 17,300 | 16,850 | 16,580 | 15,797 | 16,187 | 16,150            | 14,950 | 15,310 | 15,400 | 15,550 | 13,015 | 13,466 |
| Mg                       | 21,550            | 21,690 | 21,850 | 21,170 | 21,110 | 19,801 | 20,039 | 15,710            | 14,980 | 14,850 | 15,220 | 15,220 | 13,363 | 13,705 |
| Al                       | 25                | 12     | 12     | 11     | 10     | 6      | 7      | 72.6              | 18.4   | 17.7   | 15.8   | 15.0   | 10.8   | 10.3   |
| Si                       | 4027              | 4013   | 4042   | 3903   | 3882   | 3751   | 3781   | 4234              | 3922   | 3946   | 4007   | 4048   | 3656   | 3679   |
| K                        | 564               | 546    | 555    | 546    | 537    | 501    | 510    | 468               | 426    | 434    | 441    | 435    | 400    | 403    |
| Ca                       | 10,310            | 10,050 | 10,190 | 9717   | 9218   | 8915   | 9033   | 7437              | 7088   | 7539   | 7371   | 7151   | 6686   | 6719   |
| V                        | 0.34              | 0.18   | 0.19   | 0.18   | 0.17   | 0.11   | 0.12   | 0.27              | 0.16   | 0.16   | 0.16   | 0.16   | 0.16   | 0.15   |
| Cr                       | 1.36              | 1.16   | 1.15   | 1.08   | 1.00   | 0.61   | 0.67   | 0.87              | 0.69   | 0.68   | 0.67   | 0.69   | 0.59   | 0.54   |
| Mn                       | 31.16             | 25.40  | 25.27  | 24.87  | 24.63  | 9.55   | 9.66   | 9.77              | 9.40   | 9.41   | 9.34   | 9.49   | 2.65   | 2.67   |
| Fe                       | 955               | 35     | 34     | 21     | 25     | 6      | 7      | 98.5              | 12.1   | 11.6   | 8.0    | n.a.   | 0.0    | 0.0    |
| Co                       | 3.75              | 3.10   | 3.10   | 2.85   | 2.78   | 1.16   | 1.23   | 1.13              | 1.07   | 1.07   | 1.04   | 1.10   | 0.20   | 0.20   |
| Ni                       | 5.52              | 5.15   | 5.44   | 4.90   | 4.97   | 3.80   | 4.03   | 6.45              | 5.94   | 5.91   | 5.75   | n.a.   | 4.59   | 4.57   |
| Cu                       | 1.94              | 1.70   | 1.72   | 1.39   | 1.37   | 1.20   | 1.25   | 5.68              | 4.84   | 4.88   | 3.91   | 3.90   | 3.12   | 3.12   |
| Zn                       | 5.69              | cntd   | cntd   | cntd   | cntd   | cntd   | cntd   | 11.74             | cntd   | cntd   | cntd   | cntd   | cntd   | cntd   |
| Rb                       | 2.83              | 2.77   | 2.76   | 2.75   | 2.73   | 2.67   | 2.67   | 0.45              | 0.40   | 0.40   | 0.41   | 0.40   | 0.40   | 0.40   |
| Sr                       | 57.18             | 55.87  | 55.75  | 55.07  | 54.60  | 53.43  | 53.56  | 51.56             | 50.82  | 50.61  | 50.39  | 50.34  | 49.98  | 50.27  |
| Ba                       | 7.28              | 6.65   | 6.72   | 6.58   | 6.51   | 6.32   | 6.26   | 10.71             | 10.48  | 10.39  | 10.35  | 10.26  | 10.18  | 10.18  |
| La                       | 0.176             | 0.029  | 0.029  | 0.021  | 0.021  | 0.010  | 0.012  | 0.804             | 0.580  | 0.571  | 0.436  | 0.430  | 0.284  | 0.274  |
| Ce                       | 0.365             | 0.059  | 0.060  | 0.045  | 0.044  | 0.019  | 0.029  | 1.889             | 1.352  | 1.347  | 1.027  | 0.996  | 0.600  | 0.578  |
| Pr                       | 0.055             | 0.011  | 0.011  | 0.007  | 0.008  | 0.004  | 0.004  | 0.255             | 0.184  | 0.185  | 0.140  | 0.138  | 0.095  | 0.091  |
| Nd                       | 0.239             | 0.053  | 0.050  | 0.041  | 0.042  | 0.016  | 0.019  | 1.105             | 0.833  | 0.819  | 0.630  | 0.618  | 0.417  | 0.404  |
| Sm                       | 0.050             | 0.012  | 0.014  | 0.010  | 0.010  | 0.005  | 0.004  | 0.194             | 0.144  | 0.140  | 0.104  | 0.100  | 0.070  | 0.067  |
| Eu                       | 0.010             | 0.003  | 0.003  | 0.003  | 0.002  | 0.000  | 0.001  | 0.037             | 0.027  | 0.026  | 0.019  | 0.019  | 0.012  | 0.012  |
| Gd                       | 0.040             | 0.012  | 0.012  | 0.010  | 0.009  | 0.003  | 0.004  | 0.135             | 0.096  | 0.095  | 0.075  | 0.071  | 0.046  | 0.044  |
| Tb                       | 0.005             | 0.001  | 0.002  | 0.001  | 0.001  | 0.000  | 0.001  | 0.013             | 0.010  | 0.009  | 0.007  | 0.007  | 0.004  | 0.004  |
| Dy                       | 0.026             | 0.009  | 0.008  | 0.007  | 0.007  | 0.003  | 0.003  | 0.067             | 0.049  | 0.047  | 0.035  | 0.037  | 0.022  | 0.021  |
| Ho                       | 0.005             | 0.002  | 0.002  | 0.002  | 0.002  | 0.001  | 0.001  | 0.013             | 0.009  | 0.010  | 0.007  | 0.007  | 0.004  | 0.004  |
| Er                       | 0.015             | 0.006  | 0.007  | 0.006  | 0.005  | 0.002  | 0.002  | 0.035             | 0.027  | 0.026  | 0.019  | 0.020  | 0.012  | 0.013  |
| Tm                       | 0.002             | 0.001  | 0.001  | 0.001  | 0.001  | 0.000  | 0.000  | 0.005             | 0.004  | 0.004  | 0.003  | 0.003  | 0.002  | 0.002  |
| Yb                       | 0.015             | 0.006  | 0.007  | 0.006  | 0.005  | 0.002  | 0.003  | 0.030             | 0.025  | 0.023  | 0.018  | 0.018  | 0.012  | 0.012  |
| Lu                       | 0.003             | 0.001  | 0.001  | 0.001  | 0.001  | 0.000  | 0.001  | 0.005             | 0.004  | 0.004  | 0.003  | 0.003  | 0.002  | 0.002  |
| $\Sigma\text{REE}$       | 1.005             | 0.205  | 0.206  | 0.161  | 0.158  | 0.067  | 0.083  | 4.587             | 3.344  | 3.307  | 2.524  | 2.468  | 1.584  | 1.527  |
| Pb                       | 0.784             | cntd   | cntd   | cntd   | cntd   | cntd   | cntd   | 0.128             | cntd   | cntd   | cntd   | cntd   | cntd   | cntd   |
| Th                       | 0.045             | 0.027  | 0.027  | 0.023  | 0.019  | 0.003  | 0.005  | 0.063             | 0.025  | 0.024  | 0.016  | 0.014  | 0.008  | 0.006  |
| U                        | 0.046             | 0.035  | 0.036  | 0.030  | 0.028  | 0.022  | 0.023  | 0.049             | 0.035  | 0.034  | 0.024  | 0.014  | 0.012  |        |

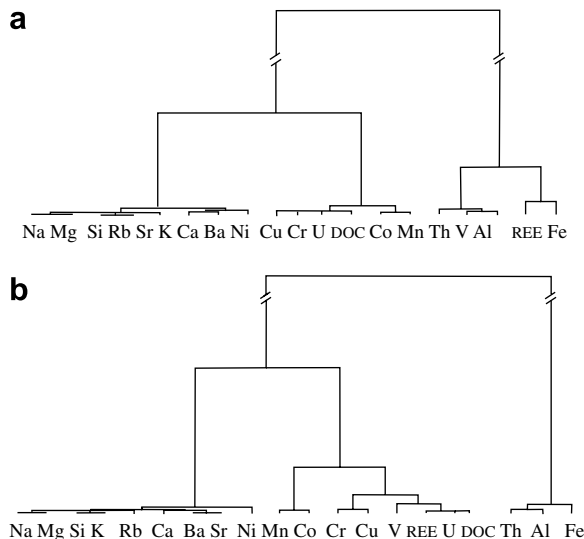


Fig. 2. Dendograms of samples (a) PF1 and (b) PF3 showing the hierarchical classification of the elements in three clusters.

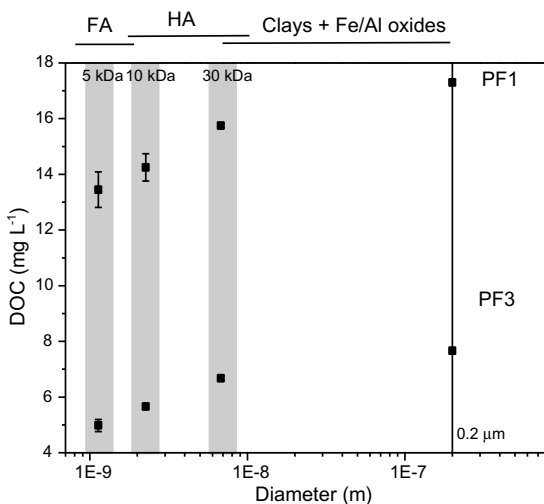


Fig. 3. DOC concentrations versus molecular weight cut-offs. Values for molecular weight are approximated, since the spatial extension of macromolecules such as humic substances is dependant on molecular structure and surrounding conditions. FA, fulvic acid; HA, humic acid.

suggest that these elements do not occur as free species in solution, and that two types of colloids can carry these metals (i.e., Al-, Fe-rich inorganic colloids or organic-, Al-, Fe-complexing colloids). Aluminium and Fe concentrations vary following the same trend (Table 1) both strongly affected by a large drop of concentrations between 0.2 μm and 30 kDa filtrations. Up to 96% and 75% for

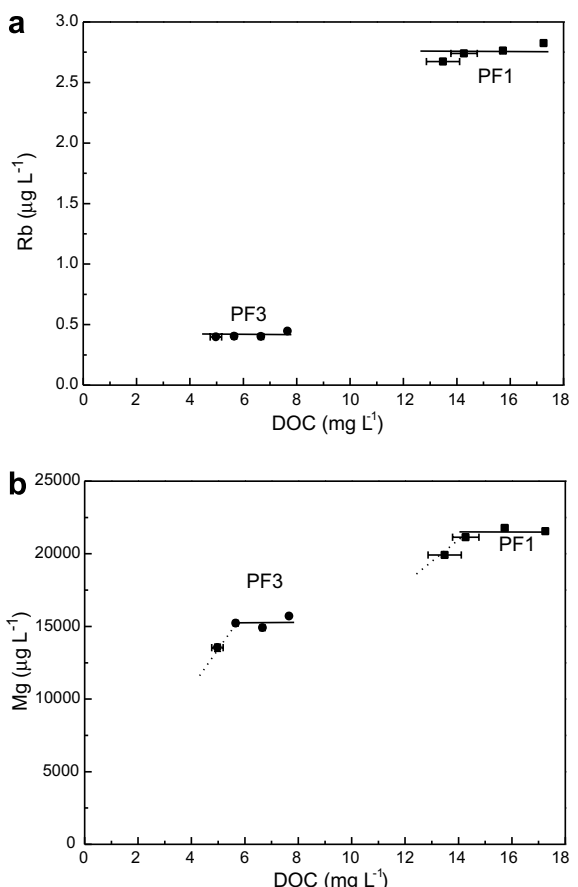


Fig. 4. Variations of (a) Rb and (b) Mg concentrations versus DOC concentrations in the different filtrates. Error bars correspond to standard deviation for two replicates, some error bars are within the symbol size.

Fe and Al, respectively, are removed by the first ultrafiltration step. This indicates a major control of Al by inorganic mixed Fe/Al oxyhydroxides as already reported (Pokrovsky and Schott, 2002; Geckes et al., 2003). This is particularly true for the Al-rich PF3 sample as compared to PF1 where Fe dominates relative to Al. However, a small part of Al and Fe could be partially bound to low-molecular weight organic-rich colloids. Aluminium concentration tends to zero before DOC does for both samples. This is not the case for Fe, since Fe disappears before DOC does. This suggests that the Fe budget between organic and inorganic carrier phases has to be different from that of Al, depending also on which sample is considered. Furthermore, Al could be carried by another low-molecular weight DOC-poor phase which does not trap Fe in

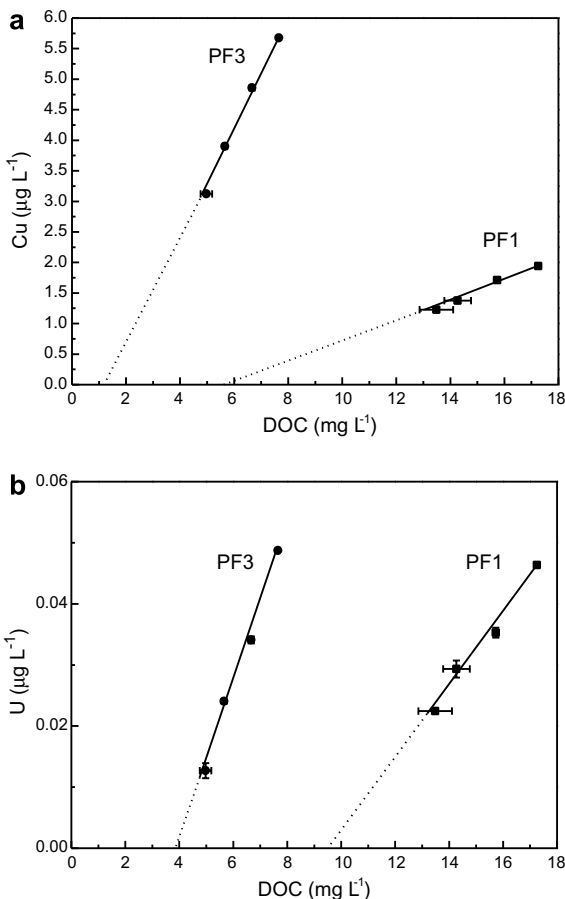


Fig. 5. Variations of (a) Cu and (b) U concentrations versus DOC concentrations in the different filtrates. Error bars correspond to standard deviation for two replicates, some error bars are within the symbol size.

PF1, but not in PF3. Aluminium cannot be present as clay colloids since Si occurs in a “truly” dissolved state.

Thorium concentrations regularly decrease through the successive decreasing pore size cut-offs with a large drop (up to 40%) between 0.2  $\mu\text{m}$  and 30 kDa (Fig. 6c). This suggests that this fraction of Th has to be associated with large size organic colloids while about 60% of Th appears to be carried by colloids smaller than 30 kDa. Thorium concentrations decrease quicker than do DOC concentrations suggesting that Th is probably mostly carried in solution by high-molecular weight organic-rich colloids. The Th concentration versus Al concentration diagram (Fig. 6d) suggests that Th might be also partly carried by

Al-rich phases as well as DOC-rich ones. Clays and clay-organic complexes could be possible Th carriers in these waters.

#### 4.1.2. Peculiar elemental distribution in the DOC-depleted sample

Rare Earth Elements and V display an ambivalent behaviour with regard to the sample considered. A plot of  $\Sigma\text{REE}$  concentrations versus DOC concentrations for the successive ultrafiltrations (Fig. 7a) show a general decreasing tendency going through zero REE that illustrates the removing of REE jointly to DOC. However, there is still DOC left in solution as REE concentrations are close to zero, which allows the extrapolation that not all the organic pool is able to complex REE. The REE appear to be strongly complexed by high-molecular weight organic matter as previously stated in other ultrafiltration studies (Sholkovitz, 1995; Viers et al., 1997; Dia et al., 2000). However, a recurrent problem of ultrafiltration studies is that Fe and Mn oxyhydroxides can be present in the waters along with organic colloids, some of them being potentially strong competitors of organic matter for REE complexation (Bau, 1999; Dupré et al., 1999). The PF1 sample presents a significant decrease in its Fe content upon ultrafiltration at the 30 kDa ultrafiltration step. This decrease corresponds to a marked change in the slope of the REE-DOC linear relationships otherwise observed in the REE versus DOC variation diagram (Fig. 7a). About 80% of the REE and 96% of the Fe, but only 9% of the DOC, are removed during the first ultrafiltration step of this sample. Such a relationship strongly suggests that the “colloidal” REE budget of PF1 samples is controlled, in part, by REE-bearing Fe colloids as suspected by looking at Fig. 7b. By contrast for the PF3 sample, REE concentrations display a strong correlation versus DOC concentrations, as reported, irrespective of the cut-off. The linear relationship suggests that in this sample REE are strongly bound to organic matter.

Vanadium concentrations reported versus DOC concentrations display a large drop between 0.2  $\mu\text{m}$  and 30 kDa filtrations in the two samples (Fig. 7c). This suggests that a significant fraction (about 40%) of V has to be carried by large size organic colloids. By contrast, when looking at the lower cut-off the V concentrations behave differently in the two samples. On one side for the uppermost sample (PF1) a three step-shape decrease following

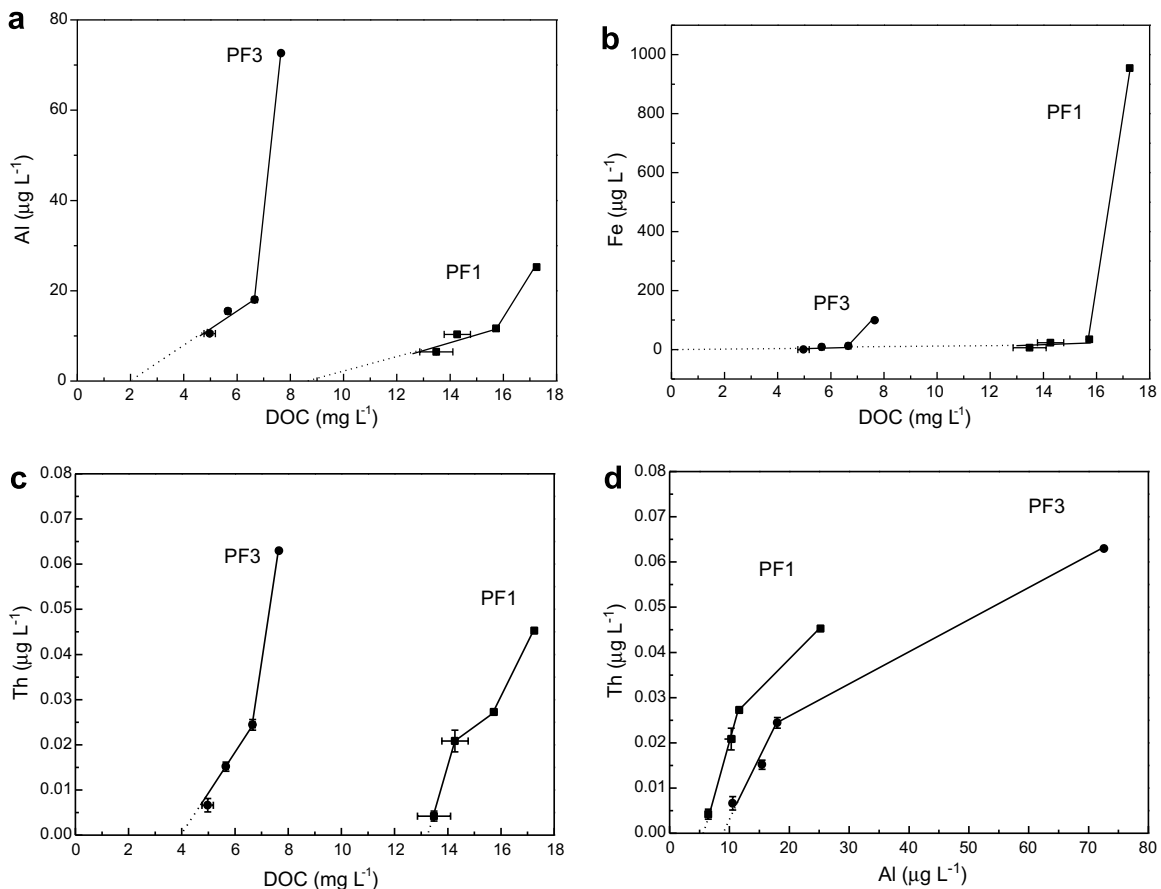


Fig. 6. Variations of (a) Al, (b) Fe, (c) Th concentrations versus DOC concentrations and (d) Th concentrations versus Al concentrations in the different filtrates. Error bars correspond to standard deviation for two replicates, some error bars are within the symbol size.

DOC concentrations lowering suggesting that V remains carried by the organic phase (low and high-molecular weight). Whereas on the other side, the decrease of V concentrations follows that of Al. This suggests that as Th concentrations vary relative to DOC and Al concentrations, V concentrations follow the same trend (Fig. 7d). Both V and Th concentrations in the organic-rich upper level seem to be controlled by mixed DOC/Al-rich phases, whatever may be the pore size cut-off. Moreover, the large decrease of V concentrations following that of Fe between 0.2  $\mu\text{m}$  and 30 kDa suggests that Fe-rich phases also exert an important control on the speciation of V at this cut-off as earlier reported (Pokrovsky and Schott, 2002). At lower filtration sizes, V concentrations tend to zero, suggesting that V has also to be carried by a mixed Al/Fe/DOC-rich phase. The lower sample (PF3) displays a strong decrease in the first filtration step which implies that V is strongly bound to high-molecular weight organic material, and a constant V concen-

tration after the 30 kDa filtration which implies that V behaves independently of DOC. However, the V concentration pattern is different in the DOC-depleted sample with no variation versus Al concentrations after the 30 kDa filtration. This suggests that V is not carried by an Al-rich phase, but mostly occurs as “truly” dissolved species as a free hydrated ion.

#### 4.2. Speciation calculations

The aqueous speciation of some major (Ca, Mg, Al, Fe) and trace elements (Cr, Ni, Cu, Eu, Dy, Th) in the two samples were calculated using Model VI (Tipping, 1998). The pH values were fixed at 7.08 and 6.93, for PF1 and PF3 samples, respectively. The DOC concentrations as well as major and trace elements concentration input in the model were those displayed in Table 1. The humic acid (HA) and fulvic acid (FA) contents necessary to run both models are assumed to be equal to the difference

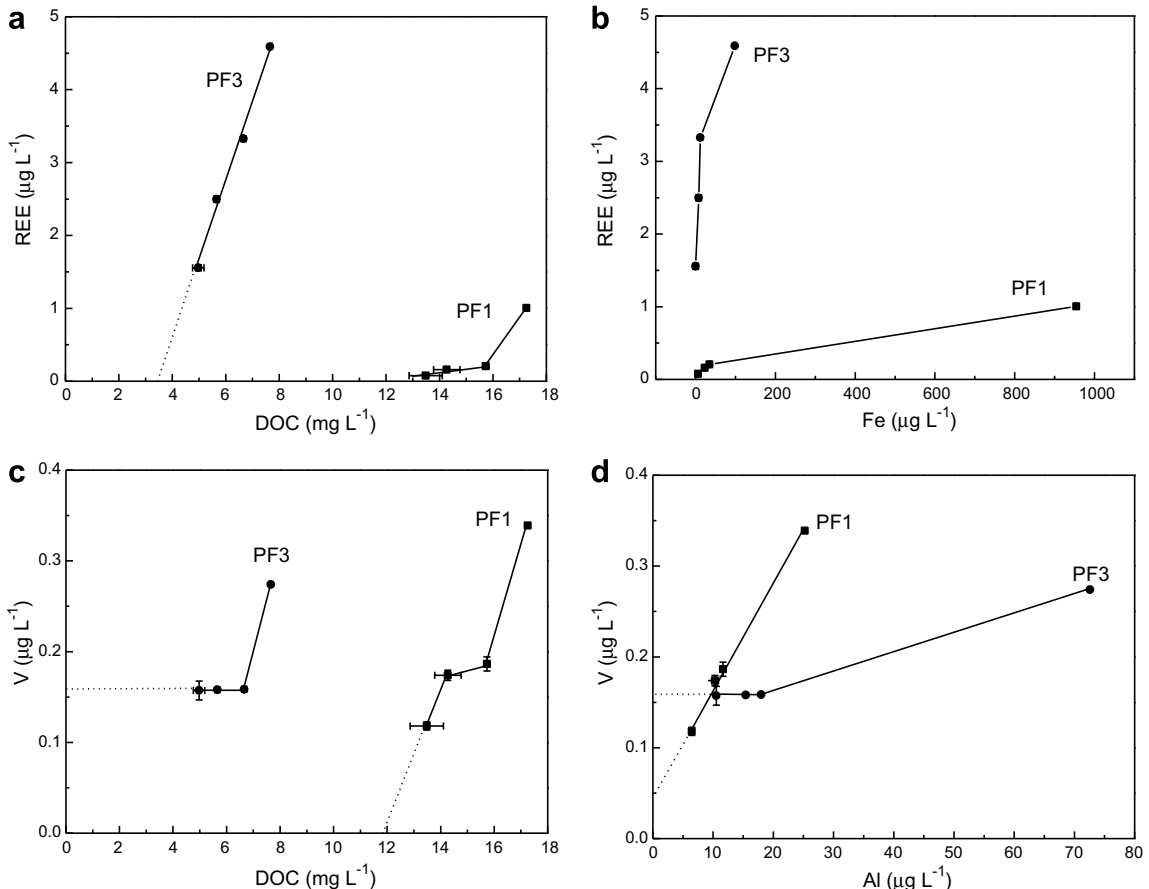


Fig. 7. Variations of REE concentrations versus (a) DOC and (b) Fe concentrations, and V concentrations versus (c) DOC and (d) Al concentrations in the different filtrates. Error bars correspond to standard deviation for two replicates, some error bars are within the symbol size.

between the DOC content of the  $<0.2 \mu\text{m}$  fraction and that of the  $<5 \text{kDa}$  fraction for HA, and to the DOC content of the  $<5 \text{kDa}$  fraction for FA. Fractions of elements complexed to humic substance samples are reported in Table 2. As for the ultrafiltration experiments three distinct groups appear from the calculations: (i) Mg, Ca, Ni appear to be mainly present as “truly” dissolved species in the solution,  $<8\%$  of elements are complexed to humic substances. (ii) Fe and Al are partly complexed to organic matter; between 16% and 81% of these elements are bound to humic substances. Aluminium is more strongly bound to humic sub-

stances than is Fe. (iii) According to calculations Cr, Cu, Eu, Dy and Th exhibit comparable speciation:  $>86\%$  (except Cu for PF1 sample) of elements are complexed by humic substances.

## 5. Confronting speciation calculations with ultrafiltration data

The need for the knowledge of “truly” dissolved and colloidal concentrations includes several points such as (i) an understanding of element geochemical cycles and partitioning, (ii) a better prediction of element fate in polluted environments, or (iii) the relevance to bioavailability issues. The comparison between results obtained by ultrafiltration and by speciation calculation leads to some comments. Three groups can be considered.

For Mg and Ca the results of speciation calculation are in good agreement with the ultrafiltration

Table 2  
Speciation calculations results: proportion of elements complexed with humic substances

|     | Mg | Al | Ca | Cr | Fe | Ni | Cu | Eu | Dy  | Th |
|-----|----|----|----|----|----|----|----|----|-----|----|
| PF1 | 3  | 58 | 5  | 86 | 16 | 6  | 61 | 96 | 100 | 89 |
| PF3 | 2  | 81 | 3  | 94 | 43 | 8  | 95 | 99 | 100 | 96 |

data. These elements behave as “free” ions in the dissolved pool in the form of inorganic species. Speciation calculations performed for Cr, Cu, Dy, Eu and Th give a higher proportion of elements bound to humic substances than those recovered from ultrafiltration data. By contrast, for Al, Fe and Ni speciation calculations give a slightly lower proportion of elements bound to humic substances as compared to those obtained from ultrafiltration data. Even if there are slight differences between ultrafiltration and speciation calculations, trends are relatively similar for Al, Dy, Eu and Th. Major differences evidenced for Cr, Cu, Fe and Ni could be explained by the fact that models need improvement as already stated for Cu and Ni (Unsworth et al., 2006).

Since the binding constants with humic substances are not available for the whole set of studied elements, the speciation calculations were performed for part of them. However, the calculations were achieved for one or several elements belonging to each of the three groups, allowing these elements to be considered as a “pilot study” for each group. In the following, the discussion will be focused on these “pilot study” elements considering that these latter are representative of the elements within the different groups.

### 5.1. “Truly” dissolved elements

Concentrations of alkalis and alkaline earth elements (major and trace ones) appear to be not significantly affected by ultrafiltrations suggesting that they are part of the dissolved pool. Since there is no clear relationship between DOC or Fe and these elemental concentrations, one can consider that these species do not occur as small-size organic or inorganic complexes in the dissolved pool. The speciation calculations performed during this study for alkalis and alkaline earth metals agree with the ultrafiltration data. The occurrence of these metals in the dissolved pool was predictable since these elements belong to the class A ion group following the Nieboer and Richardson (1980) classification of elements. The so called A group corresponds to metals with spherical symmetry and low polarizability. Aside from the metallic form, they always have a single oxidation state (+1) or (+2) for alkalis and alkaline earth elements, respectively (Ahrland et al., 1958; Nieboer and Richardson, 1980). This implies that they are not directly influenced by the redox status of the water and that they display the

lowest stability complexes. Silicon, which also belongs to the type A group following the Nieboer and Richardson (1980) classification, displays no significant variation of concentrations throughout the ultrafiltration procedure. This suggests that Si has also to be considered as a “truly” dissolved element. Although not part of the A class group, but part of the so-called “borderline” group (Nieboer and Richardson, 1980), Ni and Co behave also as “truly” dissolved ions as do alkalis and alkaline earth metals.

### 5.2. Complexed metals

It is now widely accepted that colloidal material plays a significant role in the transport and cycling of trace metals in waters. However, as often debated elsewhere (Lyven et al., 2003, and references therein) the key question is which is the true competition between Fe- and C-based colloidal carriers for trace metals?

#### 5.2.1. The inorganic colloidal pool as a metal carrier

Iron, unlike DOC is strongly affected by the first ultrafiltration step (i.e., 30 kDa). Iron is present as large-size colloids and is almost completely removed from solution after this first step. Iron and DOC behave independently during the ultrafiltration. Aluminium, like Fe, is strongly affected by the first ultrafiltration step. Iron oxyhydroxides are though much more soluble than Al ones (Stumm and Morgan, 1996). The PF1 sample displays a strong dominance of Fe over Al, with a Fe/Al molar ratio as high as 20. In PF3 the Fe/Al molar ratio is smaller with Fe and Al concentrations being present in equal proportion. Moreover, Al concentration is well correlated with that of Fe and is only weakly dependent on DOC. This indicates a control of Al by inorganic mixed Fe/Al oxyhydroxide colloids. However, the major controlling parameter remains pH which governs solubility of Fe oxyhydroxides and therefore the release and trapping of associated trace metals.

Thorium closely follows Al, being mostly controlled by Fe/Al oxyhydroxides. Its concentration strongly decreases with the decrease of Al and Fe concentrations in the filtrate whereas it does not depend on DOC concentrations. Thorium is generally known to be immobile during weathering, accumulating in residual phases. However, its migration is possible in organic- and Fe/Al-rich waters (Pokrovsky and Schott, 2002). Mixed Fe/Al colloids are essentially responsible for these concentrations

as already observed elsewhere (Pokrovsky and Schott, 2002; Geckes et al., 2003). However, this result is different from those already published by Viers et al. (1997) where this element appears to be exclusively controlled by DOC. Even if adsorption of organic matter would result in a negative surface charge on the Fe colloid surface, the negative surface charge density would be significantly less than that on purely humic colloids so that a significant difference in electrostatic binding would still be expected. Thus, Fe/Al oxyhydroxides remain the major complexing agent of Th and in this case Th is mostly controlled by Fe/Al oxyhydroxide colloids.

Model VI tends to underestimate the proportion of metal bound to humic substances as compared to ultrafiltration data (Fig. 8). It is important to note that the <5 kDa fraction is considered as free species, which is not true as fulvic acids are characterized by lower molecular weight. Thus, if the fraction >5 kDa is considered to be the humic bound fraction and as the correlation between DOC and Fe and Al shows no common behaviour, ultrafiltration experiments should be taken into account carefully. Such a direct use of ultrafiltration results led to an overestimation of elements bound to humic substances with regard to Model VI calculations.

#### 5.2.2. The organic colloidal pool as a metal carrier

REE and (+2) cations (V, Cr, Mn, Co, Cu) of the first transition series show strong correlation with DOC. These cations are all A-Type (Nieboer and Richardson, 1980), where electrostatic binding dominates over covalent ones. It is therefore more likely for the smaller cations in each series to be associated

with strongly negatively charged organic (humic) colloids than with Fe colloids with small positive charge for circumneutral pH samples (Stumm and Morgan, 1996). Among the transition metals, the sequence of complex stability is known to be  $Mn^{2+} < Co^{2+} < Ni^{2+} < Cu^{2+}$ , a sequence known as the Irving-Williams Series. As expected Cu appears to be the most strongly bound to organic ligands as evidenced elsewhere (Buerge-Weirich et al., 2003). Xue and Sigg (1993) and Tipping et al. (2002) suggested that such strong binding has to be related to highly selective organic ligands, released by phytoplankton in order to control metal levels in their immediate environment. Pronounced differences are observed in this study as compared to what is expected for the other transition metals (Eyrolle et al., 1996) with for example Ni occurring in the “truly” dissolved pool. This may be caused by the fact that organic molecules can often be characterized by more than one functional group and hence can coordinate a metal at several positions (Stumm and Morgan, 1996). Moreover, data are consistent with dominance of organic matter complexation of REE (Johannesson et al., 2004), even if REE in the high-molecular weight fraction (i.e., >30 kDa) of PF1 sample seem to be complexed with Fe oxyhydroxides. These results are also consistent with evaluation made on model calculations on REE speciation (Pourret et al., 2007).

In contrast, U may form the oxycation  $UO_2^{2+}$  at equilibrium in oxic waters. This cation is known to have a very strong affinity for carbonate ions. While carbonate concentrations are very low in the circumneutral pH groundwaters, binding to carboxylate and/or phenolate groups, which represent major functional group in humic substances (Aiken et al., 1985), may contribute to the observed association of U with organic colloids.

Model VI tends to overestimate the proportion of metals (Cu, Cr and REE) bound to humic substances (Fig. 8). It is important to note that the <5 kDa fraction is considered as free species, which is not true as fulvic acids are characterized by lower molecular weight. Thus, if all these elements (Cu, Cr and REE) are considered to be bound to organic ligands due to the good correlation they formed with DOC, model calculation results are in good agreement for these elements.

#### 5.3. Limitations of Model VI speciation calculations

Although the 5 kDa cut-off allows very small colloids to stay in solution, the lack of integration of

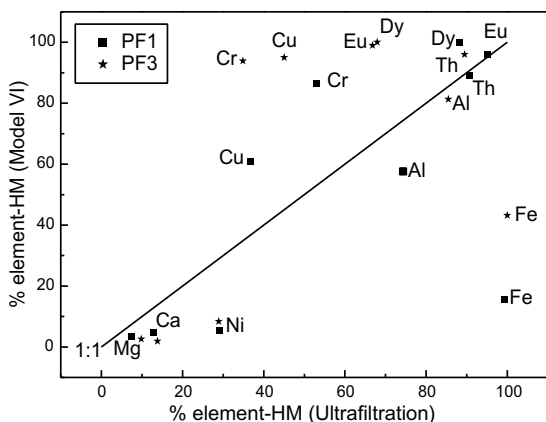


Fig. 8. Proportion of elements complexed with humic substances calculated (with Model VI) versus proportion of elements complexed with humic substances observed (by ultrafiltration).

adsorption processes onto inorganic species, as well as coprecipitation of inorganic species appear to be the major causes of disagreement between ultrafiltration data and speciation calculations for V and REE. It is then important to be aware that such a model does not take into account any uptake of metals resulting from competitive reactions between Fe- and DOC-rich colloids. Moreover as stated by Unsworth et al. (2006) model predictions of free ion activities generally do not agree with measurements (e.g., for Cd, Cu, Ni and Zn), highlighting the need for further work and difficulties in obtaining appropriate data.

The studied samples are organic-rich groundwaters with an organic pool that seems to be in excess regarding the metals available for complexation: in such samples the speciation appears to be constrained only by organic species. But, what does happen when the samples are organic-poor? Oxides, hydroxides, clay minerals, and organic matter present in the natural system all become potential sites for adsorption. Scavenging between oxyhydroxides and organic matter will occur and form ternary surface complexes (surface/ligand/metal). However, such competition is still difficult to interpret from ultrafiltration data. As evidenced by previous experimental data and calculations, it appears that the competitive reactions and the formation of ternary surface complexes on oxyhydroxides represent the major interferences of the organic ligands on metal adsorption (Buerge-Weirich et al., 2003). Cation ligand complexes can adsorb onto solid to form ternary surface complexes either as cation linked to the mineral surface over the ligand or as ligand linked to the surface over the cation. As an example, recently published experimental REE data (Davranche et al., 2004, 2005) show the impact of ternary surface complexes (humates/oxyhydroxides/REE) on metal speciation. Thus, it appears absolutely necessary in such speciation models to take into account, processes such as adsorption onto Mn and Fe oxyhydroxides, considering that the lack of such reaction precludes any true speciation to be assessed, the competition between Fe- and C-based colloidal carriers being required for constraining element geochemical cycles or element fate in polluted environments.

## 6. Conclusions

An ultracentrifugation method that allows the study of DOM-trace metal distribution at different

pore size cut-offs was tested on two shallow, circumneutral pH waters: one dissolved DOC- and Fe-rich and a second DOC-rich and Fe-poor. Data were analyzed using an ascendant hierarchical classification. Three groups of elements were identified regards to their affinity for DOM, which implies several consequences regarding their respective bioavailability or fate in the environment: (i) a “truly” dissolved behaviour group (Na, K, Rb, Ca, Mg, Ba, Sr, Si and Ni), (ii) an inorganic colloidal pool (Fe, Al and Th) and (iii) an organic colloidal pool (Cr, Mn, Co, Cu and U). However, REE and V have an ambivalent behaviour, being alternatively in the organic pool and in the inorganic pool depending on sample. Moreover, speciation calculations using Model VI were performed on both samples for some elements (Ca, Mg, Ni, Fe, Al, Th, Cr, Cu, Dy, Eu). Calculations show relatively comparable elemental distribution with regards to ultrafiltration. Although some limitations appear: a direct use of ultrafiltration results tends to overestimate the fraction of elements bound to humic material in the inorganic pool as well as, a direct use of speciation calculation results tends to overestimate the fraction of elements bound to humic material in the organic pool with regard to ultrafiltration data. Both techniques, ultrafiltration and speciation calculation, give complementary information, especially for more complex samples where inorganic and organic colloids compete. The formation of water-soluble complexes between humic materials and metal ions (radioactive, toxic or none) can increase the concentrations of these species in natural water to higher levels than expected from their thermodynamic solubilities. Since the retention, transport and fate of trace metals mediated by organic matter has still to be better constrained to understand the functional role played by DOM at the soil–water interface with regard to trace metal dynamics, further studies dedicated to space- and time-linked variations of the joined colloidal pool and trace element partitioning has to be now undertaken in waters from different DOM-rich environments.

## Acknowledgements

We thank the technical staff and undergraduates at Geosciences Rennes Laboratory for their assistance during the experimental and analytical work. Dr. R.E. Martinez is deeply acknowledged for English corrections. This research was supported by the

CPER programs “Développement de la Recherche sur la Maîtrise de la Qualité de l'Eau en Bretagne” jointly funded by the French Government and the Council of Rennes Métropole. Two anonymous reviewers are acknowledged for their useful advice and Dr. S. Smith is acknowledged for editorial handling.

## References

- Ahrland, S., Chatt, S.J., Davies, N.R., 1958. The relative affinities of ligand atoms for acceptor molecules and ions. *Quart. Rev. Chem. Soc. London* 12, 265–276.
- Aiken, G.R., McKnight, D.M., Wershaw, R.L., MacCarthy, P., 1985. Humic Substances in Soil, Sediment and Water: Geochemistry, Isolation and Characterization. John Wiley and Sons, New York.
- Bau, M., 1999. Scavenging of dissolved yttrium and rare earths by precipitating iron oxyhydroxides: experimental evidence for Ce oxidation, Y-Ho fractionation, and lanthanide tetrad effect. *Geochim. Cosmochim. Acta* 63, 67–77.
- Benedetti, M.F., Van Riemsdijk, W.H., Koopal, L.K., Kinniburgh, D.G., Goodey, D.C., Milne, C.J., 1996. Metal ion binding by natural organic matter: from the model to the field. *Geochim. Cosmochim. Acta* 60, 2503–2513.
- Bennett, P., Siegel, D.I., 1987. Increased solubility of quartz in water due to complexing by organic compounds. *Nature* 326, 684–686.
- Braun, J.-J., Ndam Ngoupayou, J.R., Viers, J., Dupré, B., Bedimo Bedimo, J.-P., Boeglin, J.L., Robain, H., Nyeck, B., Freydier, R., Sigha Nkamdjou, L., Rouiller, J., Muller, J.-P., 2005. Present weathering rates in a humid tropical watershed: Nsimi, South Cameroon. *Geochim. Cosmochim. Acta* 69, 357–387.
- Buerge-Weirich, D., Behra, P., Sigg, L., 2003. Adsorption of copper, nickel, and cadmium on goethite in the presence of organic ligands. *Aquat. Chem.* 9, 65–85.
- Buffle, J., 1988. Complexation Reactions in Aquatic Systems: An Analytical Approach. Ellis Norwood, Chichester.
- Cabaniss, S.E., Shuman, M.S., 1988. Copper binding by dissolved organic matter: I. Suwannee River fulvic acid equilibria. *Geochim. Cosmochim. Acta* 52, 185–193.
- Christensen, J.B., Jensen, D.L., Christensen, T.H., 1996. Effect of dissolved organic carbon on the mobility of cadmium, nickel, and zinc in leachate polluted groundwater. *Water Res.* 30, 3037–3049.
- Curmi, P., Durand, P., Gascuel-Odoux, C., Hallaire, V., Mérot, P., Robin, P., Trolard, F., Walter, C., Bourrié, G., 1995. Le programme CORMORAN-INRA: de l'importance du milieu physique dans la régulation biogéochimique de la teneur en nitrate des eaux superficielles. *J. Eur. Hydrol.* 26, 37–56.
- Dabard, M.P., Loi, A., Peucat, J.J., 1996. Zircon typology combined with Sm–Nd whole - rock isotope analysis to study Brioverian sediments from the Armorican Massif. *Sed. Geol.* 101, 243–260.
- Dahlqvist, R., Benedetti, M.F., Andersson, K., Turner, D., Larsson, T., Stolpe, b., Ingri, J., 2004. Association of calcium with colloidal particles and speciation of calcium in the Kalix and Amazon rivers. *Geochim. Cosmochim. Acta* 68, 4059–4075.
- Davranche, M., Pourret, O., Gruau, G., Dia, A., 2004. Impact of humate complexation on the adsorption of REE onto Fe oxyhydroxide. *J. Colloid Interf. Sci.* 277, 271–279.
- Davranche, M., Pourret, O., Gruau, G., Dia, A., Le Coz-Bouhnik, M., 2005. Adsorption of REE(III)-humate complexes onto MnO<sub>2</sub>: experimental evidence for cerium anomaly and lanthanide tetrad effect suppression. *Geochim. Cosmochim. Acta* 69, 4825–4835.
- Dia, A., Gruau, G., Olivie-Lauquet, G., Riou, C., Molénat, J., Curmi, P., 2000. The distribution of rare earth elements in groundwaters: assessing the role of source-rock composition, redox changes and colloidal particles. *Geochim. Cosmochim. Acta* 64, 4131–4151.
- Dillon, W.R., Goldstein, M., 1984. Multivariate Analysis: Methods and Applications. Wiley, New York.
- Dupré, B., Viers, J., Dandurand, J.-L., Polve, M., Bénézeth, P., Vervier, P., Braun, J.-J., 1999. Major and trace elements associated with colloids in organic-rich river waters: ultrafiltration of natural and spiked solutions. *Chem. Geol.* 160, 63–80.
- Durand, P., Juan Torres, J.L., 1996. Solute transfer in agricultural catchments: the interest and limits of mixing models. *J. Hydrol.* 181, 1–22.
- Eyrolle, F., Benedetti, M.F., Benaim, J.Y., Février, D., 1996. The distributions of colloidal and dissolved organic carbon, major elements, and trace elements in small tropical catchments. *Geochim. Cosmochim. Acta* 60, 3643–3656.
- Geckeis, H., Ngo Manh, Th., Bouby, M., Kim, J.I., 2003. Aquatic colloids relevant to radionuclide migration: characterization by size fractionation and ICP-mass spectrometric detection. *Colloids Surf. A: Physicochem. Engin. Aspects* 217, 101–108.
- Gruau, G., Dia, A., Olivie-Lauquet, G., Davranche, M., Pinay, G., 2004. Controls on the distribution of rare earth elements in shallow groundwaters. *Water Res.* 38, 3576–3586.
- Iler, R.K., 1979. In: Yariv, S., Cross, H. (Eds.), *The Geochemistry of Colloid Systems for Earth Scientists*. Springer-Verlag, Berlin, Heidelberg and New York, 1979 (Book review). *J. Colloid. Interface Sci.* 72, 177–178.
- Ingri, J., Widerlund, A., Land, M., Gustafsson, O., Andersson, P., Ohlander, B., 2000. Temporal variations in the fractionation of the rare earth elements in a boreal river: the role of colloidal particles. *Chem. Geol.* 166, 23–45.
- Jaffrézic, A., 1997. Géochimie des éléments métalliques, des nitrates et du carbone organique dissous dans les eaux et les sols hydromorphes. Agriculture intensive et qualité des eaux dans les zones humides en Bretagne. Ph.D. Diss., Univ. Rennes I.
- Johannesson, K.H., Tang, J., Daniels, J.M., Bounds, W.J., Burdige, D.J., 2004. Rare earth element concentrations and speciation in organic-rich blackwaters of the Great Dismal Swamp, Virginia, USA. *Chem. Geol.* 209, 271–294.
- Lyven, B., Hassellöv, M., Turner, D.R., Haraldsson, C., Andersson, K., 2003. Competition between iron- and carbon-based colloidal carriers for trace metals in a freshwater assessed using flow field-flow fractionation coupled to ICP MS. *Geochim. Cosmochim. Acta* 67, 3791–3802.
- Macalady, D.L., 1998. Perspectives in Environmental Chemistry. Oxford University Press.
- McCarthy, J.F., Sanford, W.E., Stafford, P.L., 1998. Lanthanide field tracers demonstrate enhanced transport of transuranic radionuclides by natural organic matter. *Environ. Sci. Technol.* 32, 3901–3906.

- Molénat, J., Durand, P., Gascuel-Odoux, C., Davy, P., Gruau, G., 2002. Mechanisms of nitrate transfer from soil to stream in an agricultural watershed of French Brittany. *Water Air Soil Pollut.* 133, 161–183.
- Nieboer, E., Richardson, D.H.S., 1980. The replacement of the nondescriptive term heavy metals by a biologically and chemically significant classification of metal ions. *Environ. Pollut. Ser. B* 1, 3–26.
- Pauwels, H., Kloppmann, W., Foucher, J.-C., Martelat, A., Fritzsche, V., 1998. Field tracer test for denitrification in a pyrite-bearing schist aquifer. *Appl. Geochem.* 13, 767–778.
- Pellerin, J., Van Vliet-Lanoë, B., 1998. Le bassin du Coët-Dan au cœur du Massif armoricain. 2. Analyse cartographique de la région de Naizin. In: Cheverry, C. (Ed.), *Agriculture Intensive et Qualité des Eaux*. pp. 17–24. INRA.
- Pokrovski, O.S., Schott, J., 1998. Experimental study of the complexation of silicon and germanium with aqueous organic species: implications for germanium and silicon transport and Ge/Si ratio in natural waters. *Geochim. Cosmochim. Acta* 62, 3413–3428.
- Pokrovsky, G.S., Schott, J., 2002. Iron colloids/organic matter associated transport of major and trace elements in small boreal rivers and their estuaries (NW Russia). *Chem. Geol.* 190, 141–179.
- Pourret, O., Davranche, M., Gruau, G., Dia, A., 2007. Organic complexation of rare earth elements in natural waters: evaluating model calculations from ultrafiltration data. *Geochim. Cosmochim. Acta*, doi:10.1016/j.gca.2007.04.001.
- Schmitt, D., Saravia, F., Frimmel, F.H., Schuessler, W., 2003. NOM-facilitated transport of metal ions in aquifers: importance of complex-dissociation kinetics and colloid formation. *Water Res.* 37, 3541–3550.
- Shapiro, J., 1964. Effect of yellow organic acids on iron and other metals in water. *Am. Water Works Assoc. J.* 55, 1062–1082.
- Sholkovitz, E.R., 1995. The aquatic chemistry of rare earth elements in rivers and estuaries. *Aquat. Geochem.* 1, 1–34.
- Sigg, L., Xue, H., Kistler, D., Schönenberger, R., 2000. Size fractionation (dissolved, colloidal and particulate) of trace metals in the Thur river, Switzerland. *Aquat. Geochem.* 6, 413–434.
- Stumm, W., Morgan, J.J., 1996. *Aquatic chemistry*. John Wiley and Sons, New York.
- Tanizaki, Y., Shimokawa, T., Nakamura, M., 1992. Physico-chemical speciation of trace elements in river waters by size fractionation. *Environ. Sci. Technol.* 26, 1433–1444.
- Tipping, E., 1998. Humic Ion-Binding Model VI: an improved description of the interactions of protons and metal ions with humic substances. *Aquat. Geochem.* 4, 3–48.
- Tipping, E., Hurley, M.A., 1992. A unifying model of cation binding by humic substances. *Geochim. Cosmochim. Acta* 56, 3627–3641.
- Tipping, E., Rey-Castro, C., Bryan, S.E., Hamilton-Taylor, J., 2002. Al(III) and Fe(III) binding by humic substances in freshwaters, and implication for trace metal speciation. *Geochim. Cosmochim. Acta* 66, 3211–3224.
- Tosiani, T., Loubet, M., Viers, J., Valladon, M., Tapia, J., Marrero, S., Yanes, C., Ramirez, A., Dupré, B., 2004. Major and trace elements in river-borne materials from the Cuyuni basin (southern Venezuela): evidence for organo-colloidal control on the dissolved load and element redistribution between the suspended and dissolved load. *Chem. Geol.* 211, 305–334.
- Unsworth, E.R., Warnken, K.W., Zhang, H., Davison, W., Black, F., Buffle, J., Cao, J., Cleven, R., Galceran, J., Gunkel, P., Kalis, E., Kistler, D., Van Leeuwen, H.P., Martin, M., Noël, S., Nur, Y., Odzak, N., Puy, J., Van Riemsdijk, W., Sigg, L., Temminghoff, E., Tercier-Waeber, M.-L., Toepperwien, S., Town, R.M., Weng, L., Xue, H., 2006. Model predictions of metal speciation in freshwaters compared to measurements by in situ techniques. *Environ. Sci. Technol.* 40, 1942–1949.
- Viers, J., Dupré, B., Polvé, M., Schott, J., Dandurand, J.-L., Braun, J.-J., 1997. Chemical weathering in the drainage basin of a tropical watershed (Nsimi-Zoetele site, Cameroon): comparison between organic-poor and organic-rich waters. *Chem. Geol.* 140, 181–206.
- Wells, M.L., Goldberg, E.D., 1991. Occurrence of small colloids in sea water. *Nature* 353, 342–346.
- Xue, H., Sigg, L., 1993. Free cupric ion concentration and Cu(II) speciation in a eutrophic lake. *Limnol. Oceanog.* 38, 1200–1213.
- Xue, H., Kistler, D., Sigg, L., 1995. Competition of copper and zinc for strong ligands in a eutrophic lake. *Limnol. Oceanog.* 40, 1142–1152.

## Colloidal Control on the Distribution of Rare Earth Elements in Shallow Groundwaters

Olivier Pourret · Gérard Gruau · Aline Dia · Mélanie Davranche · Jérôme Molénat

Received: 4 May 2009 / Accepted: 24 July 2009 / Published online: 12 August 2009  
© Springer Science+Business Media B.V. 2009

**Abstract** A 7-year monitoring period of rare earth element (REE) concentrations and REE pattern shapes was carried out in well water samples from a 450 m long transect setup in the Kervidy/Coët-Dan experimental catchment, France. The new dataset confirms systematic, topography-related REE signatures and REE concentrations variability but challenges the validity of a groundwater mixing hypothesis. Most likely, this is due to REE preferential adsorption upon mixing. However, the coupled mixing–adsorption mechanism still fails to explain the strong spatial variation in negative Ce anomaly amplitude. A third mechanism—namely, the input into the aquifer of REE-rich, Ce anomaly free, organic colloids—is required to account for this variation. Ultrafiltration results and speciation calculations made using Model VI agree with this interpretation. Indeed, the data reveal that Ce anomaly amplitude downslope decrease corresponds to REE speciation change, downhill groundwaters REE being mainly bound to organic colloids. Water table depth monitoring shows that the colloid source is located in the uppermost, organic-rich soil horizons, and that the colloid input occurs mainly when water table rises in response to rainfall events. It appears that the colloids amount that reaches groundwater increases downhill as the distance between soil organic-rich horizons and water table decreases. Topography is, therefore, the ultimate key factor that controls Ce anomaly spatial variability in these shallow groundwaters. Finally, the <0.2 µm REE fraction ultimately comes from two solid sources in these groundwaters: one located in the deep basement schist; another located in the upper, organic-rich soil horizon.

---

O. Pourret · G. Gruau · A. Dia · M. Davranche  
CNRS, UMR 6118, Géosciences Rennes, Université Rennes 1, FR CAREN, Campus Beaulieu, 35042  
Rennes Cedex, France  
e-mail: grua@univ-rennes1.fr

O. Pourret (✉)  
Département Géosciences, Institut Polytechnique LaSalle-Beauvais, 19 rue Pierre Waguet, 60026  
Beauvais Cedex, France  
e-mail: olivier.pourret@lasalle-beauvais.fr

J. Molénat  
INRA-Agrocampus Rennes, UMR 1069 Sol, Agronomie Spatialisation, FR CAREN, 65 rue de Saint-Brieuc, 35042 Rennes Cedex, France

**Keywords** Rare earth elements · Dissolved organic matter · Speciation modeling · Natural waters · Ultrafiltration

## 1 Introduction

Numerous studies over the past two decades have been dedicated to the aquatic geochemistry of rare earth elements (REE; Byrne and Sholkovitz 1996; De Baar et al. 1988, 1991; Duncan and Shaw 2003; Elderfield and Greaves 1982; Elderfield et al. 1990; Gosselin et al. 1992; Johannesson et al. 1997, 2000; Johannesson and Hendry 2000; Lawrence et al. 2006; Sholkovitz 1995; Smedley 1991). In particular, REEs have received much attention from hydrochemists in recent years because of their potential to be used as sensitive tracers of water–rock interaction processes and/or of groundwater mixing. However, this use of REE has to be developed with caution regard to the numerous processes and factors that may modify REE signatures in groundwaters. For example, processes such as REE complexation by inorganic ligands, or REE adsorption onto mineral phases can fractionate the REE patterns inherited from aquifer materials (e.g., De Carlo et al. 1998; Coppin et al. 2002; Johannesson et al. 1999; Tang and Johannesson 2005). REE complexation with natural organic ligands can also affect REE signatures of shallow groundwaters (Dia et al. 2000; Dupré et al. 1999; Ingri et al. 2000; Johannesson et al. 2004; Pourret et al. 2007a, b; Sonke and Salters 2006; Stern et al. 2007; Tanizaki et al. 1992; Viers et al. 1997), as can changes in pH that influence REE adsorption behavior (e.g., Byrne and Sholkovitz 1996; Johannesson and Burdige 2007). A thorough knowledge of the processes and factors that control REE concentrations and REE patterns in groundwater is thus required before the REE can be used as reliable hydrochemical tracers.

In this respect, it is important to understand the origin and significance of the systematic, topography-related spatial variability of REE signatures that occur in shallow groundwaters flowing in aquifer rocks of homogeneous composition. Three studies conducted on such groundwaters from Western Europe (Kervidy/Coët-Dan; Dia et al. 2000 and Petit Hermitage catchments; Gruau et al. 2004) and Western Africa (Goyoum area; Braun et al. 1998) indeed revealed the same extreme spatial variation of REE signatures. In all three cases, the same progressive disappearance of a negative Ce anomaly (i.e., registering redox equilibrium between dissolved  $\text{Ce}^{3+}$  and  $\text{Ce}^{4+}$  species) and the same progressive decrease in REE concentrations and of the Light REE (LREE; i.e., from La to Eu) over the Heavy REE (HREE; i.e., from Gd to Lu) ratio appear from top to bottom of the toposequence. In the case of the Kervidy/Coët-Dan catchment, this spatial change in REE signatures was interpreted as due to groundwater mixing processes (Dia et al. 2000).

However, bottomland domain groundwaters showing no negative Ce anomaly are generally organic rich and less acidic than groundwaters from upland domains showing a large negative Ce anomaly (e.g., Gruau et al. 2004). Thus, it is possible that other factors such as pH variation and/or organic matter complexation also play a role in the observed gradients. In this study, the spatial variation of REE signatures in the shallow groundwaters of the Kervidy/Coët-Dan catchment (France) was re-investigated in more detail. This was realized by the regular sampling of these groundwaters over a 7-year period (from March 2000 to July 2007) coupled with ultrafiltration experiments (i.e., 30, 10, and 5 kDa) and speciation modeling using the Humic Ion-Binding Model VI (Tipping 1998). The primary aims of this study are (1) to test the temporal stability of the spatially variable REE signatures that occur in these groundwaters; (2) to evaluate the respective roles of organic

matter, pH and groundwater mixing on this variation and (3) to identify the ultimate sources of REE in the aquifer system.

## 2 Hydrogeology and Previous Hydrochemical Data

The Kervidy/Coët-Dan catchment is located in Naizin, a small rural village located in the center of Brittany, France (latitude:  $48^{\circ}$ ; longitude:  $357^{\circ}10'$ ; Fig. 1) and supplies the Coët-Dan tributary of the Evel river. The catchment drains a surface of  $4.9 \text{ km}^2$ . The Kervidy/Coët-Dan catchment is a sub-basin of the Naizin catchment ( $12 \text{ km}^2$ ). The bedrock is made of fissured and fractured upper Proterozoic schists (Dabard et al. 1996). The soils, developed into a loamy material derived from bedrock weathering and eolian Quaternary deposits, exhibit facies variations, which are locally, dominated by silt, clay or sandstone materials (Pellerin and Van Vliet-Lanoë 1998). The mineralogical composition of schist was determined from drill-cutting analysis and includes (in decreasing relative proportion) quartz, muscovite, chlorite, K-feldspar and plagioclase (Pauwels et al. 1998). The soil horizons comprise a large number of secondary mineral phases including illite, smectite, kaolinite, various Fe-oxides and Fe-oxyhydroxides (hematite, goethite...) and Mn oxides

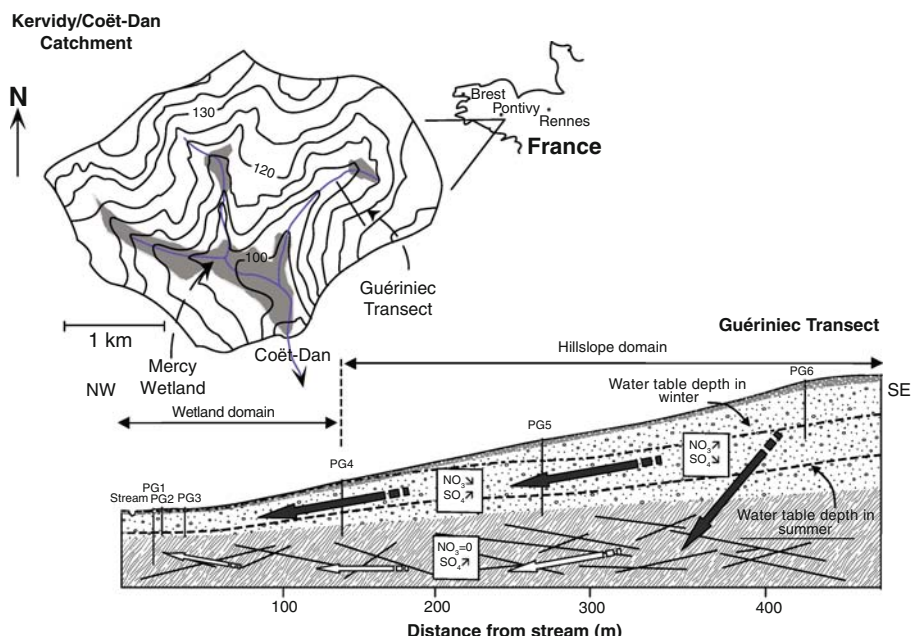


**Fig. 1** Location map of the Kervidy/Coët-Dan catchment (Brittany, France) showing the Guériniec transect and the groundwater sampling wells setup along this transect. Average groundwater levels for wet (winter) and dry (summer) periods are shown for comparison. Scheme conceptualizing the hydrochemical behavior of the Guériniec transect is adapted from Dia et al. (2000) and Molénat et al. (2002). Black arrows correspond to nitrate-rich fluxes, whereas white arrows correspond to nitrate-poor fluxes. The small black arrows on nitrate and sulfate white boxes correspond to increasing or decreasing contents. Shaded areas located close to the channel network on the catchment map indicate the location of wetland zones. The Mercy area corresponds to the wetland zone where DOC-rich, shallow (<0.5 m) groundwaters from piezometers PF1 and PF3 were investigated for major and trace elements including REE geochemistry by Pourret et al. (2007a, c)

(Pauwels et al. 1998). Both the soils and the bedrock schist of the Kervidy/Coët-Dan catchment display shale-like REE pattern signatures (Dia et al. 2000).  $(\text{LREE}/\text{HREE})_{\text{UCC}}$  ratios vary little from the soil surface down to the fresh schist horizons, always remaining close to 1.0. UCC subscript refers to normalization with respect to the estimated average composition of the upper continental crust (UCC; Taylor and McLennan 1985). Moreover, negative Ce anomalies are not observed, neither in the fresh schist nor in the different soil horizons (Fig. 6 in Dia et al. 2000).

The land use in the Kervidy/Coët-Dan catchment is intensive farming dominated by maize, wheat and temporary pastures for dairy production and a high density of indoor pig-stock breeding. This land use has caused heavy nitrate pollution of the catchment waters with a mean nitrate concentration in the upland up to  $140 \text{ mg L}^{-1} \text{ NO}_3^-$ , which decreased along the flow paths toward the stream to ca.  $80 \text{ mg L}^{-1} \text{ NO}_3^-$  (Molénat et al. 2002, 2008).

Previous hydrochemical studies (Dia et al. 2000; Durand and Juan Torres 1996; Molénat et al. 2002, 2008) showed that the Kervidy/Coët-Dan groundwater could be summarized by two spatially distributed hydrogeological and chemical domains. The first domain includes the bottomland areas or wetland domains. In these domains, the water table usually reaches the organic-rich upper soil horizons during the wet season (Fig. 1), namely, in winter and spring, leading to development of temporary reducing conditions. The shallowest levels of the water table (i.e., <1 m deep) in the wetlands comprise colored, DOC-rich ( $5 < \text{DOC} < 40 \text{ mg L}^{-1}$ ) groundwater, whereas deeper in the water table (i.e., >1 m deep), groundwater is colorless and DOC-poor (i.e., <5 mg L<sup>-1</sup>). Nitrate, sulfate and REE concentrations vary vertically in the wetland groundwaters. In general, nitrate concentrations are low (<0.1 mg L<sup>-1</sup>) in the upper (<1 m), organic-rich (<30 mg L<sup>-1</sup>) groundwater, high below 1 m (up to 50 mg L<sup>-1</sup>), then decreasing again below 3 m to reach 0 mg L<sup>-1</sup> at a depth of ca. 4 m. REE concentrations are high in the shallow organic-rich groundwater (up to 15 µg L<sup>-1</sup>), then decreasing with depth (i.e., at higher than 4 m depth) to reach  $10^{-2}$  times this concentration. Sulfate concentration varies oppositely with the highest concentrations (ca. 16 mg L<sup>-1</sup>) below 4 m. The second domain includes the hillslope domains, where the water table always remains a few meters below the soil surface (Fig. 1). Groundwaters in these domains are always oxidizing, colorless and DOC-poor ( $\text{DOC} < 5 \text{ mg L}^{-1}$ ). As in the wetland domains, the composition of the groundwater below the hillslope domains varies vertically: above ca. 15 m, groundwaters exhibit high nitrate (up to 200 mg L<sup>-1</sup>, locally), high REE (up to 30 µg L<sup>-1</sup>), but low sulfate concentrations (<5 mg L<sup>-1</sup>). By contrast, below 15 m, nitrate and REE concentrations are much lower (close to 0.2 mg L<sup>-1</sup>, detection limit, and <0.1 µg L<sup>-1</sup>, respectively), whereas sulfate concentrations increase markedly, from 1 to 20 mg L<sup>-1</sup>.

Previous investigations of the REE geochemistry in groundwaters of the Kervidy/Coët-Dan catchment (Dia et al. 2000; Pourret et al. 2007a, c) showed a systematic, topography-related variation of REE signatures in the upper part (i.e., at depth between ca. 3 and 15 m) of the DOC-poor groundwater. An upslope development of a large, negative Ce anomaly and a progressive enrichment of the LREE over the HREE were also noted. Based on the chemical variability of the groundwater composition with depth and taking into account the hydrological modeling studies, this topography-related variation of groundwater REE signatures was interpreted as a progressive mixing along the hillslope of the upper nitrate and REE-rich water in the upland domain and a return flow of the deep, denitrified, REE-poor groundwater. Secondly, it was demonstrated that REE in the DOC-rich, uppermest part (i.e., <1 m) of the wetland water table did not occur as free dissolved species but were bound to organic colloids (Pourret et al. 2007a, c). As previously shown by Davranche et al. (2005, 2008) and Pourret et al. (2007a) the organic speciation of the REE prevent any

oxidative scavenging and preferential removal of Ce from the solution, hence explaining why these waters do not show any negative Ce anomaly.

### 3 Sampling and Analytical Procedure

Six wells were sampled for the purpose of this study. These six wells (PG1 to PG6) all come from a transect set perpendicular to the topographic slope (i.e., along a direction parallel to the groundwater flow path) in the eastern part of the catchment the so-called Guériniec transect (Fig. 1). These wells collect groundwater at a depth between –3 and –6 m. Water samples were regularly collected (every 3 months on average) from March 2000 to July 2007.

#### 3.1 Field Measurements and Sample Preparation

Physico-chemical parameters (pH, Eh, temperature and conductivity) were directly measured in the field. The pH was measured with a combined Sentix 50 electrode after a calibration performed with WTW standard solutions (pH = 4.01 and 7.00 at 25°C). The accuracy of the pH measurement is  $\pm 0.05$  pH unit. Conductivity was measured with a special conductivity cell (WTW TetraCon 325). Conductivity ( $\sigma$ ) values are presented in  $\mu\text{S cm}^{-1}$ . Eh was measured using a platinum combination electrode (Metler Pt 4805). Electrodes are inserted into a cell constructed to minimize diffusion of atmospheric oxygen into the sample during measurement. Eh values are presented in mV relative to standard hydrogen electrode.

Groundwater samples were pumped using Teflon tubing connected to a polyethylene syringe. About 60 mL of each sample was immediately filtered on site through 0.2  $\mu\text{m}$  cellulose acetate filter (Sartorius Minisart). An aliquot of 30 mL was acidified and subsequently used to measure REE concentrations. The remaining 30 mL was not acidified and used to measure alkalinity (only for May and November 2004 sampling campaign), nitrate, sulfate and DOC concentrations. During the November 2004 sampling campaign, an extra 1 L aliquot was collected from PG3 and PG4 piezometers to perform ultrafiltration experiments. This extra aliquot was filtered in the laboratory through 0.2  $\mu\text{m}$  cellulose acetate membrane using a Sartorius Teflon filtration unit. About 30 mL of the filtrate was acidified and used to measure REE concentrations, while 10 mL was used to measure nitrate, sulfate and DOC content. Ultrafiltration experiments were performed with the remaining filtrate.

#### 3.2 Ultrafiltration

Ultrafiltration experiments were performed using 15 mL centrifugal tubes (Millipore Amicon Ultra-15) equipped with permeable membranes of decreasing pore sizes (<30, <10, and <5 kDa with 1 Da (Dalton) = 1 g mol $^{-1}$  for H). Each centrifugal filter device was washed and rinsed with HCl 0.1 mol L $^{-1}$  and MilliQ water twice before use. The starting filtrate was passed through 0.2  $\mu\text{m}$  filter, and then aliquots of these filtrates were passed through membranes of smaller pore sizes. All ultrafiltrations of the 0.2  $\mu\text{m}$  filtrates were done in parallel. The centrifugations were performed using a Jouan G4.12 centrifuge equipped with swinging bucket at about 3,000g for 20 and 30 min, for 30, 10 and 5 kDa devices, respectively. All experiments were carried out at room temperature: 20  $\pm$  2°C. The ultrafiltration procedure prevents any mass balance between the filtrate and the

retentate to be achieved because the retentate volumes are limited (0.2 mL). However, as the same material was used for all filtrations, molecular size exclusion rather than adsorption onto membranes should control the colloid distributions between ultrafiltrates. Such a feature has been further tested using synthetic REE solution (Pourret et al. 2007b). All ultrafiltrations were performed in duplicates. A good reproducibility was observed for DOC and major and trace elements concentrations. Duplicates were better than 5% for most elements except for some trace elements in the lower pore size cutoff fraction (i.e., in the <5 kDa fraction, about 10%). Further information on the ultrafiltration procedure can be found in Pourret et al. (2007c).

### 3.3 Chemical Analyses

Major anions ( $\text{SO}_4^{2-}$  and  $\text{NO}_3^-$ ) concentrations were measured by ionic chromatography (Dionex DX-120) with an uncertainty below  $\pm 4\%$  (by using a Dionex seven anions standard solution). Rare earth element concentrations were determined by ICPMS (Agilent 4500), using indium as an internal standard. The method is described in more detail in Davranche et al. (2004). The international geostandard SLRS-4 was used to check the validity and reproducibility of the results. Typical uncertainties including all error sources are below  $\pm 5\%$  for all the trace elements, whereas for major cations, the uncertainty lies between  $\pm 2$  and  $\pm 5\%$ , depending on the concentration levels. Dissolved organic carbon concentrations were analyzed on a total organic carbon analyzer (Shimadzu TOC-5050A). Accuracy of DOC measurement is estimated at  $\pm 5\%$  (by using a standard solution of K-biphtalate). Alkalinity was determined by potentiometric titration with an automatic titrating device (794 Basic Titrino Methrom). The uncertainty is better than 5%.

All procedures (sampling, filtration, storing and analysis) were carried out in order to minimize contamination. Samples were stored in acid-washed Nalgene polypropylene containers before analyses. Blank concentrations for DOC and REE were  $<0.5 \text{ mg L}^{-1}$  and  $<1 \text{ ng L}^{-1}$ , respectively. All reported DOC concentrations are blank corrected (maximum correction = 8%). For the REE, there was no need for blank corrections, because the sample concentrations were systematically two to three orders of magnitude higher than blank levels. The instrumental error on REE analysis in our laboratory, as established from repeated analyses of multi-REE standard solution (Accu Trace Reference, USA) and of the SLRS-4 water standard, is below 2% (e.g., Davranche et al. 2004; Yeghicheyan et al. 2001). Interference corrections are detailed in Davranche et al. (2004).

### 3.4 Speciation Calculation

Speciation calculations were performed using the computer program WHAM 6 (Version 6.0.13) including Humic Ion-Binding Model VI (Model VI; Tipping 1998). It was used to calculate the speciation of REE in three wells, namely, PG3, PG4 and PG5 sampled in May and November 2004. It must be unfortunately noted that data necessary to model speciation were only available for these three wells (PG6 well was empty as the water table was below, and PG1 and PG2 REE concentrations were below the detection limits at these two sampling dates). Model VI was modified by building a database that included  $\log K_{\text{MA}}$  for the whole REE series and values for REE complexation with HM, along with well-accepted infinite-dilution (25°C) stability constants for REE inorganic complexes (hydroxide, sulfate and carbonate; Klungness and Byrne 2000; Luo and Byrne 2004; Schijf and Byrne 2004). Model VI is described in more detail in Tipping (1998), and adaptation of Model VI to REE is detailed in Pourret et al. (2007a, b). Model VI parameters for humic

acid (HA) and fulvic acid (FA) and REE are presented in Table 4 (Appendix). As Model VI does not consider saturation index and mineral precipitation, inorganic speciation was further performed using PHREEQC (Parkhurst and Appelo 1999). For this purpose, Nagra/PSI database (Hummel et al. 2002) was used and updated including the same well-accepted infinite-dilution (25°C) stability constants for REE inorganic complexes (hydroxide, sulfate and carbonate; Klungness and Byrne 2000; Luo and Byrne 2004; Schijf and Byrne 2004).

## 4 Results

### 4.1 Spatial Variability of Water Chemistry and REE Signatures

The entire dataset can be obtained from the authors on request. Average REE, DOC,  $\text{SO}_4^{2-}$ ,  $\text{NO}_3^-$ , major cations (including Mn and Fe), Eh, conductivity, temperature and alkalinity concentrations, as well as average pH values for the six investigated wells are presented in Table 1 and further displayed on Fig. 2. REE patterns are portrayed in Fig. 3.

As can be seen on Fig. 2,  $\text{SO}_4^{2-}$  concentrations increase (from 0.7 to 16.8 mg L<sup>-1</sup>) as groundwater moves downslope toward the stream, whereas  $\text{NO}_3^-$  concentrations show the opposite trend (i.e., concentrations decrease along the same flow path: from 124 to  $\leq 1$  mg L<sup>-1</sup>). The pH values also vary spatially, with groundwaters from upland wells PG6 and PG5 being slightly more acidic (i.e., pH between 5.6 and 5.8) than groundwaters from bottomland wells PG1 and PG2 (i.e., pH between 6.5 and 6.2). Groundwaters are oxidized and display relatively the same oxidation state (Eh values ranging from 484 to 406 mV, from top to bottom of the toposequence). Alkalinity values determined during May 2004 and November 2004 were lower in upland domain wells (i.e., 100–300  $\mu\text{mol L}^{-1}$  for PG5 water) compared to bottomland wells (i.e., between 1,241 and 3,741  $\mu\text{mol L}^{-1}$  in PG1 well). This increase in alkalinity values downslope is consistent with the observed downslope pH increase (from 5.4 to 6.6 on May 2004, and from 6.0 to 7.1 on November 2004 from PG5 to PG1, respectively). Major elements and pH variations thus provide signature of end-members and help validating the water mixing model that consist of a mixing of nitrate-rich, low pH subsurface water with nitrate-poor, comparatively higher pH, deep groundwater in agreement with studies of Dia et al. (2000) and Molénat et al. (2002).

Rare earth element concentrations and profiles also exhibit a systematic spatial variability in these groundwaters, thereby confirming the previous findings by Dia et al. (2000). As can be seen in Figs. 1 and 3, REE concentrations progressively decrease from wells PG6 to PG1 (from 17.3 to 0.028 mg L<sup>-1</sup>, on average). The size of the negative Ce anomaly progressively decreases along the inferred groundwater flow path as well ( $\text{Ce}/\text{Ce}^* = 0.07$  in PG5 groundwater compared to 0.77 in PG1 groundwater; Fig. 4). Secondly, a progressive depletion of the LREE over the HREE is noted from PG6 [ $(\text{LREE}/\text{HREE})_{\text{UCC}} = 3.2$ ] to PG1 wells [ $(\text{LREE}/\text{HREE})_{\text{UCC}} = 0.9$ ; Fig. 4].

### 4.2 Temporal Stability of REE Signatures

Although REE patterns shape widely spatially vary in Guériniec groundwaters, they appear to be remarkably temporally stable. Indeed, both the  $\text{Ce}/\text{Ce}^*$  value and the  $(\text{LREE}/\text{HREE})_{\text{UCC}}$  ratio remain virtually constant in any given piezometer (Fig. 4). This feature was already emphasized by Dia et al. (2000) and Olivié-Lauquet et al. (2001). However,

**Table 1** Average concentrations for Guériniec groundwaters

| Well no.:                     | PG1 mean | RSD    | PG2 mean | RSD    | PG3 mean | RSD    | PG4 mean | RSD    | PG5 mean | RSD    | PG6 mean | RSD    |
|-------------------------------|----------|--------|----------|--------|----------|--------|----------|--------|----------|--------|----------|--------|
| pH                            | 6.6      | 0.2    | 6.2      | 0.3    | 5.8      | 0.4    | 5.7      | 0.4    | 5.9      | 0.6    | 5.8      | 0.4    |
| Eh                            | 406      | 94     | 471      | 45     | 465      | 43     | 465      | 45     | 414      | 91     | 484      | 24     |
| Temperature                   | 12.6     | 2.9    | 12.2     | 3.4    | 12.2     | 3.6    | 12.5     | 3.3    | 12.8     | 3.2    | 10.5     | 3.1    |
| Conductivity                  | 204      | 19     | 227      | 17     | 244      | 33     | 286      | 39     | 285      | 33     | 341      | 126    |
| Cl <sup>-</sup>               | 16.06    | 0.75   | 26.87    | 1.47   | 31.56    | 2.24   | 32.84    | 2.01   | 28.14    | 1.27   | 28.18    | 3.13   |
| SO <sub>4</sub> <sup>2-</sup> | 15.68    | 0.45   | 6.96     | 1.10   | 4.88     | 1.57   | 5.30     | 2.98   | 1.63     | 0.53   | 2.51     | 0.89   |
| NO <sub>3</sub> <sup>-</sup>  | 0.76     | 0.87   | 41.60    | 4.04   | 63.78    | 13.06  | 91.97    | 9.13   | 97.16    | 6.29   | 104.45   | 15.03  |
| Alkalinity                    | 2,491    | 1,768  | 660      | 84     | 347      | 207    | 193      | 117    | 200      | 141    | 2,491    | 1,768  |
| DOC                           | 1.05     | 0.90   | 0.87     | 0.68   | 2.73     | 2.15   | 1.28     | 0.74   | 0.53     | 0.14   | NA       | NA     |
| Na                            | 19,247   | 1,488  | 18,461   | 1,500  | 18,287   | 1,273  | 18,855   | 1,782  | 15,545   | 1,198  | 16,867   | 1,158  |
| K                             | 613      | 119    | 534      | 53     | 1,140    | 479    | 2,629    | 1,062  | 1,030    | 133    | 2,712    | 806    |
| Ca                            | 5,927    | 250    | 6,768    | 333    | 7,431    | 1,362  | 9,580    | 2,671  | 7,060    | 395    | 18,561   | 1,659  |
| Mg                            | 10,308   | 930    | 11,690   | 1,124  | 13,208   | 1,348  | 15,578   | 1,951  | 17,869   | 1,200  | 14,654   | 2,591  |
| Mn                            | 317.80   | 117.89 | 6.10     | 17.88  | 15.54    | 7.59   | 46.02    | 85.64  | 9.97     | 2.73   | 44.9     | 24.8   |
| Fe                            | 95.50    | 313.58 | 10.07    | 11.03  | 32.13    | 33.06  | 15.62    | 8.83   | 12.14    | 9.57   | 33.7     | 26.8   |
| La                            | 0.0056   | 0.0065 | 0.0257   | 0.0236 | 1.1505   | 1.0308 | 2.1090   | 1.0126 | 2.0020   | 0.4930 | 6.1794   | 4.2460 |
| Ce                            | 0.0087   | 0.0065 | 0.0297   | 0.0297 | 1.6947   | 1.4973 | 1.3966   | 0.9040 | 0.2095   | 0.0535 | 2.1466   | 1.5822 |
| Pr                            | 0.0014   | 0.0018 | 0.0092   | 0.0095 | 0.3587   | 0.3157 | 0.7243   | 0.4580 | 0.5142   | 0.1404 | 1.4181   | 0.8162 |
| Nd                            | 0.0071   | 0.0075 | 0.0495   | 0.0500 | 1.6018   | 1.3897 | 3.1060   | 2.0403 | 2.0524   | 0.5757 | 5.4842   | 3.0260 |
| Sm                            | 0.0015   | 0.0013 | 0.0147   | 0.0152 | 0.3216   | 0.2748 | 0.6494   | 0.4345 | 0.3708   | 0.1119 | 0.8890   | 0.4795 |
| Eu                            | 0.0003   | 0.0005 | 0.0035   | 0.0037 | 0.0690   | 0.0571 | 0.1342   | 0.9867 | 0.0712   | 0.0221 | 0.1523   | 0.0863 |
| Gd                            | 0.0013   | 0.0012 | 0.0178   | 0.0190 | 0.2985   | 0.2480 | 0.4516   | 0.2736 | 0.2458   | 0.0717 | 0.5327   | 0.3161 |
| Tb                            | 0.0001   | 0.0003 | 0.0018   | 0.0020 | 0.0300   | 0.0250 | 0.0507   | 0.0297 | 0.0235   | 0.0070 | 0.0500   | 0.0317 |
| Dy                            | 0.0009   | 0.0008 | 0.0095   | 0.0099 | 0.1475   | 0.1191 | 0.2652   | 0.1527 | 0.1086   | 0.0313 | 0.2256   | 0.1465 |
| Ho                            | 0.0001   | 0.0003 | 0.0019   | 0.0020 | 0.0295   | 0.0235 | 0.0505   | 0.0293 | 0.0194   | 0.0053 | 0.0406   | 0.0261 |

**Table 1** continued

| Well no.:                  | PG1 mean | RSD    | PG2 mean | RSD    | PG3 mean | RSD    | PG4 mean | RSD    | PG5 mean | RSD    | PG6 mean | RSD     |
|----------------------------|----------|--------|----------|--------|----------|--------|----------|--------|----------|--------|----------|---------|
| Er                         | 0.0004   | 0.0006 | 0.0058   | 0.0054 | 0.0830   | 0.0641 | 0.1413   | 0.0821 | 0.0337   | 0.0152 | 0.1129   | 0.0694  |
| Tm                         | 0.0000   | 0.0003 | 0.0007   | 0.0008 | 0.0108   | 0.0083 | 0.0187   | 0.0112 | 0.0067   | 0.0019 | 0.0144   | 0.0088  |
| Yb                         | 0.0004   | 0.0005 | 0.0045   | 0.0043 | 0.0679   | 0.0512 | 0.1145   | 0.0696 | 0.0401   | 0.0119 | 0.0867   | 0.0500  |
| Lu                         | 0.0001   | 0.0003 | 0.0008   | 0.0008 | 0.0135   | 0.0098 | 0.0189   | 0.0116 | 0.0067   | 0.0020 | 0.0151   | 0.0085  |
| ΣREE                       | 0.0279   | 0.0255 | 0.1751   | 0.1747 | 5.8769   | 5.1097 | 9.2309   | 5.5458 | 5.7245   | 1.5325 | 17.3477  | 10.7038 |
| Ce/Ce <sup>*</sup>         | 0.77     | 0.30   | 0.42     | 0.05   | 0.59     | 0.04   | 0.26     | 0.08   | 0.05     | 0.01   | 0.15     | 0.03    |
| (LREE/HREE) <sub>UCC</sub> | 1.14     | 0.78   | 0.91     | 0.13   | 1.45     | 0.12   | 1.60     | 0.09   | 2.57     | 0.05   | 3.22     | 0.23    |

Major solute and REE are in  $\mu\text{g L}^{-1}$ . DOC and major anions ( $\text{Cl}^-$ ,  $\text{SO}_4^{2-}$ ,  $\text{NO}_3^-$ ) are in  $\text{mg L}^{-1}$ . Alkalinity data are in  $\mu\text{mol L}^{-1}$ . The amplitude of the Ce anomaly was calculated as follows  $\text{Ce/Ce}^* = 2 * \text{Ce}_{\text{UCC}} / (\text{La}_{\text{UCC}} + \text{Pr}_{\text{UCC}})$

RSD relative standard deviation; NA not available

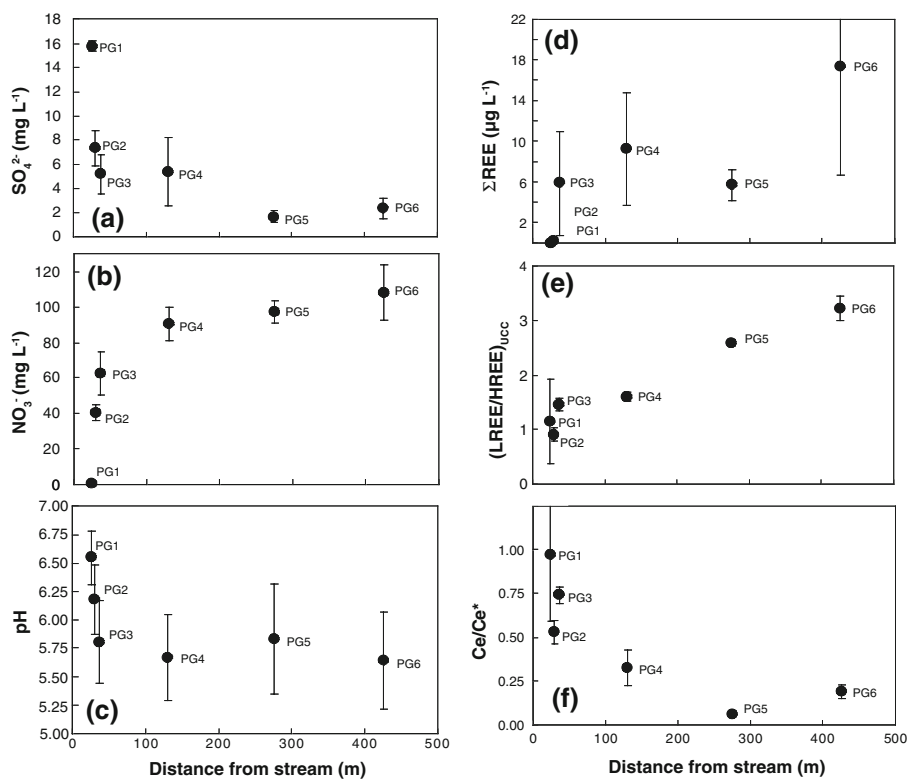


**Fig. 2** Diagrams illustrating systematic variation of the chemistry of Guériniec groundwater depending on the topographic position of sampling wells. Presented values are average values calculated by pooling chemical analyses collected during the 7-year monitoring period. Error bars correspond to relative standard deviations (data are displayed in Table 1)

the temporal stability of the REE pattern shapes in Guériniec groundwaters was established at that time only for one hydrological year. With the new dataset, the temporal stability is demonstrated to exist over a much longer period of time (7-year period), thereby demonstrating that the observed REE variations are long-term, and stationary, key features of these groundwaters.

### 4.3 REE Speciation

#### 4.3.1 Ultrafiltration Data

In order to establish the role of organic colloids on REE concentrations and REE pattern shapes, waters from two Guériniec wells (i.e., PG3 and PG4) were successively filtered through membranes of decreasing pore size (i.e., <30, <10 and <5 kDa; Table 2). As

**Fig. 3** Sketch diagram showing downslope evolution of upper continental crust (UCC)-normalized REE profiles in groundwaters from the Guériniec transect (UCC values are from Taylor and McLennan 1985). Many PG1 well samples have middle and heavy REE concentrations close to or below the detection limits (i.e., <10  $\text{ng L}^{-1}$ ), which explains the irregular shape of their REE patterns

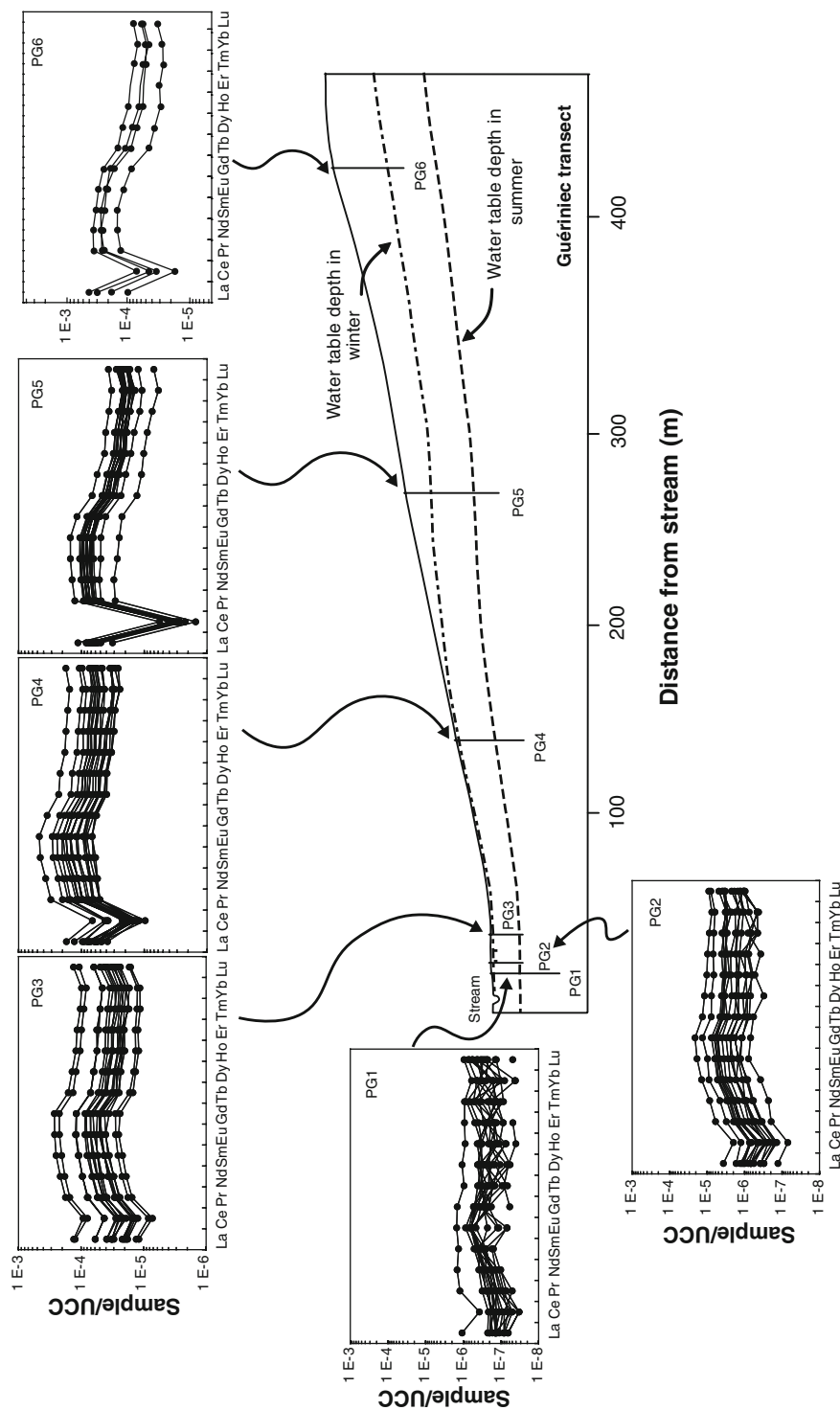
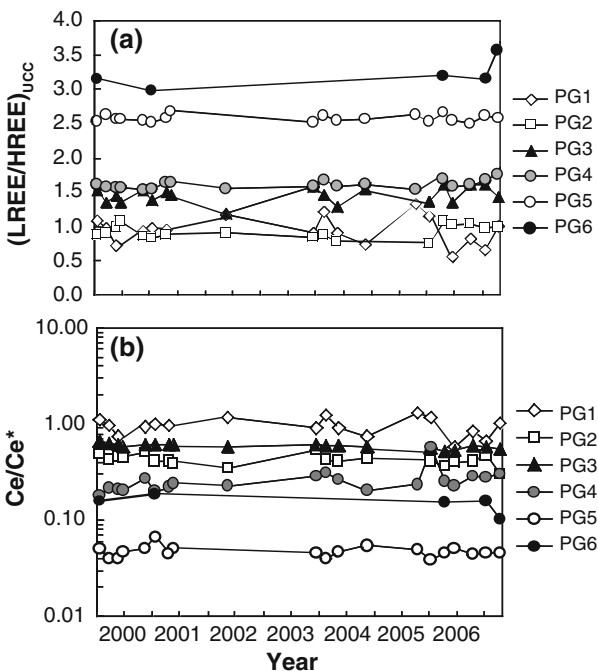


**Fig. 4** Temporal monitoring of **a** LREE/HREE)<sub>UCC</sub> ratios and **b** negative Ce anomaly amplitude in Guériniec groundwater samples



expected, both DOC and REE concentrations decreased upon successive filtrations (Fig. 5a, b), suggesting that part of the REE is effectively complexed by organic colloids in these waters. The possibility that REE were associated with FeOOH colloid was eliminated as iron is present under free and complexed Fe(III) species to dissolved organic matter (Lofts et al. 2008; Pokrovsky et al. 2005; Pourret et al. 2007c). The shape of the REE patterns remains globally unchanged, even though a slight Ce/Ce\* ratio decrease occurred in the most organic-rich sample (i.e., Ce/Ce\* decreasing from 0.58 to 0.41 in PG3 water with DOC of  $4.3 \text{ mg L}^{-1}$ ). However, differences regarding the quantitative partitioning of the REE between the organic and inorganic phases of the samples were noted. Indeed, comparison between REE concentrations in the  $<5 \text{ kDa}$  and  $<0.2 \mu\text{m}$  solutions implies that about 56% of the REE in PG3 groundwater occur as colloidal compounds, against only 21% in PG4 groundwater. Albeit it should be noted that such observation was only made on replicates from two samples. However, Dia et al. (2000) reported an even smaller fraction of colloidal REE for PG5 water (6%). Thus, it appears that the changes in negative Ce anomaly amplitude and  $(\text{LREE}/\text{HREE})_{\text{UCC}}$  ratios that are observed along the Guériniec toposequence occur simultaneously with changes in REE speciation. Indeed, REEs in upland domain waters show low Ce/Ce\* ratios (i.e., large negative Ce anomalies) and high  $(\text{LREE}/\text{HREE})_{\text{UCC}}$ , and speciation is dominated by REE inorganic species, whereas REE in waters showing high Ce/Ce\* ratios (i.e., reduced Ce anomaly), but low  $(\text{LREE}/\text{HREE})_{\text{UCC}}$  are complexed with organic colloids.

#### 4.3.2 Modeling Results

Model VI (Tipping 1998) was used to calculate REE speciation in PG3, PG4, and PG5 groundwaters, and the results were compared to the earlier mentioned ultrafiltration data.

**Table 2** Ultrafiltration results for PG3 and PG4 samples (November 2004)

| Well no.:                     | PG3    |        |        |        |        | PG4    |        |        |        |        |
|-------------------------------|--------|--------|--------|--------|--------|--------|--------|--------|--------|--------|
|                               | 0.2 µm | 30 kDa | 30 kDa | 10 kDa | 5 kDa  | 0.2 µm | 30 kDa | 30 kDa | 10 kDa | 5 kDa  |
| pH                            | 6.7    |        |        |        |        | 6.1    |        |        |        |        |
| Cl <sup>-</sup>               | 31.09  |        |        |        |        | 30.88  |        |        |        |        |
| SO <sub>4</sub> <sup>2-</sup> | 5.75   |        |        |        |        | 6.57   |        |        |        |        |
| NO <sub>3</sub> <sup>-</sup>  | 55.95  |        |        |        |        | 80.59  |        |        |        |        |
| Alkalinity                    | 493    |        |        |        |        | 275    |        |        |        |        |
| DOC                           | 4.34   | 4.19   | 4.16   | 4.02   | 3.96   | 3.07   | 2.02   | 1.93   | 1.93   | 1.47   |
| Na                            | 20,580 | 20,600 | 20,410 | 20,990 | 20,750 | 15,930 | 18,790 | 16,970 | 17,540 | 15,740 |
| K                             | 1,125  | 1,160  | 1,137  | 1,173  | 1,133  | 961    | 1,081  | 3,138  | 3,141  | 3,103  |
| Ca                            | 7,414  | 7,499  | 7,395  | 7,623  | 7,838  | 6,501  | 7,221  | 10,210 | 10,390 | 9,884  |
| Mg                            | 13,160 | 13,320 | 13,150 | 13,380 | 13,230 | 10,302 | 12,382 | 13,470 | 13,670 | 12,670 |
| Mn                            | 5.93   | 5.95   | 5.88   | 6.03   | 5.75   | 1.57   | 1.72   | 33.31  | 33.53  | 33.05  |
| Fe                            | 18.34  | 3.70   | 2.78   | 2.47   | 3.21   | BDL    | BDL    | 12.13  | 4.07   | 2.42   |
| La                            | 0.7870 | 0.6070 | 0.6040 | 0.4790 | 0.4470 | 0.3359 | 0.3851 | 1.5470 | 1.5090 | 1.5000 |
| Ce                            | 1.1810 | 0.9020 | 0.9010 | 0.6970 | 0.6550 | 0.3683 | 0.4233 | 0.8180 | 0.7920 | 0.7800 |
| Pr                            | 0.2620 | 0.2040 | 0.2040 | 0.1600 | 0.1480 | 0.1199 | 0.1347 | 0.5490 | 0.5230 | 0.5240 |
| Nd                            | 1.2350 | 0.9630 | 0.9650 | 0.7830 | 0.7120 | 0.5767 | 0.6493 | 2.4360 | 2.3270 | 2.2960 |
| Sm                            | 0.2290 | 0.1840 | 0.1850 | 0.1350 | 0.1230 | 0.1022 | 0.1210 | 0.5150 | 0.4750 | 0.4770 |
| Eu                            | 0.0478 | 0.0364 | 0.0362 | 0.0269 | 0.0249 | 0.0211 | 0.0240 | 0.1020 | 0.0945 | 0.0966 |
| Gd                            | 0.2210 | 0.1680 | 0.1660 | 0.1200 | 0.1040 | 0.0983 | 0.1082 | 0.3370 | 0.3240 | 0.3200 |
| Tb                            | 0.0209 | 0.0157 | 0.0160 | 0.0103 | 0.0093 | 0.0085 | 0.0095 | 0.0372 | 0.0340 | 0.0335 |
| Dy                            | 0.1020 | 0.0762 | 0.0721 | 0.0525 | 0.0472 | 0.0436 | 0.0479 | 0.1860 | 0.1780 | 0.1760 |
| Ho                            | 0.0223 | 0.0164 | 0.0170 | 0.0122 | 0.0107 | 0.0092 | 0.0107 | 0.0378 | 0.0350 | 0.0351 |
| Er                            | 0.0649 | 0.0506 | 0.0494 | 0.0362 | 0.0316 | 0.0292 | 0.0321 | 0.1070 | 0.1020 | 0.1040 |
| Tm                            | 0.0089 | 0.0067 | 0.0062 | 0.0051 | 0.0046 | 0.0037 | 0.0040 | 0.0154 | 0.0143 | 0.0118 |

**Table 2** continued

| Well no.: | PG3    |        |        |        |        |        | PG4    |        |        |        |        |        |
|-----------|--------|--------|--------|--------|--------|--------|--------|--------|--------|--------|--------|--------|
|           | 0.2 μm | 30 kDa | 30 kDa | 10 kDa | 10 kDa | 5 kDa  | 5 kDa  | 0.2 μm | 30 kDa | 30 kDa | 10 kDa | 10 kDa |
| Yb        | 0.0533 | 0.0432 | 0.0426 | 0.0306 | 0.0303 | 0.0262 | 0.0273 | 0.0954 | 0.0875 | 0.0863 | 0.0776 | 0.0796 |
| Lu        | 0.0108 | 0.0093 | 0.0088 | 0.0068 | 0.0062 | 0.0055 | 0.0060 | 0.0168 | 0.0154 | 0.0154 | 0.0135 | 0.0142 |
| ZREE      | 4.2459 | 3.2825 | 3.2732 | 2.5546 | 2.3539 | 1.7482 | 1.9834 | 6.7996 | 6.5104 | 6.4581 | 5.8382 | 6.0145 |
| Ce/Ce*    | 0.58   | 0.58   | 0.58   | 0.57   | 0.57   | 0.41   | 0.42   | 0.20   | 0.20   | 0.20   | 0.20   | 0.20   |

Major solute and REE are in  $\mu\text{g L}^{-1}$ . DOC and major anions ( $\text{Cl}^-$ ,  $\text{SO}_4^{2-}$ ,  $\text{NO}_3^-$ ) are in  $\text{mg L}^{-1}$ . Alkalinity data are in  $\mu\text{mol L}^{-1}$

BDL below detection limit

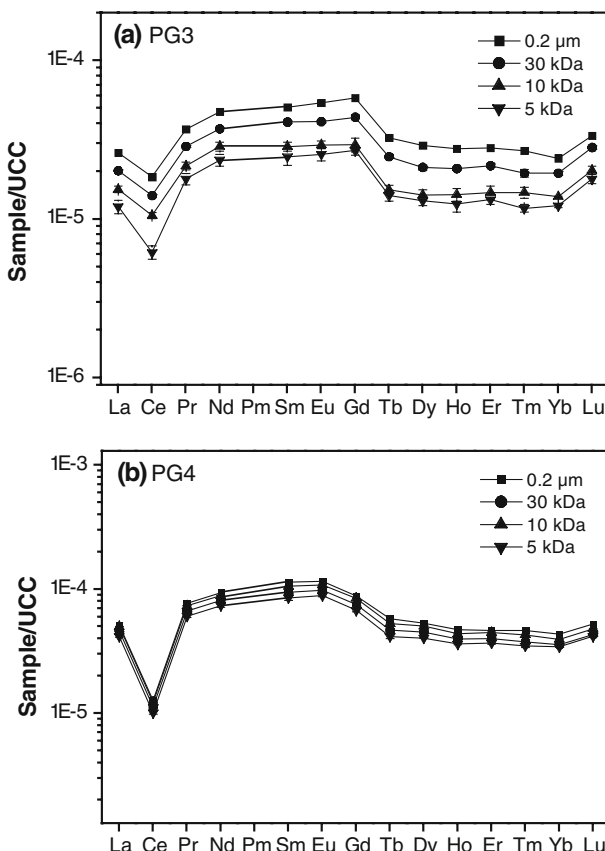


**Fig. 5** UCC-normalized REE patterns after successive ultrafiltration (i.e., 0.2  $\mu$ m; 30, 10 and 5 kDa) of groundwaters from **a** PG3 and **b** PG4 wells. Error bars correspond to standard deviations obtained from duplicate measurements, with some error bars being smaller than the symbol size (data are displayed in Table 2)

Major cation and anion concentrations and Fe and Al concentrations were taken into account in these calculations. In WHAM 6.0 (Tipping 1998), no solid precipitation is allowed to occur. Only complexation, either by organic colloids or by aqueous inorganic complexes, is modeled. In this study, it is assumed that 50% of the dissolved organic matter (DOM) is active as REE-complexing, humic matter (HM; Thurman 1985), of which 80% is present as HA and 20% as FA (Pourret et al. 2007a; Viers et al. 1997). Even if this active DOM ratio could be higher than 50%, such a value is a good compromise (see sensitive analysis in Pourret et al. 2007a).

The modeling results are displayed in Table 3 for La (La-HA and La-FA species are gathered together under La-HM). Modeling results for the others REE are coherent with La (data not shown). Consistently with the ultrafiltration results, speciation calculations show that La-HM is the dominant La species in PG3 groundwater (between 92.5 and 100% depending on the sampling date). Conversely, but also consistently with the ultrafiltration results, the proportion of La complexed with HM is lower in PG4 and PG5 groundwaters. Indeed, between 67 and 49% of La occur as free inorganic species in PG4 groundwater, and  $\sim$ 75% in PG5 groundwater. In PG4 groundwater, the remaining La occurs as sulfate

**Table 3** Speciation results obtained using model VI for PG3, PG4 and PG5 groundwaters sampled in May and November 2004

|     | % of species | La <sup>3+</sup> | LaSO <sub>4</sub> <sup>+</sup> | La-HM | Other species |
|-----|--------------|------------------|--------------------------------|-------|---------------|
| PG3 | May          | 7.0              | 0.5                            | 92.5  | 0.0           |
|     | November     | 0.0              | 0.0                            | 100.0 | 0.0           |
| PG4 | May          | 67.0             | 6.0                            | 26.1  | 0.9           |
|     | November     | 49.0             | 7.1                            | 43.1  | 0.8           |
| PG5 | May          | 74.0             | 2.5                            | 22.2  | 1.2           |
|     | November     | 75.6             | 2.3                            | 19.9  | 2.1           |

(from 6.0 to 7.1%) and La-HM complexes (from 26.1 to 43.1%). Other species consist of La hydroxide or carbonate complexes. Moreover, PHREEQC inorganic speciation does not evidence any peculiar mineral precipitation involving REE.

The modeling calculations thus demonstrate the same progressive spatial change in REE speciation as that evidenced by the ultrafiltration experiments (predominance of inorganic species in upland domain groundwaters against predominance of organic colloidal REE complexes in bottom land groundwaters). They also demonstrate that the observed spatial variability in REE speciation is likely a stable feature of these groundwaters, given that the good agreement observed between the present modeling and ultrafiltration data and the ultrafiltration data published previously by Dia et al. (2000).

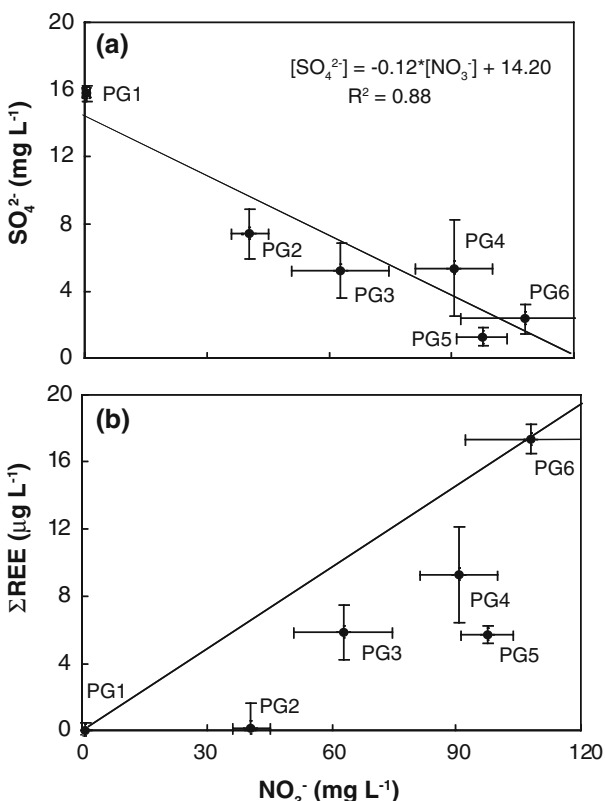
## 5 Discussion

The new REE data reported for Guériniec groundwaters confirm the spatial variability of REE signatures established previously by Dia et al. (2000) for this groundwater system. The new dataset is especially significant because both REE pattern shape and Ce anomaly amplitude spatial variability are proved to be stationary on a 7-year period. It is also significant that REE signatures and Ce anomaly amplitude spatial variability also corresponds to REE speciation spatial variability: REE become progressively more organically bound downslope. In this context, three important questions arise: (1) Is the hypothesis previously put forward by Dia et al. (2000) of a spatial variability of REE signatures due to a mixing process confirmed? (2) What is the role of REE speciation on the spatial variation of REE concentrations and REE signatures? (3) How do the Guériniec groundwaters compare themselves with similar shallow groundwaters elsewhere in the world, and what are the ultimate REE sources in these groundwaters?

### 5.1 The Role of Groundwater Mixing and pH Variation on REE Signatures

In their paper, Dia et al. (2000) concluded that the progressive change in dissolved REE signature from top to bottom of the toposequence may indicate a progressive mixing phenomenon along the hillslope between a nitrate-rich water coming from the recharge zone in the upland domain (i.e., a water similar in composition to PG6 groundwater) and a return flow water comprising deep, denitrified water (i.e., a water similar in composition to PG2 groundwater). The occurrence of such a progressive mixing phenomenon along the Guériniec transect is confirmed by this new dataset, specifically by the SO<sub>4</sub><sup>2-</sup> and NO<sub>3</sub><sup>-</sup> concentrations that define a mixing line relationship (see Sect. 4.1 and Fig. 6a). As evidenced previously by Molénat et al. (2002), a dilution mechanism occurs between these two end-members. However, the two components mixing hypothesis failed to explain the

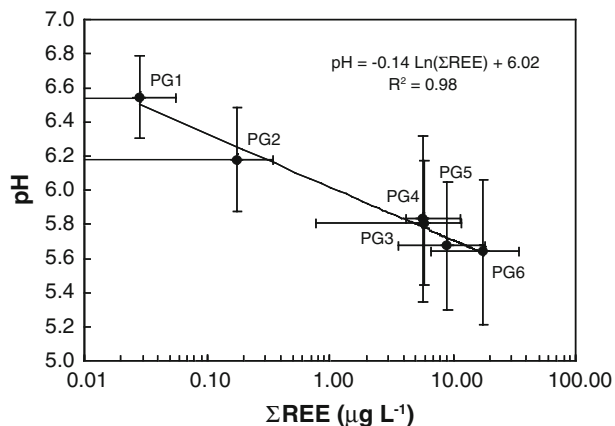
**Fig. 6** **a**  $\text{SO}_4^{2-}$  concentrations ( $\text{mg L}^{-1}$ ) and **b**  $\Sigma\text{REE}$  concentrations ( $\mu\text{g L}^{-1}$ ) as a function of  $\text{NO}_3^-$  concentrations ( $\text{mg L}^{-1}$ ) for the six studied wells. Solid lines represent **a** linear regression between  $\text{SO}_4^{2-}$  and  $\text{NO}_3^-$  and **b** the mixing line between PG6 and PG1



variation in REE concentrations. Actually, REE concentrations do not define a mixing line when reported along with  $\text{NO}_3^-$  concentrations (Fig. 6b). This is due to a nonconservative behavior of the REE during mixing, likely caused by the pH increase that accompanies the groundwater mixing process (Fig. 2).

As shown by Elderfield et al. (1990), REE concentrations in waters are indeed highly pH dependent: high pH results in low REE concentrations. Changes in pH can also fractionate dissolved REE patterns (Koeppenkastrop and De Carlo 1992, 1993; Ohta and Kawabe 2001). Alkaline pH results in waters being relatively enriched in HREE, which contrasts with more acidic waters in which the REE patterns generally exhibit relative LREE enrichments (e.g., Andersson et al. 2006). This behavior is due to the fact that REE are preferentially adsorbed onto aquifer minerals when pH increases and that LREE generally adsorb more efficiently onto solid phases than HREE do. At high pH, the deprotonation of surface hydroxyl groups generates a negative charge onto mineral surfaces, favoring adsorption of positively charged REE. With increasing pH, the order of REE adsorption onto mineral surfaces is LREE > MREE > HREE. With decreasing pH, REEs are released from mineral surfaces in the same order, LREE > MREE > HREE (Gammons et al. 2005; Johannesson et al. 2006; Leybourne and Johannesson 2008; Sholkovitz 1995; Welch et al. 2009). Thus, REE concentrations and REE pattern shapes in groundwaters are determined to a large extent by pH-driven adsorption/desorption reactions between the solution and mineral surfaces.

**Fig. 7** pH as a function of ΣREE concentrations ( $\mu\text{g L}^{-1}$ ) for the six studied wells, solid line represents linear regression



As shown in Fig. 2, the groundwater mixing that occurs along the Guériniec transect does not occur at constant pH. As evidenced by Molénat et al. (2002), the evolution of the weathered aquifer along flow path could be due to upward flows. The pH of Guériniec groundwaters indeed increases from top (pH = 5.6, on average) to bottom (pH = 6.5, on average) of the toposequence, implying that PG6 groundwater, the high REE content mixing end-member, experiences a marked pH increase when mix together with the low REE PG1 groundwater end-member. This pH increase must result in a partial adsorption of the REE brought about by PG6 groundwater, thereby explaining why REE concentrations and pH are inversely correlated in Guériniec groundwaters (Fig. 7). It should be noted that speciation calculation evidenced that none REE minerals precipitation occurs in the system. Similar negative relationships between pH and REE concentrations have already been reported for neutral to slightly acidic waters (e.g., Byrne and Sholkovitz 1996; Goldstein and Jacobsen 1988; Johannesson and Burdige 2007).

The  $(\text{LREE}/\text{HREE})_{\text{UCC}}$  ratio decrease that follows the REE concentrations decrease along the Guériniec toposequence supports the earlier mentioned conclusion of a non-conservative mixing due to REE adsorption in response to pH rise. Indeed, LREE preferentially adsorbed onto mineral aquifers as compared to HREE (e.g., Gammons et al. 2005). A decrease in  $(\text{LREE}/\text{HREE})_{\text{UCC}}$  is thus a fully expected feature in groundwaters subjected to progressive adsorption of their dissolved REE onto mineral aquifers in response to pH increase (e.g., Johannesson and Burdige 2007).

## 5.2 Origin of Negative Ce Anomaly Variations

The second most important feature displayed by the Guériniec groundwaters is that Ce anomaly gets smaller from top to bottom of the toposequence (Fig. 3). The next question to be answered is, thus, could the combined groundwater mixing and REE adsorption process also account for the spatial variation in Ce anomaly amplitude?

A simple mixing model was developed to evaluate this possibility. In this model,  $\text{NO}_3^-$  concentrations were used to calculate the proportions of the two end-member groundwaters (i.e., PG6 and PG1) that should be mixed to account for PG5, PG4, PG3 and PG2 groundwater compositions. The proportions of PG6 groundwater obtained this way were 63% for PG5, 42% for PG4, 16% for PG3 and 10% for PG2. To model the decrease in REE concentration due to adsorption, a three-step approach was followed: (1) the average pH

value measured in PG5, PG4, PG3 and PG2 well waters was inputted into Eq. 1 (i.e., regression line from Fig. 7).

$$\text{pH} = -0.14 \ln (\Sigma\text{REE}) + 6.02 \quad (1)$$

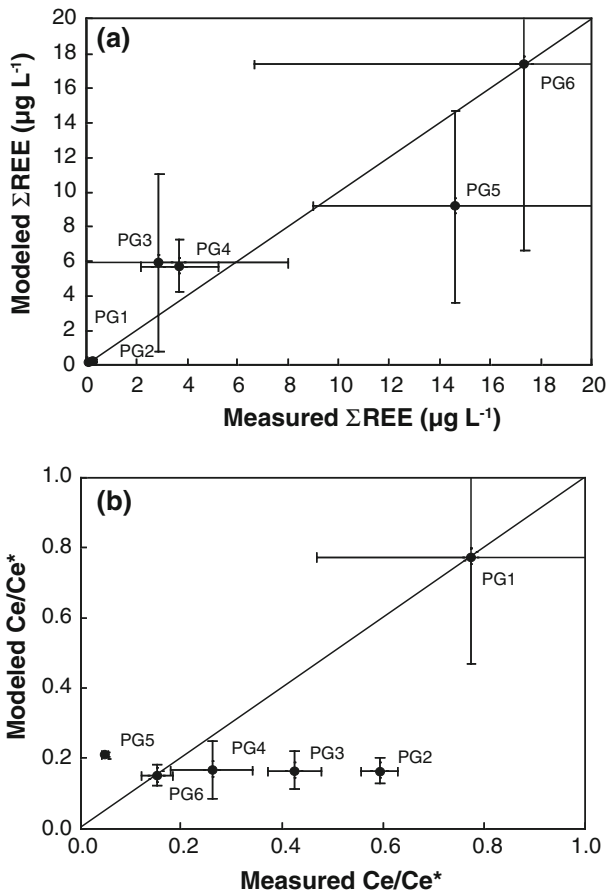
This allowed calculating REE amount that should be obtained in PG5, PG4, PG3 and PG2 well waters after mixing; (2) because REE in the mixture must dominantly come from PG6 groundwater (i.e., REE content of PG6 groundwater is higher about three orders of magnitude than that of PG1; Table 1), the REE concentration decrease that occurred during mixing could be essentially modeled by diluting PG6 groundwater before mixing. Dilution factors were calculated by dividing the measured average REE content of PG6 by the REE concentrations one should be obtained for PG5, PG4, PG3 and PG2 groundwaters as indicated by Fig. 7; (3) in the final step, diluted PG6 concentrations were inputted into the mixing equation and REE concentrations and Ce/Ce\* ratios calculated for PG2, PG3, PG4 and PG5 groundwaters.

It should be pointed out here that this simple model does not take into account the preferential adsorption of the LREE over the HREE onto the mineral aquifers. Indeed, the LREE/HRRE is kept constant during dilution of PG6 groundwater. However, the procedure used is judged valid with regard to the objective of the modeling (i.e., testing if the combined mixing–adsorption can account for the reduction in negative Ce anomaly amplitude), given the fact that the Ce anomaly amplitude in the mixture will depend essentially on only two parameters, namely, (1) the Ce anomaly amplitude of each end-member and (2) the relative REE proportion brought about into the mixture by each end-member.

Results are presented in Fig. 8a, b. As can be seen, the fit between modeled and measured values is quite good for REE concentrations (considering standard deviation, data plot on a 1:1 line), but poor for Ce/Ce\* ratios, three groundwaters (PG3, PG4 and PG5) yielding calculated Ce/Ce\* ratios that plot significantly below the 1:1 line (Fig. 8b). In other words, for these three groundwaters, the amplitude of the modeled negative Ce anomalies is much larger than that effectively measured. This discrepancy provides evidence that the downward decrease in the Ce anomaly amplitude along the Guériniec transect is not controlled by the combined mixing–adsorption process. A third mechanism is required. As discussed here, this third mechanism could be an organic colloid input. Three arguments support this interpretation:

- (1) Except for the somewhat deeper PG1 groundwater (Fig. 1) with very low REE concentrations (Fig. 2), positive correlations are observed between REE and DOC contents in bottomland groundwaters exhibiting moderate negative Ce anomalies (i.e., PG2, PG3, and PG4; Fig. 9). Combined with ultrafiltration and speciation modeling data, this observation revealed that Ce anomaly amplitude decrease with an increase in the REE proportion bound to organic colloids. Moreover, ultrafiltration data show that negative Ce anomaly amplitude in PG3 ultrafiltrates increases with decreasing pore size (Table 2; Fig. 5). This indicates that colloidal fraction REE pattern present in PG3 either exhibits no negative Ce anomaly or, a negative Ce anomaly of much lower amplitude than that occurring in the truly dissolved, inorganic REE fraction of this sample. Thus, the DOC–Ce anomaly relationship of these downhill groundwaters looks just as if REE budget of these waters was a mixture between REE-bearing organic colloids having no or reduced Ce anomaly, and an inorganic REE pool having a marked negative Ce anomaly.
- (2) A classical feature of shallow water tables developed on low-permeability basement is that rainfall event during wet season generally result in a rapid and marked rise of

**Fig. 8** **a** Modeled  $\Sigma$ REE concentrations ( $\mu\text{g L}^{-1}$ ) as a function of measured  $\Sigma$ REE concentrations ( $\mu\text{g L}^{-1}$ ) and corresponding **b** modeled Ce/Ce\* as a function of measured Ce/Ce\* for the six studied wells. Solid line represents the 1:1 line



the water table, the latter reaching the uppermost, organic-rich soil horizons in the bottomland areas of the catchments. This water table rise may result in incorporation of large proportions of soil organic colloids into the uppermost parts of the shallow groundwater. Figure 10 compares the 2006–2007 fluctuations of the Guériniec water table roof with the DOC content and Ce anomaly amplitude of PG3 well water. The 2.5 m water table rise that occurs in October–November 2006 in response to intense autumn rainfalls resulted in a marked DOC content increase (from 1 to 8  $\text{mg L}^{-1}$ ; Fig. 10a) of PG3 well water. Quite clearly, this increase occurred in phase with a marked increase in the Ce/Ce\* ratio (from 0.52 to 0.60; Fig. 10b).

- (3) As shown by Dia et al. (2000) and Pourret et al. (2007a, c), organic-rich soil horizons of the Kervidy/Coët-Dan catchment may deliver large quantities of REE-bearing organic colloids to the groundwaters. Moreover, and most importantly, REE patterns of these organic colloids do not show any negative Ce anomaly. Davranche et al. (2004, 2005, and 2008) experimentally demonstrated that REE complexation by organic matter prevents Ce oxidative scavenging by iron and manganese oxyhydroxides (and consequently the Ce anomaly development) and Pourret et al. (2008) proposed that the preferential Ce(IV) is masked rather than inhibited.

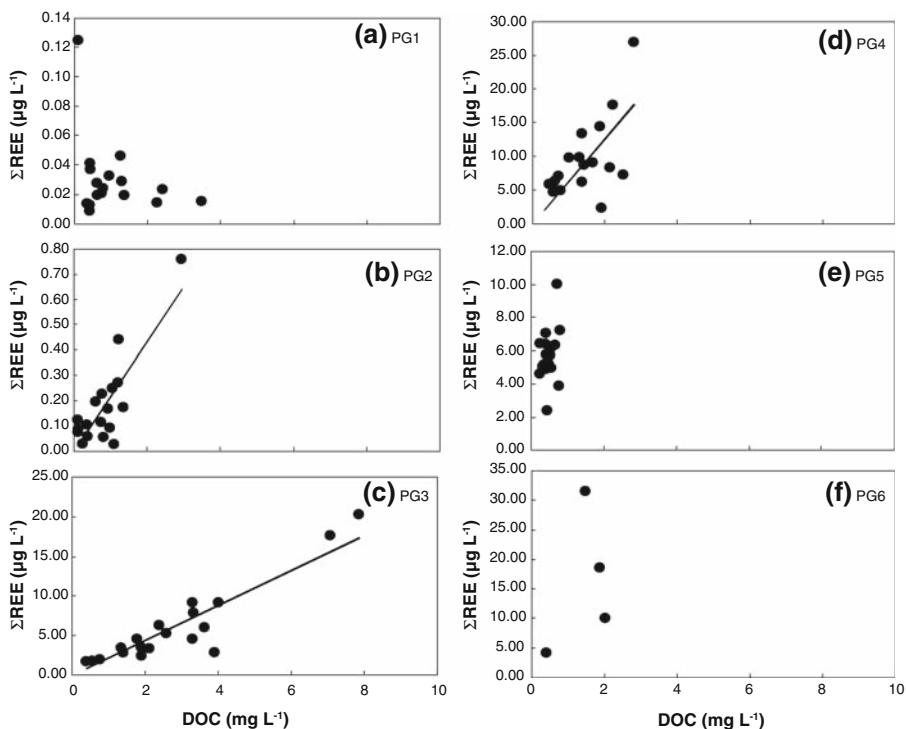


**Fig. 9**  $\Sigma\text{REE}$  concentrations ( $\mu\text{g L}^{-1}$ ) as compared to DOC concentrations ( $\text{mg L}^{-1}$ ) for **a** PG1, **b** PG2, **c** PG3, **d** PG4, **e** PG5 and **f** PG6 samples, respectively. Solid lines represent linear regression when applicable

A simple modeling approach was used to further test the hypothesis of a Ce anomaly reduction due to REE-bearing organic colloids input. In this approach, REE amount brought by organic colloids into the Guériniec groundwater was calculated from the DOC content and the DOC/REE ratios measured by Dia et al. (2000) in PF1 and PF3 wells (i.e., the two wells installed on the Kervidy/Coët-Dan catchment to monitor the composition of the groundwater that flows with the uppermost—between 20 and 50 cm—organic soil horizons). Initial groundwater REE concentrations (i.e., REE concentrations in groundwater wells prior to colloid input) were calculated using the earlier described mixing–adsorption process. In other words, the amount of REE bring by the organic colloids was added to the previous calculations that considered only groundwater mixing and REE adsorption. Results are presented in Fig. 11, which compares Ce/Ce\* ratios calculated by combining the earlier described mixing–adsorption mechanism and the proposed colloid input process, and Ce/Ce\* ratios effectively measured in Guériniec groundwaters. As can be seen, a reasonably good fit arises between measured and calculated Ce/Ce\* ratios (see legend of Fig. 11 for further explanation). Indeed, a colloidal addition of PF1 water type to the inorganic groundwater mixing allows to model PG2, whereas PF3 is required to model PG3 and PG4.

To sum up, the regular and progressive change in REE signatures and Ce anomaly amplitude that is recorded by Guériniec groundwaters likely arises from the superimposition of three processes (Fig. 12): (1) progressive mixing along the hillslope between a shallow, acidic, REE-rich groundwater component coming from the recharge zone in the

**Fig. 10** **a** DOC concentrations ( $\text{mg L}^{-1}$ ) and **b** ( $\text{Ce}/\text{Ce}^*$ ) ratio evolution from February 2006 to June 2007 both represented by full black circles, as compared to the water table depth (m), represented by solid line, in PG3

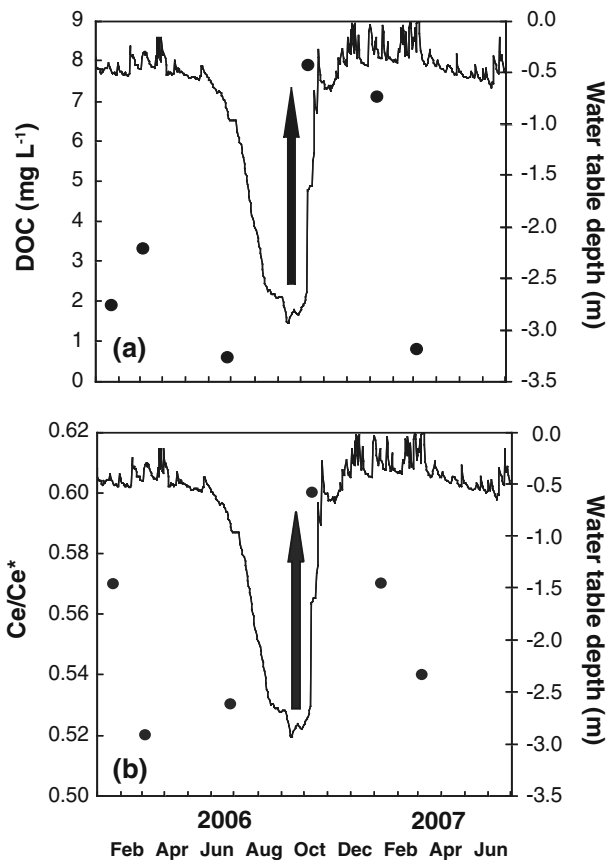
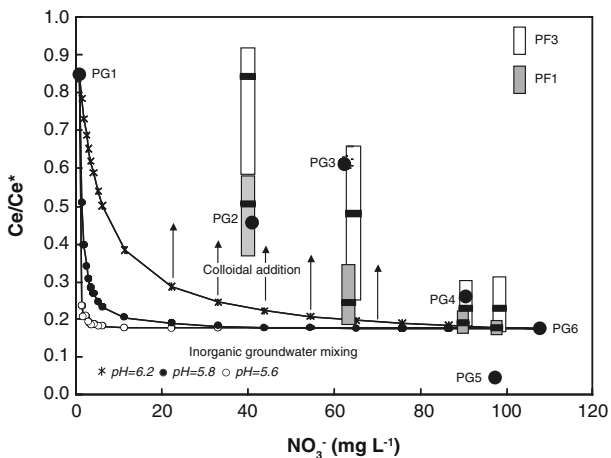


**Fig. 11**  $\text{Ce}/\text{Ce}^*$  ratios evolution as a function of  $\text{NO}_3^-$  concentrations ( $\text{mg L}^{-1}$ ) illustrating the inorganic groundwater mixing (i.e., solid lines) for various pH (i.e., 5.6, 5.8, and 6.2) and the corresponding colloidal addition (materialized by black vertical arrows) necessary to fit the measured  $\text{Ce}/\text{Ce}^*$  in PG2, PG3, PG4 and PG5 groundwater samples. Gray and white rectangles represent the colloidal addition if considering PF1 and PF3, respectively



upland domain and flowing downwards (flow path no. 1), and a deep, REE-poor, less-acidic groundwater component (flow path no. 2); (2) adsorption of part of the dissolved REE brought about by the REE-rich component due to pH increase; (3) addition of REE-

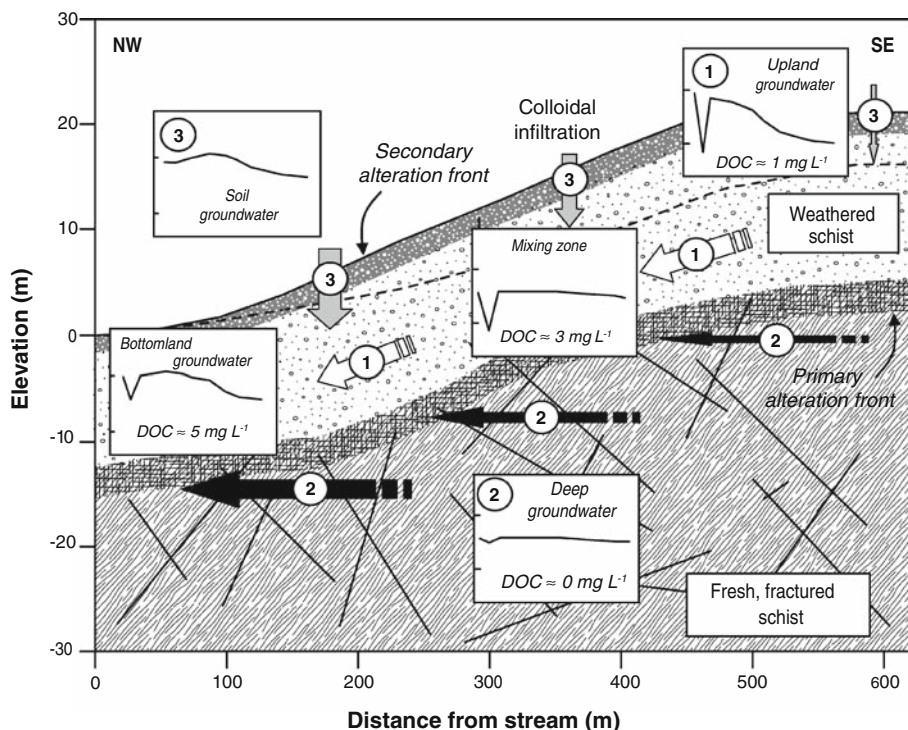


**Fig. 12** Sketch diagram illustrating the presence of three-groundwater flow paths in the Kervidy/Coët-Dan aquifer

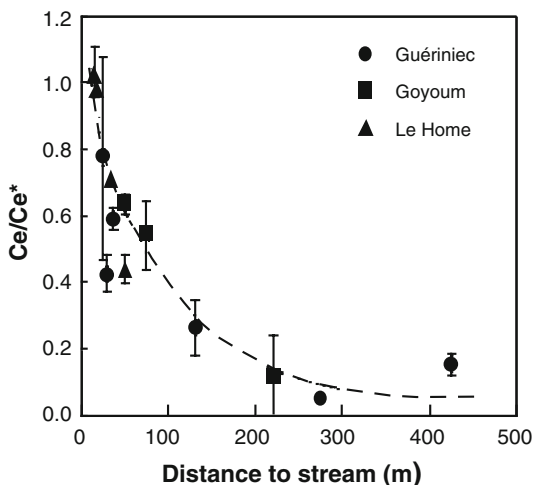
bearing, Ce anomaly free organic colloids from the uppermost, organic-rich soil horizons (flow path no. 3).

With regard to the latter process, topography is expected to play a dominant role on organic colloids amount that can effectively reach the Guériniec water table and, thus, on the colloid addition process capacity to reduce the negative Ce anomalies amplitude in these groundwaters. Topography is indeed expected to control the surface area in which the water table may rise into the soil uppermost, organic-rich horizons. More specifically, water table depth monitoring revealed that in the upland domains located above the convex-concave reversal of the topography the water table always remained well below the uppermost, organic-rich soil horizons (Fig. 1). Organic colloids flux in this domain is thus expected to be low. By contrast, in the bottomland domains, water table depth monitoring indicated that water table periodically reached soil surface during wet season (i.e., late fall and winter). The flux of organic colloids is, therefore, expected to be high in this domain, leading to a strong reduction of the negative Ce anomaly of the groundwater.

### 5.3 Comparison with Similar Groundwaters and Implications for REE Sources

As pointed out in the introduction, similar spatial variability of REE signatures and negative Ce anomaly amplitude has been reported in groundwaters of the Goyoum toposequence in Cameroon (Braun et al. 1998) and of the Le Home toposequence (Gruau et al. 2004) in Western France. As in the Guériniec case, both the Goyoum and Le Home groundwaters

**Fig. 13** Ce/Ce\* ratios as a function to distance from stream (m). Data for Goyoum and Le Home toposequences are from Braun et al. (1998) and Gruau et al. (2004), respectively



flow through aquifer rock of homogeneous composition: Proterozoic gneisses at Goyoum and Proterozoic schists at Le Home. In Fig. 13, Ce/Ce\* ratios in these three-groundwater systems are reported as a function of the distance to the stream. Figure 13 shows that the three-groundwater systems plot along a single trend reflecting the Ce anomaly amplitude gradual reduction as the distance to the stream decreases. Thus, the Ce anomaly amplitude gradual reduction observed at Guériniec from top to bottom of the toposequence appears to be a general feature of shallow groundwaters flowing into aquifers developed onto low-permeability bedrock. The likely reason for this mainly relies on the fact that, in low-permeability aquifers, water table generally reaches organic soil horizons in bottomland domains, thus allowing incorporation of large quantities of organic colloids in the aquifer bottomland part. This feature is not seen in the aquifer upland part where the water table always remains far below the upper, organic-rich soil horizons. This feature needs to be expanded to other toposequences in various hydrological contexts. Indeed, as stated by Köhler et al. (2009) in boreal catchments REE export is mostly strongly controlled by landscape type.

Finally, consideration of Ce anomaly spatial variation requires the occurrence of two spatially distinct REE sources. More specifically, the presence of a large negative Ce anomaly in the upland groundwaters (e.g., PG5 well water) implies solubilization of the REE under organic-free, oxidizing conditions. Indeed, as shown by Davranche et al. (2005, 2008), the presence of organic matter inhibits the development of negative Ce anomalies in oxidizing waters, because Ce cannot be oxidized by oxidizing mineral surfaces such as Mn oxides and above all because Ce cannot be selectively removed from the solution, Ce being complexed together with other REE by organic molecules. Thus, the occurrence of groundwaters having large negative Ce anomalies (e.g., PG 5 and PG6 well waters) implies that REE in these groundwaters ultimately come from solid sources located in the aquifer where DOC concentrations are low and where REE speciation is consequently dominated by inorganic species. Conversely, the fact that REE patterns found in upper, organic-rich soil horizon waters do not exhibit any negative Ce anomaly implies to consider that REE became dissolved in these waters in an organic-rich environment. Should REE have been solubilized in a purely inorganic context similar to that encountered in the aquifer upland domain, then original REE patterns would have had a negative Ce anomaly that should still be

observed in the organic-rich waters. The fact that the organic-rich water does not show any negative Ce anomaly thus provides evidence that a second REE solid source must exist in the Guériniec aquifer. Unlike the first source that must be located deep, this second source must be located close to the surface, in the organic-rich soil horizons, i.e., in that part of the aquifer where the REE fully organic speciation makes negative Ce anomaly development impossible.

## 6 Conclusions

This paper presents new data on the REE chemistry of shallow groundwaters from the Guériniec transect of the Kervidy/Coët-Dan experimental catchment, Western France. The field database that covers a 7-year monitoring period is followed by results of ultrafiltration experiments and speciation calculations. This allows to further constraining the speciation of the dissolved REE. The new data confirmed the spatial variability of REE pattern shapes and Ce anomaly amplitude evidenced earlier in these groundwaters, which is shown to correspond to changes in REE speciation, REE in groundwaters from the bottom land domains of the toposequence being complexed by organic molecules, whereas those in groundwaters from the upland parts occur mainly as inorganic species. Simple modeling using variations in major anion concentrations and pH variations reveal that the variation in REE pattern shape and REE concentrations along the Guériniec transect may be accounted for by a combined mixing–adsorption process. However, the data show that a third mechanism of organic colloid addition must be introduced to account for the variation in Ce anomaly amplitude. According to water table depth-monitoring data, it is suggested that the colloid source is located in the uppermost, organic-rich horizons of the aquifer and that the colloid input (and thus the reduction of the Ce anomaly amplitude it implies) is high in the bottomland domains of the toposequence but low to very low in its upland domains. A comparison of the Guériniec data with data from other shallow groundwater systems from Cameroon and Western France indicates that the topographically controlled variation in Ce anomaly amplitude seems to be a common feature of these systems. Topography is indeed the ultimate key factor that controls the spatial variability of Ce anomaly in shallow groundwaters by its ability to control the thickness of the unsaturated zone, and consequently the flux of Ce anomaly free, organic-rich colloids that can effectively reach the water table. Finally, it is shown, based on the variations in Ce anomaly amplitude, that the  $<0.2\text{ }\mu\text{m}$  REE fraction ultimately comes from two solid sources in these groundwaters: one located in the deep basement schist; another located in the upper, organic-rich soil horizon.

**Acknowledgments** We thank the technical staff at Rennes (M. Le Coz-Bouhnik, O. Hénin, and P. Petitjean) and the graduate/undergraduate students for their assistance during the sampling, and the analytical work. The CPER program “Développement de la Recherche sur la Maîtrise de la Qualité de l’Eau en Bretagne” jointly funded by the French Government and the Council of Rennes Métropole supported this research. C.H. Gammons and A.M. Shiller are thanked for thorough and constructive comments of an earlier version of this paper.

## Appendix

See Table 4.

**Table 4** Model VI parameters for HA and FA (Tipping 1998)

| Parameter        | Description  | Values   |
|------------------|--|--|
| $n_A$            | Amount of type-A sites ( $\text{mol g}^{-1}$ )                                 | $4.8 \times 10^{-3}$ (FA). $3.3 \times 10^{-3}$ (HA) |
| $n_B$            | Amount of type-B sites ( $\text{mol g}^{-1}$ )                                 | $0.5 \times n_A$                                     |
| $pK_A$           | Intrinsic proton dissociation constant for type-A sites                        | 3.2 (FA). 4.1 (HA)                                   |
| $pK_B$           | Intrinsic proton dissociation constant for type-B sites                        | 9.4 (FA). 8.8 (HA)                                   |
| $\Delta pK_A$    | Distribution term that modifies $pK_A$   | 3.3 (FA). 2.1 (HA)                                   |
| $\Delta pK_B$    | Distribution term that modifies $pK_B$   | 4.9 (FA). 3.6 (HA)                                   |
| $\log K_{MA}$    | Intrinsic equilibrium constant for metal binding at type-A sites               | From experimental data <sup>a</sup>                  |
| $\log K_{MB}$    | Intrinsic equilibrium constant for metal binding at type-B sites               | $3.39 \log K_{MA} - 1.15$                            |
| $\Delta LK_1$    | Distribution term that modifies $\log K_{MA}$                                  | 2.8 (REE)  |
| $\Delta LK_2$    | Distribution term that modifies the strength of bidentate and tridentate sites | $0.55 \log K_{\text{NH}_3} = 0.29$ (REE)             |
| $P$              | Electrostatic parameter  | -115 (FA). -330 (HA)                                 |
| $K_{\text{sel}}$ | Selectivity coefficient for counterion accumulation                            | 1  |
| $M$              | Molecular weight (kDa)   | 1.5 (FA). 15 (HA)                                    |
| $r$              | Molecular radius (nm)  | 0.8 (FA). 1.72 (HA)                                  |

<sup>a</sup> Pourret et al. (2007b)

## References

- Andersson K, Dahlqvist R, Turner D, Stolpe B, Larsson T, Ingri J, Andersson P (2006) Colloidal rare earth elements in boreal river: changing sources and distributions during the spring flood. *Geochim Cosmochim Acta* 70:3261–3274. doi:[10.1016/j.gca.2006.04.021](https://doi.org/10.1016/j.gca.2006.04.021)
- Braun JJ, Viers J, Dupré B, Polvé M, Ndam J, Muller JP (1998) Solid/liquid REE fractionation in the lateritic system of Goyoum, East Cameroon: the implication for the present dynamics of the soil covers of the humid tropical regions. *Geochim Cosmochim Acta* 62:273–299. doi:[10.1016/S0016-7037\(97\)00344-X](https://doi.org/10.1016/S0016-7037(97)00344-X)
- Byrne RH, Sholkovitz ER (1996) Marine chemistry and geochemistry of the lanthanides. In: Gschneidner KA Jr, Eyring LR (eds) *Handbook on the physics and chemistry of rare earths*, vol 23. Elsevier, Amsterdam, pp 497–593
- Coppin F, Berger G, Bauer A, Castet S, Loubet M (2002) Sorption of lanthanides on smectite and kaolinite. *Chem Geol* 182:57–68. doi:[10.1016/S0009-2541\(01\)00283-2](https://doi.org/10.1016/S0009-2541(01)00283-2)
- Dabard M-P, Loi A, Peucat J-J (1996) Zircon typology combined with Sm-Nd whole rock-isotope analysis to study Brioverian sediments from the Armorican Massif. *Sediment Geol* 101:243–260. doi:[10.1016/0037-0738\(95\)00068-2](https://doi.org/10.1016/0037-0738(95)00068-2)
- Davranche M, Pourret O, Gruau G, Dia A (2004) Impact of humate complexation on the adsorption of REE onto Fe oxyhydroxide. *J Colloid Interface Sci* 277:271–279. doi:[10.1016/j.jcis.2004.04.007](https://doi.org/10.1016/j.jcis.2004.04.007)
- Davranche M, Pourret O, Gruau G, Dia A, Jin D, Gaertner D (2008) Competitive binding of REE to humic acid and manganese oxide: impact of reaction kinetics on development of Cerium anomaly and REE adsorption. *Chem Geol* 247:154–170. doi:[10.1016/j.chemgeo.2007.10.010](https://doi.org/10.1016/j.chemgeo.2007.10.010)
- Davranche M, Pourret O, Gruau G, Dia A, Le Coz-Bouhnik M (2005) Adsorption of REE(III)-humate complexes onto  $\text{MnO}_2$ : experimental evidence for cerium anomaly and lanthanide tetrad effect suppression. *Geochim Cosmochim Acta* 69:4825–4835. doi:[10.1016/j.gca.2005.06.005](https://doi.org/10.1016/j.gca.2005.06.005)
- De Baar HJW, German CR, Elderfield H, van Gaans P (1988) Rare earth element distributions in anoxic waters of the cariaco trench. *Geochim Cosmochim Acta* 52:1203–1219. doi:[10.1016/0016-7037\(88\)90275-X](https://doi.org/10.1016/0016-7037(88)90275-X)
- De Baar HJW, Schijf J, Byrne RH (1991) Solution chemistry of the rare earth elements in seawater. *Eur J Solid State Inorg Chem* 28:357–373
- De Carlo EH, Wen X-Y, Irving M (1998) The influence of redox reactions on the uptake of dissolved Ce by suspended Fe and Mn oxide particles. *Aquat Geochem* 3:357–389. doi:[10.1023/A:1009664626181](https://doi.org/10.1023/A:1009664626181)

- Dia A, Gruau G, Olivie-Lauquet G, Riou C, Molénat J, Curmi P (2000) The distribution of rare earth elements in groundwaters: assessing the role of source-rock composition, redox changes and colloidal particle. *Geochim Cosmochim Acta* 64:4131–4151. doi:[10.1016/S0016-7037\(00\)00494-4](https://doi.org/10.1016/S0016-7037(00)00494-4)
- Duncan T, Shaw TJ (2003) The mobility of rare earth elements and redox sensitive elements in the groundwater/seawater mixing zone of a shallow coastal aquifer. *Aquat Geochem* 9:223–255. doi:[10.1023/B:AQUA.0000022956.20338.26](https://doi.org/10.1023/B:AQUA.0000022956.20338.26)
- Dupré B, Viers J, Dandurand J-L, Polvé M, Bénézeth P, Vervier P, Braun J-J (1999) Major and trace elements associated with colloids in organic-rich river waters: ultrafiltration of natural and spiked solutions. *Chem Geol* 160:63–80. doi:[10.1016/S0009-2541\(99\)00060-1](https://doi.org/10.1016/S0009-2541(99)00060-1)
- Durand P, Juan Torres JL (1996) Solute transfer in agricultural catchments: the interest and limits of mixing models. *J Hydrol* 181:1–22. doi:[10.1016/0022-1694\(95\)02922-2](https://doi.org/10.1016/0022-1694(95)02922-2)
- Elderfield H, Greaves MJ (1982) The rare earth elements in seawater. *Nature* 296:214–219. doi:[10.1038/296214a0](https://doi.org/10.1038/296214a0)
- Elderfield H, Upstill-Goddard R, Sholkovitz ER (1990) The rare earth elements in rivers, estuaries, and coastal seas and their significance to the composition of ocean waters. *Geochim Cosmochim Acta* 54:971–991. doi:[10.1016/0016-7037\(90\)90432-K](https://doi.org/10.1016/0016-7037(90)90432-K)
- Gammons CH, Wood SA, Nimick DA (2005) Diel behavior of rare earth elements in a mountain stream with acidic to neutral pH. *Geochim Cosmochim Acta* 69:3747–3758. doi:[10.1016/j.gca.2005.03.019](https://doi.org/10.1016/j.gca.2005.03.019)
- Goldstein SJ, Jacobsen SB (1988) Rare earth elements in river waters. *Earth Planet Sci Lett* 89:35–47. doi:[10.1016/0012-821X\(88\)90031-3](https://doi.org/10.1016/0012-821X(88)90031-3)
- Gosselin DC, Smith MR, Lepel EA, Laul JC (1992) Rare earth elements in chloride-rich groundwater, Palo Duro Basin, Texas, USA. *Geochim Cosmochim Acta* 56:1495–1505. doi:[10.1016/0016-7037\(92\)90219-9](https://doi.org/10.1016/0016-7037(92)90219-9)
- Gruau G, Dia A, Olivie-Lauquet G, Davranche M, Pinay G (2004) Controls on the distribution of rare earth elements in shallow groundwaters. *Water Res* 38:3576–3586. doi:[10.1016/j.watres.2004.04.056](https://doi.org/10.1016/j.watres.2004.04.056)
- Hummel W, Berner U, Curti E, Pearson FJ, Thoenen T (2002) Nagra/PSI chemical thermodynamic data base 01/01. Universal Publishers/uPUBLISH.com, Parkland
- Ingri J, Widerlund A, Land M, Gustafsson Ö, Andersson P, Öhlander B (2000) Temporal variations in the fractionation of the rare earth elements in a boreal river; the role of colloidal particles. *Chem Geol* 166:23–45. doi:[10.1016/S0009-2541\(99\)00178-3](https://doi.org/10.1016/S0009-2541(99)00178-3)
- Johannesson KH, Burdige DJ (2007) Balancing the global oceanic neodymium budget: evaluating the role of groundwater. *Earth Planet Sci Lett* 253:129–142. doi:[10.1016/j.epsl.2006.10.021](https://doi.org/10.1016/j.epsl.2006.10.021)
- Johannesson KH, Farnham IM, Guo C, Stetzenbach KJ (1999) Rare earth element fractionation and concentration variations along a groundwater flow path within a shallow, basin-fill aquifer, southern Nevada, USA. *Geochim Cosmochim Acta* 63:2697–2708. doi:[10.1016/S0016-7037\(99\)00184-2](https://doi.org/10.1016/S0016-7037(99)00184-2)
- Johannesson KH, Hawkins DL Jr, Cortés A (2006) Do archean chemical sediments record ancient seawater rare earth element patterns? *Geochim Cosmochim Acta* 70:871–890. doi:[10.1016/j.gca.2005.10.013](https://doi.org/10.1016/j.gca.2005.10.013)
- Johannesson KH, Hendry MJ (2000) Rare earth element geochemistry of groundwaters from a thick till and clay-rich aquitard sequence, Saskatchewan, Canada. *Geochim Cosmochim Acta* 64:1493–1509. doi:[10.1016/S0016-7037\(99\)00402-0](https://doi.org/10.1016/S0016-7037(99)00402-0)
- Johannesson KH, Stetzenbach KJ, Hodge VF (1997) Rare earth elements as geochemical tracers of regional groundwater mixing. *Geochim Cosmochim Acta* 61:3605–3618. doi:[10.1016/S0016-7037\(97\)00177-4](https://doi.org/10.1016/S0016-7037(97)00177-4)
- Johannesson KH, Tang J, Daniels JM, Bounds WJ, Burdige DJ (2004) Rare earth element concentrations and speciation in organic-rich blackwaters of the Great Dismal Swamp, Virginia, USA. *Chem Geol* 209:271–294. doi:[10.1016/j.chemgeo.2004.06.012](https://doi.org/10.1016/j.chemgeo.2004.06.012)
- Johannesson KH, Zhou X, Guo C, Stetzenbach KJ, Hodge VF (2000) Origin of rare earth element signatures in groundwaters of circumneutral pH from southern Nevada and eastern California, USA. *Chem Geol* 164:239–257. doi:[10.1016/S0009-2541\(99\)00152-7](https://doi.org/10.1016/S0009-2541(99)00152-7)
- Klungness GD, Byrne RH (2000) Comparative hydrolysis behavior of the rare earths and yttrium: the influence of temperature and ionic strength. *Polyhedron* 19:99–107. doi:[10.1016/S0277-5387\(99\)00332-0](https://doi.org/10.1016/S0277-5387(99)00332-0)
- Koeppenkastrop D, De Carlo EH (1992) Sorption of rare-earth elements from seawater onto synthetic mineral particles: an experimental approach. *Chem Geol* 95:251–263. doi:[10.1016/0009-2541\(92\)90015-W](https://doi.org/10.1016/0009-2541(92)90015-W)
- Koeppenkastrop D, De Carlo EH (1993) Uptake of rare earth elements from solution by metal oxides. *Environ Sci Technol* 27:1796–1802. doi:[10.1021/es00046a006](https://doi.org/10.1021/es00046a006)
- Köhler SJ, Lidman F, Hassellöv M, Stolpe B, Mört M, Björkvald L, Laudon H (2009) Temporal variations in the export of REE in boreal catchments of varying character and size. *Geochim Cosmochim Acta* 73:A674. doi:[10.1016/j.gca.2009.05.009](https://doi.org/10.1016/j.gca.2009.05.009)

- Lawrence MG, Greig A, Collerson KD, Kamber BS (2006) Rare earth element and yttrium variability in South East Queensland waterways. *Aquat Geochem* 12:39–72. doi:[10.1007/s10498-005-4471-8](https://doi.org/10.1007/s10498-005-4471-8)
- Leybourne MI, Johannesson KH (2008) Rare earth elements (REE) and yttrium in stream waters, stream sediments, and Fe-Mn oxyhydroxides: fractionation, speciation, and controls over REE + Y patterns in the surface environment. *Geochim Cosmochim Acta* 72:5962–5983. doi:[10.1016/j.gca.2008.09.022](https://doi.org/10.1016/j.gca.2008.09.022)
- Lofts S, Tipping E, Hamilton-Taylor J (2008) The chemical speciation of Fe(III) in freshwaters. *Aquat Geochem* 14:337–358. doi:[10.1007/s10498-008-9040-5](https://doi.org/10.1007/s10498-008-9040-5)
- Luo Y-R, Byrne RH (2004) Carbonate complexation of yttrium and the rare earth elements in natural rivers. *Geochim Cosmochim Acta* 68:691–699. doi:[10.1016/S0016-7037\(03\)00495-2](https://doi.org/10.1016/S0016-7037(03)00495-2)
- Molénat J, Durand P, Gascuel-Odoux C, Davy P, Gruau G (2002) Mechanisms of nitrate transfer from soil to stream in an agricultural watershed of French Brittany. *Water Air Soil Pollut* 133:161–183. doi:[10.1023/A:1012903626192](https://doi.org/10.1023/A:1012903626192)
- Molénat J, Gascuel-Odoux C, Ruiz L, Gruau G (2008) Role of water table dynamics on stream nitrate export and concentration in agricultural headwater catchment (France). *J Hydrol* 348:363–378. doi:[10.1016/j.jhydrol.2007.10.005](https://doi.org/10.1016/j.jhydrol.2007.10.005)
- Ohta A, Kawabe I (2001) REE(III) adsorption onto Mn dioxide and Fe oxyhydroxide: Ce(III) oxidation by Mn dioxide. *Geochim Cosmochim Acta* 65:695–703. doi:[10.1016/S0016-7037\(00\)00578-0](https://doi.org/10.1016/S0016-7037(00)00578-0)
- Olivié-Lauquet G, Gruau G, Dia A, Riou C, Jaffrezic A, Hénin O (2001) Release of trace elements in wetlands: role of seasonal variability. *Water Res* 35:943–952. doi:[10.1016/S0043-1354\(00\)00328-6](https://doi.org/10.1016/S0043-1354(00)00328-6)
- Parkhurst DL, Appelo CAJ (1999) User's guide to PHREEQC (version 2)—a computer program for speciation, batch-reaction, one-dimensional transport, and inverse geochemical calculations. Water-resources investigations report 99-4259, US geological survey, Denver
- Pauwels H, Kloppmann W, Foucher JC, Martelat A, Fritzsche V (1998) Field tracer test for denitrification in a pyrite-bearing schist aquifer. *Appl Geochem* 13:767–778. doi:[10.1016/S0883-2927\(98\)00003-1](https://doi.org/10.1016/S0883-2927(98)00003-1)
- Pellerin J, Van Vliet-Lanôe B (1998) Le bassin du Coët-Dan au coeur du Massif armoricain. 2. Analyse cartographique de la région de Naizin. In: Cheverry C (ed) Agriculture intensive et qualité des eaux. INRA, Paris, pp 17–24 (in French)
- Pokrovsky OS, Dupré B, Schott J (2005) Fe-Al-organic colloids control of trace elements in peat soil solutions: results of ultrafiltration and dialysis. *Aquat Geochem* 11:241–278. doi:[10.1007/s10498-004-4765-2](https://doi.org/10.1007/s10498-004-4765-2)
- Pourret O, Davranche M, Gruau G, Dia A (2007a) Organic complexation of rare earth elements in natural waters: evaluating model calculations from ultrafiltration data. *Geochim Cosmochim Acta* 71:2718–2735. doi:[10.1016/j.gca.2007.04.001](https://doi.org/10.1016/j.gca.2007.04.001)
- Pourret O, Davranche M, Gruau G, Dia A (2007b) Rare earth elements complexation with humic acid. *Chem Geol* 243:128–141. doi:[10.1016/j.chemgeo.2007.05.018](https://doi.org/10.1016/j.chemgeo.2007.05.018)
- Pourret O, Davranche M, Gruau G, Dia A (2008) New insights into cerium anomalies in organic rich alkaline waters. *Chem Geol* 251:120–127. doi:[10.1016/j.chemgeo.2008.03.002](https://doi.org/10.1016/j.chemgeo.2008.03.002)
- Pourret O, Dia A, Davranche M, Gruau G, Hénin O, Angée M (2007c) Organo-colloidal control on major- and trace-element partitioning in shallow groundwaters: confronting ultrafiltration and modelling. *Appl Geochem* 22:1568–1582. doi:[10.1016/j.apgeochem.2007.03.022](https://doi.org/10.1016/j.apgeochem.2007.03.022)
- Schijf J, Byrne RH (2004) Determination of  $\text{SO}_4\beta_1$  for yttrium and the rare earth elements at  $I = 0.66 \text{ m}$  and  $t = 25^\circ\text{C}$ -implications for YREE solution speciation in sulfate-rich waters. *Geochim Cosmochim Acta* 68:2825–2837. doi:[10.1016/j.gca.2003.12.003](https://doi.org/10.1016/j.gca.2003.12.003)
- Sholkovitz ER (1995) The aquatic chemistry of rare earth elements in rivers and estuaries. *Aquat Geochem* 1:1–34. doi:[10.1007/BF01025229](https://doi.org/10.1007/BF01025229)
- Smedley PL (1991) The geochemistry of rare earth elements in groundwater from the Carnmenellis area, southwest England. *Geochim Cosmochim Acta* 55:2767–2779. doi:[10.1016/0016-7037\(91\)90443-9](https://doi.org/10.1016/0016-7037(91)90443-9)
- Sonke JE, Salters VJM (2006) Lanthanide-humic substances complexation. I. Experimental evidence for a lanthanide contraction effect. *Geochim Cosmochim Acta* 70:1495–1506. doi:[10.1016/j.gca.2005.11.017](https://doi.org/10.1016/j.gca.2005.11.017)
- Stern JC, Sonke JE, Salters VJM (2007) A capillary electrophoresis-ICP-MS study of rare earth element complexation by humic acids. *Chem Geol* 246:170–180. doi:[10.1016/j.chemgeo.2007.09.008](https://doi.org/10.1016/j.chemgeo.2007.09.008)
- Tang J, Johannesson KH (2005) Adsorption of rare earth elements onto carrizo sand: experimental investigations and modeling with surface complexation. *Geochim Cosmochim Acta* 69:5247–5261. doi:[10.1016/j.gca.2005.06.021](https://doi.org/10.1016/j.gca.2005.06.021)
- Tanizaki Y, Shimokawa T, Nakamura M (1992) Physicochemical speciation of trace elements in river waters by size fractionation. *Environ Sci Technol* 26:1433–1444. doi:[10.1021/es00031a023](https://doi.org/10.1021/es00031a023)
- Taylor SR, McLennan SM (1985) The continental crust: its composition and evolution. Blackwell, Oxford
- Thurman EM (1985) Organic geochemistry of natural waters. Nijhoff/Junk, Dordrecht

- Tipping E (1998) Humic ion-binding model VI: an improved description of the interactions of protons and metal ions with humic substances. *Aquat Geochem* 4:3–48. doi:[10.1023/A:1009627214459](https://doi.org/10.1023/A:1009627214459)
- Viers J, Dupré B, Polvé M, Schott J, Dandurand J-L, Braun JJ (1997) Chemical weathering in the drainage basin of a tropical watershed (Nsimi-Zoetele site, Cameroon): comparison between organic-poor and organic-rich waters. *Chem Geol* 140:181–206. doi:[10.1016/S0009-2541\(97\)00048-X](https://doi.org/10.1016/S0009-2541(97)00048-X)
- Welch SA, Christy AG, Isaacson L, Kirste D (2009) Mineralogical control of rare earth elements in acidic sulfate soils. *Geochim Cosmochim Acta* 73:44–64. doi:[10.1016/j.gca.2008.10.017](https://doi.org/10.1016/j.gca.2008.10.017)
- Yeghicheyan D, Carignan J, Valladon M, Bouhnik Le Coz M, Le Cornec F, Castrec-Rouelle M, Robert M, Aquilina L, Aubry E, Churlaud C, Dia A, Deberdt S, Dupré B, Freydier R, Gruau G, Hénin O, de Kersabiec A-M, Macé J, Marin L, Morin N, Petitjean P, Serrat E (2001) Compilation of silicon and thirty-one trace elements measured in the natural river water reference material SLRS-4 (NRC-CNRC). *Geostand Newslett* 25:465–474. doi:[10.1111/j.1751-908X.2001.tb00617.x](https://doi.org/10.1111/j.1751-908X.2001.tb00617.x)